



HAL
open science

Catalytic conversion of carbon oxides to new polymeric materials

Zdeněk Hošťálek

► **To cite this version:**

Zdeněk Hošťálek. Catalytic conversion of carbon oxides to new polymeric materials. Polymers. Université de Bordeaux; Vysoká škola chemicko-technologická (Praze), 2016. English. NNT: 2016BORD0016 . tel-01308191

HAL Id: tel-01308191

<https://theses.hal.science/tel-01308191>

Submitted on 27 Apr 2016

HAL is a multi-disciplinary open access archive for the deposit and dissemination of scientific research documents, whether they are published or not. The documents may come from teaching and research institutions in France or abroad, or from public or private research centers.

L'archive ouverte pluridisciplinaire **HAL**, est destinée au dépôt et à la diffusion de documents scientifiques de niveau recherche, publiés ou non, émanant des établissements d'enseignement et de recherche français ou étrangers, des laboratoires publics ou privés.

THÈSE EN COTUTELLE PRÉSENTÉE

POUR OBTENIR LE GRADE DE

**DOCTEUR DE
L'UNIVERSITÉ DE BORDEAUX
ET DE
L'ÉCOLE NATIONALE SUPÉRIEURE DES TECHNOLOGIES
CHIMIQUES DE PRAGUE**

ÉCOLE DOCTORALE DE SCIENCES CHIMIQUES DE BORDEAUX

SPÉCIALITÉ POLYMÈRES

Par **Zdeněk HOŠŤÁLEK**

**CATALYTIC CONVERSION OF CARBON OXIDES TO NEW
POLYMERIC MATERIALS**

Sous la direction de **Jan MERNA** et de **Henri CRAMAIL**

Soutenue le 5 Février 2016

Membres du jury :

M. PERUCH, Frédéric	DR CNRS, Université de Bordeaux	Président
Mme. GUILLAUME, Sophie	DR CNRS, Institut des Sciences Chimiques de Rennes	Rapporteur
M. DAGORNE, Samuel	DR CNRS, Université de Strasbourg	Rapporteur
M. ZINCK, Philippe	Professeur, Université de Lille	Examineur
M. LORBER, Christian	DR CNRS, Université de Toulouse	Examineur
M. CRAMAIL, Henri	Professeur, Université de Bordeaux	Examineur
M. MERNA, Jan	Ass-Prof, University of Chemistry and Technology, Prague	Examineur
M. BROŽEK, Jiří	Professeur, University of Chemistry and Technology, Prague	Examineur

ABSTRACT

A series of salphen complexes based on Cr, Co and Fe was synthesized and used as catalysts in ring-opening copolymerization of different substrates: (i) epoxides with carbon monoxide (CO), (ii) epoxides with anhydrides and (iii) epoxides with carbon dioxide (CO₂). Additionally, a screening of catalytic activity for the last substrate was performed with novel Zn, Al and Mg non-salen based complexes.

The first part of the Thesis deals with the copolymerization of propylene oxide with carbon monoxide using asymmetric salphen chromium complex and Co₂(CO)₈ in order to prepare a synthetic equivalent of polyhydroxybutyrate (PHB) otherwise accessible by fermentation of various substrates. Very poor catalytic performances towards carbonylated products (PHB or β -butyrolactone (BBL)) were observed with any of the two complexes. The combination of both salphen chromium and Co₂(CO)₈ complexes led to increased formation of BBL. Low molar mass poly(ester-co-ether) was only prepared, suggesting a poor compatibility of selected complexes.

The second part of the work is focused on the copolymerization of epoxides with anhydrides catalyzed by salphen chromium or iron complexes combined with simple organic bases as cocatalysts. Salphen complexes alone were almost inactive, while in the presence of bis(triphenylphosphineiminium)chloride (PPNCl) they afforded highly alternating polyesters with molar mass up to 10 kg.mol⁻¹ and low dispersity. Surprisingly, organic bases alone afforded similar, highly alternating polyesters at five-time lower polymerization rate. PPNCl was found to be an effective catalyst for the highly alternating copolymerization of various epoxides and anhydrides.

The last part of our investigations refers to the copolymerization of epoxides with CO₂ using salphen chromium and especially salphen cobalt complexes. Cobalt catalysts were significantly more active in propylene oxide (PO)/CO₂ and cyclohexene oxide (CHO)/CO₂ copolymerization compared to their chromium analogues. Highly alternating polycarbonates (> 99%) with low dispersity and molar mass 10-35 kg.mol⁻¹ were prepared by salphen cobalt complexes. Kinetic studies showed that these polymerizations are controlled and MALDI-TOF MS analysis was used for initiation mechanism clarification. Compared to widely investigated salen Co catalysts, salphen Co complexes exhibit lower activity (100-450 h⁻¹) and selectivity to polymer (40-90%) in propylene oxide/CO₂ copolymerization, while 100% selectivity to polycarbonate was achieved in the copolymerization of CHO and CO₂. Alternatively, new Al, Zn and Mg-based catalysts were tested for CO₂ activation, however, they usually led only to epoxide homopolymerization.

Key words: Catalysis, carbon oxides, epoxides, anhydrides, ring-opening copolymerization, salphen complexes.

RESUMÉ

Plusieurs complexes de salphen à base de métaux transition (Cr, Co, Fe) ont été synthétisés et utilisés comme catalyseurs pour la copolymérisation d'époxydes avec du monoxyde de carbone (CO), des anhydrides ou du dioxyde de carbone (CO₂). De nouveaux complexes à base de Zn, Al, Mg ont également été testés pour la copolymérisation d'époxydes avec CO₂.

La partie première s'intéresse principalement à la copolymérisation d'oxyde de propylène avec du monoxyde de carbone. Le complexe salphen de chrome et Co₂(CO)₈ ont été utilisés comme catalyseurs. Quel que soit le complexe utilisé, il a été observé une faible activité et les produits de carbonylation attendus (polyester et lactone) ont été obtenus en faible quantité. En revanche, la combinaison in-situ de ces deux catalyseurs a montré une activité supérieure. Cela a conduit à la formation de la lactone cyclique (β -butyrolactone) et de poly(ester-co-éther) de faible masse molaire, ce qui marque une faible compatibilité de ces complexes.

La partie suivante traite de la copolymérisation d'époxydes avec des anhydrides catalysée par des complexes de salphen à base de chrome et fer ou d'une base organique simple. Les complexes utilisés sans co-catalyseur ont été inactifs, mais la combinaison avec la base organique (PPNCl) comme co-catalyseur a conduit à la copolymérisation alternée des deux monomères, produisant des polyesters avec des masses molaires jusqu' à 10 kg.mol⁻¹ et une faible dispersité. PPNCl s'est révélée être la base la plus efficace pour la copolymérisation alternée des époxydes et des anhydrides. Les bases organiques simples utilisées seules ont aussi permis l'obtention de polyesters, mais avec des temps de polymérisation cinq fois plus longs.

Enfin, la troisième partie présente la copolymérisation des époxydes avec CO₂ en présence de complexes salphen de Cr ou de Co. Les complexes salphen cobalt ont été significativement plus efficaces pour la copolymérisation de l'oxyde de propylène (PO) ou de l'oxyde de cyclohexène (CHO) avec CO₂ que leurs homologues à base de chrome. Les polycarbonates obtenus avec les complexes de cobalt ont plus de 99% d'unités carbonate, des masses molaires allant de 10 à 35 kg.mol⁻¹ et une faible dispersité. Les études cinétiques ont permis de montrer que la polymérisation est contrôlée. Des analyses par spectrométrie de masse MALDI-TOF ont permis de vérifier la microstructure et le mécanisme d'activation. Toutefois, pour la copolymérisation de PO avec CO₂, les complexes salphen cobalt ont une activité plus faible (100-450 h⁻¹) ainsi qu'une sélectivité en polycarbonate moindre (40-90%) que les complexes salen cobalt. Une sélectivité de 100% vers la synthèse de polycarbonate a néanmoins pu être obtenue lors de la copolymérisation de CHO avec CO₂. Enfin, les complexes β -diminate, ketiminate et amidate d'Al, Zn et Mg utilisés pour la copolymérisation d'époxydes avec CO₂ se sont révélés décevants car présentant une activité très faible et seuls des homopolyéthers ont été obtenus.

Mot clés: Catalyse, oxyde de carbone, époxydes, anhydrides, ROCOP, complexes salphen

Titre : Conversion de catalyseurs d'oxydes de carbone en nouveaux matériaux polymères

SOUHRN

V této práci byla připravena řada sulfenových komplexů na bázi chromu, kobaltu a železa. Tyto komplexy byly použity jako katalyzátory pro kopolymerizace epoxidů s různými substráty: (i) s oxidem uhelnatým (CO), (ii) s anhydridy a (iii) s oxidem uhličitým (CO₂). U nových komplexů na bázi zinku, hliníku a hořčíku byla dále testována možnost jejich použití jako katalyzátorů pro kopolymerizace epoxidů s CO₂.

První část práce se zabývá kopolymerizací epoxidů s oxidem uhelnatým s využitím asymetrického sulfenového komplexu na bázi chromu a Co₂(CO)₈ s cílem připravit kopolymer na bázi přírodního polyhydroxybutyrátu (PHB). Sulfenový komplex chromu i Co₂(CO)₈ vykazovaly velmi nízké aktivity při karbonylaci propylenoxidu a poskytovaly pouze nepatrné množství produktů (cyklického β-butyrolaktonu a PHB). Kombinace obou katalytických komplexů vedla k výraznému zvýšení aktivity ve prospěch cyklického produktu (β-butyrolaktonu) i polymeru. Kopolymerizací PO s CO byl získán pouze nízkomolekulární poly(ester-co-ether), což naznačuje špatnou vzájemnou kompatibilitu těchto komplexů.

Druhá část je zaměřena na kopolymerizace epoxidů s anhydridy katalyzované sulfenovými komplexy chromu a železa v kombinaci s jednoduchými organickými bázemi. Samotné sulfenové komplexy chromu a železa nevedly ke vzniku polymeru. V kombinaci s nukleofilním kokatalyzátorem bis(trifenylfosfin)iminium chloridem (PPNCl) ovšem tyto komplexy poskytly alternující kopolymery epoxidu a anhydridu (polyestery) s molárními hmotnostmi do 10 kg.mol⁻¹ a nízkou dispersitou. Dále bylo zjištěno, že samotné organické báze poskytují podobně jako sulfenové komplexy vysoce alternující kopolymery se srovnatelnou molární hmotností i úzkou dispersitou, i když je zapotřebí 5x delších polymerizačních časů. Nejvyšší účinnost ze všech testovaných bází měl PPNCl. Tato báze byla dále efektivně použita pro kopolymerizace řady epoxidů a anhydridů za vzniku vysoce alternujících kopolymerů.

Třetí část pojednává o kopolymerizacích epoxidů s CO₂ s využitím sulfenových komplexů chromu a kobaltu. Bylo zjištěno, že kobaltové komplexy jsou oproti chromovým mnohem efektivnější katalyzátory jak při kopolymerizacích propylenoxidu (PO) s CO₂ tak i cyklohexenoxidu (CHO) s CO₂. Sulfenové komplexy kobaltu poskytly polykarbonáty s vysokým obsahem karbonátových jednotek v kopolymeru (> 99%), úzkou dispersitou a s molárními hmotnostmi 10-35 kg.mol⁻¹. Studie kinetiky odhalila kontrolovaný průběh kopolymerizace. Dále byla provedena MALDI-TOF analýza výsledných polykarbonátů s cílem objasnit mechanismus iniciace kopolymerizace. Ve srovnání se sulfenovými komplexy kobaltu vykazují sulfenové komplexy při kopolymerizacích PO s CO₂ nižší aktivitu (100-450 h⁻¹) i selektivitu na polykarbonát (40-90%). Při kopolymerizacích CHO s CO₂ byla ovšem selektivita 100%. Nové komplexy na bázi Al, Mg a Zn byly také testovány jako katalyzátory pro kopolymerizace epoxidů s CO₂, nicméně jejich aktivita byla nízká a výsledkem těchto reakcí byly pouze polykarbonáty s nízkým podílem karbonátových jednotek nebo polyethery.

Klíčová slova: Katalýza, oxidy uhlíku, epoxidy, anhydridy, kopolymerizace, sulfenové komplexy

ACKNOWLEDGEMENTS

On the first place I would like thank to my supervisors Dr. Jan Merna (UCT Prague) and prof. Cramail (ENSCBP) for their guidance, advices and patience during my Ph. D. studies. My sincere thanks belong also to my co-supervisors Dr. Peruch and Dr. Etienne Grau, who also guided me during my internships at LCPO.

Further I would like to mention all people, who contributed to this thesis. Particularly, I would like to thank to Prof. Růžička and his research team from University Pardubice, who kindly provided a series of β -diiminate, ketiminate and aminidate complexes. My thanks belong also to Martina Štekrová for kind supplying of indene oxide and to Prof. Gläser from University Leipzig, for kind supplying of methyl stearate oxide.

My further acknowledgements belongs especially to Robert Mundil for the synthesis and characterization of salphen Fe complexes and also to short-term students Duygu Özfidan from Turkey and Thomas Martinez from France, who performed some copolymerization experiments of anhydrides and epoxides.

I cannot forget to mention all the people, who helped a lot with the characterization of complexes and polymers. My grateful thanks belongs especially to: Olga Trhlíková and Zuzana Walterová for MALDI-TOF MS analyses of polyesters and polycarbonates, Mrs. Ivana Císařová for X-ray crystallography of complexes, Mrs. Ivana Bartošová for uncountable ^1H and ^{13}C NMR analyses of synthesized polymers, Mrs. Miroslava Novotná for FT-IR analyses, Mrs. Zdeňka Rottnerová for MS-ESI analyses and Mrs. Anna Bruthansová for elemental analyses of complexes.

Finally, I would like to thank all members of our laboratory B128 and Department of polymers at UCT Prague and to all members of LCPO laboratories at ENSCBP for their never-ending enthusiasm and their kind help whenever it was needed. My heartiest thanks belong to my family and girlfriend for their love, patience and support.

LIST OF ABBREVIATIONS

APO	α -Pinene oxide
BBL	β -Butyrolactone
BDI	β -diiminate (complexes)
BPO	β -Pinene oxide
CC	Cyclic carbonate
CHA	Cyclohexene anhydride
CHC	Cyclohexene carbonate
CHO	Cyclohexene oxide
CL	Carbonate linkage (% of carbonate units in copolymer)
CO _x	Carbon oxides (=CO+CO ₂)
CPrA	Cyclopropane anhydride
\bar{D}	Dispersity (M_w/M_n)
DABCO	1,4-Diazabicyclo[2.2.2]octane
DMAP	4-Dimethylaminopyridine
DMC	Double metal cyanide (complexes)
DMSO	Dimethyl sulfoxide
DNP	Dinitrophenolate
<i>ee</i>	Enantiomeric excess
HT	Ratio of head-tail linkage in copolymer [%]
<i>i</i>	isotactic
k_{rel}	Kinetic resolution; enantioselectivity; $k_{rel}=\ln[(1-c)(1-ee)]/\ln[(1-c)(1+ee)]$, where <i>c</i> is a conversion of epoxide and the <i>ee</i> value is of unreacted epoxide
LA	Lewis acid
L _n	Ligand framework
LO	Limonene oxide
M	Metal
MA	Maleic anhydride
M_n	Number average molar mass (kg.mol ⁻¹)
MTBD	Methyltriazabicyclodec-1-ene
MSO	Methyl stearate oxide
MUO	Methylundec-10-enoate oxide
Nu	Nucleophile
OAc	Acetate
OBzF ₅	Pentafluorobenzoate
OR	Alkoxy group
P	Growing polymer chain
<i>p</i> -TsOH	<i>Para</i> -toluenesulfonic acid
PA	Phthalic anhydride
PC	Propylene carbonate (cyclic propylene carbonate)
PCHC	Poly(cyclohexene carbonate)
PCL	Poly(ϵ -caprolactone)
PET	Poly(ethylene terephthalate)
PES	Polyesters
PHA	Poly(hydroxyalkanoates)

PHB	Poly(3-hydroxybutyrate)
PLA	Poly(L-lactide)
P_m	Probability of <i>meso</i> dyad linkages (isotacticity) of substituents in polymer chain
PO	Propylene oxide
PPC	Poly(propylene carbonate)
PPN ⁺	Bis(triphenylphosphine)iminium cation
PPNCl	Bis(triphenylphosphine)iminium chloride
P_r	Probability of <i>racemo</i> dyad linkages (syndiotacticity) of substituents in polymer chain
PSC	Poly(styrene carbonate)
PVA	Poly(vinylalcohol)
<i>rac</i>	racemic
ROCOP	Ring-Opening Copolymerization
ROP	Ring-Opening Polymerization
SA	Succinic anhydride
sc	supercritical
S_N2	Nucleophilic substitution (bi-molecular)
SO	Styrene oxide
TBD	Triazabicyclodecene
tCIPA	Tetrachlorophthalic anhydride
$T_{deg(5\%)}$	Thermal decomposition temperature (corresponding to 5% polymer loss)
T_g	Glass transition temperature
THF	Tetrahydrofuran
T_m	Melting temperature
TMC	Trimethylene carbonate
TOF	Turnover frequency (=activity) - number of catalytic cycles per one catalytic center per hour (h^{-1})
X	Initiating nucleophilic group attached to metal center or substituent on ligand framework or halogen

CONTENT

1	GENERAL INTRODUCTION	1
2	LITERATURE PART	3
2.1	Polyesters based on CO, epoxides and their carbonylation products	3
2.1.1	Direct copolymerization of epoxides with CO	4
2.1.1.1	Mechanism of epoxide/CO copolymerization.....	4
2.1.1.2	Catalysts for direct epoxides/CO copolymerization.....	5
2.1.2	Polyesters by polymerization of β -lactones obtained by epoxide carbonylation	6
2.1.2.1	Catalysts for carbonylative expansion of epoxides	7
2.1.2.2	Ring-opening polymerization of β -butyrolactone.....	10
2.1.3	Polyesters by ring-opening copolymerization of epoxides with anhydrides.....	13
2.2	Polycarbonates by epoxide/CO₂ copolymerization.....	17
2.2.1	Mechanism of epoxide/CO ₂ copolymerization.....	17
2.2.2	Catalysts for copolymerization of commercial epoxides with CO ₂	23
2.2.2.1	Early catalysts for CO ₂ /epoxides copolymerization	23
2.2.2.2	Single site dinuclear β -diiminate complexes.....	23
2.2.2.3	Single site salen catalysts	27
2.2.2.4	Salan and salalen complexes.....	30
2.2.2.5	Multichiral and bifunctional salen complexes	32
2.2.2.6	Early and new porphyrin catalysts	36
2.2.2.7	Binuclear and bimetallic-bridged catalysts	39
2.2.2.8	Other catalysts	43
2.2.2.9	Brief summary of displayed catalytic complexes	44
2.2.3	Copolymerization of special and biobased epoxides with CO ₂	45
3	MOTIVATION AND GOALS OF THE THESIS	49
4	EXPERIMENTAL PART	51
4.1	General experimental details.....	51
4.2	Used chemicals.....	51
4.3	Synthesis of catalysts.....	52
4.3.1	Synthesis of ligands	52
4.3.2	Synthesis of complexes.....	52
4.4	Epoxidation of methylundec-10-enoate	57
4.5	Polymerization procedures	58
4.6	Analyses.....	59
5	RESULTS AND DISCUSSION	63
5.1	Synthesis and characterization of salphen catalysts.....	63
5.1.1	Salphen Cr complexes.....	63
5.1.2	Salphen Fe complexes	64
5.1.3	Salphen Co complexes	64
5.1.4	Conclusion	74
5.2	Copolymerization of epoxides with carbon monoxide.....	76
5.2.1	Copolymerization of PO and CO with 2-CrCl/Co ₂ (CO) ₈	76
5.2.2	Copolymerization of CHO or MUO with CO catalyzed by 2-CrCl/Co ₂ (CO) ₈	79

5.2.3	Conclusion	80
5.3	Copolymerization of epoxides with anhydrides	81
5.3.1	Copolymerization of epoxides and anhydrides catalyzed by Cr and Fe salphen complexes	81
5.3.2	Copolymerization of PA with CHO catalyzed with PPNCl - initial screening	83
5.3.3	MALDI-TOF analysis of PA-CHO polyesters – mechanism of initiation	87
5.3.4	The effect of PA-CHO stoichiometry, reaction temperature and solvent (incl. bulk)	91
5.3.5	Kinetic studies of CHO-PA copolymerization	93
5.3.6	Copolymerization of PA with CHO catalyzed by various organic bases	96
5.3.7	Copolymerization of various epoxides and anhydrides	97
5.3.8	Conclusion	98
5.4	Copolymerization of epoxides with CO₂.....	100
5.4.1	Alternating copolymerization of PO or CHO with CO ₂ catalyzed by Cr salphen complexes	100
5.4.2	Alternating copolymerization of PO and CO ₂ catalyzed by Co salphen complexes	103
5.4.2.1	Copolymerization of PO/CO ₂ with 1-Co-OOCCl ₃	103
5.4.2.2	Copolymerization of epoxide with series of salphen complexes 1-Co-Y and 2-Co-Y	105
5.4.2.3	Mechanism of activation and insight into PO/CO ₂ copolymer microstructure.....	107
5.4.3	Alternating copolymerization of CHO with CO ₂ in presence of 1-Co-Y and 2-Co-Y complexes	109
5.4.3.1	Kinetics of copolymerization CHO/CO ₂ and insight into copolymer microstructure	110
5.4.4	Coupling of alternative epoxides with CO ₂ catalyzed with 2-CrCl and 2-Co-OAc	111
5.4.5	Screening of catalytic activity of Al, Zn and Mg complexes for copolymerization of epoxides with CO ₂	112
5.4.6	Conclusion	114
6	GENERAL CONCLUSIONS	116
7	REFERENCES.....	118
8	SUPPLEMENTARY DATA	126
8.1	Full NMR characterization of complex 2-Co	126
8.2	Crystallographic data for complex 1-Co-OBzF ₅	129
8.3	¹ H NMR spectra of “polyesters” obtained by copolymerization of APO or BPO with PA ...	130
8.4	Spectrum of PA-CHO copolymer with PPN-OMe terminal group.....	131
8.5	¹ H NMR spectra of copolyesters prepared with PPNCl catalyst.....	131
8.6	Polymerization apparatuses used for epoxide/CO _x copolymerizations	135
9	LIST OF TABLES.....	136
10	LIST OF SCHEMES	137
11	LIST OF FIGURES.....	138
12	LIST OF SPECTRA	141
13	LIST OF PUBLICATIONS	142

1 GENERAL INTRODUCTION

In the last decades, plastic materials became an integral part of our lives and their production continuously increases as illustrated by an exponential growth of polymer world production since WWII overpassing 300 Mt per year in 2013.¹ Hand in hand with rising production of plastics, an increase of plastic waste production (which exceeded 25 Mt/year in Europe¹) is observed. A large scale produced polymers such as polyolefins, polystyrene or polyvinylchloride are highly stable towards biological or hydrological decomposition and have a large negative effect on the environment. Although there is an increasing demand to reuse and recycle plastics² and a significant effort is devoted to the development of new technologies for material valorization, (e.g. pyrolysis³ and solvolysis⁴) recycling is still, in most cases, economically unprofitable and the majority of plastics is combusted or stored in stock-yards. The solution of problems with part of polymeric waste could be a production of biodegradable polymers like aliphatic polyesters and polycarbonates which are susceptible towards biotic or abiotic degradation.

Although some biodegradable polymers are produced on industrial scale (e.g. bacterial production of PHB, production of high-molar mass PLA and PCL), larger commercial usage is impeded by their higher price compared to petroleum based polymers produced in large-ton scale by efficient chemical processes using cheap raw materials (olefins, styrene, vinylchloride).

An alternative way leading to cheaper biodegradable polymers could be the utilization of carbon oxides as a C1 feedstock for the copolymerization with other monomers. The incorporation of carbon monoxide into organic molecules is a promising strategy towards the synthesis of new valuable materials. A large number of publications was focused on the copolymerization of reactive carbon monoxide with α -olefins (ethylene, propylene...) and vinylarenes producing polyketone-based polymers.⁵ The copolymerization of CO with heterocycles such as epoxides and aziridines could be an interesting environmentally friendly alternative for the production of polyesters and polyamides.^{5b} Moreover, combining CO with imines can lead to polypeptides, which have broad applications in materials, catalysis and pharmaceuticals.⁶

Further, use of CO₂ - an abundant, renewable and nontoxic gas in polymer synthesis could be also a pathway to new "green" materials. Despite the low reactivity of CO₂ it can be activated by suitable catalysis and when copolymerized with epoxides the overall reaction is thermodynamically favorable leading to polycarbonates.⁷ In the case of the use of basic aliphatic epoxides polycarbonates susceptible to (bio)degradation can be obtained.

The development of novel catalytic processes using commodity monomers could make the production of biodegradable (and also non-biodegradable) polymers comparably effective with current synthetic polymers.

Using major petrol based epoxides (ethylene oxide, propylene oxide) with CO₂ could lead to polymers, which are composed from 20 to 50% of renewable CO₂ building blocks (e.g., poly(propylene carbonate) (PPC)). 100% biobased polymers could be achieved when CO₂ would be effectively copolymerized with epoxides derived from e.g. fatty acid or terpenes. Production of such materials could decrease the dependence of polymer industry on petrol.

Thesis Overview: A variety of catalysts have been reported to catalyze the copolymerization of epoxides with various substrates, such as anhydrides CO and CO₂. Among those, salen complexes of Al, Cr and Co were widely explored. Similar salen complexes were however studied marginally. The motivation of this thesis is therefore to explore the potential of salen complexes in ring-opening copolymerization of epoxides with various substrates, which can afford biodegradable polycarbonates and polyesters.

This work deals with:

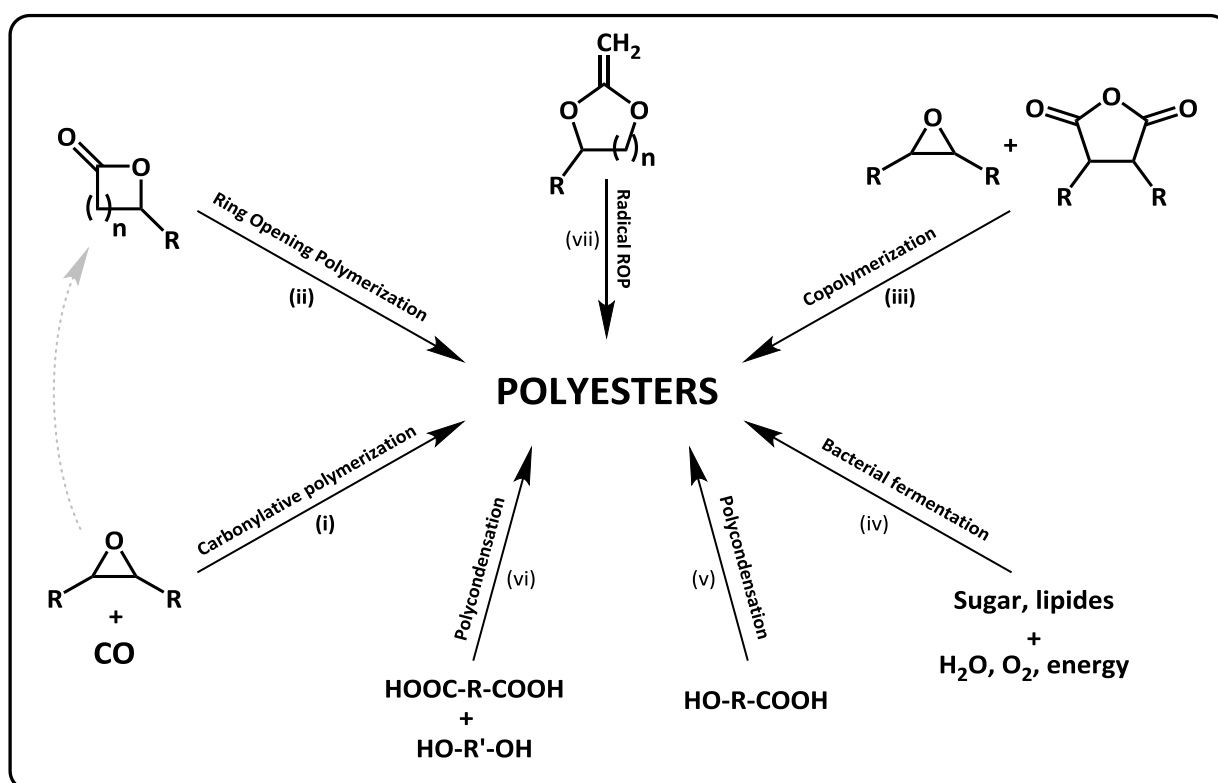
- (i) **Synthesis and characterization of salen complexes** of cobalt, chromium and iron
- (ii) **Copolymerization of epoxides with CO** using salen chromium complexes in combination with Co₂(CO)₈ in order to prepare linear polyesters
- (iii) **Copolymerization of epoxides with anhydrides** using salen chromium, iron complexes and simple organic bases for the preparation of linear polyesters, detailed mechanistic and kinetic studies of organo-catalyzed copolymerization of cyclohexene oxide with phthalic anhydride
- (iv) **Copolymerization of epoxides with CO₂** with salen chromium and cobalt complexes combined with organic base-cocatalyst leading to linear polycarbonates, investigation of activation mechanism of PO/CO₂ and CHO/CO₂ copolymerization and the effect of experimental conditions on the overall catalytic performance of individual complexes

2 LITERATURE PART

2.1 Polyesters based on CO, epoxides and their carbonylation products

Polyesters represent an important group of polymers with a broad spectrum of properties from highly resistant and tough aromatic polyesters used in aeronautics⁸ up to biodegradable and biocompatible aliphatic polyesters used in various medicinal applications.⁹

Polyesters can be prepared by many diverse synthetic routes such as polycondensation, anionic, cationic, enzymatic, coordination-insertion polymerization and even by free radical polymerization (Scheme 2.1). These methods allow the synthesis of multiple structures including polyester resins, linear homopolyesters and random, block, graft, star and hyper-branched copolyesters.¹⁰



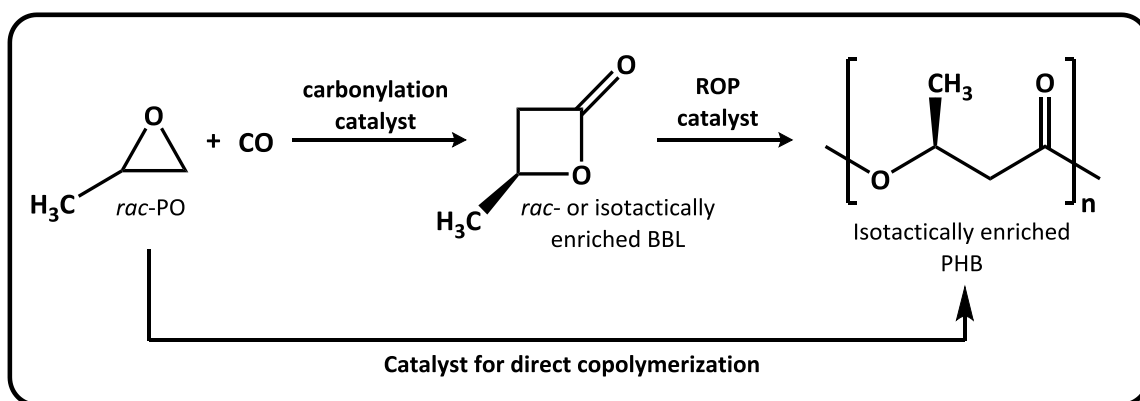
Scheme 2.1: Synthetic routes to polyesters

Compared to highly resistant linear aromatic polyesters and relatively stable semi-aromatic polyesters (PET), aliphatic polyesters are polymers containing a labile oxo-carbonyl bond which impart some interesting material properties especially susceptibility towards biological degradation and biocompatibility. The biodegradability of polyesters (and polymers in general) is a desirable property for selected applications with short life-time (e.g. foils for agriculture, medicinal materials). Moreover, their biocompatibility makes them suitable candidates for biomedical and pharmaceutical applications.¹¹ The most important representatives of such polyesters are poly(ϵ -caprolactone), poly(*L*-lactide), polyglycolide

and its copolymers prepared by ROP of cyclic monomers, and poly(hydroxyalkanoates) produced by bacteria.

Other routes to polyesters are described in the following chapters utilizing catalyzed copolymerization of epoxides with carbon monoxide or substrates potentially available through mono or double carbonylation of epoxides (β -lactones and anhydrides). The following three sub-chapters (2.1.1, 2.1.2 and 2.1.3) are focused mainly to (i) **direct propylene oxide/CO copolymerization**, (ii) **epoxide carbonylation leading to β -lactones and their following ROP** and (iii) **copolymerization of epoxides with anhydrides**. All mentioned polymerization routes (i-iii) can be catalyzed by salen or salphen transition metal complexes which are the main catalytic systems applied in this thesis.

An alternative route to bacterial production of PHA's and ROP of cyclic esters (mainly PHB) could be the direct metal catalyzed copolymerization of epoxides (propylene oxide (PO)) with carbon monoxide¹² or carbonylative expansion of epoxides followed by the ROP of in-situ formed cyclic esters (lactones) so-called carbonylative polymerization (Scheme 2.2).¹³



Scheme 2.2: Expansion carbonylation of propylene oxide with CO and subsequent ring-opening polymerization

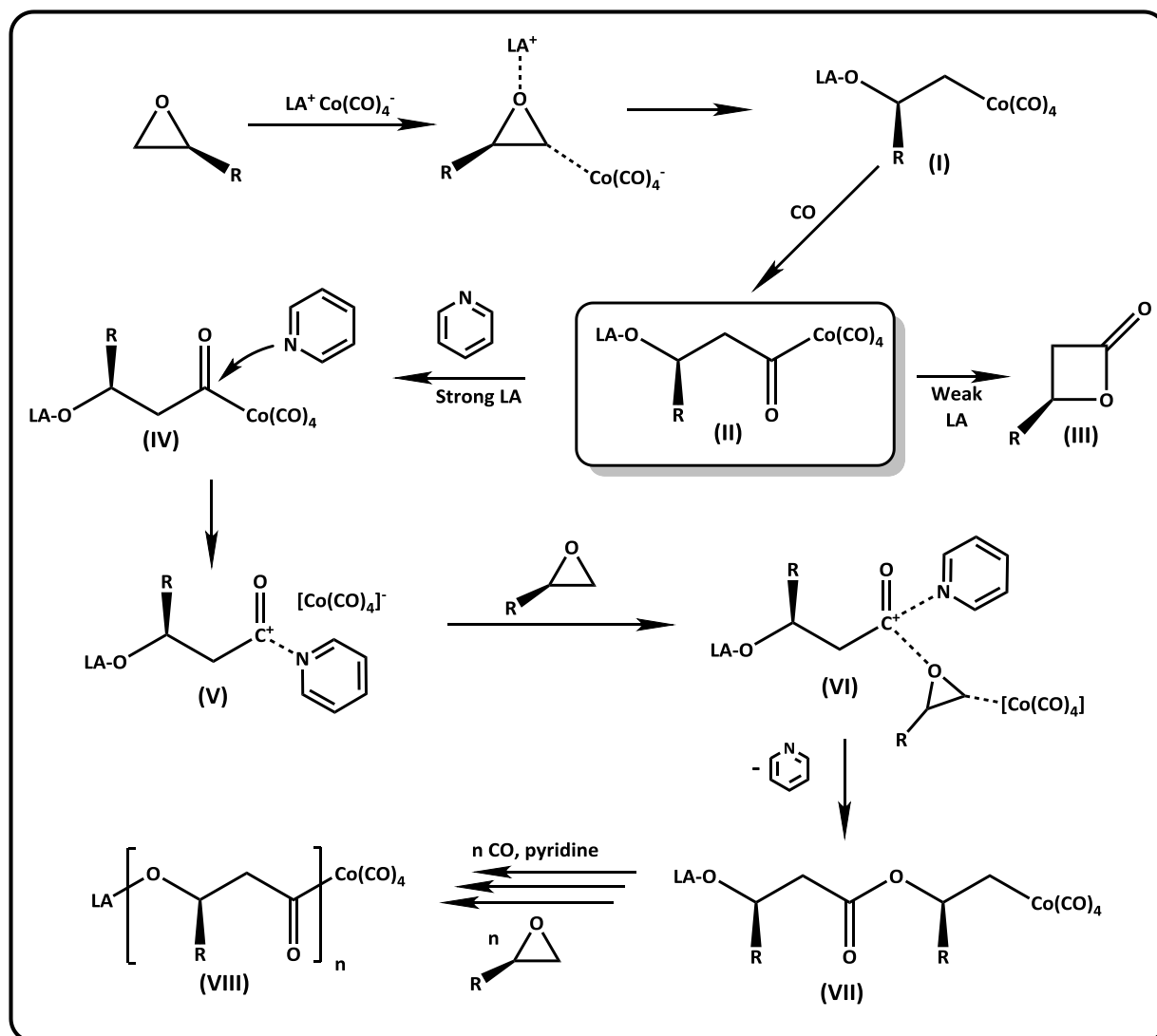
2.1.1 Direct copolymerization of epoxides with CO

2.1.1.1 Mechanism of epoxide/CO copolymerization

Although the formation of polyesters from epoxides and CO catalyzed by cobalt carbonyls was known since 1965,¹⁴ the first mechanistic studies on epoxide/CO copolymerization were performed quite recently (in 2002), when Rieger and co-workers used in situ FTIR spectroscopy for the monitoring of the reaction.¹⁵ It was clarified that the polymerization proceeds through the direct coupling of epoxides and CO rather than by the production and subsequent ring-opening polymerization of β -lactones.

The first step (Scheme 2.3) is the ring-opening of the epoxide assisted by a Lewis acid (LA) followed by the backside attack of $\text{Co}(\text{CO})_4^-$, which afford cobalt-alkyl species (I) (Scheme 2.3). Insertion of carbon monoxide (I \rightarrow II) leads to cobalt-acetyl intermediate (II). Depending on the strength of the Lewis acid, polymer or β -lactones can be produced. Labile Lewis acid-

oxygen interactions resulting from weak Lewis acids (e.g. $\text{BF}_3\cdot\text{OEt}_2$ and AlMe_3) allow the back-biting process and produce lactones (III). However, the use of stronger Lewis acid (e.g. Ph_3Si^+) in combination with pyridine cocatalyst affords a polymerization reaction. Addition of pyridine donor plays an important role in polyester formation. Pyridine attacks the carbonyl group (IV), which results in the formation of acylium cation and nucleophilic tetracarbonyl cobaltate (V). Acylium cation activates the epoxide for subsequent ring-opening via nucleophilic attack of $[\text{Co}(\text{CO})_4]^-$ (VI) and consecutive formation of new cobalt-alkyl σ -bond (VII). Subsequent iterative insertion of CO and epoxide leads to the formation of polyester (VIII).¹⁶

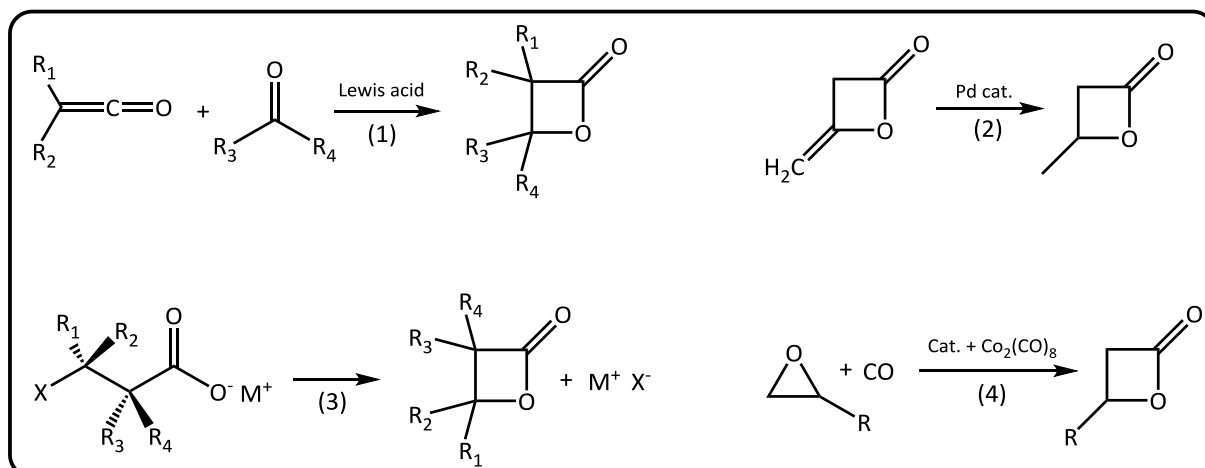


Scheme 2.3: Mechanism of direct epoxide/CO copolymerization proposed by Rieger et al.

2.1.1.2 Catalysts for direct epoxides/CO copolymerization

Coupling reactions of CO with epoxides were first reported in 1960's.¹⁷ Since then, considerable effort was devoted to the development of methods allowing activation and use of carbon monoxide as a feedstock for the synthesis of new materials. The combination of $\text{Co}(\text{acac})_3$ and AlEt_3 led to the polymer similar to poly(3-hydroxybutyrate) (PHB) prepared mostly by bacteria. In the following 30 years, various catalysts were reported to carbonylate epoxides to cyclic lactones,¹⁸ nevertheless no formation of polymer was reported until 1994,

alternative method of β -lactones production is metal catalyzed carbonylative expansion of epoxides (4) (Scheme 2.5).²⁷

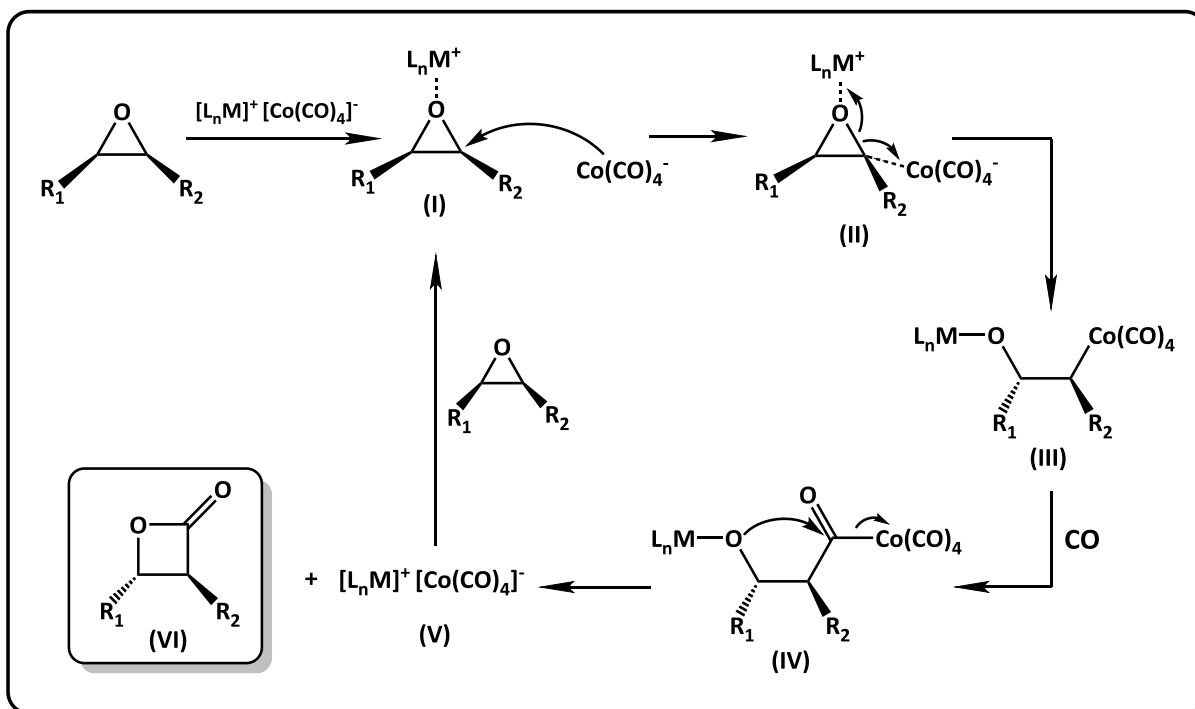


Scheme 2.5: Preparation methods to β -lactones

In the case of carbonylation of propylene oxide, β -butyrolactone (BBL) is obtained. Its polymerization leads to poly(3-hydroxybutyrate), a polymer, which is typically produced by bacteria.

2.1.2.1 Catalysts for carbonylative expansion of epoxides

The carbonylative expansion of epoxides to β -lactones is catalyzed by Lewis acid/cobalt-carbonyl catalysts and proceeds in 4 basic steps (Scheme 2.6). The first step is the activation of epoxide substrate with Lewis acidic cation (I). Then, $[Co(CO)_4]^-$ nucleophile attacks the less hindered epoxide C-O carbon (II) (S_N2 reaction), which lead to the formation of intermediate (III) with inversion of stereochemistry. 3rd step is the insertion of CO into the new cobalt-carbon bond of (III) resulting in intermediate (IV), which immediately undergoes the ring-closing via metal assisted back-biting leading to the formation of cyclic β -lactone (VI) and regeneration of the catalytic species (V).



Scheme 2.6: Mechanism of carbonylative expansion of epoxides to cyclic β -lactones

The first demonstration of epoxide ring-expansion was reported in 1963 by Heck using cobalt-carbonyl compounds to prepare β -hydroxyesters or γ -lactones.^{17c} Subsequently Nguyen and Pollock patented a method for the carbonylation of 1,2-epoxides to cyclic β -lactones using metal-carbonyl complexes of Co, Cr, Ni and Fe. The most active and selective complex was dicobaltoctacarbonyl.^{18a} Within the following 30 years new rhodium and palladium complexes were reported to carbonylate epoxides to cyclic lactones, nevertheless the conversion and selectivity were generally low.^{18b, c} Improvement of selectivity towards β -lactones production was described in the patent of Drent and Kragtwijk,¹⁹ who used 3-hydroxypyridine in combination with $\text{Co}_2(\text{CO})_8$.

Significant progress in the carbonylative expansion of epoxides was achieved after 2001 when few research groups reported new catalytic complexes with enhanced activity. Alper and co-workers reported that a mixture of neutral Lewis acid ($\text{BF}_3 \cdot \text{OEt}_2$) with bis(triphenylphosphine)iminium-tetracarbonylcobaltate, $([\text{PPN}]^+[\text{Co}(\text{CO})_4]^-)$ in combination with $\text{Co}_2(\text{CO})_8$ catalyzes the carbonylation of various epoxides to the corresponding β -lactones.²⁰ Although these catalysts required long reaction times (24-48 h) some lactones were obtained in good yields. It was also clarified that both, Lewis acid and nucleophilic cobalt-carbonyl complex have to be present in the reaction, otherwise the catalytic system is inactive. Coates et al. reported cyclopentadienyl titanium complex **1** (Figure 2.2) for the carbonylative ring-expansion of epoxides and substituted aziridines to corresponding β -lactones and β -lactams.²⁸

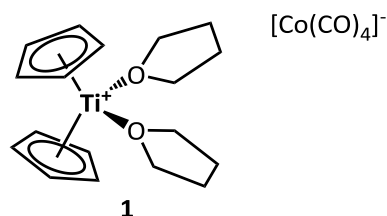


Figure 2.2: Cyclopentadienyl titanium complex for carbonylative expansion of epoxides

The same group reported a series of salen and porphyrin metal complexes (Figure 2.3), which selectively carbonylated epoxides to β -lactones at relatively mild conditions compared to the previous catalytic systems. Salphen-aluminium complex **2** carbonylated alkyl substituted epoxides and aziridines in very good yields (TOF = 83-99 h⁻¹).²⁹ (*R,R'*) chiral aluminium complex **3** produced slightly enantiomerically enriched 3,4-dimethyloxetan-2-one from *cis*- and *trans*-2,3-epoxybutane. (k_{rel} = 4.1 at 0°C, TOF \approx 4 h⁻¹).³⁰ Salphen chromium complex **4** was used for the carbonylation of various epoxides at mild condition (0.7 MPa, 22°C) to produce β -lactones with high selectivity (> 98%, TOF = 49 h⁻¹). The carbonylation of propylene oxide to BBL catalyzed by **4** was also achieved at mild conditions (1 bar CO, 22°C) with TOF = 8.2 h⁻¹.³¹ The same complex was used for the carbonylative expansion of fluorinated epoxides to corresponding β -lactones with similar activity (TOF \approx 8 h⁻¹).³² Chromium porphyrin complexes **5** and **6** were used for the carbonylation of substituted and bicyclic epoxides to the corresponding lactones.³³ Complex **6** exhibited significantly increased TOF (e.g. 580 h⁻¹ for 1,2-epoxybutane carbonylation^{33b}) compared to complex **5** (50 h⁻¹ for the same substrate^{33a}). In 2007, Coates et al. reported the double carbonylation of epoxides to anhydrides using new chloro-porphyrin aluminium complex **7**.³⁴ This double carbonylation proceeds through two different and non-overlapping steps: epoxide carbonylation to lactone and subsequent lactone carbonylation to anhydride.

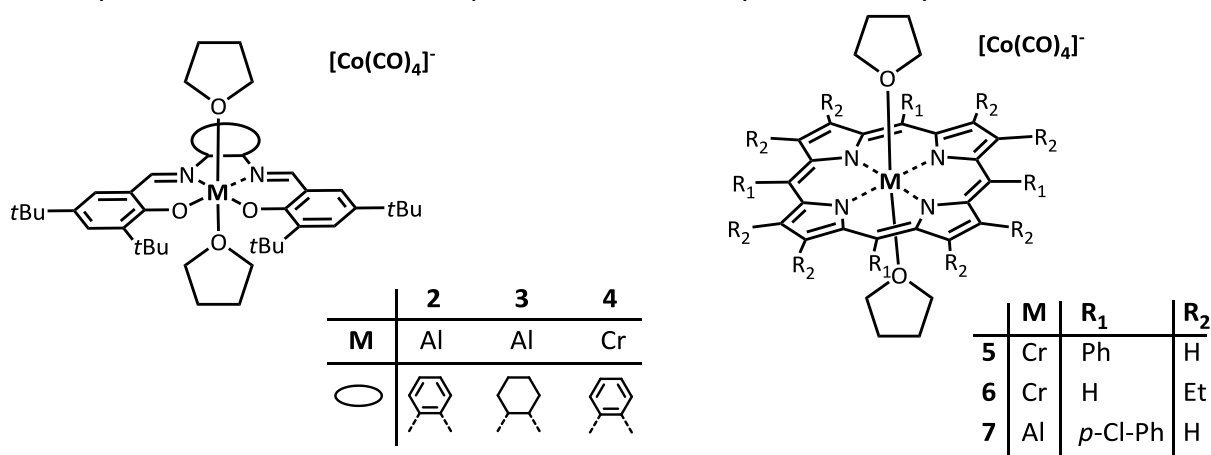


Figure 2.3: Salen and porphyrin complexes for carbonylative expansion of epoxides to lactones

Slightly enantioenriched BBL was prepared by the copolymerization of racemic propylene oxide with CO using new chiral indole-based Cr(III) catalysts (Figure 2.4).³⁵ A series of 12 complexes achieved enantiomeric excess (*ee*) 5-19 %, while the highest *ee* (19% of (*R*)-BBL) was reached with complexes **8a** and **8b** (TOF = 8 and 37 h⁻¹ respectively).

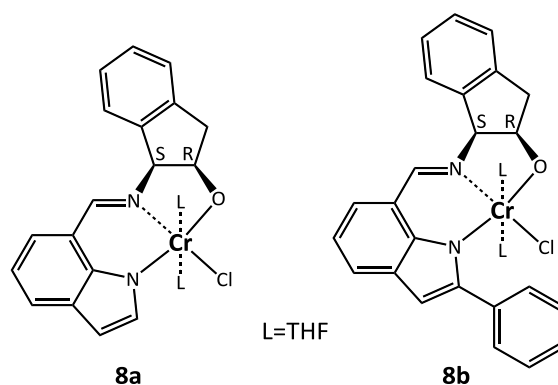


Figure 2.4: Chiral indole-based Cr(III) catalysts for carbonylation of epoxides to BBL

2.1.2.2 Ring-opening polymerization of β -butyrolactone

A second step of polyester production via multicatalytic approach is the ROP of in situ formed β -lactones. A variety of ROP processes, namely anionic, cationic, organocatalytic and coordination–insertion, can be used to transform cyclic lactones to polyesters.³⁶ The coordination–insertion process has gained the most interest for the ROP of cyclic esters since it allows the preparation of well-controlled polyesters in terms of molar mass, composition and microstructure.³⁷ A large number of catalysts for the ROP of six and seven-membered lactones (mostly lactide, glycolide³⁶ and ϵ -caprolactone³⁸) was reported but only very few of them were proven to be effective for the polymerization of four-membered ring β -lactones.

Early initiating systems for the ROP of β -butyrolactone, a four-member methyl-substituted cycle, were extremely slow and were not able to produce high molar mass PHB.³⁹ Nevertheless, in the last two decades, a few catalytic systems for the efficient polymerization of *rac*- β -butyrolactone have been reported (Figure 2.5). Moderately active distannoxane catalysts **9a,b** reported by Hori produced predominantly syndiotactic PHB with high M_n .⁴⁰ New β -diiminate zinc complexes **10a,b** prepared by Coates were highly active for β -butyrolactone polymerization at mild conditions.⁴¹ Obtained polyesters had high M_n up to 200 kg.mol⁻¹, but they were completely atactic.

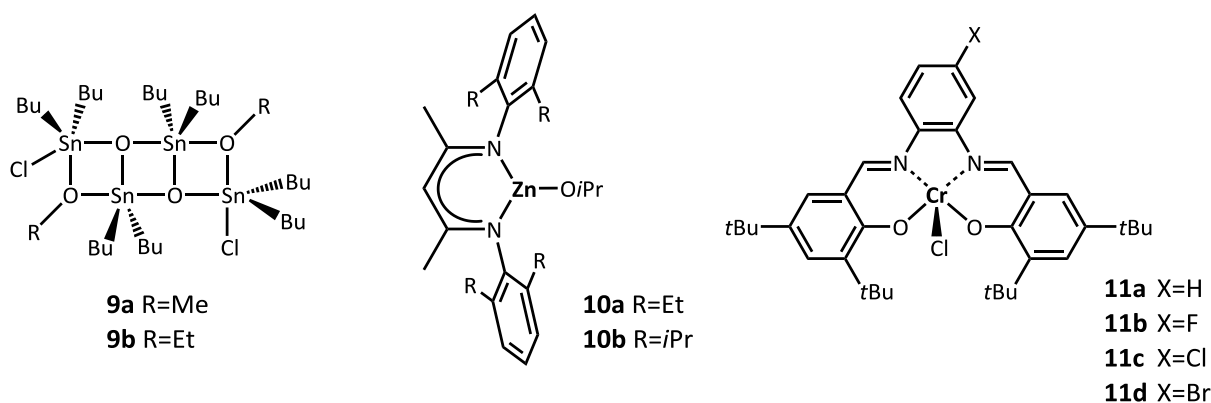


Figure 2.5: Catalysts for ROP of β -butyrolactone

Slightly isotactically enriched PHB was prepared by Rieger and co-workers, who reported a series of new symmetric and asymmetric chromium salphen complexes for BBL ROP (Figure 2.5).⁴² These achiral Cr(III) complexes (**11a-d**) afforded PHB with molar mass 33-98 kg.mol⁻¹ (\bar{D} = 5-8.5) and probability of *meso* dyad linkages (P_m) 0.60-0.67, the highest P_m value being achieved with complex **11d**. Moreover, similar monometallic and bimetallic bridged chromium complexes **12a-d** (Figure 2.6), were effective in the production of high molar mass PHB.⁴³ The highest M_n 57 kg.mol⁻¹ was achieved with bimetallic complex **12b** bridged with a short trimethylene linker.

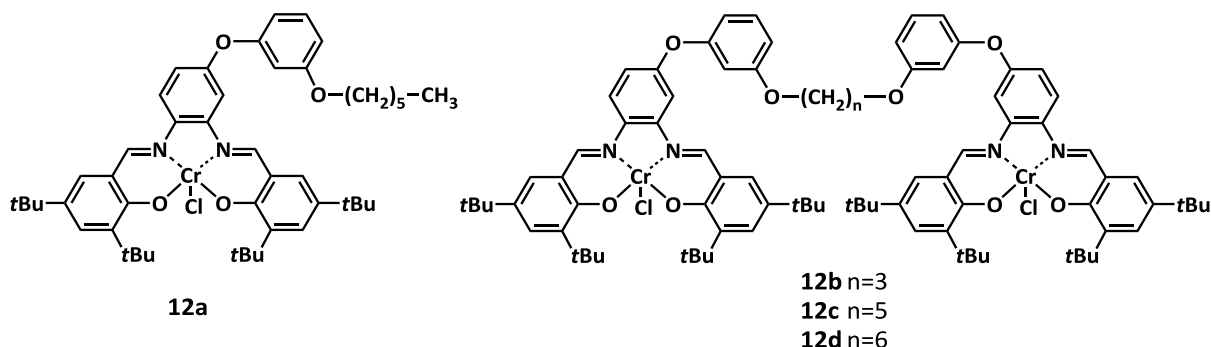


Figure 2.6: Conformationally flexible dimeric chromium salphen complexes

The highest activities and productivities under mild conditions as well as significant degree of control over the polymerization was achieved with group 3 and rare earth metal complexes (Figure 2.7).²⁴ One of the most effective catalysts, sterically crowded yttrium complexes **13a,b** and **14**, were reported by Carpentier. Highly syndiotactic PHB (*racemo* dyad linkage (P_r) in range of 0.81-0.94) was produced in controlled manner with M_n in range 20-65 kg.mol⁻¹ in high yields.⁴⁴ Yttrium complexes **15**⁴⁵ and **16**⁴⁶ also produced syndiotactic PHB (P_r 0.87 and 0.84, respectively) with $M_n \approx 15-30$ kg.mol⁻¹. On the contrary, a silica-supported neodymium borohydride complex **17**⁴⁷ afforded isotactic-enriched PHB with P_m value 0.80-0.85. Recently, an ethoxy-bridged dinuclear indium catalyst **18** was used for the ROP of BBL to form high molar mass PHB ($M_n = 315$ kg.mol⁻¹) with activity ≈ 230 h⁻¹ and remarkable control during the polymerization.⁴⁸

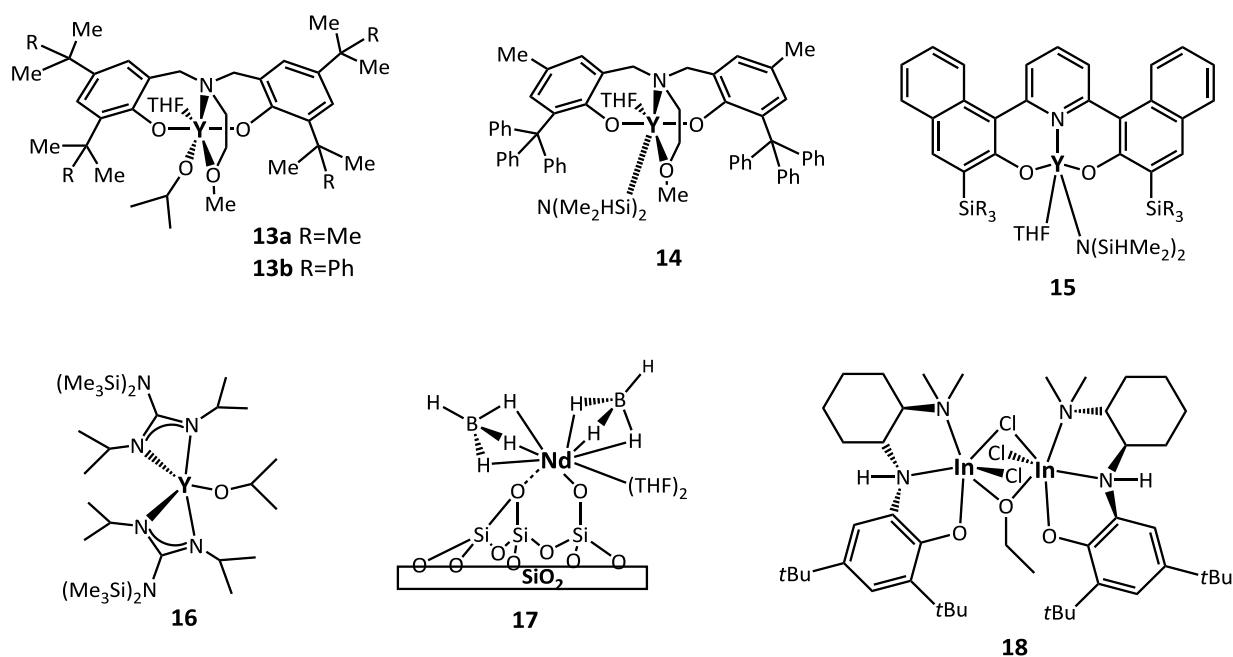


Figure 2.7: Rare earth metal catalysts for syndiospecific polymerization of β -butyrolactone

In the last three years, new yttrium complexes **19-21** (Figure 2.8) were synthesized and used for the syndiospecific ROP of β -butyrolactone.⁴⁹ Catalysts were able to polymerize BBL rapidly under mild conditions and produced *syndio*-enriched PHB ($P_r = 0.74-0.86$) with M_n between 20-30 kg.mol⁻¹ and narrow \mathcal{D} .

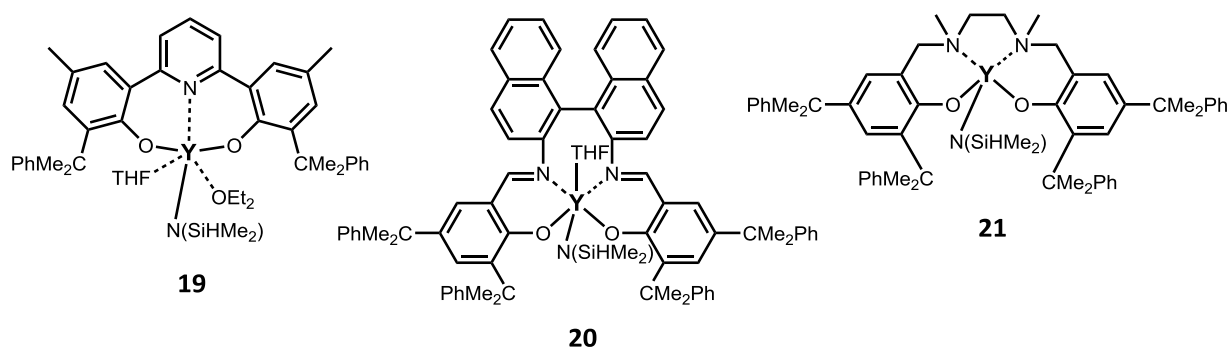


Figure 2.8: Newest yttrium complexes for syndiospecific β -butyrolactone polymerization

Since BBL is a toxic and carcinogenic compound, its direct ROP immediately after its synthesis is desirable. A multicatalytic approach for the tandem catalysis of PO carbonylation and following BBL ROP in a one-pot reaction was developed to solve this problem.¹³ The highest selectivity to PHB was achieved when Cr and Al porphyrin complexes **6** and **7** (catalysts for carbonylation of PO) (Figure 2.3, page 9) were combined with Zn β -diimine complexes **10b** (Figure 2.5, page 10) and **22a,b** (catalysts for the ROP of BBL) (Figure 2.9).

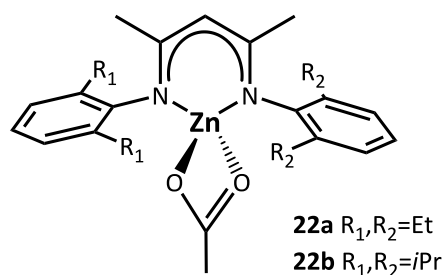
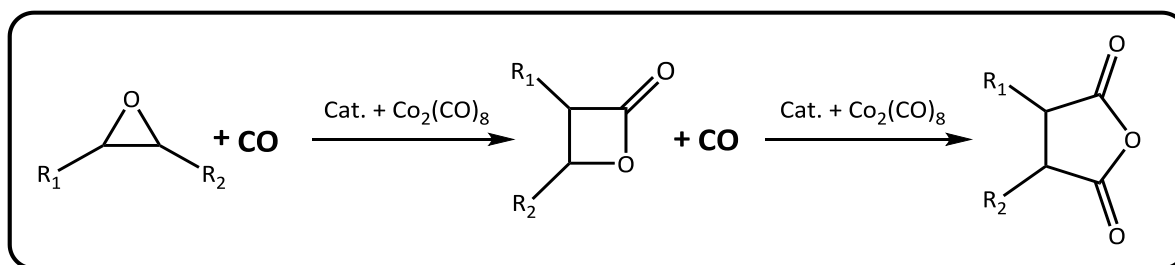


Figure 2.9: β -diiminato (BDI) zinc catalysts for ROP of in-situ formed BBL

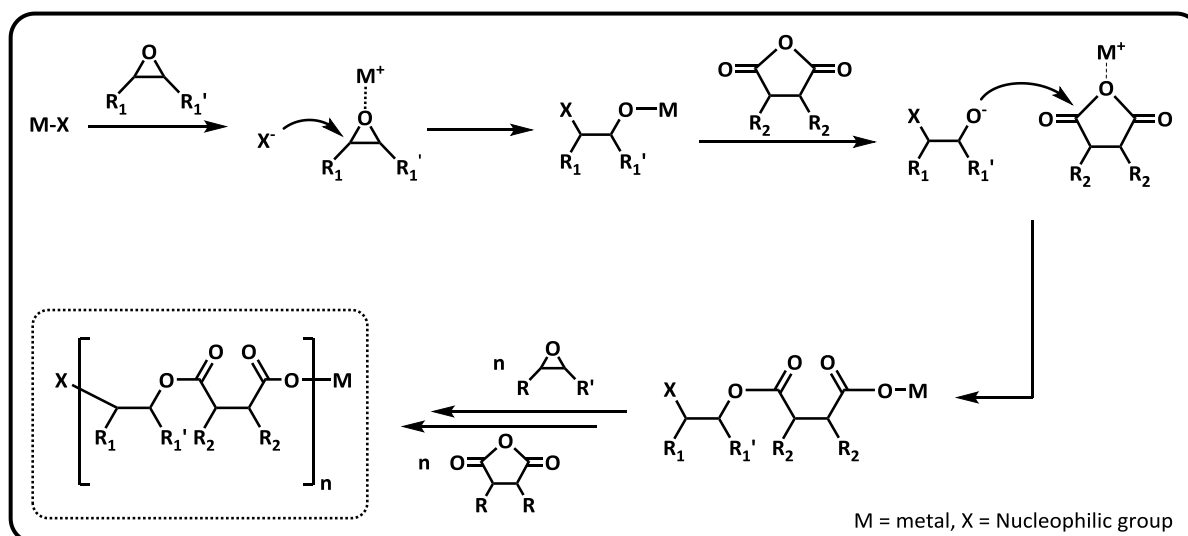
2.1.3 Polyesters by ring-opening copolymerization of epoxides with anhydrides

The ring-opening copolymerization (ROCOP) of epoxides with anhydrides can be considered as a sister polymerization method to the ROP of cyclic lactones. Considering lactones (and particularly BBL) as products of epoxide monocarbonylation (see chapter 2.1.2.1, page 7), anhydrides can be prepared by a double carbonylation of epoxides (Scheme 2.7).³⁴



Scheme 2.7: Double carbonylation of epoxides to anhydrides

Compared to the ROP of lactones, the copolymerization of epoxides with anhydrides (Scheme 2.8) allows controlled synthesis of polyesters with wide range of thermal and mechanical properties, which can be easily manipulated by the simple substitution of epoxide or anhydride comonomers.⁵⁰ Moreover, wide range of potential substrates (epoxides and anhydrides) can be copolymerized using similar conditions and catalysts.



Scheme 2.8: General scheme of metal catalyzed ROCOP of epoxides and anhydrides

Alternating copolymerization of epoxides and anhydrides was first reported in 1960 using tertiary amines as catalysts.⁵¹ In the following 20 years, various organometallic initiators (ZnEt₂, R₃Al, RZnEt₂ etc.) were reported for the ROCOP of epoxides and anhydrides.⁵² Significant progress was achieved with the development of well-defined metal catalysts with ancillary ligands.

Porphyrin aluminium complexes **23a,b** (Figure 2.10) in combination with quaternary ammonium/phosphonium salts produced perfectly alternating copolymer of propylene oxide, cyclohexene oxide (CHO), styrene oxide (SO) and but-1-ene oxide with phthalic anhydride (PA) (TOF = 5 h⁻¹).⁵³ Analogous chromium complex **24**/4-dimethylaminopyridine (DMAP) produced polyesters by the copolymerization of CHO or SO with PA, succinic anhydride (SA) or cyclopropane anhydride (CPrA) with significantly higher TOF 95h⁻¹ and molar masses 1-20 kg.mol⁻¹.⁵⁴ The substitution of Cr metal by Co and Mn metals in complex **24** led to the decrease of the activity (TOF ≤ 43 h⁻¹). A range of Al(III), Cr(III) and Co(III) porphyrin complexes **23a** and **24-28** (Figure 2.10) was also tested for the copolymerizations of various anhydride substrates such as PA, SA, maleic anhydride (MA) and methyl-succinic anhydride with PO.⁵⁵ Among these complexes, the most effective catalyst proved to be tetraphenylporphyrin chromium complex **24**.

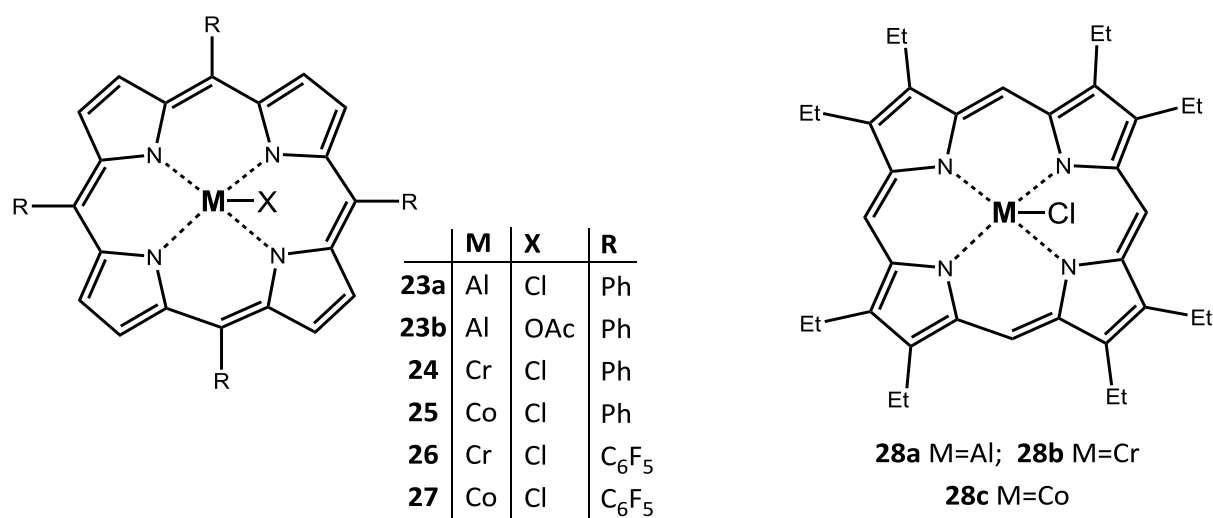


Figure 2.10: Metal-porphyrin complexes for copolymerization of epoxides with anhydrides

Another significant breakthrough in the ROCOP of epoxides and anhydrides was achieved by Coates and co-workers, who tested a series of β -diiminate (BDI) zinc complexes **29a-c** (Figure 2.11), which are well-known as effective catalysts for the ROP of cyclic esters (see chapter 2.1.2.2, page 10) and for the copolymerization of epoxides with CO₂ (see chapter 2.2.2.2, page 23). The highest activities for the copolymerization of epoxides (vinylcyclohexene oxide, limonene oxide (LO), *cis*-2-butene oxide, isobutene oxide and PO) with diglycolic anhydride were achieved with complex **29b**.⁵⁶ This complex further afforded perfectly alternating polyesters with high molar masses ($M_n \leq 55$ kg.mol⁻¹)

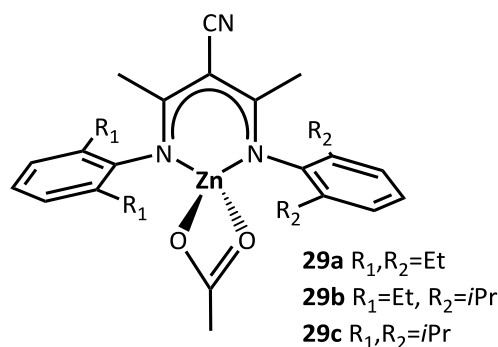


Figure 2.11: β -diiminate (BDI) zinc complexes for ROCOP of epoxides and anhydrides

Metal salen and salan complexes proved to be also effective for epoxide/anhydride copolymerization. Complex **31b** (Figure 2.12) was effectively used for the ROCOP of MA with variety of epoxides (PO, BO, epichlorohydrin, allyl glycidyl ether, phenyl glycidyl ether etc.) producing highly alternating polyesters with M_n 21-33 $\text{kg}\cdot\text{mol}^{-1}$.⁵⁷ Duchateau et al. prepared a series of Al, Cr and Co salen and salphen complexes **30-32** (Figure 2.12).^{54a,58} Using these complexes in combination with DMAP for the copolymerization of CHO with SA, PA and CPRa afforded alternating polyesters with molar masses 2-15 $\text{kg}\cdot\text{mol}^{-1}$. The best activity was achieved with chromium complexes **31a** and **31b** ($\text{TOF} \approx 150 \text{ h}^{-1}$), while the highest molar masses (15 $\text{kg}\cdot\text{mol}^{-1}$) were obtained for the copolymerization of CHO with PA. The same research group investigated LO/PA copolymerization, which yielded partially renewable polyesters with $M_n = 4\text{-}7 \text{ kg}\cdot\text{mol}^{-1}$.⁵⁹ The best performance was achieved with salphen Al(III) and Cr(III) complexes **30a** and **31a**.

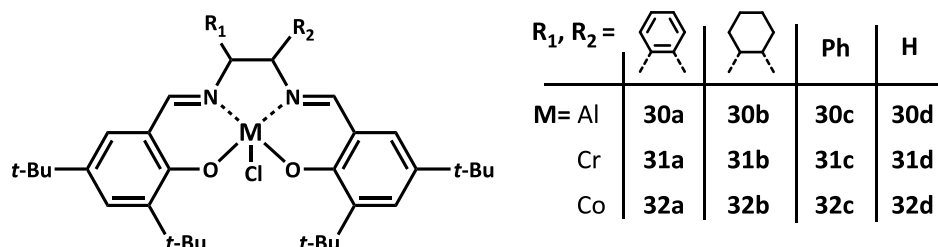


Figure 2.12: Series of salen complexes for copolymerization of epoxides with anhydrides

In the last years, a significant attention is paid to the bimetallic complexes since they often showed higher activities compared to their monometallic analogues, especially in the parallel field of epoxides/ CO_2 copolymerization (see chapter 2.2.2.7, page 39). Indeed, the copolymerization of epichlorohydrin with MA using bimetallic Cr(III) salan complex **33** (Figure 2.13) afforded alternating polyester of molar mass 32 $\text{kg}\cdot\text{mol}^{-1}$ with $\text{TOF} = 7.8 \text{ h}^{-1}$, while its monometallic analogue produced polyester with $M_n = 5 \text{ kg}\cdot\text{mol}^{-1}$ and $\text{TOF} = 0.9 \text{ h}^{-1}$ only.⁶⁰ Trinuclear zinc complex **34** in combination with DMAP reported in 2014, showed activity $\approx 116 \text{ h}^{-1}$ for the CHO/MA copolymerization.⁶¹ Another group reported new salen dizinc complex **35**/DMAP for the copolymerization of CHO and MA ($\text{TOF} = 130 \text{ h}^{-1}$).⁶²

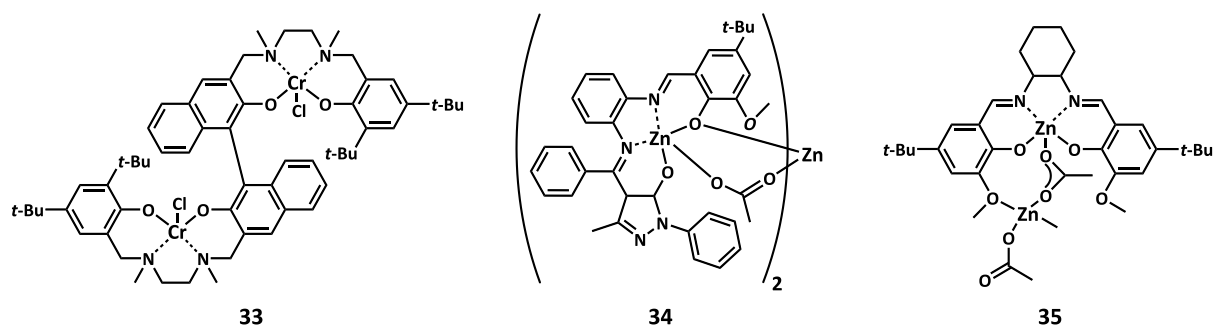


Figure 2.13: Bi- and tri-metallic salan and salen complexes for copolymerization of epoxides with anhydrides

Other dinuclear complexes, dizinc and dimagnesium homogeneous catalysts **36a,b** (Figure 2.14), produced CHO-PA copolymers with molar masses $2\text{-}21 \text{ kg}\cdot\text{mol}^{-1}$. These complexes exhibited activity up to 97 h^{-1} .⁶³

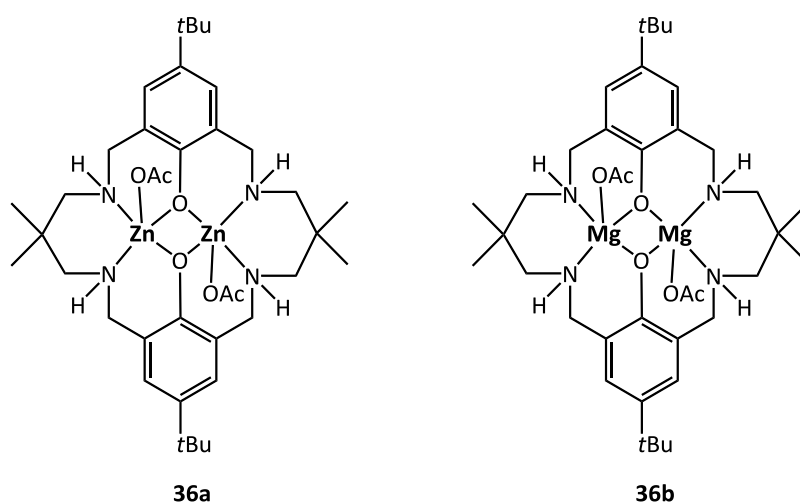


Figure 2.14: Di-magnesium and zinc catalysts for ROCOP of PA with CHO

Nozaki and co-workers have reported monometallic and bimetallic metal-corrole complexes **37a-d** (Figure 2.15) for the copolymerization of epoxides (PO, CHO, SO) with anhydrides (MA, SA and glutaric anhydride).⁶⁴ Manganese and iron corrole complexes in combination with $\text{PPN}^+\text{-OBzF}_5^-$ cocatalyst copolymerized aforementioned comonomers with $\text{TOF} \approx 3 \text{ h}^{-1}$, while the highest molar mass ($M_n = 8.0 \text{ kg}\cdot\text{mol}^{-1}$) was achieved with complex **37c**.

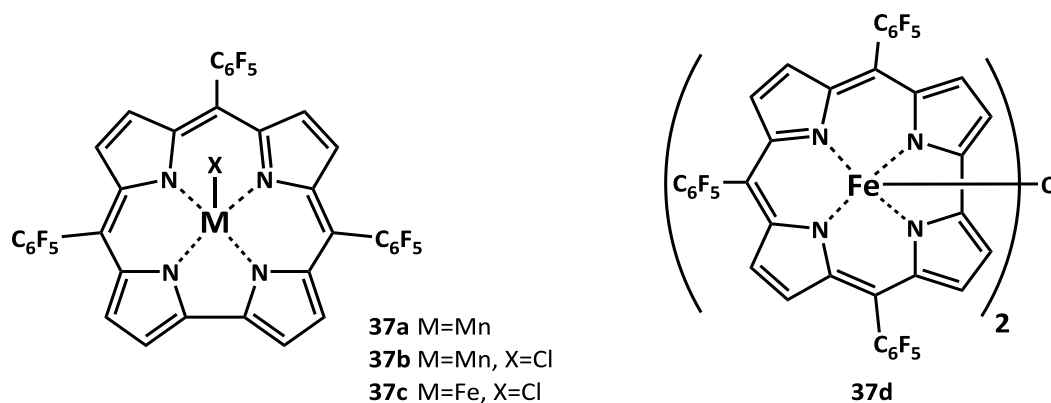
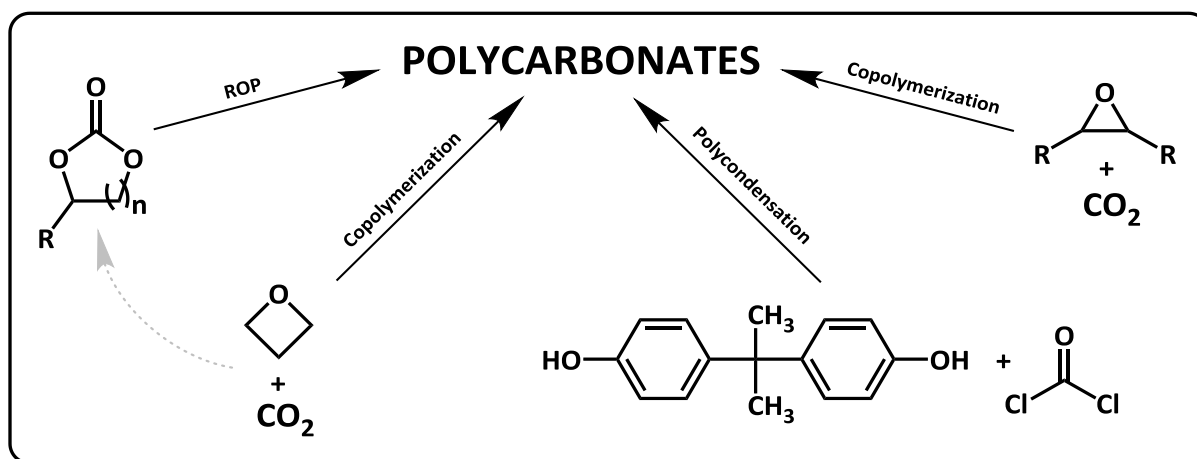


Figure 2.15: Metal corrole complexes for copolymerization of epoxides with anhydrides

2.2 Polycarbonates by epoxide/CO₂ copolymerization

Besides the polycondensation, polycarbonates can be prepared by the ROP of cyclic carbonates (e.g. trimethylene carbonate)⁶⁵ or by the alternating copolymerization of CO₂ with epoxides or oxetanes (Scheme 2.9). The area of application is related to their structure. Aromatic polycarbonates based on Bisphenol A are used mostly in automotive, electronics, building & construction and optics.⁶⁶ On the contrary, aliphatic polycarbonates found usage in biomedical and pharmaceutical applications.⁶⁷



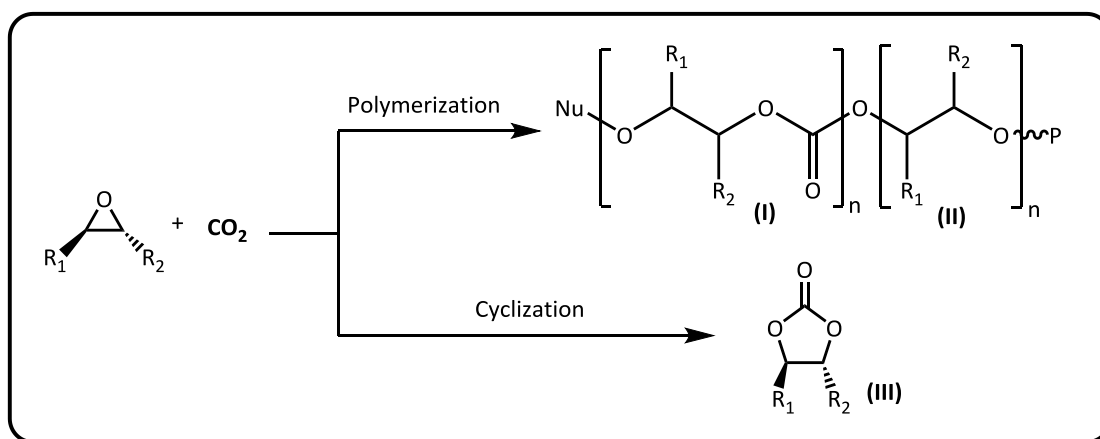
Scheme 2.9: Synthetic routes to polycarbonates

Desirable properties of aliphatic polycarbonates, susceptibility towards biotic or abiotic degradation, biocompatibility and tunable mechanical properties predestinate these materials to replace a part of synthetic polymers for disposable products. However, its average thermal stability, low temperature of thermal deformation and relatively high price compared to the large-ton scale produced polymers are the major limitations impeding their broader industrial application.

The development of highly active catalysts for CO₂/epoxide copolymerization is a key for economical routes of polycarbonate production from CO₂ as a non-traditional feedstock.

2.2.1 Mechanism of epoxide/CO₂ copolymerization

A large number of catalytic systems able to catalyze the coupling of epoxide and CO₂ have been reported in the last decades. Depending on the catalytic system and experimental conditions the reaction of epoxides with CO₂ can generate two main types of products: polycarbonates **(I)** or cyclic carbonates **(III)** (Scheme 2.10). During the copolymerization, a consecutive insertion of two epoxides in the polymer chain can occur instead of the alternating copolymerization of epoxide and CO₂. This lead to the presence of ether linkage in polycarbonate **(II)**.⁶⁸



Scheme 2.10: Products of epoxide/CO₂ copolymerization

Catalysts for epoxide/CO₂ copolymerization generally contain a specific Lewis acidic metal active center (M), which is coordinated to the ligand framework (L_n), and attached nucleophilic group (X). Catalysts (L_nMX) can be easily tailored by modifying either the ligand framework (L_n), metal center (M) or the initiating group (X).⁶⁹ The crucial role in catalyst activity during the copolymerization plays the strength of binding between metal-alkoxide and metal-carbonate intermediates (structures **V** and **VII** in Scheme 2.11). A too strong metal–oxygen bond makes the intermediate inactive towards another insertion of epoxide or CO₂ and thus prohibits the formation of the both cyclic carbonate and polycarbonate. On the contrary, a too weak metal-oxygen bond can result in the displacement of alkoxy/carbonate intermediate by another nucleophile, which leads to the decrease of activity and also favoring the back-biting reaction (as will be discussed later) resulting in increased cyclic carbonate formation. Therefore, the intermediate bond strength (Lewis acidity of metal center) is needed for a good catalytic performance.⁷⁰ Beside the Lewis acidity of the active center, which can be modified by switching the central metal or by the modification of ligand electronic effects, the steric effects of ligand also play an important role. Too bulky substituents usually hinder access of comonomers to the active center, which result in lower activity of the catalytic system.

The copolymerization of epoxide with CO₂ is realized via coordination-insertion mechanism. The first step – initiation can be realized via three different mechanisms: a monometallic, binary or bimetallic, which are dependent on the type of catalyst and its concentration (Scheme 2.11).

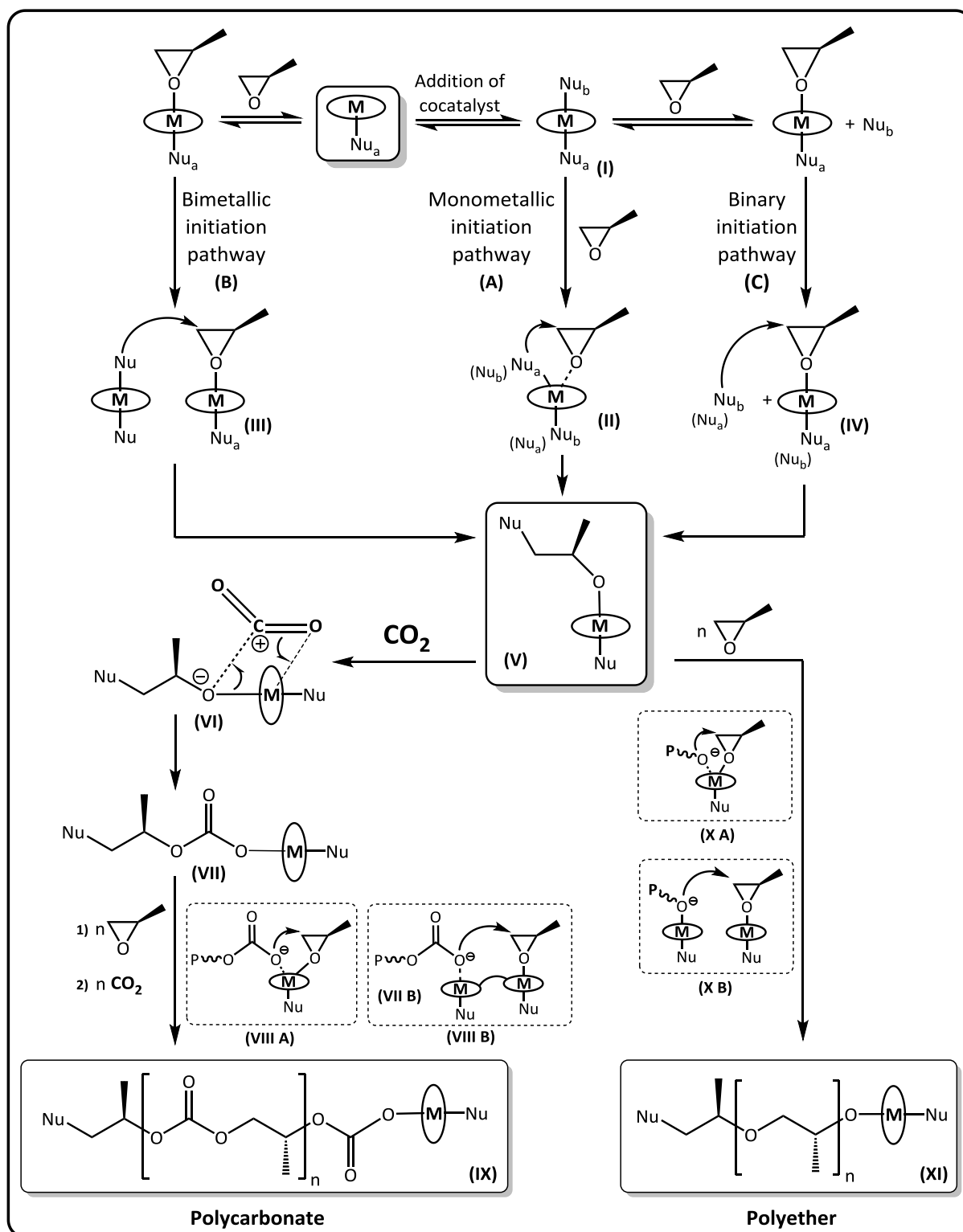
A monometallic mechanism (A) (Scheme 2.11) considers that only one metal is involved in the initiation step.⁷¹ Firstly, an addition of cocatalyst leads to the coordination of second nucleophile (Nu_b) to the metal center resulting in the formation of six-coordinated (for tetradentate ligand) structure (**I**). Coordinated second nucleophile destabilizes the original metal-nucleophile bond (Nu_a), favoring the coordination of epoxide to the Lewis-acidic metal center (**II**). Subsequent intramolecular attack of nucleophile to the less hindered C-O bond of the epoxide leads to epoxide opening and to the formation of a metal-alkoxide bond (**V**). The metal alkoxide acts as a nucleophile, which promotes CO₂ insertion into the metal alkoxide

bond (VI) generating metal-carbonate species (VII). Carbonate intermediates can undergo the cyclization reaction to form cyclic carbonates, (Scheme 2.12) or propagate by further addition of epoxide (VIII A) and CO₂ to form polycarbonates (IX).

A bimetallic mechanism (B) (Scheme 2.11) involves two separate metal complexes in the initiation step. It is similar to the monometallic mechanism with a difference that the nucleophile attacks the epoxide, which is coordinated to second metal center (III). The bimetallic mechanism occurs preferentially in the absence of cocatalyst or at low epoxide/catalyst loadings. It was also suggested that this pathway is preferred when a weaker Lewis base is used as a cocatalyst, while the monometallic mechanism takes place in the presence of stronger Lewis base, which is able to weaken the metal-nucleophile bond and simultaneously allows the opening of the epoxide.⁷² Subsequent insertion of CO₂ to the metal alkoxide bond (VI) followed by the insertion of another epoxide to the metal-carbonate bond (VII) proceeds in the same way as it was described for the monometallic (VIII A) mechanism. The bimetallic mechanism of propagation (VIII B) was assigned to dinuclear complexes where two adjacent metal centers can cooperate.⁷³ In some cases, complexes containing two adjacent metals connected with alkoxy or aryloxy groups can react first with CO₂ in the initiation step. The reaction continues with the coordination of epoxide followed by the ring-opening and insertion into metal-carbonyl bond. This mechanism was proposed for β-diiminate zinc complexes (Figure 2.18, page 24).⁷⁴

A binary mechanism (C) (Scheme 2.11) was proposed for binary catalyst/cocatalyst systems, where free nucleophilic cocatalyst (Nu_b) attacks the epoxide pre-coordinated to the metal center (IV). Added cocatalyst can also displace originally coordinated Nu_a, which can also attack the epoxide. The addition of such cocatalyst can significantly improve the activity and selectivity at low CO₂ pressures and/or elevated temperatures.⁷⁵ The best binary catalytic system was found to consist of a bulky chiral salenCo(III)X complex with an axial X group of poor leaving ability and a bulky ionic ammonium salt (bulky cation and nucleophilic anion with poor leaving ability) or a sterically hindered strong organic base with low coordination ability.⁷⁶

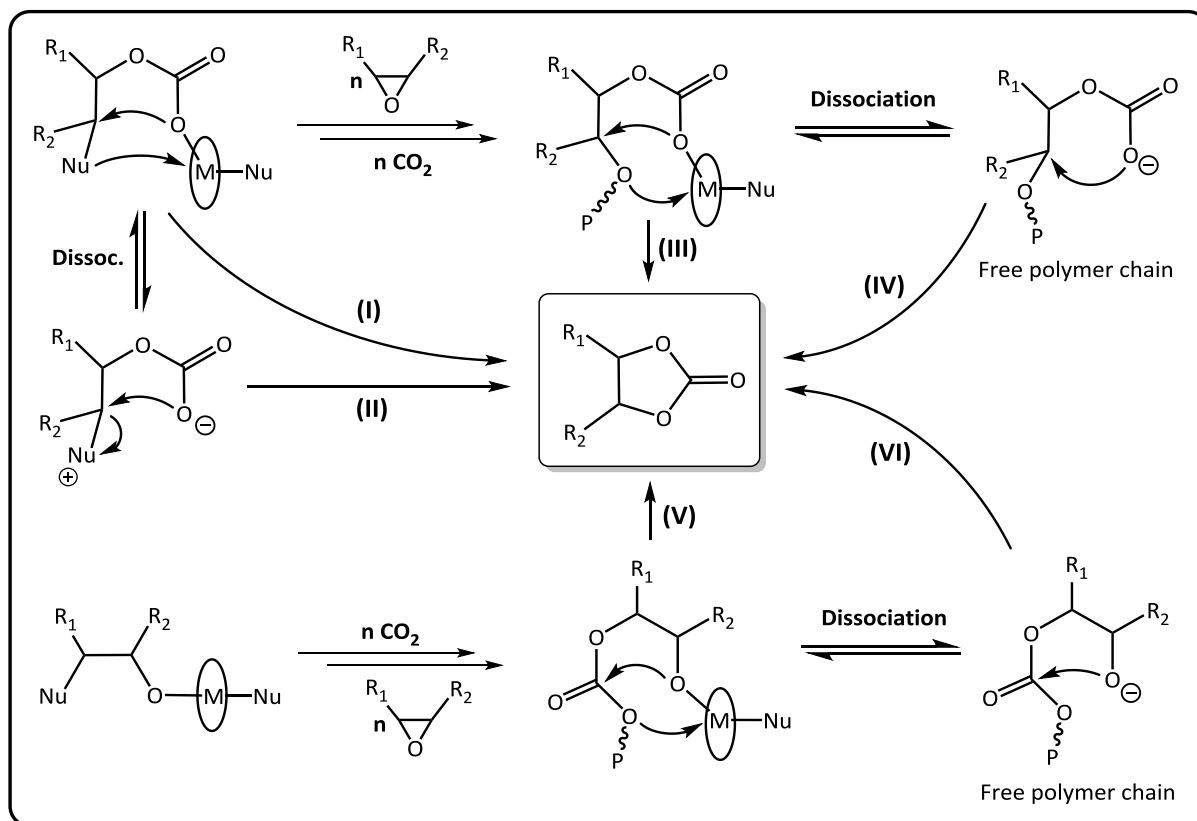
In some cases, the consecutive epoxide insertion (X) can occur within a polymerization process (Scheme 2.11). This leads to the presence of ether groups in polycarbonate chain or at specific case to the formation of polyether (XI). Consecutive epoxide insertion can be eliminated by the right choice of catalytic system, temperature, CO₂ pressure and epoxide concentration.⁷⁷



Scheme 2.11: General initiation and propagation mechanisms for epoxide/CO₂ copolymerization

A concurrent reaction to the copolymerization is the formation of cyclic carbonate by-product. Cyclic carbonate formation is observed with various epoxides and generally they are formed at higher temperatures. Cyclic carbonates are thermodynamically more stable than corresponding polycarbonates. They can be formed by an intramolecular cyclic elimination (back-biting) by two concurrent back-bite mechanisms (Scheme 2.12). One is assisted by the central metal (paths I, III, V in Scheme 2.12) and the other involves the back-

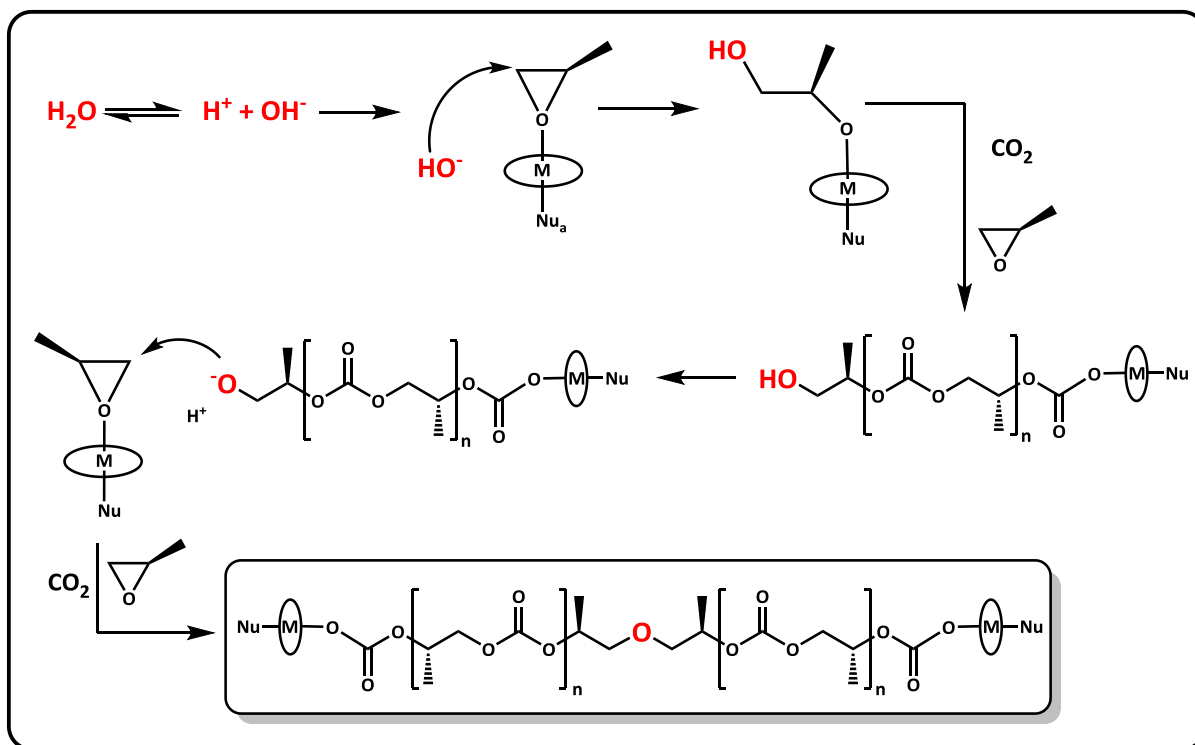
biting by dissociated linear carbonate anion (path II) or by growing polymer chain in which both carbonate and alkoxide anion can induce the cyclization reaction (paths IV and VI). The latter process has a lower activation barrier and thus it is enhanced upon increasing the reaction temperature and/or by the addition of an excess of nucleophilic cocatalyst, which facilitates a dissociation of growing polymer chain from the metal center.^{76b,78} The ratio of polymer/cyclic product can be further affected by the catalyst (electrophilicity of central metal), additives, CO₂ pressure and epoxide concentration.



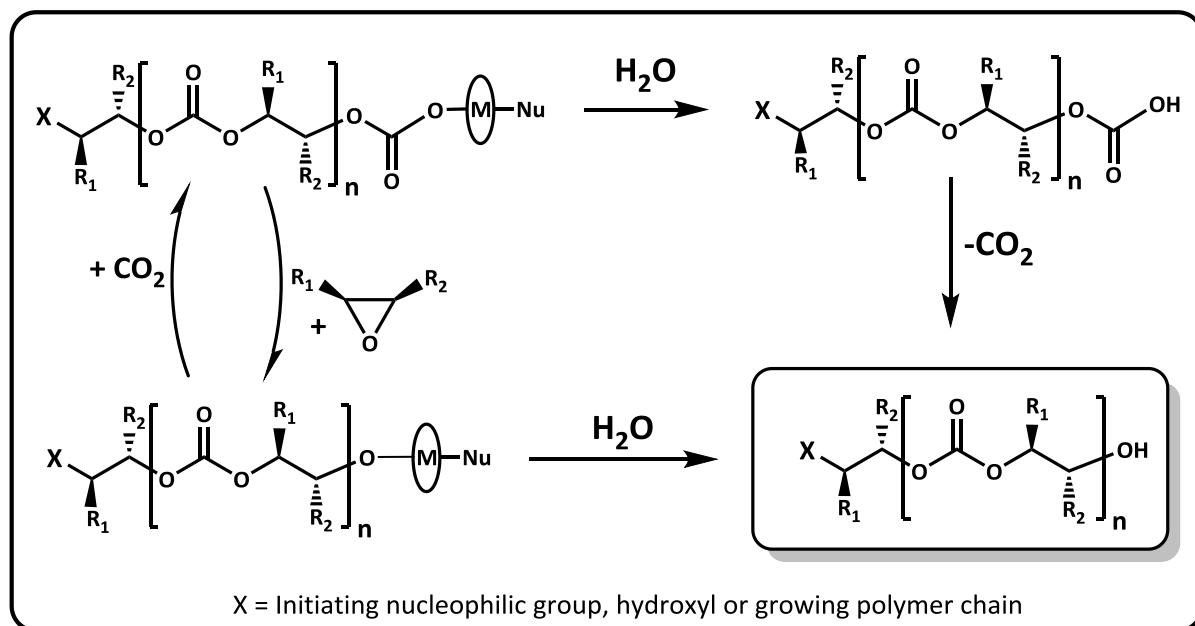
Scheme 2.12: Formation of cyclic carbonates via back-biting mechanism

Contaminant water plays an important role during the copolymerization. It can act either as a bifunctional initiator (Scheme 2.13)⁷⁹ or chain transfer agent (Scheme 2.14).⁸⁰ Dissociated hydroxyl anion (or alkoxy anion, when diol instead water is present) can activate the epoxide through nucleophilic -OH⁻ (-OR⁻) groups. Terminal hydroxyl (alcohol) group can again dissociate to form new alkoxy anion, which can propagate in the same manner to form polycarbonate with two growing polymer chains. This is often indicated by bimodal distribution of polycarbonates.⁷⁹

Water present in the reaction mixture also acts as the chain-transfer agent (Scheme 2.14). The reaction of active chain-ends with water can generate hydroxyl or carboxyl chain ends. Carboxyl groups are rather unstable and tend to convert into alcoholic terminal groups with liberation of a CO₂ molecule. Hydroxyl-terminal groups of such polycarbonates can easily dissociate upon heating and thus formed alkoxy group, which can further induce depolymerization via the back-biting mechanism as mentioned above.⁸⁰



Scheme 2.13: Bifunctional initiation by contaminant water



Scheme 2.14: Chain transfer reaction by contaminant water during the copolymerization

2.2.2 Catalysts for copolymerization of commercial epoxides with CO₂

2.2.2.1 Early catalysts for CO₂/epoxides copolymerization

The first alternating copolymerization of epoxides with carbon dioxide was realized in 1969 by Inoue, who observed a slow formation of poly(propylene carbonate) (PPC) in the presence of heterogenous catalyst ZnEt₂/H₂O (1:1).⁸¹ Subsequently, Inoue et al. reported various catalytic systems based on ZnEt₂ in combination with dihydric compounds (resorcinol, dicarboxylic acids and primary amines), which were only capable to generate catalytically active species suggesting dinuclear structures of these catalysts.⁸² Few years later Kuran and co-workers developed a catalytic system based on ZnEt₂ in combination with trihydric phenols - pyrogallol and 4-bromopyrogallol.⁸³ Because of the very low activity of these catalysts (TOF = 0.1-0.45 h⁻¹), Hatori tried to synthesize more effective catalytic system based on heterogeneous Zn(OH)₂ and glutaric acid. Subsequent copolymerization of PO with CO₂ at 30°C and 6 MPa produced PPC with TOF = 1.1 h⁻¹ and M_n = 12 kg.mol⁻¹.⁸⁴

Simple zinc-phenoxides complexes were discovered to catalyze the copolymerization of epoxides with CO₂. The first discrete zinc catalysts **38** (Figure 2.16) originated from phenolic derivatives and Zn[N(SiMe₃)₂]₂.⁸⁵ Complex **38a** and optimized complex **38b** afforded PCHC with ≈ 90% of carbonate unit and molar mass 38 kg.mol⁻¹ with TOF = 2.4 h⁻¹ and 9.6 h⁻¹, respectively. Although following derivatives of zinc phenoxide complexes (e.g. **39** and **40**) afforded PCHC with 100% of carbonate linkage, no further improvement of catalytic performance was achieved.⁸⁶

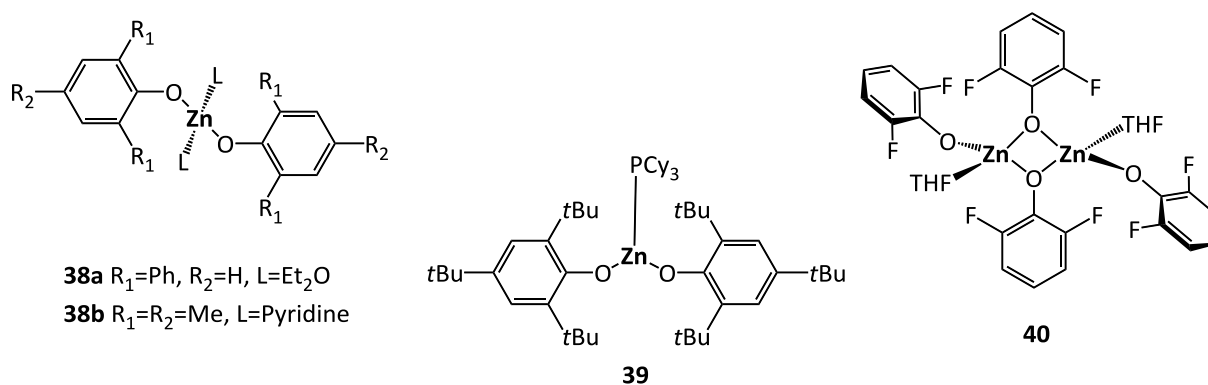


Figure 2.16: Early discrete zinc-phenoxide complexes

2.2.2.2 Single site dinuclear β-diiminate complexes

The first catalysts, which copolymerized epoxides and CO₂ at low pressure and ambient temperatures with remarkably high activities were β-diiminate (BDI) zinc complexes.

A quinoxaline zinc alkoxide complex **41** (Figure 2.17) - an ancestor of BDI catalysts, was reported in 2002. This complex displayed very poor catalytic performance (5 h⁻¹) in CHO/CO₂ copolymerization.⁸⁷

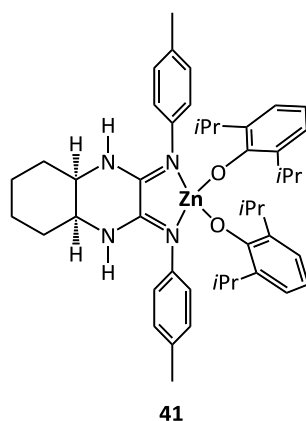


Figure 2.17: Diimine quinoxaline-derived zinc alkoxide complex for CHO/CO₂ copolymerization

Compared to complex **41**, new bulky BDI zinc catalysts **42** and **43** (Figure 2.18) synthesized by Coates afforded PCHC in controlled manner with very high activities. A detailed dynamic solution study revealed that synthesized complexes can exist in 3 forms - a monomeric and tightly bounded dimeric form, which are inactive for the copolymerization, and highly active poorly tight dimeric form.⁷⁴ The equilibrium of these 3 forms is influenced by the temperature, concentration and by steric effects of substituents. It was observed that bulkiness as well as electronic effects of R₁-R₃ substituents play the crucial role in the rate of polymerization. For example, sterically unencumbered complex **42a** is inactive in CHO/CO₂ copolymerization. On the contrary, catalysts with bulkier ethyl and isopropyl substituents **42b,c** showed TOFs of 431 h⁻¹ and 360 h⁻¹ respectively. The highest activities were achieved with unsymmetrical complex **42d** (729 h⁻¹) and with complex **42e** (917 h⁻¹) containing an electron-withdrawing cyano substituent in R₃ position. All active complexes produced PCHC with $M_n = 16\text{-}25 \text{ kg}\cdot\text{mol}^{-1}$ with very narrow dispersity ($\mathcal{D} < 1.15$).

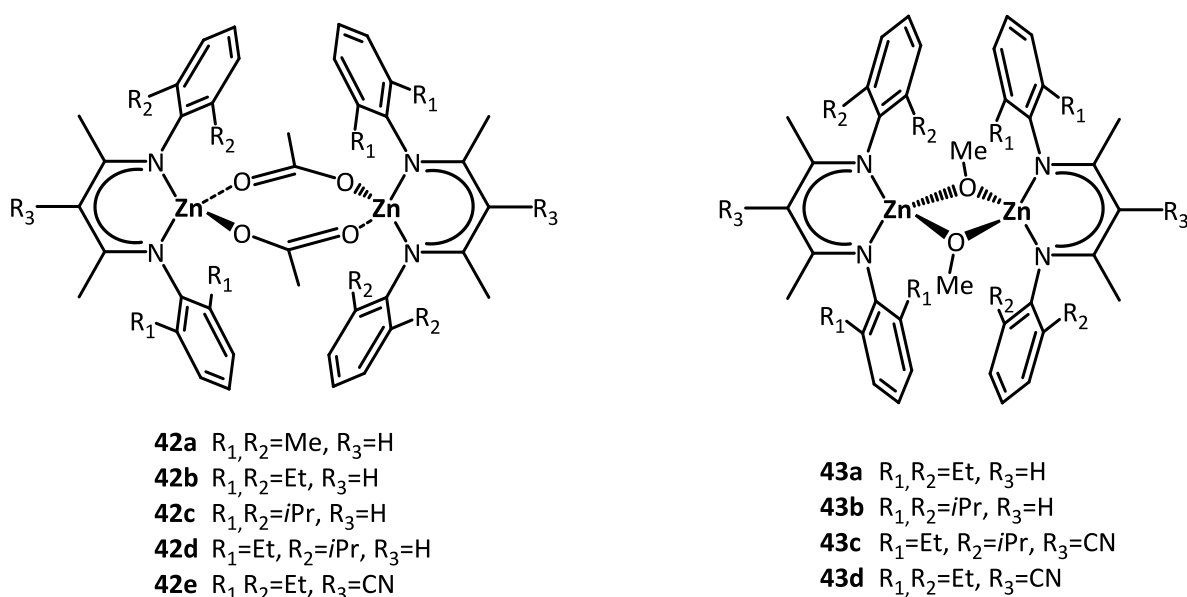


Figure 2.18: β -diimine (BDI) zinc catalysts for epoxide-CO₂ copolymerization

Similar alkoxy-zinc complexes **43a,b** (Figure 2.18) reported by the same group were also effective for CHO/CO₂ copolymerization providing PCHC with TOFs ranging from 239 h⁻¹

(**43a**) to 224 h^{-1} (**43b**).⁸⁸ An outstanding increase in the polymerization activity was observed with complexes **43c** and **43d**, where α -hydrogen in R_3 position was replaced by an electron-withdrawing cyano substituent.⁸⁹ These complexes exhibited activities of 2170 h^{-1} and 1690 h^{-1} respectively. Molar masses and dispersities of PCHCs obtained with catalysts **43a-d** were comparable with those obtained with complexes **42a-e**.

An unprecedented activity of complexes **43c,d** with the electron-withdrawing cyano group led to the development of new complexes **44**⁹⁰ and **45**⁹¹ containing CF_3 or CN and OEt groups (Figure 2.19). Complex **44** was effective in PO/ CO_2 copolymerization producing PPC with TOF 235 h^{-1} . The latter complex (**45**) copolymerized CHO with CO_2 with activity 210 h^{-1} , but carbonate linkage of obtained PCHCs reached only 88%.

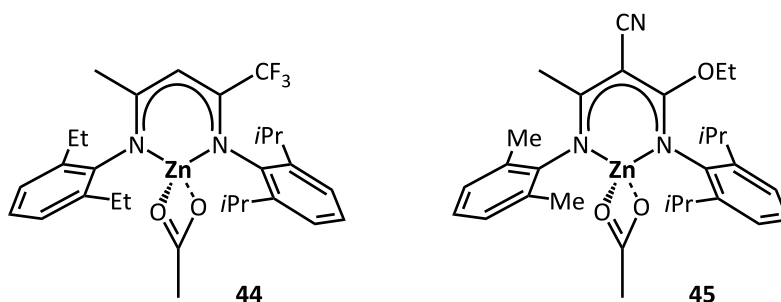


Figure 2.19: BDI zinc complexes with modified framework

Rieger's ethyl sulfinate BDI complexes **46a,b** were also viable to copolymerize CHO/ CO_2 (Figure 2.20). Both complexes showed moderate TOFs $\approx 160 \text{ h}^{-1}$ and afforded PCHC with M_n $30\text{-}40 \text{ kg}\cdot\text{mol}^{-1}$.⁹² At the same conditions, a new bimetallic BDI zinc complex **47** bridged via *meta*-substituted phenyl group showed a maximum TOF of 262 h^{-1} and M_n of PCHC in range $45\text{-}100 \text{ kg}\cdot\text{mol}^{-1}$.⁹³ BDI-derived tetramethyltetraazaannulene chromium(III) complex **48** (Figure 2.20) with an ionic cocatalyst $[\text{PPN}]\text{N}_3$ displayed high TOF (1300 h^{-1}) in CHO/ CO_2 copolymerization producing PCHC with molar mass $27 \text{ kg}\cdot\text{mol}^{-1}$ and narrow $\mathcal{D} = 1.03$.⁹⁴

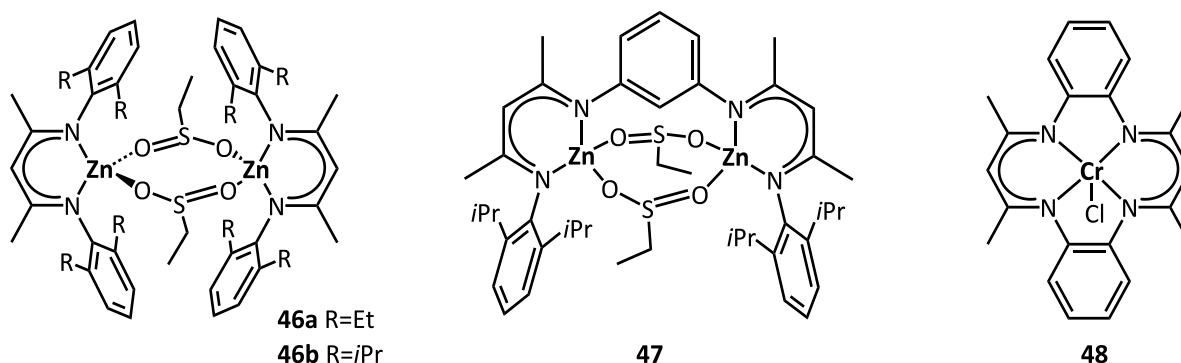


Figure 2.20: Ethyl sulfinate BDI complexes synthesized by Rieger

Another BDI-derived structure – a fluorine substituted anilido-alimine dizinc complex **49** (Figure 2.21) was reported by Lee.⁹⁵ Displayed catalyst was active at very high $[\text{CHO}]/[\text{Cat.}]$ loadings $50\,000:1$ and thus showed very high activity up to 2860 h^{-1} and afforded high molar mass PCHCs up to $245 \text{ kg}\cdot\text{mol}^{-1}$ ($\mathcal{D} = 1.20$). However, carbonate linkage in such copolymer was low (60-80%). Very recently, new extremely active dizinc complexes **50a-c** (Figure 2.21)

were reported by Rieger.⁹⁶ Complexes **50a,b** afforded PCHC with unprecedented activity $\approx 10\,000\text{ h}^{-1}$ with the selectivity 91-95% to PCHC. Further catalyst modifications in terms of different electronic properties of the ligands (**50c**) resulted in extraordinary activities for the poly(cyclohexene carbonate) formation as high as $28\,300\text{ h}^{-1}$. Molar masses of such PCHC achieved very high values $100\text{-}350\text{ kg}\cdot\text{mol}^{-1}$, while the carbonate linkage values were in range of 70-90%.

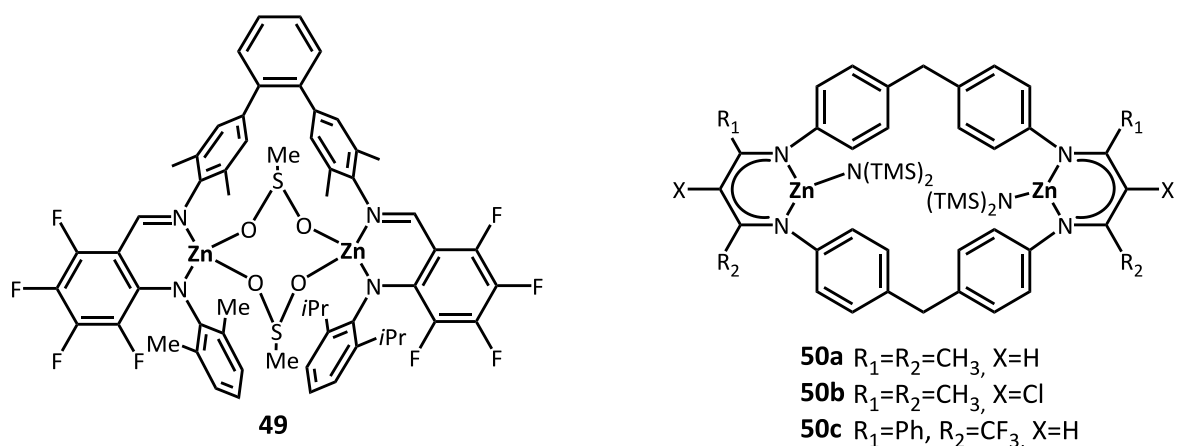


Figure 2.21: BDI-derived dizinc complex

A family of new chiral zinc complexes **51** (Figure 2.22) proved to be viable initiators for the copolymerization of CO_2 and CHO . Resultant PCHCs ($\text{TOF} = 2\text{ h}^{-1}$) are isotactic with enriched *m*-centered tetrads up to 72% and with 95% polycarbonate linkage and moderate molar masses and dispersity.⁹⁷ Compared to very slow complexes **51a-c**, a new family of enantioselective BDI zinc catalysts **52** (Figure 2.22) produced isotactic PCHC. Amongst all, complexes **52a,b** showed the best combination of activity and selectivity affording *i*PCHC with an enantiomeric excess (*ee*) 86-92% and activities as high as 190 and 160 h^{-1} respectively.⁹⁸

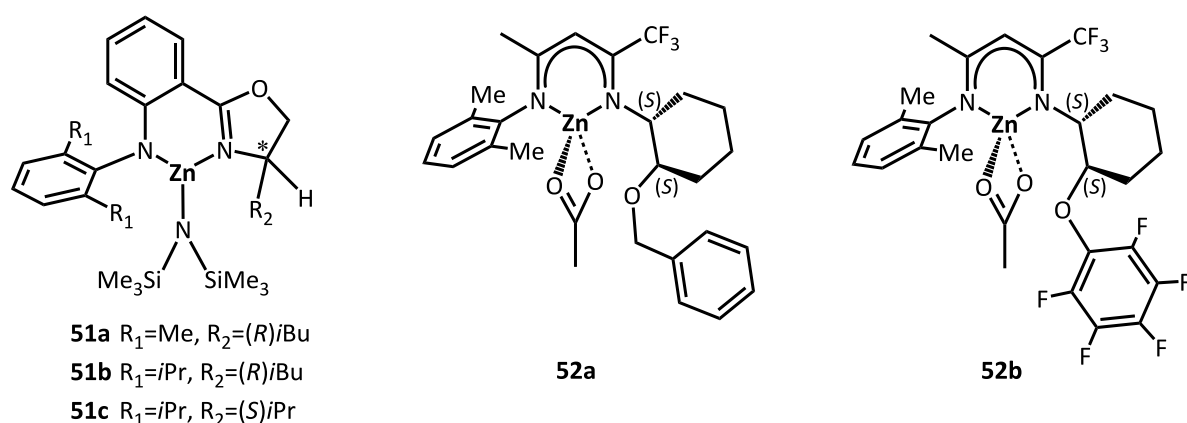


Figure 2.22: New amido-oxazolinato and BDI complexes for asymmetric copolymerization of CHO with CO_2

Recently, three new catalysts **53a-d** with varying degree of steric bulkiness having CN substituent in the *para* positions of aryl rings were highly active in CHO/CO_2 copolymerization (Figure 2.23).⁹⁹ Activity of these complexes ($690\text{-}758\text{ h}^{-1}$) lies in the range

of similar complexes with and without –CN group in ligand backbone (**43c,d** vs. **43a,b**, Figure 2.18, page 24). Percentage of carbonate linkages in obtained PCHCs ranges from 80 to 93%.

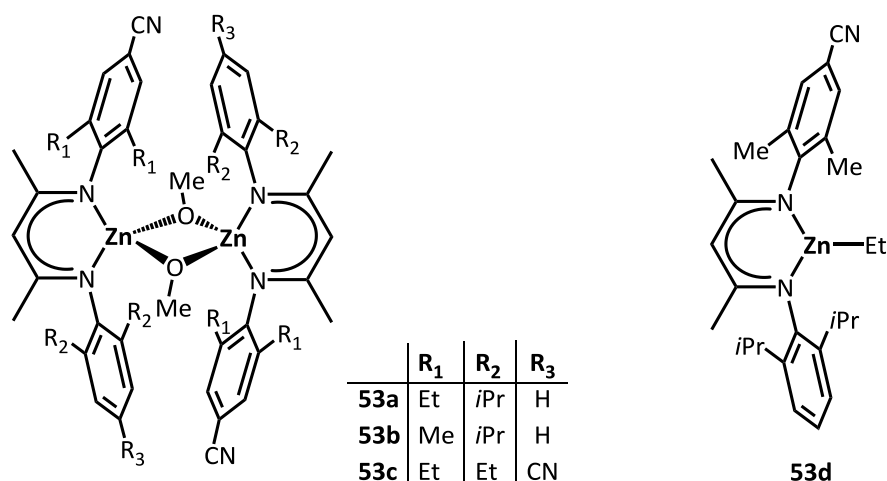


Figure 2.23: New BDI complexes with *para* CN substituents

The most active β -diiminate complexes for CHO (or PO)/CO₂ copolymerization with corresponding experimental conditions are summarized in Table 2.1.

Table 2.1: Bulk polymerization of epoxides with selected BDI Zinc complexes

Complex	Epoxide	M/CAT	<i>T</i> (<i>p</i>) (°C; MPa)	<i>t_p</i> (min)	TOF (h ⁻¹)	CL ^a (%)	<i>M_n</i> ^b (kg.mol ⁻¹)	\bar{D} ^b	Note	REF
42b	CHO	1000	50 (0.7)	30	431	97	17.3	1.15	-	74
42d	CHO	1000	50 (0.7)	30	729	99	23.3	1.15	-	74
42e	CHO	1000	50 (0.7)	20	917	90	17.9	1.15	-	74
43a	CHO	1000	50 (0.7)	120	239	96	23.7	1.14	-	88
43d	CHO	1000	50 (0.7)	10	2 170	89	22.8	1.11	-	89
44	PO	2000	50 (0.7)	120	235	99	36.7	1.13	Sel.to PPC=75%	90
46b	CHO	1000	60 (1)	120	156	97	39.8	1.11	-	92
47	CHO	3000	60 (1)	120	262	99	45.7	1.28	-	93
49	CHO	50 000	80 (1.4)	200	2 860	88	245	1.20	-	95
50c	CHO	8000	100 (1)	10	28 300	81	278	1.60	Pol. in toluene	96
52b	CHO	400	22 (0.8)	90	160	99	45	1.20	<i>ee</i> =90%	98
53b	CHO	1000	50 (0.7)	30	758	93	19.7	1.27	-	99

^a Carbonate linkage;

^b Determined by SEC

2.2.2.3 Single site salen catalysts

The use of salicylaldehyde complexes (so called salens) for the ring-opening of epoxides was first reported 15 years ago by Jacobsen. Salen-chromium complex **31b** (Figure 2.24) was used for the asymmetric ring-opening of various terminal and *meso*-epoxides.¹⁰⁰ Shortly afterwards, a series of salen aluminium,¹⁰¹ chromium¹⁰² and cobalt¹⁰³ complexes (**54a-c**,

31b,c + **55a,b** and **56a-e** respectively; Figure 2.24) were reported to catalyze the coupling reaction of epoxides and CO₂ to cyclic carbonates. In some cases, the production of optically active cyclic carbonates (*ee* = 51% with **56c**) have been reported.¹⁰³

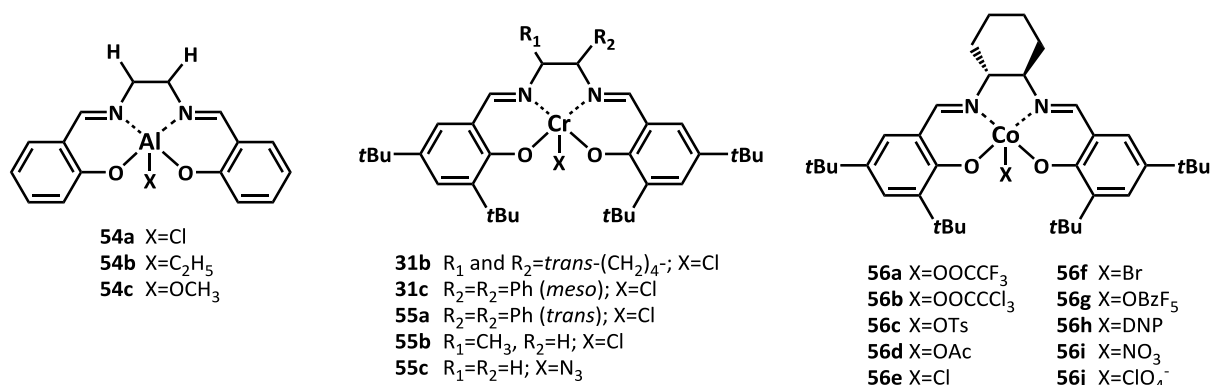


Figure 2.24: Early metal salen complexes for production of cyclic carbonates and polycarbonates

The first article describing the copolymerization of epoxides (CHO) with CO₂ by metal salen-like complexes was reported by Darensbourg in 2001.¹⁰⁴ Bis(salicylaldiminato)-zinc complexes were synthesized by reaction of Zn[N(SiMe₃)₂]₂ with two equivalents of salicylaldimine. Among all, the most active catalyst was complex **57** (Figure 2.25), which gave PCHC with 99% of carbonate units and $M_n = 41 \text{ kg}\cdot\text{mol}^{-1}$, ($\bar{D} = 10.3$) with activity 15 h^{-1} .

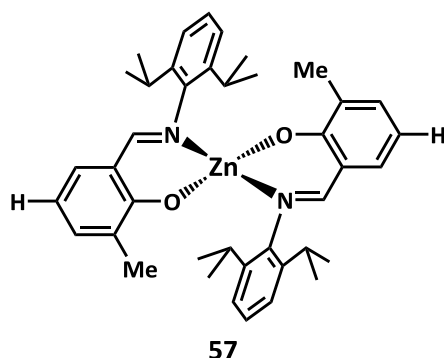


Figure 2.25: First salicyl-aldiminato complex producing PCHC

Shortly after, the same author reported the first article describing the copolymerization of epoxides (PO, CHO) with CO₂ by metal salen complexes.¹⁰⁵ Complex **31b** (Figure 2.24) in the presence of methylimidazole (5 eq.) produced CHO/CO₂ copolymer ($M_n = 8.9 \text{ kg}\cdot\text{mol}^{-1}$) with a moderate TOF of 32 h^{-1} . The copolymerization of PO and CO₂ afforded a mixture of cyclic propylene carbonate and PPC, while the selectivity to PPC was increased upon decreasing the temperature and/or cocatalyst loading. Similar complex with X group = NO₃ instead of Cl and MTBD (methyltriazabicyclodec-1-ene) cocatalyst produced PPC with 99% selectivity at optimized conditions.¹⁰⁶ Catalyst **31a** with phenylene framework (Figure 2.26) reported by the group of Rieger catalyzed the copolymerization of PO and CO₂.^{75d} **31a**/DMAP produced PPC ($M_n = 16.7 \text{ kg}\cdot\text{mol}^{-1}$) with the activity of 160 h^{-1} and selectivity to polycarbonate up to 82%. An important study referring the crucial role of the cocatalyst during epoxide/CO₂ copolymerization was reported by Darensbourg. Various cocatalysts, such as *N*-heterocyclic amines, phosphines, tetraalkylammonium salts and anions derived from

bis(triphenylphosphine) iminium (PPN⁺) were compared in the copolymerization of CHO and CO₂ with salen chromium complex **55c** (Figure 2.24). The most effective cocatalysts - P(C(CH₃)₃)₃ and PPNN₃ in combination with **55c** exhibited activity up to 600 h⁻¹.^{75c}

In 2005 and 2006 a series of chiral (salen)CoX complexes (**56**) with wide range of X anions were synthesized by few research groups. Paddock synthesized complexes bearing nucleophiles tosylate (OTs) (**56c**), OAc (**56d**), Cl (**56e**), I, BF₄, triflate (OTf) and NO₃ (**56i**) (Figure 2.24) in combination with *N,N*-dimethylaminoquinoline. They showed excellent selectivity (99%) to PPC in PO/CO₂ copolymerization.¹⁰⁷ Simultaneously, Coates et al. reported a series of complexes, e.g. **56d-g** (Figure 2.24)¹⁰⁸ and **58a-d** (Figure 2.26),^{75b} which afforded PPC (*M*_n = 10-50 kg.mol⁻¹) with activity 100-620 h⁻¹ in the presence of PPnCl. The highest activity and *M*_n was achieved with complex **56g**/PPnCl. Moreover, isotactic PPC with TOF = 1100 h⁻¹ was obtained when (*S*)-PO was employed with CO₂ copolymerization. Aforementioned complexes were effective also in CHO/CO₂ copolymerization; the highest TOF 440 h⁻¹ was achieved again with complex **56g**.¹⁰⁹ Lu et al. extensively tested the alternating copolymerization of CO₂ with *rac*-PO and CHO using **56b,e-j** complexes with various nucleophilic cocatalysts.^{76a} A detailed investigation focused on effects of salen ligand substituents, X groups and cocatalysts on the activity, selectivity to PPC, enantio- and stereo-selectivity was performed. The most effective complexes afforded PPC with TOF = 568 h⁻¹ (**56b**) and 530 h⁻¹ (**56h**) at 25°C while at higher temperature (40°C) TOF 1400 h⁻¹ was observed with **56h**.^{76a} CHO was copolymerized at ambient temperature with TOF 89 h⁻¹ (925 h⁻¹ at 80°C) (**56b**) and 83 h⁻¹ (**56h**).¹¹⁰

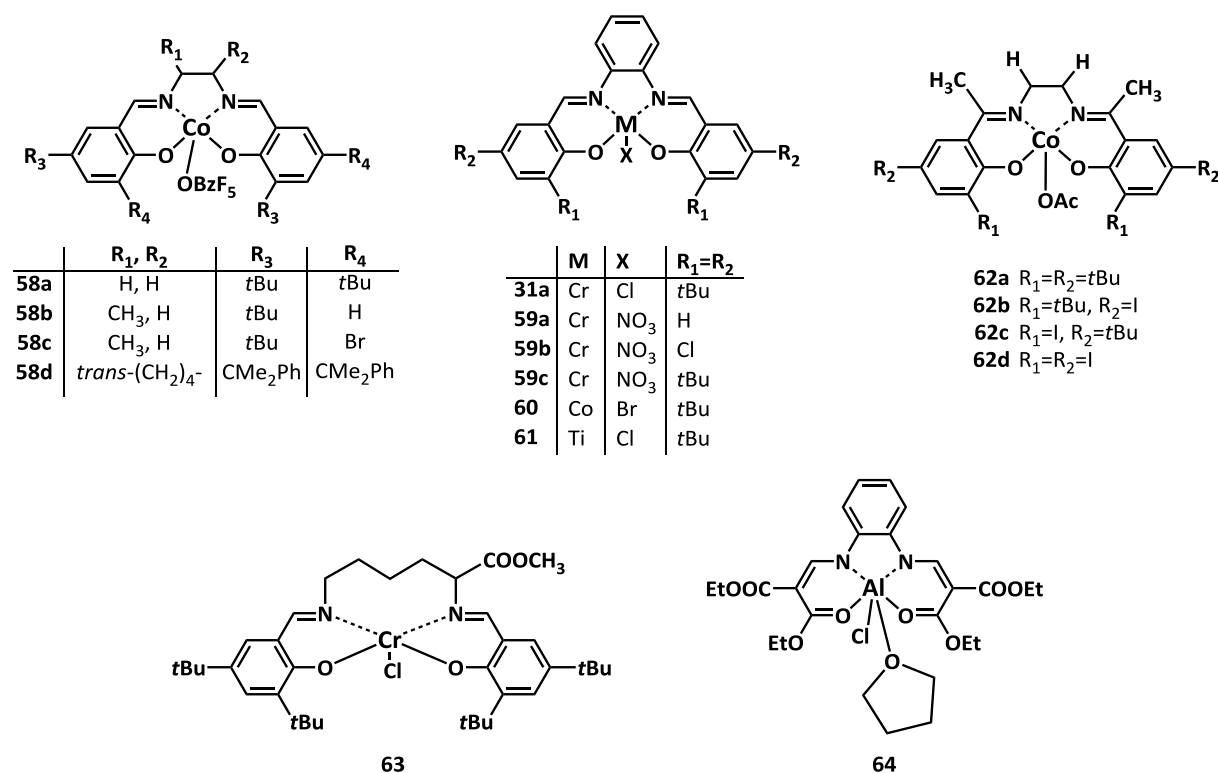


Figure 2.26: Metal salen complexes for copolymerization of epoxides with CO₂

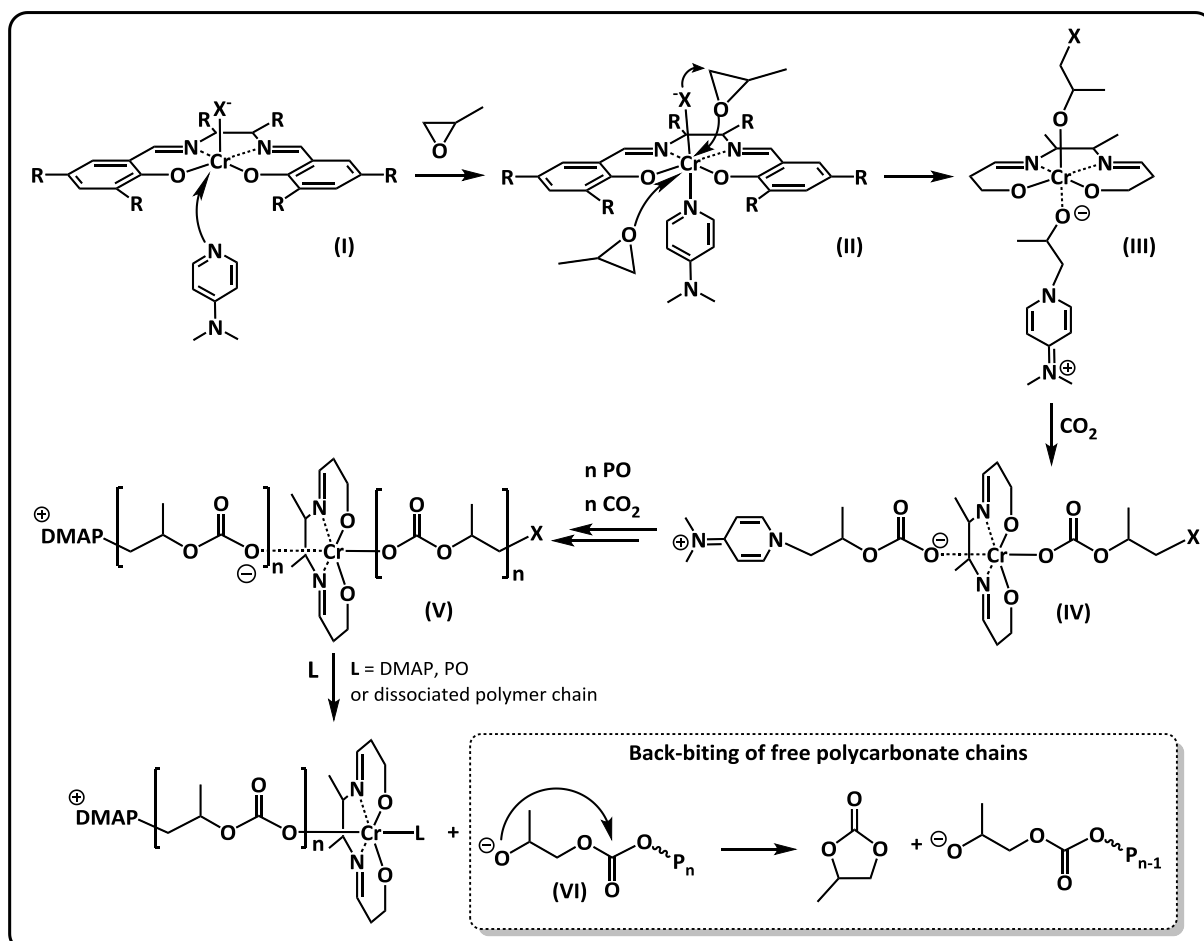
Salphen complexes containing phenylene ligand backbone were mentioned in only few publications, compared to the extensively explored salen complexes with chiral (*R,R'*) cyclohexylene backbone. Salphen chromium complex was first reported to copolymerize PO and CO₂ in 2003, where **31a**/DMAP (Figure 2.26) produced PPC with the selectivity 82% and $M_n = 15 \text{ kg}\cdot\text{mol}^{-1}$.^{75d} Comparable results were obtained with salphen chromium complexes **59a-c** differing in R₁ and R₂ substituents (Figure 2.26).¹¹¹ Compared to chromium, cobalt salphen complex **60** without any cocatalyst reported by Coates produced PPC in high selectivity to PPC (99%). Nevertheless, the activity of salphen complex **60** reached only 23 h⁻¹, which was $\approx 3x$ lower compared to analogous salen complex **56f** (Figure 2.24).^{75b} Very recently, a new salphen complex with an unusual trivalent titanium central metal **61**/PPNCl afforded PCHC ($M_n \approx 5 \text{ kg}\cdot\text{mol}^{-1}$) with 99% selectivity and TOF up to 577 h⁻¹.¹¹²

In the last years new complexes with unusual salen ligands were reported for the copolymerization of CHO and CO₂. Salen Co-OAc,¹¹³ lysin based salen Cr-Cl¹¹⁴ and salphen Al-Cl¹¹⁵ complexes **62-64** (Figure 2.26) produced PCHC with 100% selectivity over the cyclic by-product. The highest achieved TOF ranged from 20 to 70 h⁻¹. Prepared PCHCs displayed molar masses 3-10 kg·mol⁻¹ with complex **63**, $\approx 20 \text{ kg}\cdot\text{mol}^{-1}$ with complex **64** and 10-70 kg·mol⁻¹ with complex **62a**.

2.2.2.4 *Salan and salalen complexes*

Compared to salen complexes, reduced salan or half-reduced salalen complexes contain sp³-hybridized amino donors, which decrease the electrophilicity of the metal center and thus facilitate reversible epoxide/cocatalyst binding, which can significantly affect the activity.¹¹⁶ The flexibility of the ligand system also facilitates the bidentate binding of the growing polycarbonate chain and reduces the energy barrier to CO₂ insertion.¹¹⁷

In 2009, asymmetric binary salan (**65a,b**; Figure 2.27) and corresponding salen chromium complexes as well as detailed mechanism of polycarbonate formation were reported by Lu and co-workers (Scheme 2.15).^{75e} The mechanism considered that both DMAP and nucleophilic anion (X) play an initiator role during the polymerization process (see the monometallic pathway of initiation B in Scheme 2.11, page 20). Lu also suggested that copolymer growth can occur at both sides of salan- or salenCr(III) metal center. The formation of cyclic carbonates was promoted at higher concentrations of DMAP cocatalyst, which assists in the dissociation of growing polymer chains from the metal center resulting in the free alcoholate moieties, which easily undergo the cyclization via back-biting attack (see also Scheme 2.12).



Scheme 2.15: Mechanism of PO/CO₂ copolymerization for salen/salan type catalysts with DMAP

Complex **65c** (Figure 2.27) reported by Darensbourg was used for the copolymerization of CO₂ with both CHO and PO with activity 405 h⁻¹ and 21 h⁻¹ respectively.¹¹⁸ Shortly afterwards, Nozaki synthesized half-reduced salalen complexes **66a-d** (Figure 2.27), which polymerized CHO with CO₂ in the presence of PPNCI cocatalyst with TOFs of 140-230 h⁻¹ and *M_n* up to 11 kg.mol⁻¹. Moreover, TOF = 100 h⁻¹ was achieved even at 0.1 MPa of CO₂.¹¹⁷ New bimetallic zirconium salan complexes **67a-c** (Figure 2.27) efficiently catalyzed the copolymerization of PO and CHO with CO₂ as well as the ROP of cyclic lactones.¹¹⁹ Catalysts **67a-c** in combination with *n*-Bu₄NBr cocatalyst afforded PPC and PCHC with molar masses in the range of 11-16 kg.mol⁻¹ and activities of 133 and 158 h⁻¹ respectively.

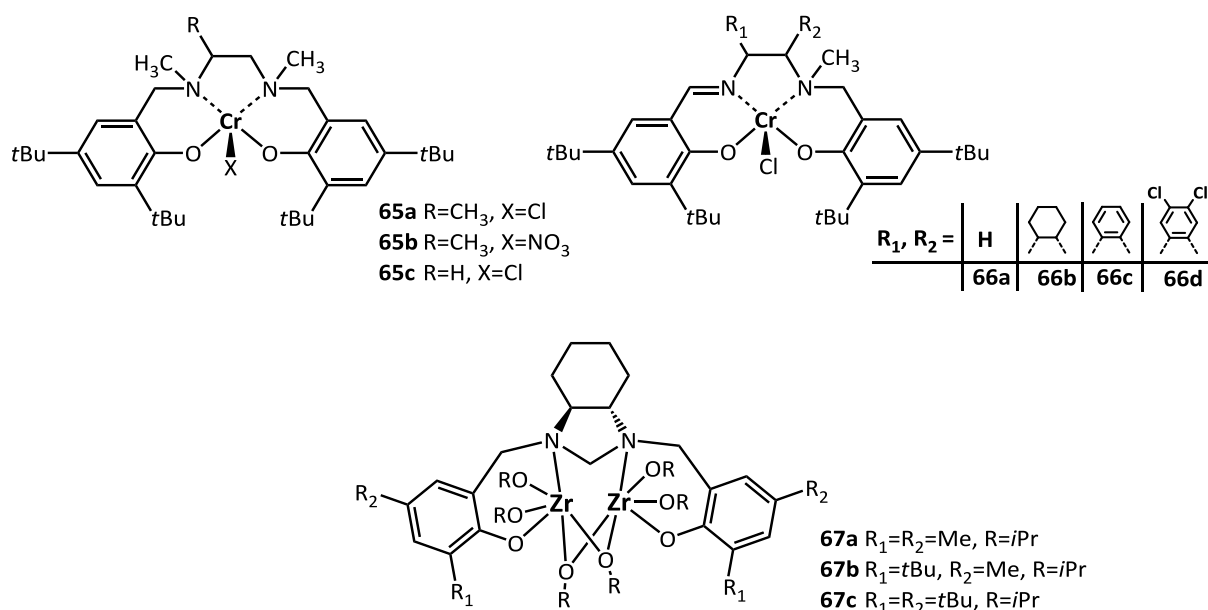


Figure 2.27: Salen and salalen Cr and Zr complexes for CHO and PO copolymerization

Table 2.2 compares the activity of binary salen (**31a**, **56-64**) and salan (**65-67**) complexes in epoxide/CO₂ copolymerization at optimized conditions.

Table 2.2: Binary salen and salan complexes for epoxide/CO₂ copolymerization in bulk

Complex /Cocatalyst	Epoxide	M/CAT	<i>T</i> (p) (°C; MPa)	<i>t</i> _p (h)	TOF (h ⁻¹)	Selectivity (%)	CL ^a (%)	<i>M</i> _n ^b (kg.mol ⁻¹)	Đ ^b	REF
31a /DMAP	PO	1500	75 (1.3)	4	160	66	98	16.7	1.38	75d
56b /PPNCl	PO	2000	25 (1.5)	1.5	568	>99	>99	28.1	1.14	76a
56b /PPNCl	CHO	1000	80 (2.5)	0.5	925	>99	>99	11.4	1.30	110
56g /PPNCl	PO	2000	22 (1.4)	1	620	>99	98	26.8	1.13	108
56h /PPNCl	PO	2000	40 (2)	0.7	1400	97	>99	25.9	1.08	76a
61 /PPNCl	CHO	1000	120 (4)	1	577	>99	>99	4.2	1.06	112
62a /PPNCl	CHO	1000	80 (1.5)	6	58	>99	>99	23.8	1.20	113
63 /PPNCl	CHO	1000	80 (4.5)	24	45	>99	>99	7.7	1.20	114
64 /Bu ₄ NBr	CHO	500	80 (5)	20	24	>99	>99	14.5	1.47	115
65c /PPN ₃	CHO	2500	60 (3.4)	4	405	-	-	19.5	1.19	118
66c /PPNCl	CHO	1000	70 (3.4)	2	230	>99	>99	9.1	1.15	117
67a /Bu ₄ NBr	CHO	1000	50 (3.5)	6	158	98	95	16.0	1.09	119

^a Carbonate linkage;

^b Determined by SEC

2.2.2.5 Multichiral and bifunctional salen complexes

Since simple catalytic systems for copolymerization of epoxides with CO₂ usually suffer from low activity (far beyond its industrial applicability) and prepared polycarbonates, whether PPC or PCHC, have insufficient thermal and mechanical properties, a significant effort was devoted to the development of new catalysts, which would overcome these

limitations. Compared to the binary catalytic system, bifunctional complexes contain ionic cocatalyst attached directly to the ligand framework, which effectively suppress the dissociation of growing polymer chain from metal center leading to the back-biting and cyclic carbonate formation. Indeed, such complexes exhibited significant increase in selectivity at high temperatures and two order of magnitude increase of activity. Improving of thermal and mechanical properties of polycarbonates from CO₂ can be realized via stereospecific polymerization, which introduces stereo-regularity into the polymer chain. For this purpose multichiral complexes, which can preferentially build one enantiomer into the polymer chain, were developed.

The first bifunctional catalyst for the highly selective formation of PPC was explored by Nozaki, who synthesized a complex containing attached piperidinium end-capping arms **68** (Figure 2.28).¹²⁰ Piperidinium arms protonated growing polymer chains upon its dissociation from the metal center, which helped to suppress the back-biting reactions leading to the cyclic carbonate formation. At 25°C, selectivity of 99% and activity of 254 h⁻¹ were observed. Moreover, due to effective suppression of back-biting, **68** allows copolymerization of PO with CO₂ at higher temperatures (60°C) with the formation of only ≈ 10% of cyclic carbonate by-product (TOF = 602 h⁻¹).

Complexes **69a-c** (Figure 2.28) containing piperidine and morpholine arms in para positions of aryl rings showed significantly lower activity (≈ 29 h⁻¹ at 40°C) in PO/CO₂ copolymerization compared to complex **68**.¹²¹ Slightly higher activity (57 h⁻¹) was achieved with complex **70** having piperidinium groups in para positions. Although this complex was still significantly less active than catalyst **68**, it exhibited increased kinetic resolution ($k_{rel} = 3.5$) allowing to prepare a stereogradient PPC with an unusually high thermal decomposition temperature that is greater than that of isotactic PPC (281 versus 245°C).¹²²

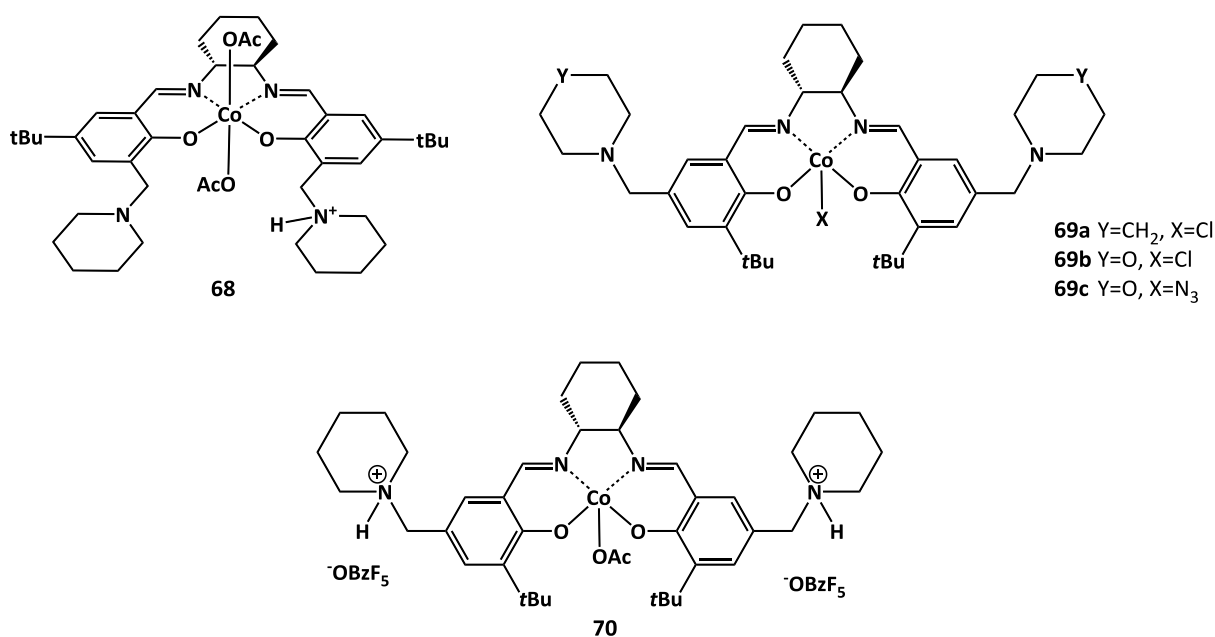


Figure 2.28: Salen(Co) complexes with pieridinium end-capping arms

Cobalt catalysts containing quaternary ammonium salts attached directly to the ligand framework were synthesized as an alternative of already known binary catalysts. The concept of intramolecular combination of (Salen)CoX complex with an ionic $\text{Bu}_4\text{N}^+\text{X}^-$ moieties led to a new type of catalysts, which showed unprecedented activities and excellent selectivity to polycarbonate at high temperatures.

Complex **71** (Figure 2.29) prepared by Lee et al. shows excellent activity 3300 h^{-1} (at 80°C) at conditions of high dilution ($[\text{epoxide}]/[\text{catalyst}] = 25\,000:1$).¹²³ High selectivity (94%) and high molar masses ($60\text{--}95 \text{ kg}\cdot\text{mol}^{-1}$) of obtained PPCs are other merits of this catalyst. Optimization of catalyst structure by removing of SiMe_2 linking groups and addition of other two side Bu_4NX arms resulted in even more effective complexes **72a-c** (Figure 2.29).¹²⁴ Activities of these complexes varied markedly with bulkiness of R substituents. The highest activity ($26\,000 \text{ h}^{-1}$) was achieved with complex **72a** containing methyl substituents in R positions, while complex **72c** with *tert*-butyl substituents exhibited $\text{TOF} = 1300 \text{ h}^{-1}$. Moreover, the final PPC had $M_n = 208 \text{ kg}\cdot\text{mol}^{-1}$ and narrow \mathcal{D} . Furthermore, catalysts **72a-c** can be removed from the reaction mixture by a simple filtration over silica gel and subsequently recovered without loss of activity, whereby catalyst cost and metal residues in the copolymer can be significantly reduced. An unusual binding mode, that differs from conventional salen-Co(III) complexes, was observed in cobalt(III) salen complex **73** bearing four quaternary ammonium arms (Figure 2.29).¹²⁵ This complex showed activity up to $16\,000 \text{ h}^{-1}$ in PO/CO₂ copolymerization, whereas molar masses of gained PPC were in range of $100\text{--}300 \text{ kg}\cdot\text{mol}^{-1}$.

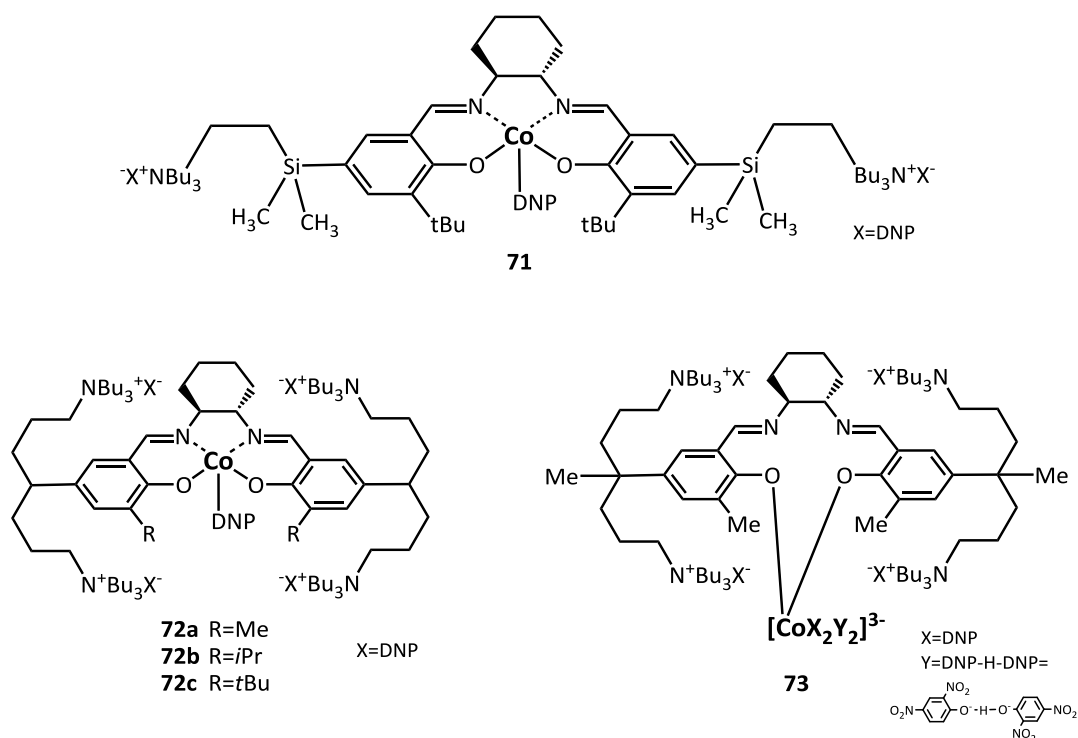


Figure 2.29: (Salen)Co complexes with tertiary amine end-capping arms

Cobalt complexes with tertiary amines attached directly to the salen framework via a pendant arm were also investigated. Complexes **74a-c** (Figure 2.30) proved to be highly active for PO/CO₂ copolymerization especially at higher temperatures.¹²⁶ The activity of these complexes ranged from 3863 h⁻¹ (**74c**) to 6290 h⁻¹ (**74b**) at 80°C. Molar masses lie in the range 100-136 kg.mol⁻¹. Another increase of activity was observed at 100°C where complex **74b** produced PPC with TOF of 10 882 h⁻¹ and $M_n = 60 \text{ kg.mol}^{-1}$ ($D = 1.18$).

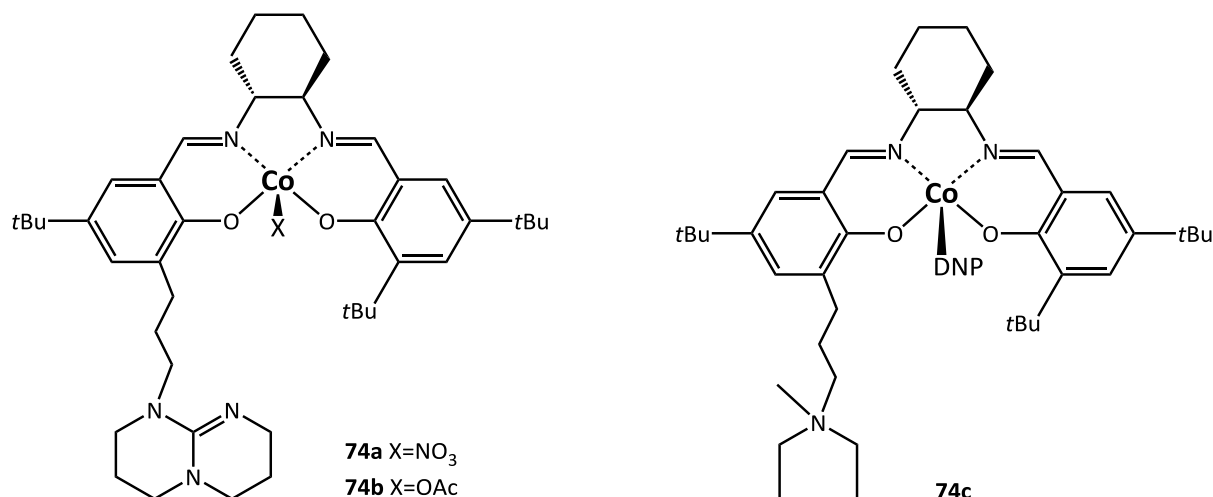


Figure 2.30: Salen Co complexes with pendant tertiary amine cocatalyst

Asymmetric (salen)Co(III) complexes **75a-c** (Figure 2.31) containing chiral 1,1'-bi-2-naphthol (BINOL) and 3-adamantyl substituents were prepared by Lu and co-workers.¹²⁷ As expected, prepared complexes showed higher enantioselectivity compared to enantiopure (salen)Co(III) complexes **56** with cyclohexylene backbone (Figure 2.24). At 25°C, multichiral complexes **75a-c** produced PPC with TOF = 336-384 h⁻¹ with enantioselectivity (k_{rel}) 9.8-12.4 compared to k_{rel} of 4.7 observed with complex **56h** with a dinitrophenolate (DNP) X group. The highest selectivity was observed with complex **75c** at -25°C ($k_{rel} = 24.0$). The highest k_{rel} reported to date (24.3) was achieved at -20 °C with a similar catalyst **76** that contains a pendant triazabicyclodecene (TBD) group (Figure 2.31).¹²⁸

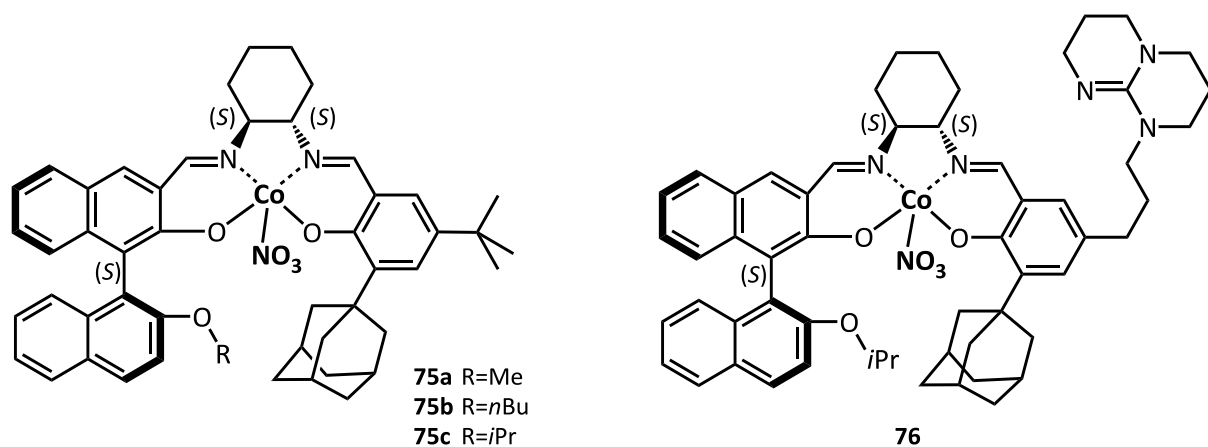


Figure 2.31: Multichiral BINOL salen Co(III) complexes

2.2.2.6 Early and new porphyrin catalysts

The first single-site catalysts for epoxide-CO₂ coupling were metal porphyrins reported first in 1978 by Inoue.¹²⁹ Polycarbonates subsequently prepared with those aluminium-porphyrin complexes (**23a** and **77**) (Figure 2.32) produced PPC over the course of 2 weeks with $M_n = 3.9 \text{ kg.mol}^{-1}$ and 30-40% of carbonate units in copolymer.¹³⁰ When 1 equivalent of ammonium or phosphonium salts (Et₄NBr and EtPh₃PBr) was added to complex **23a**, a significant increase of carbonate linkage in final copolymers (> 99%) was observed.¹³¹ The copolymerization of CO₂ with oxirane, PO, or CHO yielded corresponding polycarbonates with M_n 3.5-6.2 kg.mol⁻¹ and low \bar{D} (< 1.14), however, the activity still remained low ($\approx 0.3 \text{ h}^{-1}$). Although this catalyst yielded some amount of cyclic PC, the formation of ethylene carbonate and cyclohexene carbonate (CHC) wasn't observed. A series of Al, Cr and Co complexes **23-28** (Figure 2.32) reported for the ROCOP of epoxide and anhydride,^{53-54,55} were effectively used by Chisholm et al. also for the copolymerization of PO with CO₂.¹³²

Cobalt catalyst **25** (Figure 2.32) combined with Schiff bases was able to produce polycarbonates with controlled molar mass, narrow dispersity and 100% selectivity to PCHC.¹³³ The copolymerization of CO₂ and CHO in the presence of DMAP or pyridine cocatalyst afforded PCHC with TOF $\approx 21 \text{ h}^{-1}$, $M_n = 14\text{-}20 \text{ kg.mol}^{-1}$ and with > 99 % of carbonate units in copolymer. A dinuclear version of complex **25** linked in para-position of aryl ring via dioxopentamethylene bridge proved slightly better catalytic performance affording PCHC with an activity 64 h^{-1} .¹³⁴ In 2000 Holmes et al. synthesized a chromium porphyrin catalyst **26** modified with fluorinated aromatic moieties (Figure 2.32) to increase its solubility in supercritical CO₂ (scCO₂).¹³⁵ The copolymerization of CHO and scCO₂ (22.5MPa) at 110°C with **26** produced PCHC with $M_n = 1.5\text{-}9.4 \text{ kg.mol}^{-1}$ with TOF up to 173 h^{-1} .

Tetra-*p*-tolylporphyrinate chromium complexes **78a,b** in combination with cocatalyst methylimidazole or DMAP produced cyclic carbonates and low molar mass PCHC.¹³⁶ Manganese-porphyrine complex **79**, synthesized later by Inoue showed activity 16.3 h^{-1} in CHO/CO₂ copolymerization, while reaction of PO and CO₂ gave only cyclic PC.¹³⁷

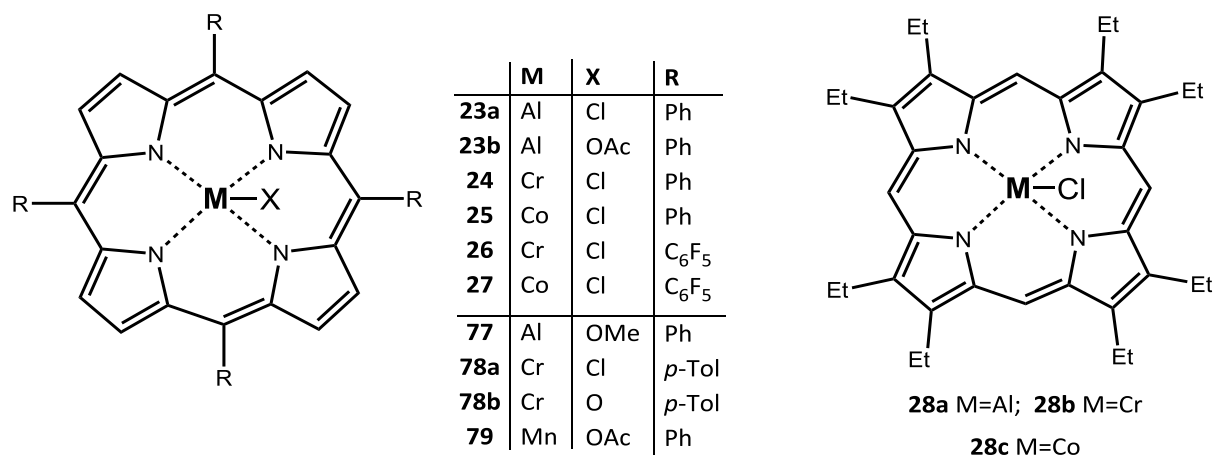


Figure 2.32: Metal porphyrin complexes for copolymerization of epoxides with CO₂

In the last years, new porphyrin-based complexes were reported to catalyze PO/CO₂ copolymerization. In 2012, Rieger reported cobalt complexes with various alkoxy substituents in *para*-position of aryl rings **80a-d** (Figure 2.33).¹³⁸ In combination with PPnCl an activity up to 103 h⁻¹ and $M_n \leq 47 \text{ kg.mol}^{-1}$ was achieved. C_{2v} symmetric complexes **81a,b** and asymmetric cobalt complex **81c** with bromo substituent in R₁ position produced PPC of $M_n = 8\text{-}17 \text{ kg.mol}^{-1}$ within 3 days (Figure 2.33). Interestingly, symmetric complex **81d** with bromo substituents in R₁ and R₂ positions produced only cyclic carbonate (PC).¹³⁹

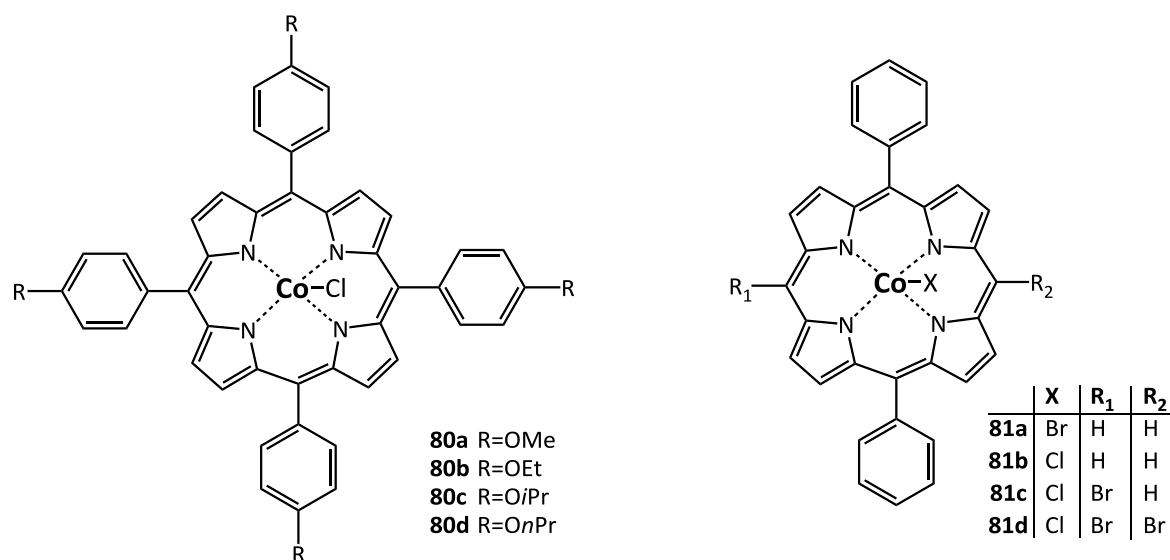


Figure 2.33: New metal porphyrin complexes for copolymerization of epoxides with CO₂

Bifunctional tetraphenylporphyrin cobalt complexes bearing two and four ammonium side arms **82a,b** (Figure 2.34) were first synthesized by group of Wang.¹⁴⁰ An unprecedented activity for metalloporphyrins (TOF = 495 h⁻¹) was observed with complex **82a** with two side NBu₃⁺ arms. M_n of synthesized PPC reached 40 kg.mol⁻¹. The activity and molar mass of PPC prepared with complex **82b** with four NBu₃⁺ side arms was lower by a half compared to **82a**.

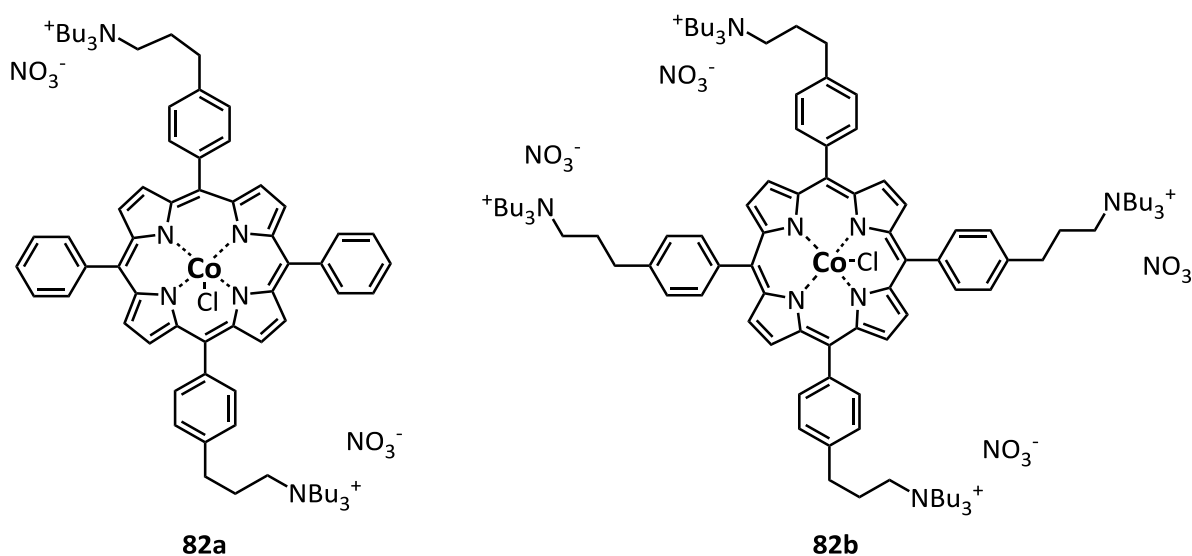


Figure 2.34: Cobalt porphyrin complexes with tetrabutylammonium side arms

Following this initial success, the same group designed a plentitude of novel aluminium complexes **83** and **84** with two side ammonium arms in combination with various R_1 - R_5 substituents on aryl rings attached to the porphyrin framework.¹⁴¹ Figure 2.35 shows a selection of the most efficient catalysts for the copolymerization of PO and CO_2 . Complexes **83** and **84** exhibited activities in range of $300\text{-}800\text{ h}^{-1}$ and afforded in most cases PPC with M_n in range $30\text{-}50\text{ kg}\cdot\text{mol}^{-1}$ (selectivity to polymer $\approx 90\%$). An optimization of conditions performed with complexes **83b** and **84e** led to the formation of PPC with very high TOF $\approx 2500\text{ h}^{-1}$.

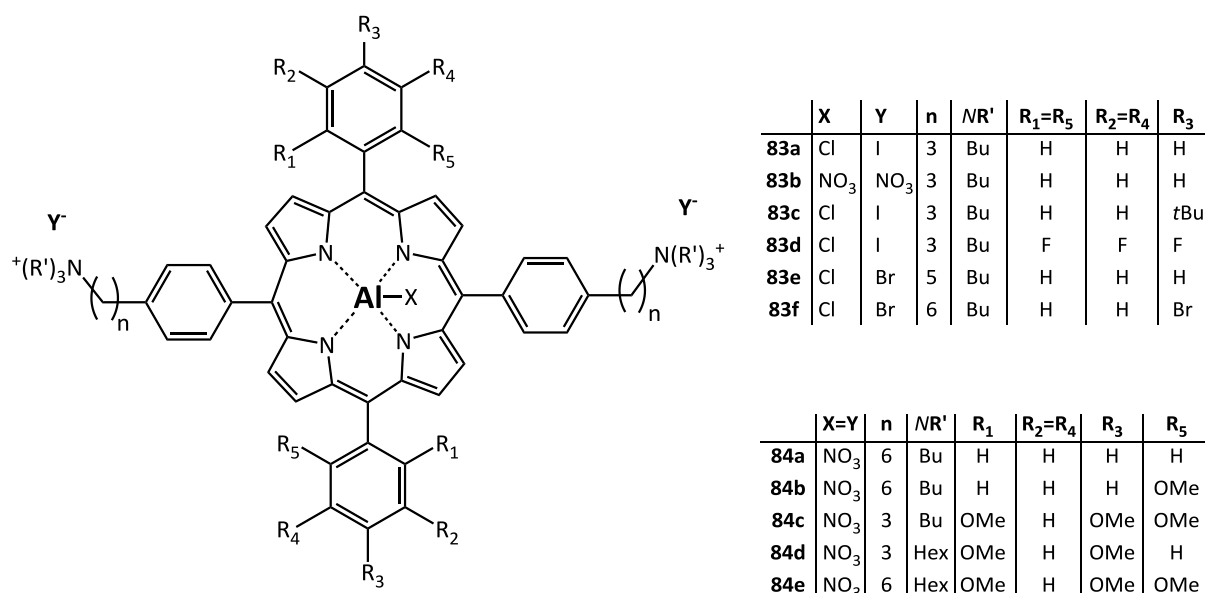


Figure 2.35: Series of aluminium porphyrin complexes with tetraalkylammonium side arms

Manganese and iron corrole complexes **37a-d** (Figure 2.36) already mentioned as efficient catalysts for epoxide/anhydride copolymerization were also successfully used as catalysts for the copolymerization of CO_2 with PO. Complexes produced PCHC with carbonate linkage up to 92%. The highest activity was achieved with **37a**/PPN-OAc, which produced PPC with M_n $50\text{ kg}\cdot\text{mol}^{-1}$ and TOF = 69 h^{-1} , however, the content of carbonate units in copolymer was very low 30%.⁶⁴

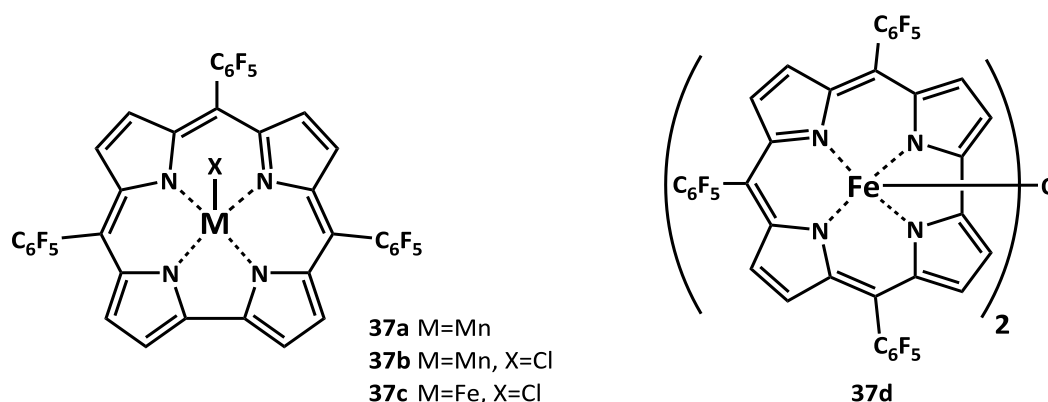


Figure 2.36: Metal corrole complexes for copolymerization of epoxides with CO_2

The most active bifunctional salen (**68-76**) and porphyrin (**80-84**) complexes for the copolymerization of PO/ CO_2 are summarized in Table 2.3.

Table 2.3: Bifunctional salen and porphyrin complexes for PO/CO₂ copolymerization

Complex /Cocat.	M/CAT	T (p) (°C; MPa)	t _p (h)	TOF (h ⁻¹)	Selectivity (%)	CL ^a (HT ^b) (%)	M _n ^c (kg.mol ⁻¹)	D	k _{REL} ^d	REF
68	2000	25 (1.4)	3	254	>99	>99 (-)	12.6	1.13	-	120
70	2000	25 (1.4)	9	57	98	>99 (92)	8.2	1.13	3.5	122
71	25 000	80 (2)	1	3300	94	>99 (94)	71	1.25	-	123
72a	50 000	80 (2)	0.5	26 000	>99	>99 (-)	208	1.20	-	124
73	100 000	75 (2)	1	16 000	>99	>99 (82)	300	1.31	-	125
74	10 000	100 (2.5)	0.25	10 880	97	>99 (-)	60.2	1.23	-	126
75c/PPNCl	1000	-25 (1)	24	18	-	>99 (99)	6.5	1.18	23.7	127
76	1000	-20 (1)	24	16	>99	>99 (99)	20.4	1.15	24.3	128
80c/PPNCl	2000	30 (3)	18	103	99	90 (93)	39	1.18	-	138
82a	1500	50 (4)	2	495	96	99 (-)	40	1.30	-	140
83b	20 000	110 (3)	2	2420	71	98 (-)	36	1.25	-	141b
84c	5000	70 (3)	2	704	93	98 (-)	45	1.09	-	141c
84e	20 000	90 (3)	2	2510	89	98 (-)	58	1.13	-	141c

^a Carbonate linkage;^b Head-to-Tail linkage;^c Determined by SEC;^d Kinetic resolution (enantioselectivity)

2.2.2.7 Binuclear and bimetallic-bridged catalysts

Catalysts containing two (or more) metal active sites often proved to be more active and selective compared to its monometallic counterparts. Compared to BDI zinc complexes, which can be in monomeric or dimeric form depending on their structure, concentration and temperature (see chapter 2.2.2.2, page 23) bimetallic complexes discussed herein contain two metal centers coordinated to a single ligand molecule. A cooperation of neighboring metals during the copolymerization can significantly improve the catalytic performance of such complexes. This is due to a) activation of epoxide and CO₂ at the same time or b) due to feasibility of growing polymer chain to attack epoxide coordinated to adjoining metal center. Moreover, bimetallic complexes also prevent a dissociation of growing polymer chain from the metal center, which often results in cyclic carbonate formation via back-biting.

The first bimetallic complexes were reported in 2005 by Xiao et al. In situ prepared dizinc and dimagnesium complexes coordinated to Trost phenolate ligands were active in CHO/CO₂ copolymerization (Figure 2.37).¹⁴² Dizinc complex **85a** was more active (TOF = 142 h⁻¹) compared to magnesium complex **85b** (20 h⁻¹). Molar masses of gained PCHC ranged from 20 to 40 kg.mol⁻¹. A derived structure **86** reported later was also effective in CHO/CO₂ copolymerization, however, its activity was very low (3 h⁻¹).¹⁴³

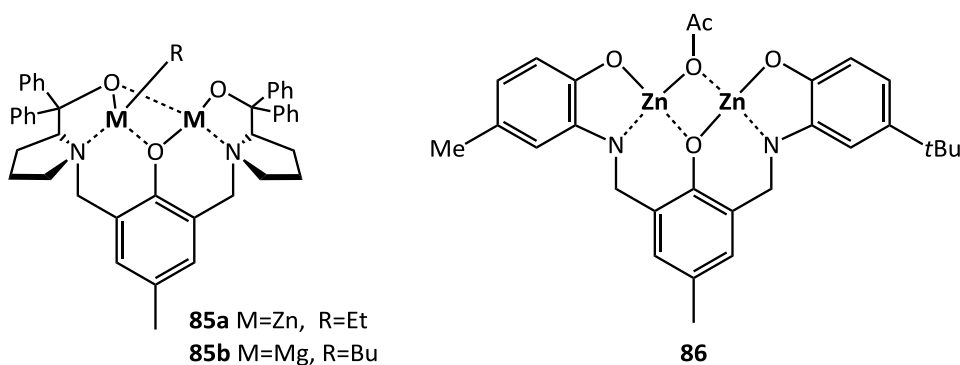


Figure 2.37: Trost phenolate complexes

Dinuclear metal complexes **36a,b** and **87a,b** (Figure 2.38) were developed by group of Williams. Up to date, various metals (Zn, Mg, Fe, Co) were successfully coordinated to so-called Robson's ligands, while all of them exhibited good catalytic performance in epoxide/ CO_2 copolymerization. The most efficient proved to be dicobalt complex **87b** ($\text{TOF} = 3700 \text{ h}^{-1}$), but corresponding dizinc, dimagnesium and diiron analogues also exhibited good catalytic performance. Complexes **36a,b** and **87a** exhibited activities 140 h^{-1} , 730 h^{-1} and 107 h^{-1} respectively in CHO/CO_2 copolymerization at $p_{\text{CO}_2} = 1 \text{ MPa}$.¹⁴⁴ Moreover, all complexes copolymerized CHO with CO_2 even at 0.1 MPa CO_2 pressure with activity 28 h^{-1} (**36a**), 152 h^{-1} (**36b**), 6 h^{-1} (**87a**) and 500 h^{-1} (**87b**) respectively. Recently, the same group reported a water-tolerant heterodinuclear complex **87c** for CHO/CO_2 copolymerization.¹⁴⁵ Although its activity was rather low, it is the first example of heterodinuclear complex so far.

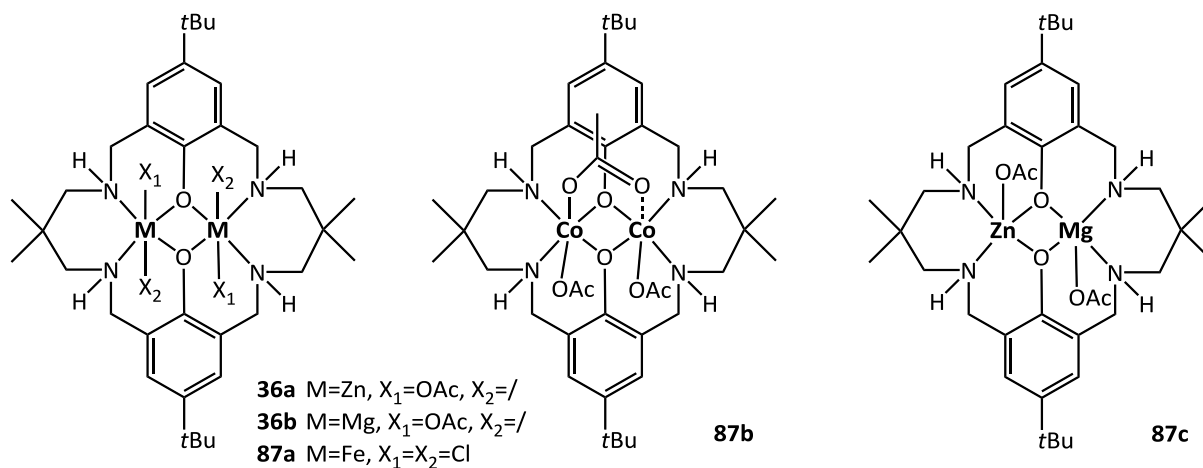


Figure 2.38: Dinuclear Robson-type complexes

Dinuclear cobalt salen complexes with a variable length of methylene linkers were synthesized by Nozaki et al.⁷³ The highest TOF (1770 h^{-1}) was achieved with dinuclear chiral (*R,R*)-(*S,S*) Co(III) complex linked with adipic acid (**88**, Figure 2.39) in combination with PPNCI, however, high activities (430 h^{-1}) were achieved also in the absence of cocatalyst. It was further found that the copolymerization with solely complex **88** proceeds via the bimetallic propagation mechanism, while in the presence of cocatalyst (PPNCI), the propagation proceeds via the monometallic mechanism.

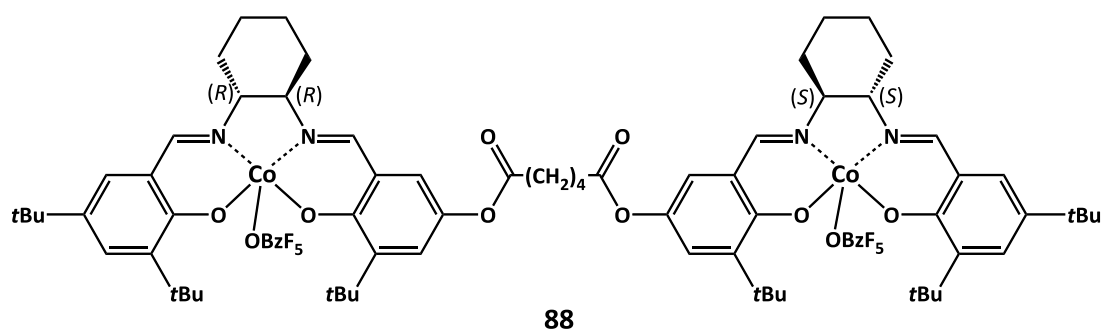


Figure 2.39: Dinuclear methylene-bridged salen complexes

Monomeric and conformationally flexible dimeric chromium salen complexes **12a** and **12d** were tested for the copolymerization of PO and CO₂ (Figure 2.40).^{43,146} The bimetallic complex **12d** exhibited slightly lower activity (49 h⁻¹) compared to the monomeric salen Cr complex **12a** (61 h⁻¹). However, the bimetallic catalyst retained its activity even upon conditions of high dilution (82 h⁻¹) compared to the monometallic counterpart (7 h⁻¹), which is an evidence of the bimetallic propagation mechanism.

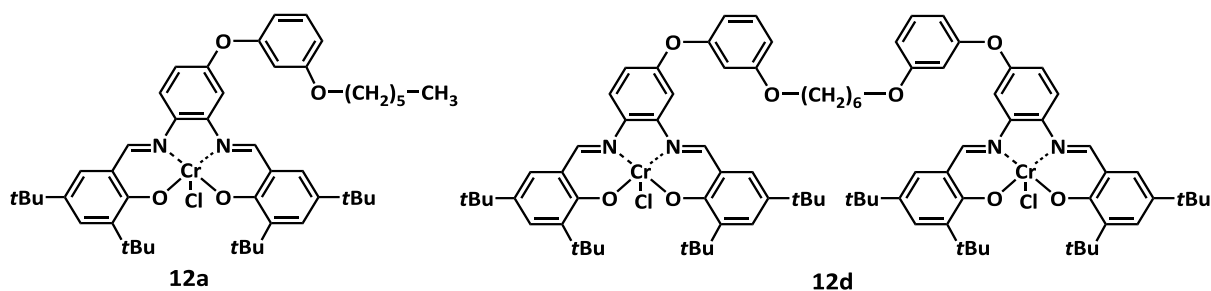


Figure 2.40: Conformationally flexible dimeric chromium salen complexes

New asymmetric enantiopure dinuclear Co(III) catalysts **89a,b** (Figure 2.41) with rigid biphenyl linker were used for the stereospecific copolymerization of cyclopentene oxide or CHO with CO₂.¹⁴⁷ The copolymerization of CHO/CO₂ with **89a,b**/PPN⁺DNP⁻ afforded optically active polycarbonates (*ee* up to 81%) with 99% selectivity to PCHC and activity up to 1409 h⁻¹. Outstanding enantioselectivity of 98% in CHO/CO₂ copolymerization was achieved with **89b** at 0°C. Related complex **90** with a binaphthol linker showed significantly lower activity and selectivity.

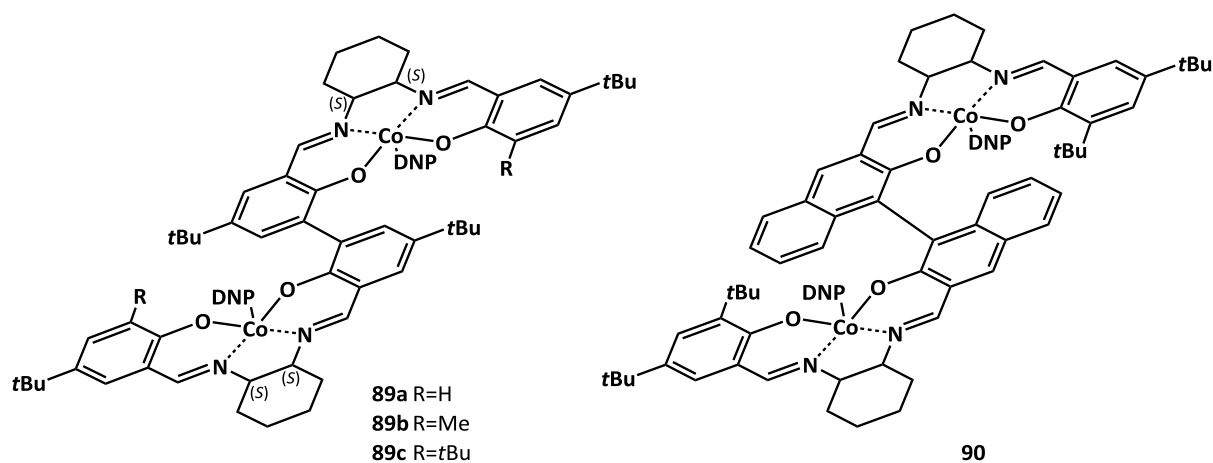


Figure 2.41: Enantiopure dinuclear Co salen complexes

Dinuclear cobalt complexes **91a-c** (Figure 2.42) linked with a chiral biphenol containing tunable linking bridge at 6,6' positions (to restrict free rotation of the complex) were also designed for the asymmetric copolymerization CHO with CO₂.¹⁴⁸ Enantiopure (*S,S,R,S,S*) complex **91a** with C₄ linking bridge combined with PPN⁺-DNP⁻ cocatalyst catalyzed CHO/CO₂ copolymerization with TOF 71 h⁻¹ producing PCHC with *ee* 20% of *R,R* configuration. The use of longer linking bridges composed of 6 methylene units (**91b**) and 8 methylene units (**91c**) significantly improved the activity (483 h⁻¹ and 758 h⁻¹). However, the enantiomeric purity of PCHCs was lower. Additionally, an enantioselectivity of 39% of *R,R*-configuration in PCHC was obtained with multichiral complex (*S,S,S,S,S,S*)-**91b**/PPN⁺-DNP⁻.

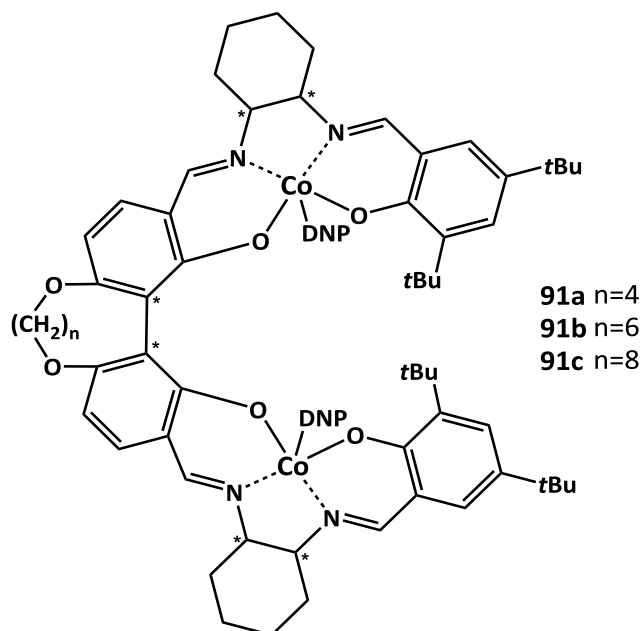


Figure 2.42: Biphenyl-linked dinuclear cobalt complexes with restricted rotation

Novel bimetallic bis(benzotriazole iminophenolate) catalysts with Ni(II), Co(II) and Zn(II) metal centers **92a-c** (Figure 2.43) were used towards CHO/CO₂ copolymerization.¹⁴⁹ Dinuclear nickel and zinc complexes **92a,b** displayed moderate activity 40-50 h⁻¹ and afforded PCHC with 99% of carbonate units and *M_n* 22-50 kg.mol⁻¹ (*Đ* < 1.25). Dicobalt complex **92c** exhibited very poor activity.

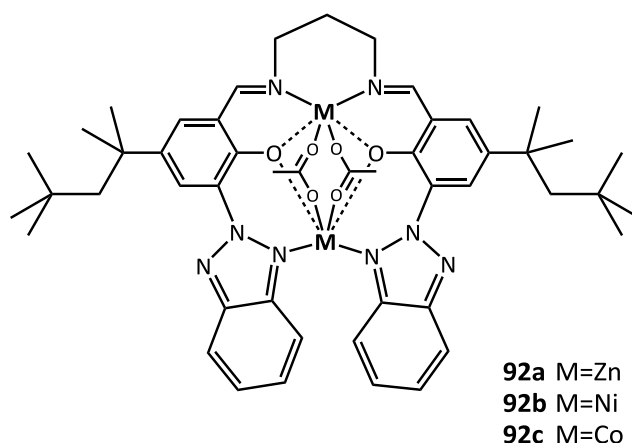


Figure 2.43: Ni(II), Co(II) and Zn(II)bis(benzotriazole iminophenolate) catalysts

2.2.2.8 Other catalysts

In the last few years, new types of catalysts for epoxide/ CO_2 copolymerization have appeared. Amine-bis-phenolate complexes proved to be efficient for the copolymerization of CHO/ CO_2 systems.

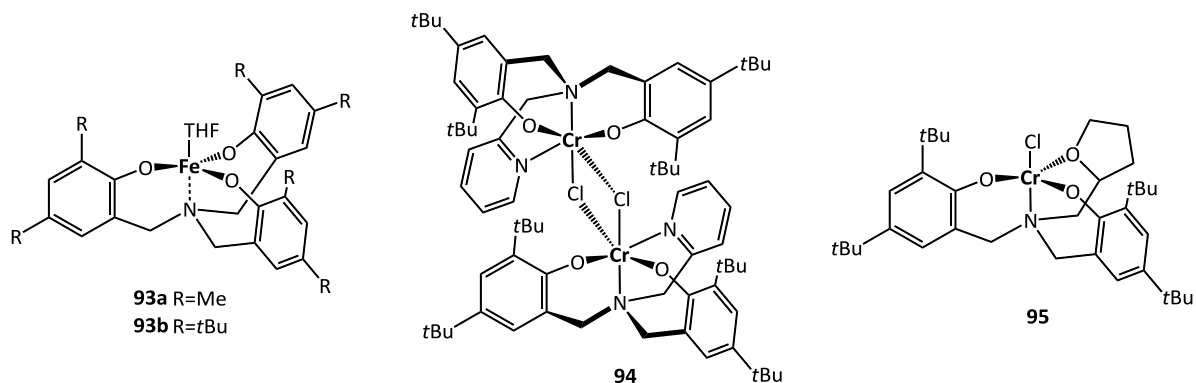
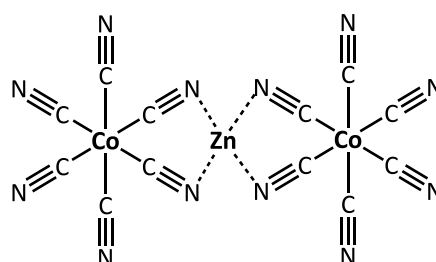


Figure 2.44: Metal amino triphenolate complexes

Iron amino-triphenolate catalysts **93a,b** (Figure 2.44) show activity up to 183 h^{-1} , but molar masses of obtained PCHC's did not overpass $6 \text{ kg}\cdot\text{mol}^{-1}$.¹⁵⁰ Chromium bis phenolate complex **94** showed activity up to 219 h^{-1} . Molar masses of prepared polycyclohexene carbonates were in range $2\text{-}13 \text{ kg}\cdot\text{mol}^{-1}$.¹⁵¹ Similarly, complex **95** afforded low molar mass PCHC ($M_n = 3\text{-}6 \text{ kg}\cdot\text{mol}^{-1}$) with activity of $12\text{-}55 \text{ h}^{-1}$.¹⁵²

Double metal cyanide (DMC) complexes were also tested for epoxide/ CO_2 copolymerization.¹⁵³ The most effective proved to be Zn-Co double metal cyanide complex **96** (Figure 2.45). In 2004, $\text{Zn}_3[\text{Co}(\text{CN})_6]$ was compared with another DMC catalyst $\text{Zn}_3[\text{Fe}(\text{CN})_6]$ in PO/ CO_2 copolymerization.¹⁵⁴ Zn-Co complex **96** afforded poly(ether-carbonate) with 40x higher activity compared to $\text{Zn}_3[\text{Fe}(\text{CN})_6]$ (180 vs. 4.5 h^{-1}). Carbonate linkage in copolymers prepared with **96** was 15-30%, selectivity to polymer reached 55-83% and molar masses of polymers were $8 \text{ kg}\cdot\text{mol}^{-1}$, however, highly crystalline $\text{Zn}_3[\text{Co}(\text{CN})_6]$, which was reported later, afforded PPC with 40% of carbonate units and molar mass $50 \text{ kg}\cdot\text{mol}^{-1}$ with activity 1200 h^{-1} .¹⁵⁵ Very recently, a comprehensive study encompassing the influence of reaction time, temperature, pressure, catalyst and comonomer loadings on

Zn₃[Co(CN)₆] catalyzed terpolymerization of PO and CHO with CO₂ was reported.¹⁵⁶ A series of poly(propylene carbonate-co-cyclohexene carbonate)s of various composition were synthesized. Afforded polycarbonates had molar masses 15-22 kg.mol⁻¹ and carbonate linkage 60-84%.



96

Figure 2.45: Structure of Zn₃[Co(CN)₆] double metal cyanide (DMC) complex

Catalytic performance of dinuclear complexes in PO/CO₂ and CHO/CO₂ copolymerization at specific experimental conditions is compared in Table 2.4.

Table 2.4: Dinuclear and bimetallic bridged complexes for epoxide/CO₂ copolymerization

Complex /Cocatalyst	Epoxide	M/CAT	T (p) (°C; MPa)	t _p (h)	TOF (h ⁻¹)	Selectivity (%)	CL ^a (%)	M _n ^b (kg.mol ⁻¹)	Đ	REF
12d/PPNCl	PO	20 000	60 (4)	24	55	90	90	15.0	1.8	146
36b	CHO	10 000	100 (1.2)	5	730	>99	>99	16.8	1.21	144a
85a	CHO	500	80 (2)	2	142	-	92	21.0	1.28	142a
87b	CHO	500	100 (1)	0.1	3700	>99	>99	8.8	1.04	144c
88/PPNCl	PO	10 000	80 (5.3)	0.5	1740	94	>99	29.9	1.07	73
89a/PPN-DNP	CHO	1000	25 (2)	0.25	1409	>99	>99	18.9	1.23	147
91c/PPN-DNP	CHO	1000	25 (2)	0.5	758	>99	92	13.8	1.15	148
92b	CHO	1600	120 (2)	24	56	>99	>99	24.9	1.21	149
94/DMAP	CHO	500	80 (2.2)	3	116	>99	98	8.0	1.10	151
96	PO	18 000	100 (8)	15	1170	98	39	49.7	3.39	155

^a Carbonate linkage;

^b Determined by SEC

2.2.2.9 Brief summary of displayed catalytic complexes

To summarize and compare basic features of displayed catalyst, we can divide aforementioned complexes into 3 main groups according to their structure.

β-diiminate zinc complexes and its derivatives are used generally for the copolymerization of CHO with CO₂ producing highly alternating PCHC with > 99% selectivity to PCHC (Table 2.1, page 27). Generally slightly higher ratio of ether linkage in copolymer can be present. These complexes did not require any cocatalyst, but they usually operate at higher temperatures and slightly higher pressure (≈ 50°C and 1 MPa). Introduction of an

electron withdrawing group into ligand framework greatly increases the activity of BDI complexes.

Metal salen complexes are versatile catalysts used for the copolymerization of various epoxide substrates from commercial PO and CHO to special epoxides with bulky substituents or polar side groups (Table 2.2, page 32). These catalysts operate even at mild conditions (1 bar, 20°C), but usually higher pressure is applied to reach the optimal activity. At higher temperatures, a significant decrease of selectivity to polymer (especially in case of PPC) can be observed. It is necessary to use nucleophilic cocatalysts with these complexes, unless bifunctional complexes are used. In this case, the formation of cyclic carbonate is efficiently suppressed even at higher temperatures. Moreover, chiral and multichiral complexes can afford iso-enriched or stereogradient PPC. Among all, cobalt salen complexes achieved the best catalytic performance and produced PPC and PCHC with > 99% of selectivity and carbonate linkage. An extensive research on this type of catalysts revealed that for the best catalytic performance a proper choice of nucleophilic group attached to metal center as well as type of cocatalyst is necessary. The best results were achieved with weak nucleophiles attached to Co metal (pentafluorobenzoate, trichloroacetate and dinitrophenolate) in combination with PPNCI cocatalyst. Introduction of ammonium side arms into the ligand framework led to tremendous increase of activity of such complexes (Table 2.3, page 39).

Porphyrin complexes were used preferentially for the copolymerization of PO with CO₂. Metal porphyrins usually require higher temperatures and pressures. The presence of neutral or nucleophilic cocatalyst is necessary except for bifunctional porphyrin complexes, which also exhibit significantly higher activities. Among various metal-porphyrin complexes, the best catalytic performance was achieved especially with cobalt and aluminium porphyrins with side arms attached to the ligand framework (Table 2.3, page 39). Produced PPC has usually slightly lower selectivity (90-96%) compared to salen catalysts.

2.2.3 Copolymerization of special and biobased epoxides with CO₂

Mostly explored polycarbonates, PPC and PCHC (from oil-based epoxides), generally suffer from poor mechanical properties such as low rigidity (PPC) and brittleness (PCHC). Although some polymer properties can be improved by a proper choice of catalytic system (e.g. by synthesis of isotactic or stereogradient polycarbonates), the use of alternative epoxide substrates is a strategy, which can lead to the significant improvement of polycarbonate properties.

In order to prepare polycarbonates from fully renewable sources, epoxides prepared by oxidation of natural compounds containing a double bond (fatty acid, terpenes) must be copolymerized with CO₂. The large library of such compounds was already tested together with special epoxides manufactured mostly in laboratory scale (Figure 2.46).

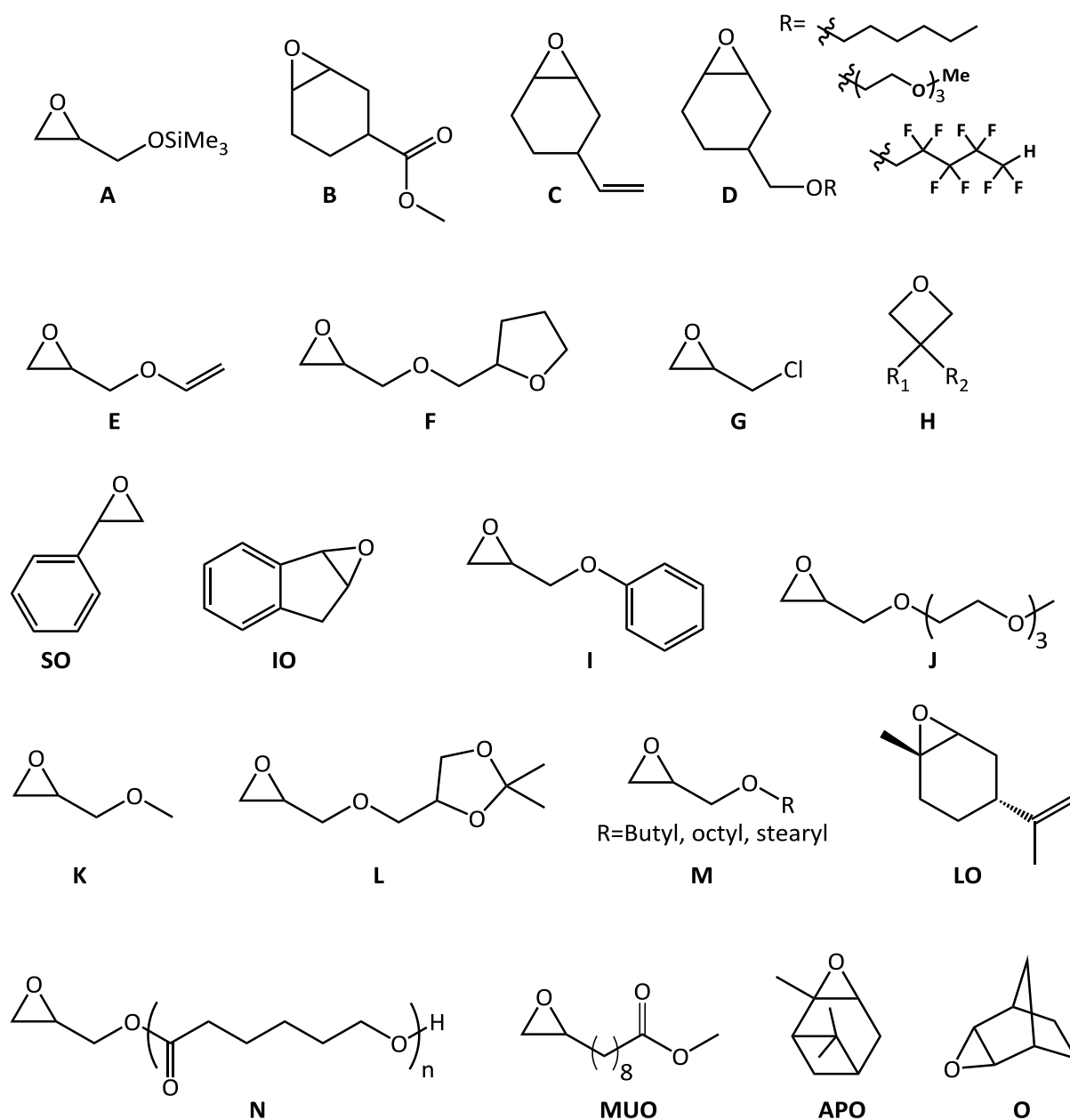


Figure 2.46: Scope of noncommercial and biobased epoxides

The first attempts to use special epoxides and CO₂ for polycarbonate syntheses were performed already in 1979 when Et₂Zn/H₂O catalytic system was used for the copolymerization of CO₂ with trimethylsilyl glycidyl ether (**A**) (Figure 2.46). Following hydrolysis of copolymer silyl groups resulted in degradable polycarbonate with side hydroxyl groups.¹⁵⁷

The copolymerization of ester-functionalized cyclohexene oxide (**B**) using BDI ZnOEt complex led to the formation of branched or cyclic polycarbonates with M_n 2.3 kg.mol⁻¹.¹⁵⁸ In 2011 Coates et al. reported living copolymerization of CHO with a series of functionalized cyclohexene oxides (**C**, **D** and others) catalyzed with BDI complex **44** (Figure 2.19, page 25) to produce block copolymers with lipophilic, hydrophilic and fluorophilic blocks.¹⁵⁹ Polycarbonates with high M_n 133 kg.mol⁻¹ and 77 kg.mol⁻¹ and glass transition temperatures around -20°C and 7°C respectively were obtained by the copolymerization of CO₂ with

allyl glycidyl ether (**E**)¹⁶⁰ or furfuryl glycidyl ether (**F**) with yttrium based complexes (e.g. $Y(\text{CCl}_3\text{OO})_3\text{-ZnEt}_2\text{-glycerine}$).¹⁶¹ With an enantiopure salen Co complex (**74a**, Figure 2.30, page 35), isotactic poly(chloropropylene carbonate) was obtained by the copolymerization of epichlorohydrin (**G**) with CO_2 .¹⁶² Poly(chloropropylene carbonate) is a typical semicrystalline thermoplastic polymer possessing T_g of 42°C and a T_m of 108°C. The yield strength and tensile strength of this crystalline copolymer are 10-30 times higher compared to its amorphous counterpart. Oxetane compounds (**H**) were also studied as monomers in the coupling reaction with CO_2 to produce polycarbonates.¹⁶³ Except the direct CO_2 -oxetane copolymerization (catalyzed by **31b**, Figure 2.12, page 15), analogous polycarbonates can be achieved via ring-opening polymerization (ROP) of generated six-membered cyclic carbonate monomers (e.g. trimethylene carbonate (TMC)).¹⁶⁴

Properties of aliphatic polycarbonates can be manipulated for example by using more rigid comonomers. The typical example could be polystyrene carbonate (PSC). It was first synthesized from styrene oxide (**SO**) and CO_2 with chiral salenCo-DNP complexes (Figure 2.30, page 35)¹⁶⁵ or with double metal cyanide complexes.¹⁶⁶ As expected, synthesized PSC exhibited high thermal stability 300°C and also relatively high glass transition temperature 80°C. The terpolymerization of SO with CO_2 and CHO led to further increase in T_g of polycarbonate to 112°C.¹⁶⁷ The use of rigid indene oxide (**IO**) as a monomer for the copolymerization with CO_2 catalyzed with **56h** (Figure 2.24, page 28) or **74c** (Figure 2.30, page 35) resulted in polycarbonates with rigid backbone with high thermal stability up to 250°C and T_g in range 109-138°C, although molar masses of resulting poly(indene carbonate)s did not overpass $10 \text{ kg}\cdot\text{mol}^{-1}$.¹⁶⁸ Isotactic semicrystalline polycarbonate with $T_m = 75^\circ\text{C}$ was recently afforded by the copolymerization of phenyl glycidyl ether (**I**) with CO_2 using salenCo-DNP complex with TBD side arm (**74**, Figure 2.30, page 35).¹⁶⁹

New hydrophilic epoxide ((2,5,8,11-tetraoxadodec-1-yl)oxirane; **J**), prepared by the reaction of epichlorohydrin with triethyleneglycol monomethyl ether, was successfully copolymerized with propylene oxide and CO_2 by complex **56e** (Figure 2.24, page 28).¹⁷⁰ Resultant polycarbonates contained variable mole fractions of monomer **J** in the copolymer and they were more hydrophilic compared to PPC. Furthermore, terpolymers with > 25% of monomer **J** showed rapid and reversible thermo-responsive properties in water, which make this copolymers a promising material for biomedical applications.

A series of functional polycarbonates were prepared by the copolymerization of glycidyl methyl ether (**K**) and protected glycidyl ether derivative (**L**) with CO_2 by $\text{ZnEt}_2/\text{pyrogallol}$.¹⁷¹ Subsequent acidic hydrolysis of acetal protecting groups afforded a new type of functional polycarbonate – poly ((glyceryl glycerol)-*co*-(glycidyl methyl ether) carbonate). Prepared glycerol-functionalized polycarbonates are amorphous with $T_g = -5^\circ\text{C}$ and molar masses $12\text{-}25 \text{ kg}\cdot\text{mol}^{-1}$. Poly(carbonate)s possessing pendant butyl, octyl and stearyl ether groups were prepared by the copolymerization of alkyl glycidyl ethers (**M**) with CO_2 catalyzed with salenCo-DNP complex with TBD side arm (**74**, Figure 2.30, page 35).¹⁷² Polycarbonates with butyl and octyl-ether substituents posed T_g below -20°C , while the polymer containing

stearyl ether groups exhibited a melting point of 55°C instead of T_g . Prepared polycarbonates were thermally stable and their molar masses varied from 8 to 32 kg.mol⁻¹. The most thermally stable ($T_{deg(5\%)} = 220^\circ\text{C}$) was the polycarbonate containing butyl ether substituents. This polymer is a viscoelastic material, it flows at elevated temperatures and moreover, it exhibits high conductivity. Therefore, this material has a potential as a thermally stable solid polymer electrolyte.

The synthesis of completely alternating polycarbonate from renewable limonene oxide (**LO**), which is derived from cyclic monoterpene limonene naturally occurring in citrus fruit, was performed by Coates et al.¹⁷³ As catalysts, a series of BDI-ZnOAc complexes was used, while the best catalytic performance exhibited complex **44** (Figure 2.19, page 25). Prepared polycarbonates had high T_g (111°C) and molar masses in the range 5-11 kg.mol⁻¹. The enzymatic synthesis of epoxy-functionalized PCL (**N**) and subsequent copolymerization with CO₂ or with anhydride catalyzed by ZnO₂/glutaric acid (and benzyldimethylamine respectively) produced novel graft and hyperbranched copolymers with hydroxyl-terminal groups.¹⁷⁴

Bio-based fatty acid derivative (methylundec-10-enoate oxide; **MUO**) was successfully transformed to completely alternating, biodegradable polycarbonate with terminal hydroxyl groups and low T_g (-40°C) using Zn-Co DMC catalyst.¹⁷⁵ This polymer, together with limonene oxide-based polycarbonate, is an example of 100% bio-based copolymer. More sterically demanding epoxides such as α -pinene oxide (**APO**) and exo-norbornene oxide (**O**) were not transferred to the polycarbonate yet.

3 MOTIVATION AND GOALS OF THE THESIS

The synthesis of new polymeric materials from renewable resources is of high research interest for both academia and industry. Several promising routes to less oil-dependent (or completely renewable) polymers were reviewed in the introduction part, namely: **polycarbonates** and **polyesters** formed by the copolymerization of **epoxides** with **CO₂** or **CO**, respectively.

The direct one-pot preparation of synthetic PHB by the reaction of CO with epoxide (through in situ formed BBL) described by Coates represents an interesting way to production of PHB without the need of manipulation of toxic BBL.¹³ The crucial point of the process is a mutual tolerance of two catalysts (for carbonylation and ROP) and their sufficient activity in the **tandem catalytic process**.

Less challenging, but recently significantly reinvestigated in the literature, is the preparation of **polyesters** by the ring-opening copolymerization of epoxides with anhydrides⁵⁰ that could be understood as products of double epoxide carbonylation. Thus, in summation, two molecules of CO react with two molecules of epoxide resulting in two monomer units that could be otherwise formed by direct copolymerization of one epoxide molecule with one CO molecule.

All the mentioned copolymerizations can be catalyzed (initiated) by similar catalytic systems. In this work the main effort was focused on the development of **salphen transition metal complexes** (Co, Cr) that were less studied compared to their salen analogues. **Iron** was decided to be used for the first time as the central atom of analogous salphen and salen complexes as a cheap and non-toxic alternative to the most popular metals like Cr and Co.¹⁷⁶ During this work we surprisingly found that the ROP of epoxides with anhydrides can be activated just by an **organic base** which is normally used as a cocatalyst of salphen or salen complexes. Despite of the lower activity of this **fully organic initiation system** compared to combined system (metal complex/organic base), it represents i) simple and ii) highly “green” initiating system. Simultaneously, an undesired polymer coloration, another serious problem of transition metal based systems (Cr, Co, Fe), can be solved by this approach.

The research of carbon oxides copolymerization with epoxides has been intensively developed in the last 15 years. However, no viable catalyst with sufficient catalytic activity and simple preparation procedure was found despite the copolymerization reactions are thermodynamically favorable. On the other hand, relatively limited library of transition metals and ligands has been investigated so far. Therefore, a **further search for completely new complexes** is necessary, similarly as it led to a great success of heterogeneous Ziegler catalysts for olefin polymerizations.

The aims of the Thesis can thus be concluded in following points:

1. Synthesis of novel Cr and Co salen complexes with variation of nucleophilic counterions as this structural motive was only marginally studied in the literature and plays an important role in the catalytic process.
2. Investigation of catalytic behavior of prepared complexes in epoxide/CO and epoxide/CO₂ copolymerizations.
3. Searching for new families of catalysts for epoxide-CO₂ copolymerization based on rarely investigated metals (iron, lanthanoids) or highly activating ligands (ketiminate, amidinates, β-diiminate). Significant part of investigated catalysts was accessible due to the collaboration with group of prof. A. Růžička (University of Pardubice).
4. Investigation of one-pot dual catalysis of salen chromium complexes (ROP) with Co₂(CO)₈ (carbonylation) in CO/epoxide reaction in order to prepare synthetic PHB.
5. Investigation of metal free initiating systems for the ROP of epoxides with anhydrides.

4 EXPERIMENTAL PART

4.1 General experimental details

All manipulations involving air and water sensitive compounds were carried out under dry nitrogen atmosphere using standard Schlenk techniques. Air and water sensitive catalysts were stored in Schlenk flasks at room temperature or in the fridge at 5°C. All solvents and monomers were dried with suitable drying agent prior to use and stored under nitrogen atmosphere unless otherwise noted.

4.2 Used chemicals

Nitrogen (5.0, SIAD) was purified by passing through deoxygenating and drying columns. Oxygen (99%, SIAD) was purified by passing through 4Å activated molecular sieves. CO (SIAD) and CO₂ (4.8, SIAD) were used without further purification. Toluene (Penta) and xylene (Chemapol) were dried by a distillation over sodium metal under N₂ atmosphere. Chloroform, dichloromethane and hexane (Penta) were dried over CaH₂ and distilled under N₂ atmosphere. THF and diethyl ether (Penta) were pre-dried by a distillation from CaH₂ and then dried over sodium with benzophenone ketyl and distilled under N₂ atmosphere.

1,2-phenylenediamine (98%), 4-chloro-1,2-phenylenediamine (97%), 3,5-ditertbutyl-2-hydroxybenzaldehyde (99%) (Aldrich), cobalt(II)acetate tetrahydrate (98%) chromium(II) chloride (97%, anhydrous), pentafluorobenzoic acid (99%) and trichloroacetic acid (99%), (Alfa Aesar) and dicobaltoctacarbonyl (stabilized with 1-5% of hexane, STREM) were used as received. 2,4-Dinitrophenol (Aldrich, stabilized with 15% H₂O) was dried under high vacuum to remove water prior to use. DMAP (99%, Aldrich) was recrystallized twice from dry hot toluene, PPNCl (97%, ABCR) was recrystallized from dry CH₂Cl₂/Et₂O, *n*-Bu₄NCl (98%, TCI) and *n*-Bu₄NBr (p.a. Lachema) were recrystallized from dry acetone/Et₂O, triphenylphosphine (97%, Fluka) was recrystallized from dry hexane. 1,5,7-Triazabicyclo[4.4.0]dec-5-ene (98%) and 1,4-diazabicyclo[2.2.2]octane (99%) (both from Aldrich) were used as received.

Propylene oxide (99%), styrene oxide (97%), cyclohexene oxide (98%) and α and β-pinene oxide (98%) (Sigma-Aldrich) were dried over CaH₂, distilled under vacuum and stored under N₂ atmosphere. Methylundec-10-enoate oxide and indene oxide (obtained by Ru catalyzed epoxidation of indene and kindly provided by M. Štekrová, UCT Prague) were dried over 4Å activated molecular sieves. Technical methyl stearate oxide prepared by epoxidation of biodiesel was kindly provided by Prof. Gläser (University of Leipzig) and used as received. β-Diiminate, ketiminate and aminidate complexes of Al, Zn and Mg used in chapter 5.4.5 were kindly supplied by Prof. Růžička (University Pardubice) and used as received.

Phthalic anhydride (99%, Aldrich and Alfa Aesar), tetrachlorophthalic anhydride (96%), cyclohexane anhydride (95%) (Aldrich), maleic anhydride (99%, Fluka) and succinic anhydride

(99%, Acros) were used as received or purified by sublimation or recrystallization. Methylundec-10-enoate (96%, TCI) and *meta*-chloroperoxybenzoic acid (77%, Aldrich) were used as received.

Water content of liquid monomers and solvents was determined by Karl Fischer titration.

4.3 Synthesis of catalysts

4.3.1 Synthesis of ligands

N,N'-Bis(3,5-di-*tert*-butylsalicylidene)-1,2-phenylenediamine (**1**) and *N,N'*-Bis(3,5-di-*tert*-butylsalicylidene)-4-chloro-1,2-phenylenediamine (**2**) were synthesized according to the literature.^{42b}

N,N'-Bis(3,5-di-*tert*-butylsalicylidene)-1,2-phenylenediamine (**1**)

A 250 mL round bottom flask was charged with 1,2-phenylenediamine (1.17 g, 10.6 mmol) and 2.4 equivalent of 3,5-ditertbutyl-2-hydroxybenzaldehyde (6.09 g, 26 mmol). Reactants were flushed with nitrogen. Absolute ethanol (150 mL) was then added. The reaction mixture was refluxed for 24 h and then slowly cooled to room temperature. The suspension was filtered in air atmosphere, recrystallized from ethanol and dried at room temperature under high vacuum overnight. Yellow needle-like crystals were obtained. $Y_w = 79\%$.

¹H NMR (CDCl₃, 500 MHz): δ (ppm) 1.33(s, 18H, -CH₃), 1.44 (s, 18H, -CH₃), 7.22-7.44 (m, 4H, Ar-H); 8.67 (s, 2H, =NH-), 13.53 (s, 2H, Ar-OH).

N,N'-Bis(3,5-di-*tert*-butylsalicylidene)-4-chloro-1,2-phenylenediamine (**2**)

Ligand **2** was synthesized by a similar procedure as ligand **1**. Ligand was recrystallized twice from ethanol. Orange needle-like crystals were obtained. $Y_w = 88\%$.

¹H NMR (CDCl₃, 500 MHz): δ (ppm) 1.32 (s, 18H, -CH₃), 1.43 (s, 18H, -CH₃), 7.17-7.47 (m, 3H, Ar-H); 8.64 (s, 2H, =NH-), 13.27 (s, 1H, Ar-OH), 13.36 (s, 1H, Ar-OH).

4.3.2 Synthesis of complexes

(N,N'-Bis(3,5-di-*tert*-butylsalicylidene)-1,2-phenylenediamine) Chromium (III) chloride (**1-CrCl**)

1-CrCl complex was synthesized according to the literature procedure.¹⁷⁷ A 100 mL Schlenk flask purified by a few vacuum/N₂ cycles was charged with 0.87 g (1.6 mmol) of **1** and 1.3 equivalent of chromium(II)chloride (0.26 g, 2.1 mmol). Reactants were dissolved in 30 mL of dry THF and stirred under nitrogen at ambient temperature for 24 h. The reaction mixture was then exposed to air and stirred another 24 h. Subsequently, 30 mL of diethyl ether was added. The organic layer was washed with aqueous saturated solution of NH₄Cl

(4x100 mL) and with brine (4x 100 mL). Organic phase was then dried with Na₂SO₄ for 48 h. After filtration, solvent was removed in vacuo and resultant dark brown powder was dried at room temperature under high vacuum for 24 h. Y_w = 98%.

MS-ESI⁺ (m/z, M⁺) = 590.2956; Calcd. for [C₃₆H₄₆N₂O₂Cr]⁺: 590.2959.

IR (ATR, cm⁻¹): 2951, 2903, 2866, 1601, 1577, 1524, 1482, 1460, 1425, 1255, 1195, 1170, 1133, 1025, 869, 837, 785, 747, 537.

EA calculated for [C₃₆H₄₅N₂O₂ClCr.(C₄H₈O)] (%): C 68.80; H 7.79; N 4.01; Found: C 68.53; H 7.71; N 4.14.

(N,N'-Bis(3,5-di-tert-butylsalicylidene)-4-chloro--1,2-phenylenediamine) Chromium (III) chloride (2-CrCl)

2-CrCl complex was synthesized by a similar procedure as complex **1-CrCl**, with exception, that 0.749 g (1.3 mmol) of ligand **2** was used. Y_w = 99%.

MS-ESI⁺ (m/z, M⁺) = 624.2568; Calcd. for [C₃₆H₄₅ClN₂O₂Cr]⁺: 624.2569.

IR (ATR, cm⁻¹): 2952, 2903, 2866, 1596, 1573, 1522, 1481, 1422, 1358, 1255, 1195, 1171, 1120, 1022, 930, 839, 804, 784, 749, 539.

EA calculated for [C₃₆H₄₅N₂O₂Cl₂Cr.(C₄H₈O)] (%): C 65.56; H 7.29; N 3.82; Found: C 65.80; H 8.13; N 4.19.

(N,N'-Bis(3,5-di-tert-butylsalicylidene)-1,2-phenylenediamine) Iron (III) chloride (1-FeCl)

N,N'-Bis(3,5-di-tert-butylsalicylidene)- 1,2-phenylene diamine (**1**) (0.239 g, 0.44 mmol) was transferred to a Schlenk flask filled with 1.3 eq. of FeCl₂ (0.074 g, 0.58mmol) under nitrogen. The mixture was dissolved in dried THF and stirred for 20 h at room temperature. Then the Schlenk flask was opened to air and solution was allowed to stir for at least 48 h. After the addition of 2,6-lutidine (2.6 eq.) the solution was stirred for another 24 hours. The organic solution was diluted with *tert*-butyl methyl ether and washed three times with saturated NaCl and NH₄Cl solutions and dried over Na₂SO₄. The filtered solution was evaporated and the obtained black powder was dried under high vacuum. Y_w = 87%.

MS-ESI⁺ (m/z, M⁺) = 594.2909; Calcd. for [C₃₆H₄₆N₂O₂Fe]⁺: 594.2903.

EA calculated for [C₃₆H₄₆N₂O₂ClFe.C₄H₈O)] (%): C 68.42; H 7.75; N 3.99; Found: C 68.62; H 7.46; N 4.15.

IR (ATR, cm⁻¹): 2957, 2867, 1607, 1597, 1577, 1530, 1461, 1424, 1379, 1356, 1315, 1250, 1197, 1180, 839, 782, 744, 543.

(N,N'-Bis(3,5-di-tert-butylsalicylidene)-4-chloro-1,2-phenylenediamine) Iron (III) Chloride (2-FeCl)

The complex **2-FeCl** was prepared by the same procedure as complex **1-FeCl** using *N,N'*-bis(3,5-di-*tert*-butylsalicylidene)-4-chloro-1,2-phenylenediamine (**2**) (0.186 g, 0.32 mmol) and 1.3 eq. of FeCl₂ (0.054 g, 0.43 mmol). $Y_w = 99\%$.

MS-ESI⁺ (m/z, M⁺) = 628.2523; Calcd. for [C₃₆H₄₅ClN₂O₂Fe]⁺: 628.2514.

EA calculated for [C₃₆H₄₅N₂O₂Cl₂Fe.(C₄H₈O)] (%): C 65.22; H 7.25; N 3.80; Found: C 66.13; H 7.30; N 3.59.

IR (ATR, cm⁻¹): 2959, 2868, 1609, 1595, 1575, 1530, 1484, 1462, 1424, 1379, 1361, 1316, 1250, 1196, 1178, 841, 782, 744, 542.

(N,N'-Bis(3,5-di-tert-butylsalicylidene)-1,2-phenylenediamine) Cobalt(II) (1-Co)

Complex **1-Co** was synthesized according to the modified literature procedure.¹⁷⁸ A 250 mL Schlenk flask was charged with ligand **1** (2.06 g, 3.8 mmol) and degassed ethanol (150 mL). Suspension was heated to 50 °C until complete ligand dissolution. Then 0.85 eq. of cobalt(II)acetate tetrahydrate (0.8 g, 3.2 mmol) was dissolved in 30mL of degassed EtOH and immediately added dropwise to the solution of ligand **1**. The flask was heated to 80 °C for 30 min and then slowly cooled to room temperature. Suspension was concentrated to ca. 70 mL, filtered under nitrogen atmosphere and washed with cold (-20 °C) dried methanol. The dark red/brown powder was recrystallized by dissolving it in dry dichloromethane (30 mL) and layered with dry hexane (700 mL). The solution was let few days to recrystallize in the fridge and then filtered under nitrogen atmosphere and dried 24 h under high vacuum. $Y_w = 80\%$.

MS-ESI⁺ (m/z, M⁺) = 597.2888; Calcd. for [C₃₆H₄₆N₂O₂Co]⁺: 597.2886.

It was not possible to determine ¹H NMR spectrum of **1-Co** due to its poor solubility in organic solvents.

IR (ATR, cm⁻¹): 2954, 2902, 2866, 1613, 1574, 1543, 1519, 1489, 1463, 1424, 1386, 1355, 1323, 1249, 1198, 1178, 1161, 1131, 930, 918, 785, 740, 638.

(N,N'-Bis(3,5-di-tert-butylsalicylidene)-4-chloro-1,2-phenylenediamine) Cobalt(II) (2-Co)

Complex was synthesized by a similar procedure as complex **1-Co**, with an exception, that 2.05 g (3.57 mmol) of ligand **2** was used. $Y_w = 90\%$

MS-ESI⁺ (m/z, M⁺) = 631.2499; Calcd. for [C₃₆H₄₅N₂O₂ClCo]⁺: 631.2496.

IR (ATR, cm⁻¹): 2953, 2904, 2867, 1607, 1574, 1543, 1519, 1484, 1463, 1425, 1387, 1358, 1334, 1261, 1197, 1170, 1161, 1131, 1122, 1090, 935, 910, 785, 806, 748.

¹H NMR (DMSO-d₆, 500 MHz): δ (ppm) 1.33 (s, 18H, -CH₃ (b)), 1.69 (s, 18H, -CH₃ (a)), 7.39 (s, 2H, Ar-H (g)); 7.47 (m, 2H, Ar-H (i)), 7.50 (d, 1H, Ar-H (o)), 8.47 (d, 1H, Ar-H (p)), 8.61 (s, 1H, Ar-H (m)), 8.71 (s, 1H, -N=CH- (k')), 8.77 (s, 1H, -N=CH- (k)).

^{13}C NMR (DMSO- d_6 , 500 MHz): 30.09 (-CH₃ (a)), 31.24 (-CH₃(c)), 33.61 (-C(CH₃)₃ (d)), 35.84 (-C(CH₃)₃ (b)), 116.10 (=CH-Ar, (m)), 116.91 (=CH-Ar, (p)), 117.76 (=C-Ar, (j)), 125.90 (=C-Ar, (o)), 129.13(=CH-Ar, (i)), 129.57 (=CH-Ar, (g)), 131.09 (=CCl-Ar (n)), 134.59 (=C-Ar (f)), 141.63 (=C-Ar (h)), 145.31(=C-Ar, (q)), 147.35(=C-Ar, (l)), 159.97 (-N=CH-, (k')), 160.48 (-N=CH-, (k)), 166.06 (=C-O Ar (e')), 166.46 (=C-O Ar (e)).

(N,N'-Bis(3,5-di-tert-butylsalicylidene)-1,2-phenylenediamine) Cobalt(III)-OCCCl₃ (1-Co-OCCCl₃)

A 1 eq. of trichloroacetic acid (0.1840 g, 1 mmol) in CH₂Cl₂ (15 mL) was added to a stirred mixture of **1-Co** (0.6040g, 1 mmol) dissolved in dry CH₂Cl₂ (20 mL). The solution was stirred under dry oxygen atmosphere at room temperature for 90 min. The solvent was removed in vacuo and dark red/brown solid was dried under high vacuum. Crude product was washed with dry hexane (3x20 mL) and dried 24h under high vacuum. $Y_w = 78\%$.

MS-ESI^{+/-} (m/z, M⁺) = 597.2883; Calcd. for [C₃₆H₄₆N₂O₂Co]⁺: 597.2886; MS-ESI^{+/-} (m/z, M⁻): 163.8383.

^1H NMR (DMSO- d_6 , 500 MHz): δ (ppm) 1.35 (s, 18H, -CH₃ (c)), 1.78 (s, 18H, -CH₃ (a)) 7.56 (-,4H, Ar-H (i,g)), 7.66 (s, 2H, Ar-H (n)), 8.63 (m, 2H, Ar-H (m)), 8.94 (s, 2H, -N=CH-(k)), 9.61 (broad, 1H, COO-H-O-Ar(z)).

IR (ATR, cm⁻¹): 2959, 2905, 2868, 1718, 1704 (C=O vibrations of CCl₃COO⁻), 1612, 1578, 1546, 1519, 1486, 1461, 1418, 1387, 1358, 1330, 1288 (C-O vibration of CCl₃COO⁻), 1199, 1182, 1167, 1133, 1110, 883 (C-Cl vibration of CCl₃COO⁻), 753, 676.

EA calculated for [C₃₆H₄₆N₂O₂Co.(C₂Cl₃O₂)_{1.75}] (%): C 53.80; H 7.76; N 3.18; Found: C 53.93; H 5.37; N 3.28.

(N,N'-Bis(3,5-di-tert-butylsalicylidene)-1,2-phenylenediamine) Cobalt(III)-DNP (1-Co-DNP)

It was synthesized as a similar procedure of the complex **1-Co-OCCCl₃**. Crude product was washed with a mixture of dry hexane/ethyl acetate (50/50) (3x20 mL) and dried 24 h under high vacuum. $Y_w = 61\%$.

MS-ESI^{+/-} (m/z, M⁺) = 597.2888; Calcd. for [C₃₆H₄₆N₂O₂Co]⁺: 597.2886; (m/z, M⁻): 183.0041; Calcd. for [C₆H₃N₂O₅]⁻: 183.0036.

^1H NMR (DMSO- d_6 , 500 MHz): δ (ppm) 1.35 (s, 18H, -CH₃ (c)), 1.78 (s, 18H, -CH₃ (a)), 6.42 (broad, 1H, Ar-H (DNP)), 7.56 (4H, Ar-H (i,g)), 7.65 (s, 2H, Ar-H (n)), 7.84 (broad, 1H, Ar-H (DNP)), 8.63 (3H, Ar-H (m+r(DNP))), 8.93 (s, 2H, -N=CH-(k)).

IR (ATR, cm⁻¹): 2952, 2904, 2867, 1610, 1576 (N=O vibration of DNP), 1519, 1519, 1489, 1462, 1428, 1389, 1358, 1319 (N=O vibration of DNP), 1267, 1248, 1197, 1174, 1130, 936, 919, 833, 784, 743.

EA calculated for [C₃₆H₄₆N₂O₂Co.(C₆N₂O₅)_{0.85}] (%): C 65.53; H 6.50; N 6.88; Found: C 65.53; H 6.76; N 6.28.

(*N,N'*-Bis(3,5-di-*tert*-butylsalicylidene)-1,2-phenylenediamine) Cobalt(III)-OBzF₅ (1-Co-OBzF₅)

It was synthesized by a similar procedure as the complex **1-Co-OOCCCl₃**. $Y_w = 53\%$.

MS-ESI⁺ (m/z, M⁺) = 597.2893; Calcd. for [C₃₆H₄₆N₂O₂Co]⁺: 597.2886; (m/z, M⁻): 166.9932; Calcd. for [C₆F₅]⁻: 166.9926; and (m/z, M⁻): 210.9817; Calcd. for [C₇F₅O₂]⁻: 210.9824.

¹H NMR (DMSO-d₆, 500 MHz): δ (ppm) 1.35 (s, 18H, -CH₃ (c)), 1.79 (s, 18H, -CH₃ (a)) 7.57 (-, 4H, Ar-H (i,g)), 7.67 (s, 2H, Ar-H (n)), 8.65 (dd, 2H, Ar-H (m)), 8.95 (s, 2H, -N=CH-(k)), 9.57 (broad, 1H, COO-H-O-Ar(z)).

¹⁹F NMR (500 MHz, DMSO-d₆): -138.96, -143.73, -154.57, -157.57, -162.28.

IR (ATR, cm⁻¹): 2955, 2906, 2869, 1734, 1666, 1651 (C=O vibrations of OBzF₅⁻), 1612, 1592, 1581, 1520, 1485, 1463, 1423, 1387 (C-F vibration of OBzF₅⁻), 1356, 1331, 1274, 1241, 1197, 1170, 1133, 1112, 995 (C-F vibration of OBzF₅⁻), 761, 749.

EA calculated for [C₃₆H₄₆N₂O₂Co.(C₇F₅O₂)_{1.75}](%): C 59.93; H 4.79; N 2.90; Found: C 60.00; H 5.32; N 2.89.

Crystals suitable for X-ray analysis were prepared by a layering technique (solvent diffusion). Ca. 10 mg of complex **1-Co-OBzF₅** was placed into a dry clean NMR tube under nitrogen and dissolved in ca. 0.3 mL of dry CH₂Cl₂. The solution was then layered by slow dribbling of dry hexane (2.5-3 mL). The NMR tube was then carefully placed in a quiet place for 2-3 weeks until dark red block-shaped crystals occurred. Supplementary crystallographic data for the complex **1-Co-OBzF₅** are displayed in chapter 8.2 page 129.

(*N,N'*-Bis(3,5-di-*tert*-butylsalicylidene)-4-chloro-1,2-phenylenediamine) Cobalt(III)-OBzF₅ (2-Co-OOCCCl₃)

It was synthesized by a similar procedure as the complex **1-Co-OOCCCl₃** using precursor **2-Co**. $Y_w = 52\%$.

MS-ESI^{+/-} (m/z, M⁺) = 631.2497; Calcd. for [C₃₆H₄₅N₂O₂ClCo]⁺: 631.2496; MS-ESI^{+/-} (m/z, M⁻) = 163.8381.

¹H NMR (DMSO-d₆, 500 MHz): δ (ppm) 1.35 (s, 18H, -CH₃ (c)), 1.77(s, 18H, -CH₃ (a)), 7.40 (s, 2H, Ar-H (g)); 7.56 (m, 2H, Ar-H (i)), 7.65 (d, 1H, Ar-H (o)), 8.55 (d, 1H, Ar-H (p)), 8.70 (s, 1H, Ar-H (m)), 8.93 (s, 1H, -N=CH- (k')), 8.97 (s, 1H, -N=CH- (k)).

IR (ATR, cm⁻¹): 2958, 2907, 2869, 1761, 1697 (C=O vibrations of CCl₃COO⁻), 1603, 1580, 1522, 1483, 1418, 1383, 1359, 1307 (C-O vibration of CCl₃COO⁻), 1254, 1197, 1167, 1126, 1092, 937, 836 (C-Cl vibration of CCl₃COO⁻), 755, 683.

EA calculated for [C₃₆H₄₅N₂O₂ClCo.(C₂Cl₃O₂)_{2.05}] (%): C 49.91; H 4.70; N 2.90; Found: C 50.01; H 5.13; N 2.81.

(N,N'-Bis(3,5-di-tert-butylsalicylidene)-4-chloro-1,2-phenylenediamine) Cobalt(III)-DNP (2-Co-DNP)

It was synthesized by a similar procedure as the complex **2-Co-OCCCl₃**. Crude product was washed with mixture of dry hexane/ethyl acetate (50/50) (3x20 mL) and dried 24 h under high vacuum. $Y_w = 65\%$.

MS-ESI^{+/-} (m/z, M⁺) = 631.2499; Calcd. for [C₃₆H₄₅N₂O₂ClCo]⁺: 631.2496; (m/z, M⁻): 183.0055; Calcd. for [C₆H₃N₂O₅]⁻: 183.0047.

¹H NMR (DMSO-d₆, 500 MHz): δ 1.35 (s, 18H, -CH₃ (c)), 1.78 (s, 18H, -CH₃ (a)), 6.99 (broad, 1H, Ar-H (t(DNP))), 7.40 (s, 2H, =CH- (g)); 7.56 (s, 2H, Ar-H (i)), 7.65 (s, 1H, Ar-H (o)), 8.20 (broad, 1H, Ar-H (s(DNP))), 8.55 (d, 1H, Ar-H (p)), 8.70 (m, 2H, Ar-H (m+r(DNP))), 8.93 (s, 1H, -N=CH- (k')), 8.97 (s, 1H, -N=CH-(k)).

IR (ATR, cm⁻¹): 2952, 2904, 2867, 1600, 1573, 1545, 1519, 1483, 1462, 1424, 1389, 1357, 1327 (N=O vibration of DNP), 1262, 1196, 1174, 1131, 1122, 934, 912, 835, 783, 744.

EA calculated for [C₃₆H₄₅N₂O₂ClCo.(C₆N₂O₅)_{1.80}] (%): C 58.45; H 5.28; N 8.16; Found: C 58.40; H 5.75; N 6.37.

(N,N'-Bis(3,5-di-tert-butylsalicylidene)-4-chloro-1,2-phenylenediamine) Cobalt(III)-OAc (2-Co-OAc)

It was synthesized according to the modified literature procedure.¹⁷⁸ Complex **2-Co** (1.20 g, 1.90 mmol) was dissolved in tetrahydrofuran (25 mL). 1.2 eq. of acetic acid (0.05 mL, 2.30 mmol) was then added and brown suspension was stirred for one week open to air at room temperature while solvent was allowed to evaporate. The resulting reddish brown powder was washed with pentane and dried under high vacuum for 18 h. $Y_w = 99\%$.

MS-ESI⁺ (m/z, M⁺) = 631.2484; Calcd. for [C₃₆H₄₅N₂O₂ClCo]⁺: 631.2496.

Complex **2-Co-OAc** was very poorly soluble in organic solvents. Displayed NMR spectrum of **2-Co-OAc** in DMSO is therefore not quantitative. ¹H NMR (DMSO-d₆, 500 MHz): δ (ppm) 1.35 (-CH₃ (c)), 1.77 (-CH₃ (a)), 7.40 (Ar-H (g)); 7.57 (Ar-H (i)), 7.65 (Ar-H (o)), 8.66 (Ar-H (p)), 8.80 (Ar-H (m)), 8.93 (-N=CH- (k')), 8.97 (-N=CH- (k)).

IR (ATR, cm⁻¹): 3550, 2950, 2903, 2866, 1603, 1572, 1519, 1484, 1462, 1424, 1357, 1263, 1197, 1173, 1159, 1121, 934, 785.

EA calculated for [C₃₆H₄₅N₂O₂ClCo.(C₂H₃O₂)_{1.30}] (%): C 65.40; H 6.95; N 3.95; Found: C 65.43; H 7.25; N 4.18.

4.4 Epoxidation of methylundec-10-enoate

A 2 L round bottom flask was charged with 53 g (≈ 0.27 mol) of methylundec-10-enoate and 1.1 L of dichloromethane. A 162 g (≈ 0.73 mol) of *meta*-chloroperoxybenzoic acid was added in small portions to stirred solution. The reaction mixture was stirred at room

temperature for 20 h. The solution was filtered over the frit S4. After reduction of volume to ca. 500 mL, extraction with 1M soln. of Na₂SO₃ (3x500 mL), saturated soln. of NaHCO₃ (3x500 mL) and finally with saturated soln. of NaCl (3x500 mL) was performed. Organic phase was dried 3 days over Na₂SO₄ (50 g). Drying agent was then filtered-off and solvent was removed in vacuo. Obtained MUO ($Y_w > 80\%$) was further dried over the molecular sieves 4Å and then distilled under reduced pressure.

¹H NMR (CDCl₃, 500 MHz): δ (ppm) 1.29 (m, 8H -CH₂-(e)), 1.43 (m, 2H -CH₂-(f)), 1.51 (m, 2H -CH₂-(d)), 1.60 (m, 2H -CH₂-(c)), 2.28 (t, 2H -CH₂-(b)), 2.45 (m, 1H -CH-(g)), 2.45 (t, 1H -O-CH₂-(g)), 2.72 (t, 1H -O-CH₂-(i)), 2.88 (m, 1H -CH-(g)), 3.65 (s, 3H, COO-CH₃, (a)) (Figure 4.1).

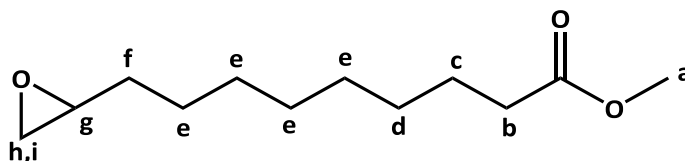


Figure 4.1: Methylundec-10-enoate oxide (MUO)

4.5 Polymerization procedures

Copolymerization of epoxides with CO

The copolymerization of epoxides with CO up to 1MPa CO pressure was performed in a 100 mL glass reactor (Fischer-Porter bottle, Figure 8.1 in supplementary data). The copolymerization at pressure 5 MPa was performed in a 10 mL stainless steel reactor (Figure 8.2 in supplementary data). The reactor with a teflon-coated magnetic stirrer was heated in an oven to 100°C for 60 minutes. Immediately after removing from an oven, the reactor was connected to a pressure pipe and purified by few vacuum/N₂ cycles. The reactor was then shortly opened to air. Solid catalyst and cocatalyst were introduced rapidly and the reactor was closed and purified by vacuum/CO cycles. An epoxide (1-2 mL) was then introduced via a syringe through a ball valve against flow of CO. The reactor was pressurized to appropriate pressure and heated to desired temperature using an oil bath. After allotted polymerization time, the reaction mixture was cooled by ethanol/dry ice bath, excess of pressure was carefully vented of and polymerization vessel was disassembled. A small aliquot of reaction mixture was removed from the reactor for ¹H NMR analysis. A viscous reaction mixture was then dissolved in small amount of CH₂Cl₂ and precipitated into excess of MeOH. Final polymer was separated by filtration and dried 24 h under high vacuum at 60°C.

Copolymerization of epoxides with anhydrides (in solution)

A 25 mL Schlenk ampoule equipped with a magnetic stirring bar was purified with 3 vacuum/N₂ cycles and then charged with catalyst (generally 20 μ mol), epoxide (5 mmol, 250 eq. to catalyst), anhydride (5 mmol, 250 eq. to catalyst) and 3 mL of dry toluene. The Schlenk ampoule was then placed into a preheated oil bath. After allotted polymerization time, the ampoule was removed from the bath and a small aliquot of crude reaction mixture

was taken for ^1H NMR analysis to determine the conversion, when appropriate. The rest of the reaction mixture was precipitated in 200 mL of methanol and filtered. In case of insufficient polymer precipitation, the solution was cooled to -20°C and 1 mL of 36% HCl was added. The solution was stirred until complete precipitation of polymer (≈ 30 min) and then immediately filtered and washed with excess of ethanol. All polymers were dried 16-24 h at 60°C under vacuum.

Copolymerization of epoxides with anhydrides (in bulk)

A 5 mL Schlenk ampoule equipped with a magnetic stirring bar was purified with 3 vacuum/ N_2 cycles and then charged with catalyst (20 μmol), epoxide (5 mmol, 250 eq. to catalyst), anhydride (5 mmol, 250 eq. to catalyst). The Schlenk ampoule was then placed into a preheated oil bath. After allotted polymerization time, the ampoule was removed from the oil bath and the viscous polymer mixture was dissolved in a small amount of toluene and then poured into 200 mL of methanol. Precipitated polymer was then filtered and dried at 60°C under reduced pressure for 24 h.

Copolymerization of PO or CHO with CO_2

A 100 mL Fischer-Porter bottle (Figure 8.1 in supplementary data) was heated to 100°C in an oven for 60 minutes. Immediately after removing from the oven, the Fischer-Porter bottle was screwed to the pressure pipe and purified by few vacuum/ N_2 cycles. The reactor was shortly opened to air to allow the dosage of solid catalyst and cocatalyst. Then the reactor was closed and purified by vacuum/ CO_2 cycles. An epoxide (1.5-2 mL) was then introduced via a syringe through the ball valve against flow of CO_2 . The reactor was pressurized by CO_2 to 1 MPa and heated to desired temperature using an oil bath. After desired polymerization time, the reaction mixture was cooled to -78°C , excess of pressure was carefully vented of and the polymerization vessel was disassembled. A small aliquot of the reaction mixture was removed from the reactor for ^1H NMR analysis. A viscous reaction mixture was then dissolved in small amount of CH_2Cl_2 and precipitated into excess of MeOH. Final polymer was separated by filtration and dried 24 h under high vacuum at 60°C .

4.6 Analyses

Evaluation of Y_w , TOF, selectivity and calculation of theoretic M_n

Yield was calculated by using equation (1):

$$(1) Y_w = m_{\text{POLYMER}} \times \frac{M_{\text{EPOXIDE}}}{M_{\text{RU}}} / m_{\text{EPOXIDE}} ;$$

where m_{POLYMER} and m_{EPOXIDE} is mass of isolated polymer and epoxide in feed, respectively, M_{EPOXIDE} is molar mass of monomer unit and M_{RU} corresponds to the molar mass of repeating (carbonate) unit in polymer.

Turnover frequency to polymer was calculated using formula (2):

$$(2) \text{TOF}_{\text{POL}} = \frac{m_{\text{POLYMER}} \times \text{CL}/100}{M_{\text{RU}} \times n_{\text{CAT}} \times t_p} + \frac{m_{\text{POLYMER}} \times (1 - \text{CL}/100)}{M_{\text{EPOXIDE}} \times n_{\text{CAT}} \times t_p};$$

where n_{CAT} is molar amount of catalyst and t_p is time of polymerization and CL is content of carbonate units in copolymer (in %).

Turnover frequency to cyclic carbonate or cyclic ester (TOF_{CC}) was calculated from equation (3):

$$(3) \text{TOF}_{\text{CC}} = \frac{m_{\text{CC}}}{M_{\text{CC}} \times n_{\text{CAT}} \times t_p};$$

where M_{CC} is molar mass of cyclic carbonate (ester) and m_{CC} is mass of cyclic carbonate (ester) calculated according to equation (4):

$$(4) m_{\text{CC}} = (m_{\text{EPOXIDE}} - (m_{\text{EPOXIDE}} \times Y_{\text{W POL}})) \times \frac{I_{\text{CH}}(\text{CC})}{I_{\text{CH}}(\text{CC}) + I_{\text{CH}}(\text{EPOXIDE})};$$

where $I_{\text{CH}}(\text{CC})$ and $I_{\text{CH}}(\text{EPOXIDE})$, are integrals of ^1H NMR signals of methine groups present in cyclic carbonate and epoxide, respectively.

Selectivity to polycarbonate over cyclic carbonate by-products was calculated according to equation (5)

$$(5) \text{Selectivity} = \frac{\text{TOF}_{\text{POL}}}{\text{TOF}_{\text{POL}} + \text{TOF}_{\text{CC}}} \times 100;$$

Theoretical molar masses of polymers (M_n^{THEOR}) were calculated according to equation (6):

$$(6) M_n^{\text{THEOR}} = \frac{m_{\text{POLYMER}}}{n_{\text{CAT}}}.$$

^1H and ^{13}C NMR spectroscopy

^1H and ^{13}C (and ^{19}F) spectra of ligands, complexes, reaction mixtures and polymers were recorded on Bruker 500 Avance III at room temperature. Ligands, reaction mixtures and polymers were analyzed using CDCl_3 as a solvent. Cobalt complexes were dissolved and analyzed in deuterated DMSO dried over molecular sieves 4Å.

Elemental analysis

Elemental analysis of complexes was measured on EI III instrument, from Elementar Vario. The resulting values are average values of two analyses.

Mass spectrometry

Mass spectra were recorded on spectrometer Orbitrap Velos (Thermo, USA). Samples were dissolved in CH_2Cl_2 and then transferred into MeOH. The isocratic methanol was used as mobile phase.

FT-IR spectroscopy

FT-IR spectra were recorded on spectrometer Nicolet 6700 by ATR technique.

X-Ray crystallography

Crystallographic data for complex **1-Co-OBzF₅** were collected on Nonius KappaCCD diffractometer equipped with Bruker APEX-II CCD detector by monochromatized MoK α radiation ($\lambda = 0.71073 \text{ \AA}$) at the temperature of 150 K.

MALDI-TOF mass spectrometry

MALDI-TOF mass spectra were acquired with a spectrometer UltrafleXtreme (Bruker Daltonics, Bremen, Germany) in the positive ion reflectron mode. The spectra were the sum of 25000 shots with a DPSS, Nd: YAG laser (355 nm, 1000 Hz). Delayed extraction and external calibration was used. The samples were prepared by the dried droplet method: solutions of polycarbonate sample ($10 \text{ mg}\cdot\text{mL}^{-1}$), DCTB (trans-2-[3-(4-*tert*-butylphenyl)-2-methyl-2-propenyldiene]malonitrile; $10 \text{ mg}\cdot\text{mL}^{-1}$) as a matrix and sodium trifluoroacetate (CF_3COONa ; $10 \text{ mg}\cdot\text{mL}^{-1}$) as a cationization agent in DMF were mixed in the volume ratio 4:20:1. 1 mL of the mixture was deposited on the ground-steel target plate. Drop was dried at ambient atmosphere.

Size-exclusion chromatography (SEC)

Molar masses of polyesters and polycarbonates were determined using a Waters Breeze chromatograph with RI detector operating at 880 nm and with MALLS detector miniDawn TREOS (Wyatt) operating at 658 nm. Both methods (absolute and PS calibration) were used for polymer molar mass determination and subsequently correlated (Figure 4.2). The dn/dc increments were determined on RI detector by on-line method by analyses of polycarbonate (PPC and PCHC) or polyester samples of precisely known concentration.¹⁷⁹ The average values of dn/dc increments of polycarbonates were obtained from analyses of 17 PPC samples with $M_n = 10\text{-}32 \text{ kg}\cdot\text{mol}^{-1}$ and 11 PCHC samples with $M_n = 9\text{-}23 \text{ kg}\cdot\text{mol}^{-1}$, respectively. Average dn/dc value of polyester (PA-CHO copolymer) was obtained from analyses of 19 samples with $M_n = 4\text{-}13 \text{ kg}\cdot\text{mol}^{-1}$.

Absolute molar masses of polypropylene carbonates were determined using dn/dc increment $0.050 \pm 0.003 \text{ mL}\cdot\text{g}^{-1}$. Analyzed PPC's were in average 12% superior compared to PS calibration values. Absolute molar masses of analyzed polycyclohexene carbonates were calculated with dn/dc increment $0.087 \pm 0.002 \text{ mL}\cdot\text{g}^{-1}$ and they are of 29% higher compared to

M_n 's obtained from PS calibration method. Absolute molar masses of polyesters from PA and CHO were determined using dn/dc increment $0.139 \pm 0.005 \text{ mL.g}^{-1}$.

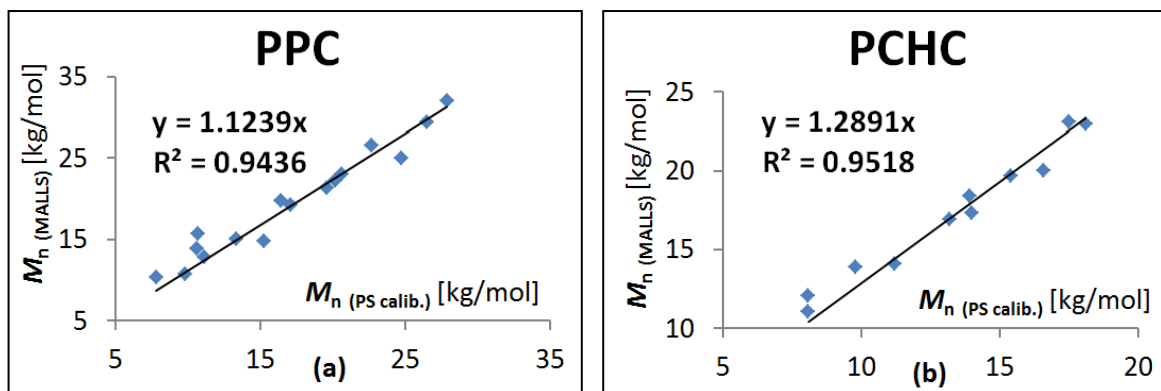
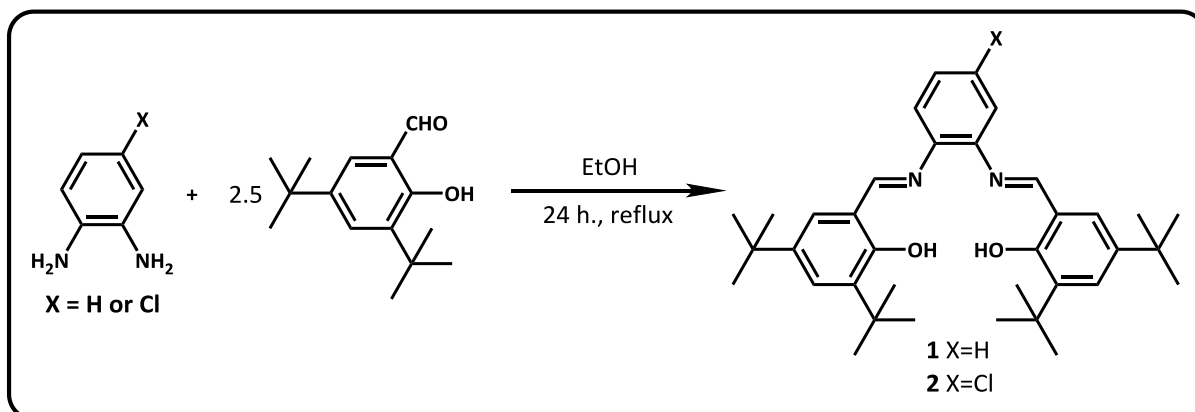


Figure 4.2: Correlation of molar masses of PPC (a) and PCHC (b) obtained by SEC-MALLS and PS calibration method

5 RESULTS AND DISCUSSION

5.1 Synthesis and characterization of salphen catalysts

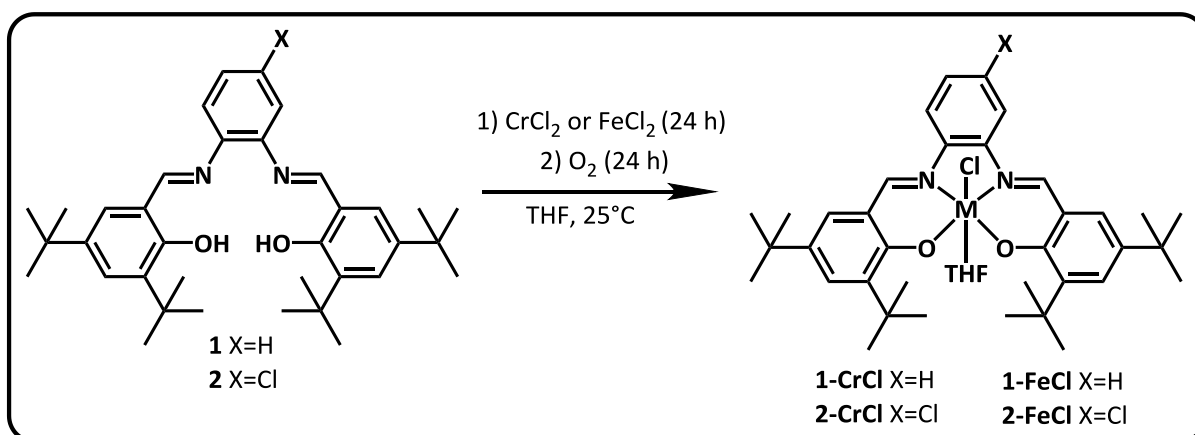
Salphen ligands were prepared by condensation reaction of 1,2-diamines with substituted benzaldehyde in ethanol (Scheme 5.1). Subsequent recrystallization from ethanol gave pure compounds as yellow (**1**) and orange (**2**) needle-like crystals.



Scheme 5.1: Synthesis of salphen ligands **1** and **2**

5.1.1 Salphen Cr complexes

Chromium salphen complexes (**1-CrCl** and **2-CrCl**) were prepared by the coordination of anhydrous CrCl_2 to the corresponding ligands **1** and **2** in THF at room temperature followed by oxidation using air according to the literature procedure (Scheme 5.2).¹⁷⁷



Scheme 5.2: General synthesis procedure of salphen Cr and Fe complexes

Since both chromium complexes are paramagnetic, it was not possible to confirm their structure via ^1H NMR spectroscopy. Both complexes were characterized with HRMS-ESI⁺ mass spectrometry, FT-IR spectroscopy and elemental analysis.

Mass spectrometry confirmed both $[\text{1-Cr}]^+$ (590.2956) and $[\text{2-Cr}]^+$ (624.2568) cations. The elemental composition of both chromium complexes did not entirely correspond with anticipated structures (Scheme 5.2). However a good correlation was achieved with

complexes assuming THF as another ligand attached to the chromium metal together with Cl anion, as was already described earlier by Rieger *et al.*^{42b} (Table 5.1) .

Table 5.1: Elemental analysis of **1-CrCl** and **2-CrCl**

EA	1-CrCl C ₃₆ H ₄₆ N ₂ O ₂ CrCl	1-CrCl. THF C ₄₀ H ₅₄ O ₃ N ₂ CrCl	FOUND	EA	2-CrCl C ₃₆ H ₄₅ N ₂ O ₂ CrCl ₂	2-CrCl. THF C ₄₀ H ₅₃ N ₂ O ₃ CrCl ₂	FOUND
C	0.6905	0.6880	0.6853	C	0.6545	0.6556	0.6580
H	0.0740	0.0779	0.0771	H	0.0687	0.0729	0.0813
N	0.0447	0.0401	0.0414	N	0.0424	0.0382	0.0419

5.1.2 Salphen Fe complexes

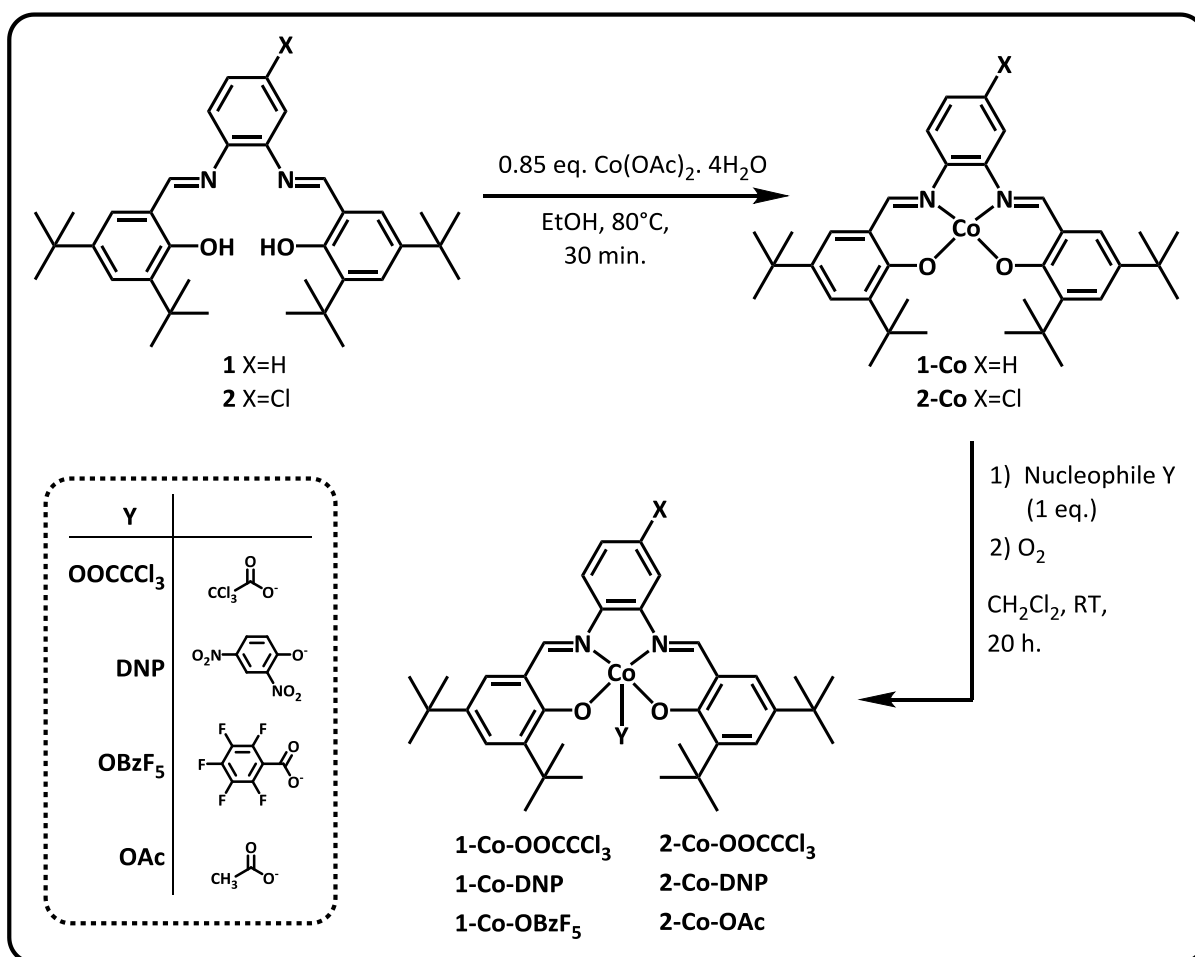
Salphen iron complexes **1-FeCl** and **2-FeCl** were synthesized in THF in similar way as chromium complexes using the FeCl₂ precursor (Scheme 5.2). Mass spectrometry of iron complexes confirmed formation of both [1-Fe]⁺ (594.2909) and [2-Fe]⁺ (628.2523) cations. Elemental analysis of salphen Fe complexes also indicate the presence of coordinated THF (Table 5.2), however, a clear evidence for this anticipation cannot be given. Elemental analysis of **1-FeCl** indicates the presence of both penta- and hexacoordinated iron complexes, while the elemental analysis of complex **2-FeCl** shows better correlation with hexacoordinated structure with one Cl and one THF molecule attached to the Fe metal.

Table 5.2: Elemental analysis of **1-FeCl** and **2-FeCl**

EA	1-FeCl C ₃₆ H ₄₆ N ₂ O ₂ FeCl	1-FeCl. THF C ₄₀ H ₅₄ O ₃ N ₂ FeCl	FOUND	EA	2-FeCl C ₃₆ H ₄₅ N ₂ O ₂ FeCl ₂	2-FeCl. THF C ₄₀ H ₅₃ N ₂ O ₃ FeCl ₂	FOUND
C	0.6863	0.6842	0.6862	C	0.6507	0.6522	0.6613
H	0.0736	0.0775	0.0746	H	0.0683	0.0725	0.0730
N	0.0445	0.0399	0.0415	N	0.0422	0.0380	0.0359

5.1.3 Salphen Co complexes

Intermediate neutral cobalt (II) salphen complexes **1-Co** and **2-Co** (Scheme 5.3) were synthesized according to the previously published procedures^{76a,178} by the coordination of ligands **1** and **2** to Co(OAc)₂.4H₂O precursor. Recrystallized and dried complexes **1-Co** and **2-Co** were then treated with 1 eq. of Y-H nucleophile (trichloroacetic acid, 2,4-dinitrophenol, pentafluorobenzoic acid and acetic acid) and let oxidize to afford final complexes **1-Co-Y** and **2-Co-Y** (Scheme 5.3). Prepared complexes were obtained in most of cases as microcrystalline dark red powders.



Scheme 5.3: General scheme of salphen **Co-Y** synthesis

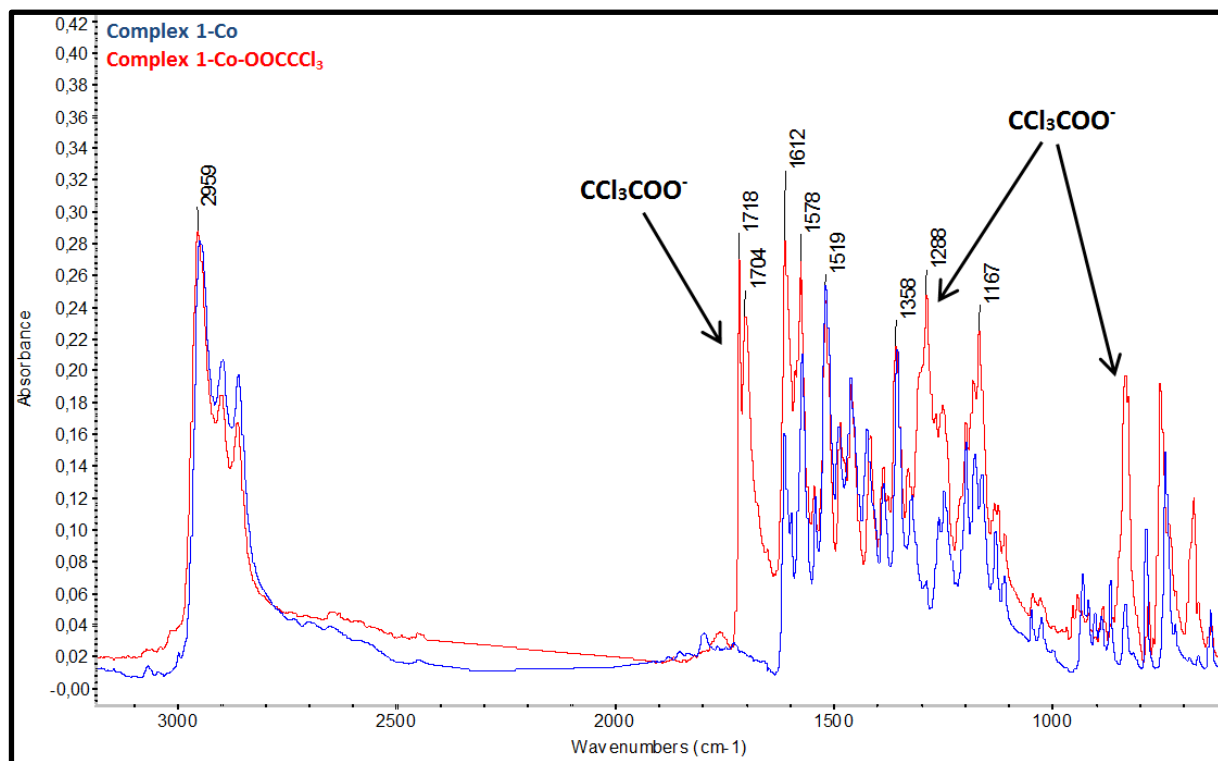
Intermediate complexes **1-Co** and **2-Co** were characterized by FT-IR spectroscopy and MS-ESI⁺, which confirmed expected [**1-Co**]⁺ (597.2888) and [**2-Co**]⁺ (631.2499) cations. Detailed COSY, HSQC and HMBC experiments were used to fully assign the ¹H and ¹³C NMR spectra of new asymmetric salphen cobalt complex **2-Co** (Spectrum 8.1-Spectrum 8.6 in supplementary data, pages 126-128). On the contrary, the complex **1-Co** was very poorly soluble in organic solvents, therefore it was not possible to use NMR analyses for complex characterization.

¹H NMR, FT-IR, HR-MS spectroscopy and elemental analysis were used for structural characterization of **1-Co-Y** and **2-Co-Y** complexes. Although several attempts to prepare monocrystals suitable for solid state structure analysis were performed, only **1-Co-OBzF₅** afforded suitable crystals allowing to determine its molecular structure.

Complex 1-Co-OOCCCl₃

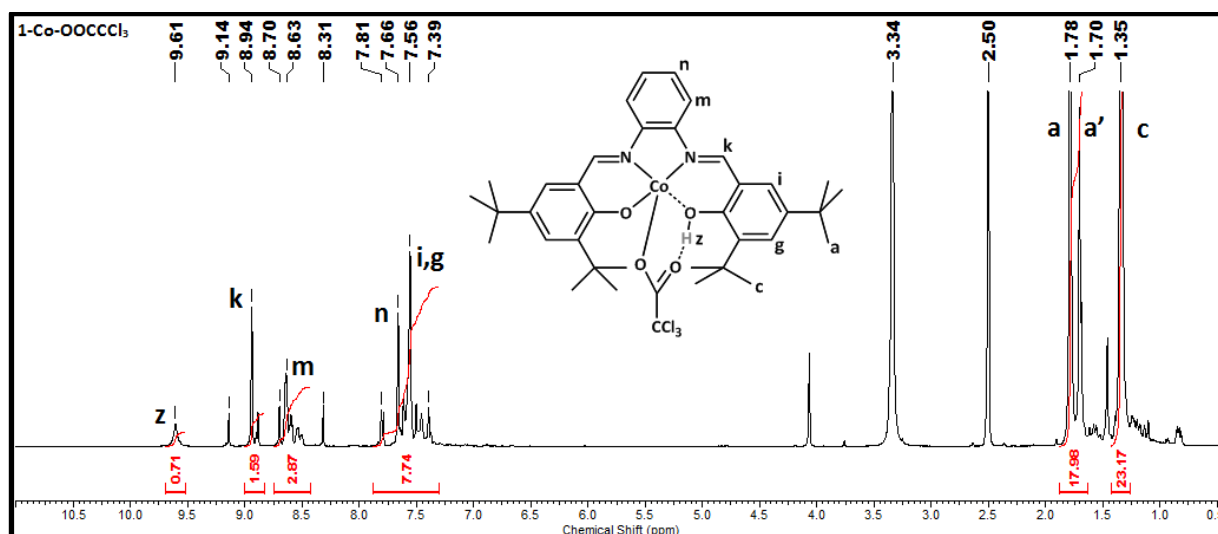
The mass spectrum of complex **1-Co-OOCCCl₃** confirmed the presence of [**1-Co**]⁺ (597.2883). The presence of trichloroacetate counterpart in complex **1-Co-OOCCCl₃** was not confirmed by MS-ESI⁻, however, the formation of anionic species with mass 163.8383, which is close to the molar mass of trichloroacetic acid was observed. Interestingly, the same peak (163.8381) was found in MS-ESI⁻ spectra of **2-Co-OOCCCl₃**. Trichloroacetate group was

confirmed by ATR-IR spectroscopy, which clearly showed the presence of typical vibration of C=O group at $\approx 1700\text{ cm}^{-1}$ and another C-O and C-Cl vibrations at 1288 and 883 cm^{-1} respectively, which were not present in starting **1-Co** complex (Spectrum 5.1).



Spectrum 5.1: FT-IR spectra of complexes **1-Co** and **1-Co-OOCCl₃**

^1H NMR spectrum of complex **1-Co-OOCCl₃** (Spectrum 5.2) shows the presence of multiple peaks, which cannot be clearly attributed to the single structure as depicted in Scheme 5.3. Moreover, two methyl hydrogens peaks observed at δ 1.78 ppm and 1.70 ppm (corresponding to *a tert*-butyl groups) suggest the presence of two chemically unequal species, probably with one and two trichloroacetate groups coordinated to the central metal.

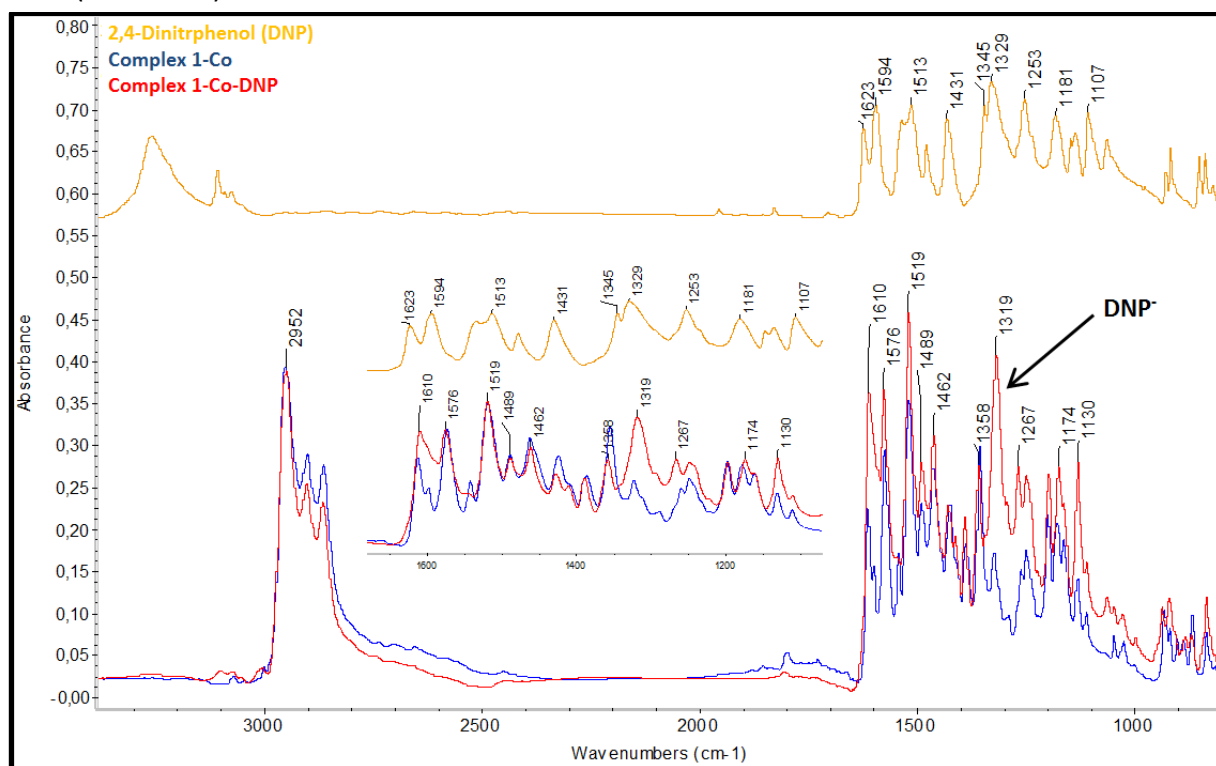


Spectrum 5.2: ^1H NMR spectrum of complex **1-Co-OOCCl₃** in DMSO

Additional elemental analysis of complex **1-Co-OCCCCl₃** shows better agreement with structure calculated for hexacoordinated salenCo(III) complex with one nucleophile Y and one Y-H molecule attached to the Co metal. EA calculated for [C₃₆H₄₆N₂O₂Co.(C₂Cl₃O₂)1.75] (%): C 53.80; H 7.76; N 3.18; Found: C 53.93; H 5.37; N 3.28.

Complex 1-Co-DNP

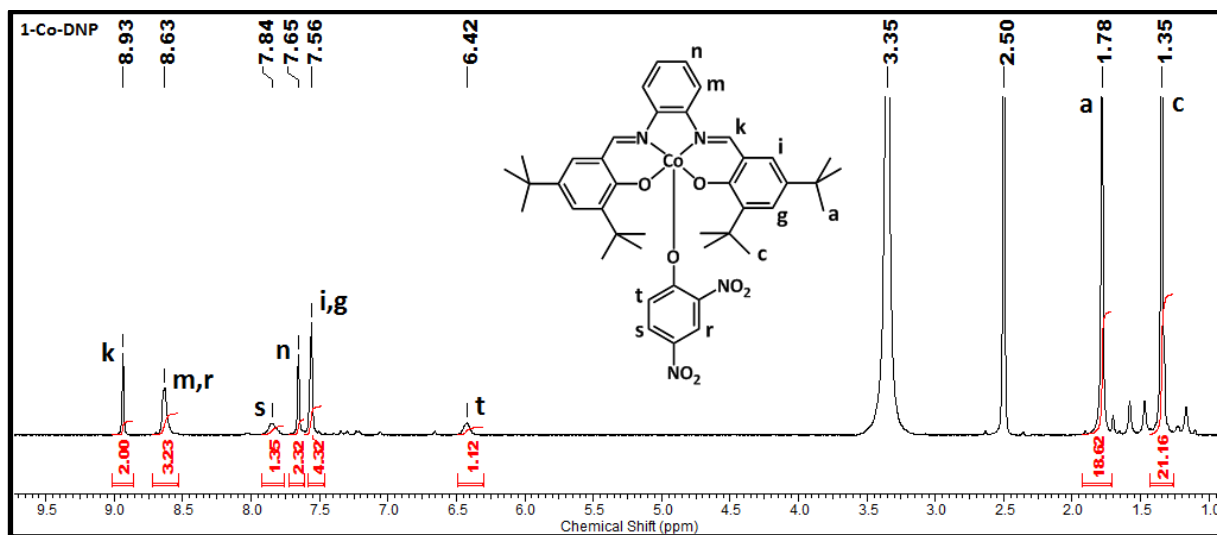
Mass spectrometry of **1-Co-DNP** confirmed the presence of both, [1-Co]⁺ cation (597.2886) and DNP⁻ nucleophile (183.0041). The presence of DNP⁻ anion was confirmed also by FT-IR spectroscopy (Spectrum 5.3), where the peak corresponding to N=O vibration of DNP (1319 cm⁻¹) was observed.



Spectrum 5.3: FT-IR spectra of complexes **1-Co** and **1-Co-DNP**

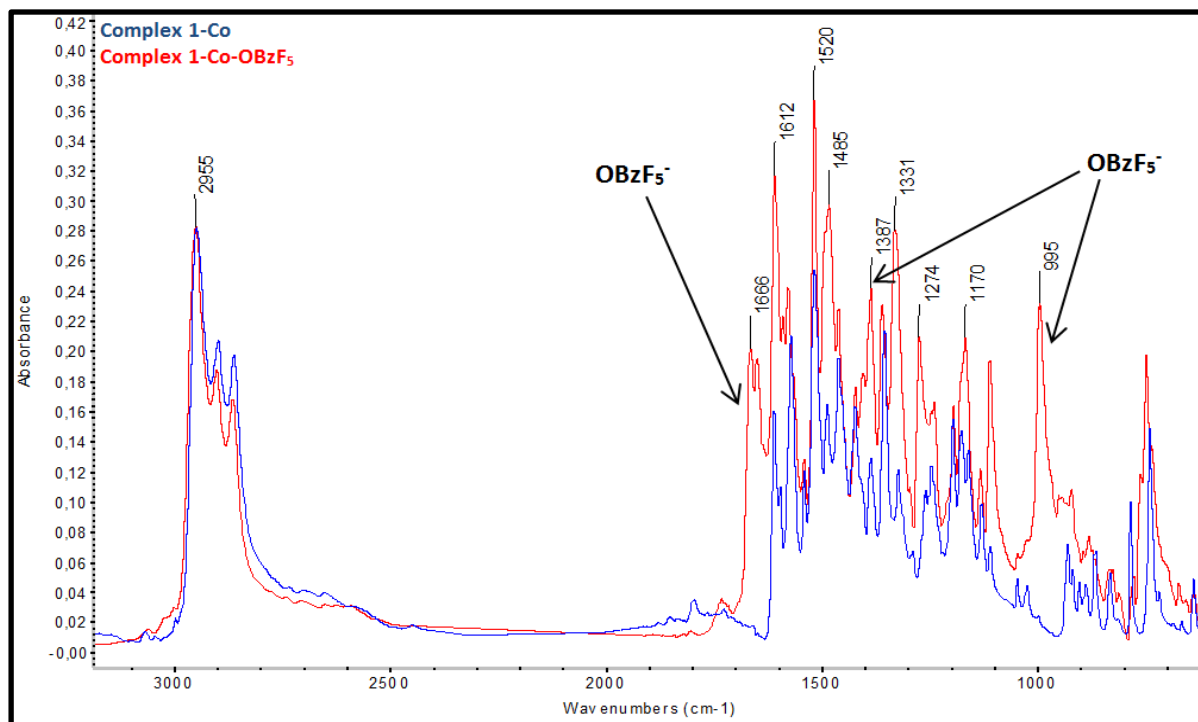
¹H NMR of **1-Co-DNP** is presented in Spectrum 5.4. Singlet signals **a** (1.78 ppm) and **c** (1.35 ppm), corresponding to the *ortho*- and *para-tert*-butyl groups, suggest the formation of only one species, most probably a pentacoordinated complex with one DNP anion attached to the Co metal. Integral values of DNP signals (**r,s,t**) are equal to one, which also suggest the presence of only one DNP molecule in the complex.

The presence of single species (pentacoordinated complex **1-Co-DNP**) was implied also by elemental analysis, where the elemental composition was attributed to the structure with one DNP anion. EA calculated for: [C₃₆H₄₆N₂O₂Co.(C₆N₂O₅)0.85] (%): C 65.53; H 6.50; N 6.88; Found: C 65.53; H 6.76; N 6.28.



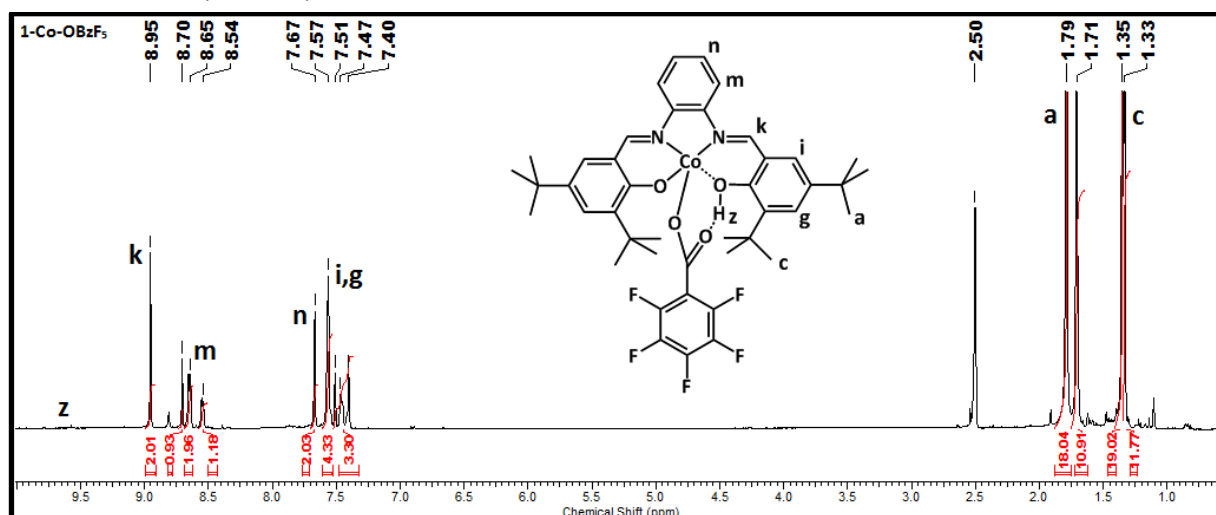
Complex **1-Co-OBzF₅**

Mass spectrometry of complex **1-Co-OBzF₅** confirmed the presence of $[\text{1-Co}]^+$ cation (597.2893) as well as C_6F_5^- (166.9932) and $\text{C}_7\text{O}_2\text{F}_5^-$ (210.9817) moieties of pentafluorobenzoic acid. FT-IR spectra (Spectrum 5.5) show the presence of $\text{C}=\text{O}$ (1666 cm^{-1}) and $\text{C}-\text{F}$ vibrations (1387 and 995 cm^{-1}), which is another clear evidence for the presence of pentafluorobenzoic acid in the complex.

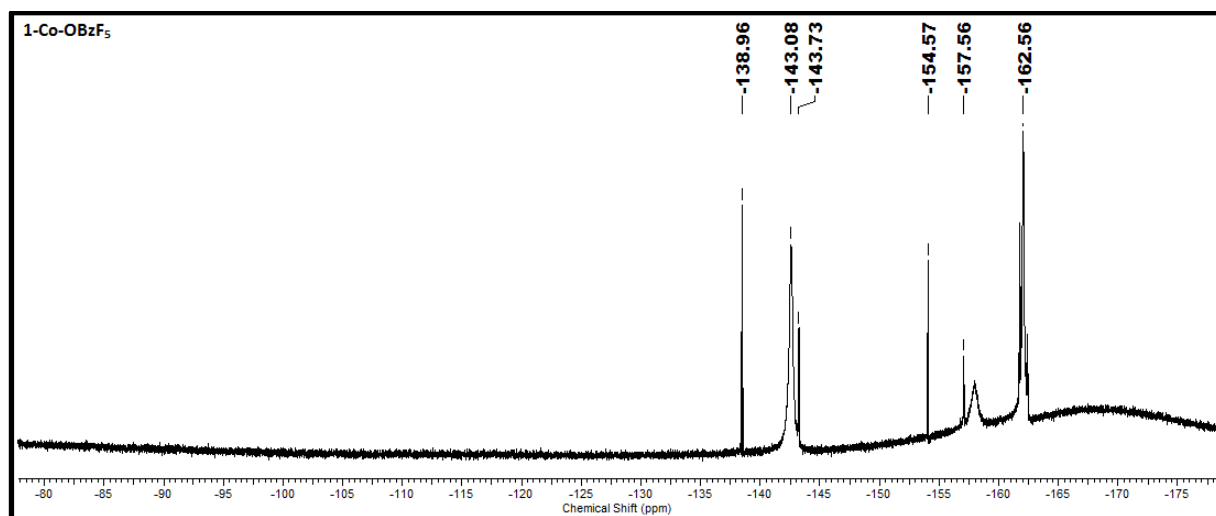


^1H NMR spectrum of **1-Co-OBzF₅** (Spectrum 5.6) shows the presence of multiple peaks in aromatic region and pair signals corresponding to the peak **a** (δ 1.71 and 1.79). This suggests the formation of two catalytic species, probably penta- and hexacoordinated structures of complex **1-Co-OBzF₅**. ^{19}F NMR (Spectrum 5.7) confirmed the presence of pentafluorobenzoic

acid, nevertheless the spectrum also contain other peaks, which cannot be assigned to the solely pentafluorobenzoate moiety. It can be explained by different binding mode of two pentafluorobenzoic acids in the complex. This presumption was confirmed later from molecular structure of the complex obtained by X-Ray crystallography (Figure 5.1). The presence of two pentafluorobenzoic acid molecules in the complex is suggested also by elemental analysis. EA calculated for $[C_{36}H_{46}N_2O_2Co.(C_7F_5O_2)_{1.75}]$ (%): C 59.93; H 4.79; N 2.90; Found: C 60.00; H 5.32; N 2.89.



Spectrum 5.6: ^1H NMR spectrum of complex 1-Co-OBzF₅ in DMSO



Spectrum 5.7: ^{19}F NMR of complex 1-Co-OBzF₅

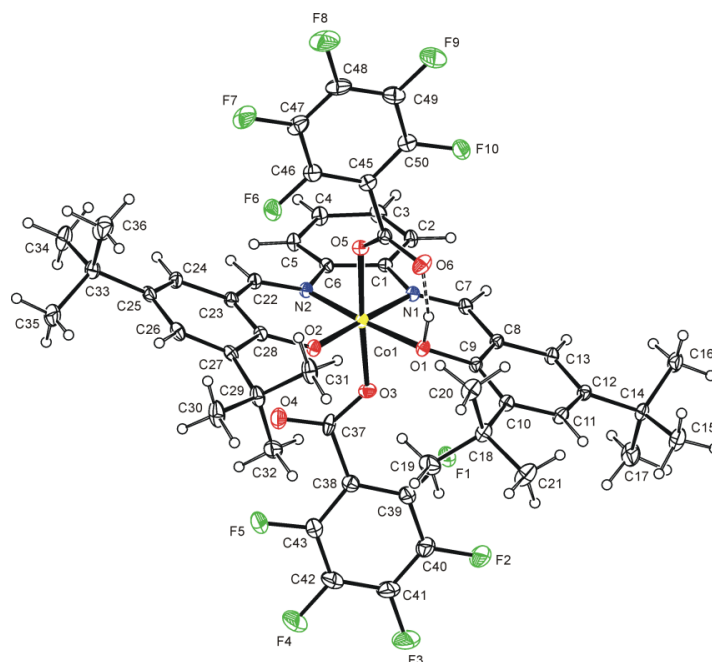
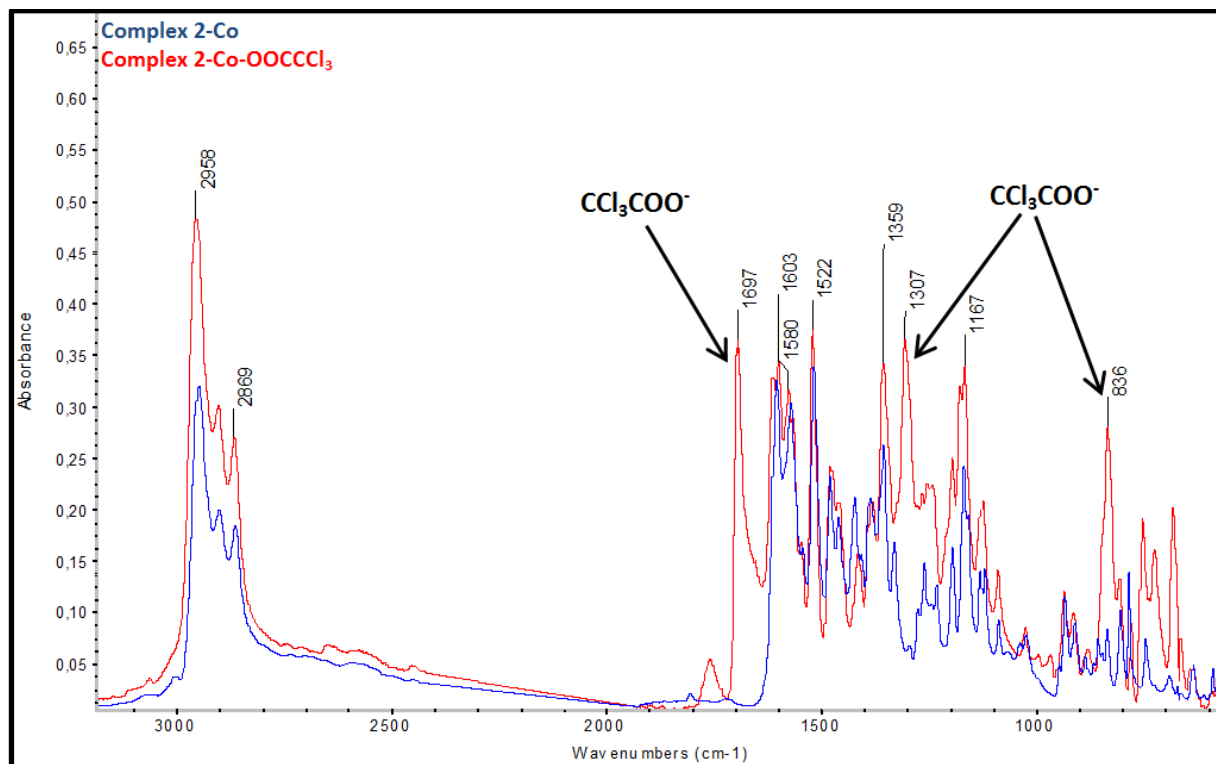


Figure 5.1: View on the molecular structure of complex **1-Co-OBzF₅** determined by X-Ray crystallography

Complex 2-Co-OOCCCl₃

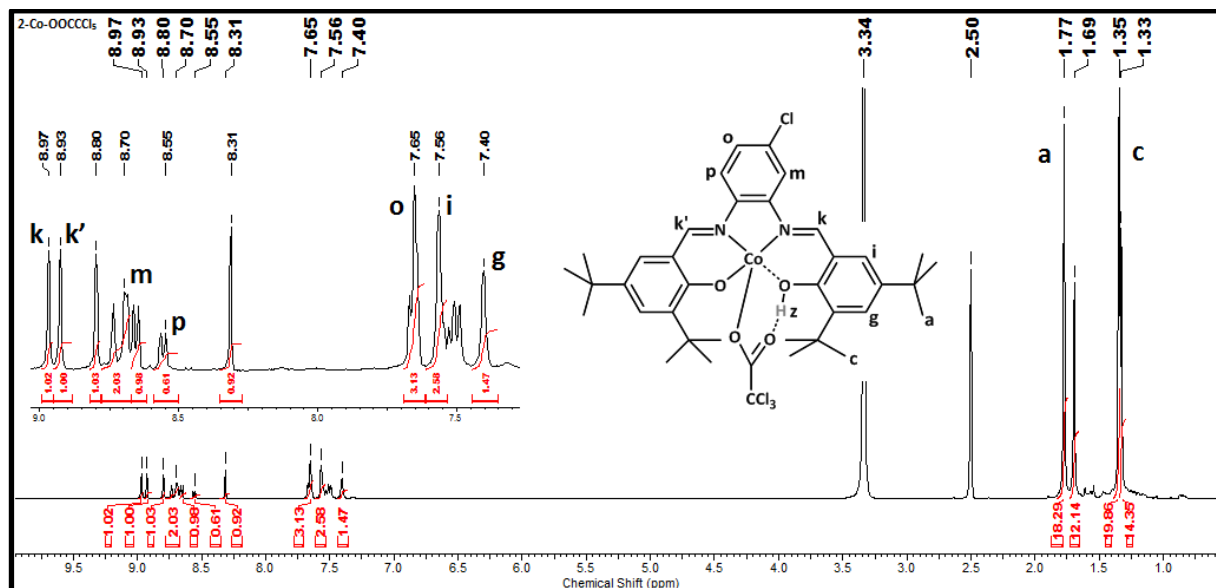
MS-ESI⁺ analysis of complex **2-Co-OOCCCl₃** confirmed the presence of [2-Co]⁺ adduct. MS-ESI analysis in negative mode showed a peak with mass 163.8381.

FT-IR spectrum of **2-Co-OOCCCl₃** (Spectrum 5.8) shows typical C=O vibrations of trichloroacetic acid at 1697 cm⁻¹ and another C-O and C-Cl vibrations at 1307 and 836 cm⁻¹ respectively.



Spectrum 5.8: FT-IR spectra of complexes **2-Co** and **2-Co-OOCCCl₃**

^1H NMR spectrum (Spectrum 5.9) shows splitting of methyl peaks at δ 1.35 ppm and 1.77 ppm suggesting again the presence of both penta- and hexacoordinated complex. This anticipation was supported by elemental analysis, where the best coincidence of theoretical and found composition was achieved assuming two trichloroacetate moieties attached to the Co metal. EA calculated for $[\text{C}_{36}\text{H}_{45}\text{N}_2\text{O}_2\text{ClCo}(\text{C}_2\text{Cl}_3\text{O}_2)_2]_{2.05}$ (%): C 49.91; H 4.70; N 2.90; Found: C 50.01; H 5.13; N 2.81.

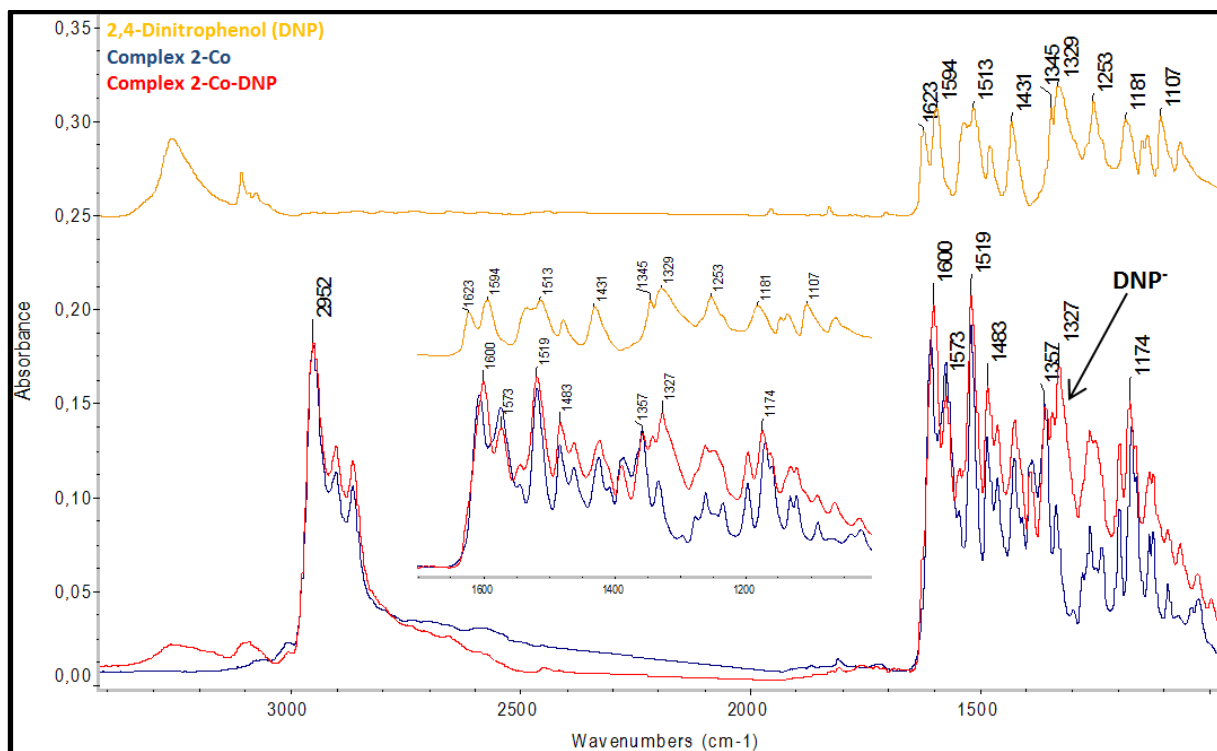


Spectrum 5.9: ^1H NMR spectrum of complex **2-Co-OOCCl₃** in DMSO

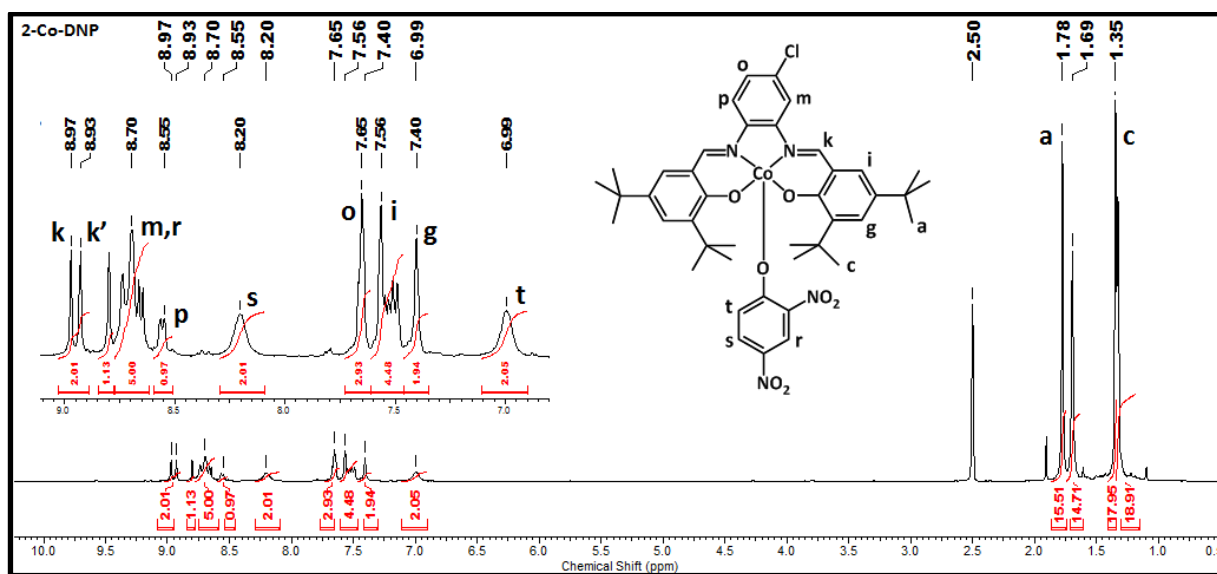
Complex **2-Co-DNP**

Mass spectrometry of **2-Co-DNP** confirmed the presence of $[\text{2-Co}]^+$ cation (631.2499) and DNP^- nucleophile (183.0047). DNP^- anion was confirmed also by FT-IR spectroscopy, which displayed peak at 1327 cm^{-1} corresponding to $\text{N}=\text{O}$ vibration of dinitrophenolate (Spectrum 5.10).

Compared to the complex **1-Co-DNP**, which was determined to be pentacoordinated, complex **2-Co-DNP** is probably a mixture of penta- and hexacoordinated structures, as it can be deduced from ^1H NMR of complex **2-Co-DNP** (Spectrum 5.11), which shows split methyl peaks **a** and **c** and also double integral values of peaks **r,s,t** corresponding to DNP moieties. Elemental analysis also suggests the hexacoordinated structure of the complex. EA calculated for $[\text{C}_{36}\text{H}_{45}\text{N}_2\text{O}_2\text{ClCo}(\text{C}_6\text{N}_2\text{O}_5)_1.80]$ (%): C 58.45; H 5.28; N 8.16; Found: C 58.40; H 5.75; N 6.37.



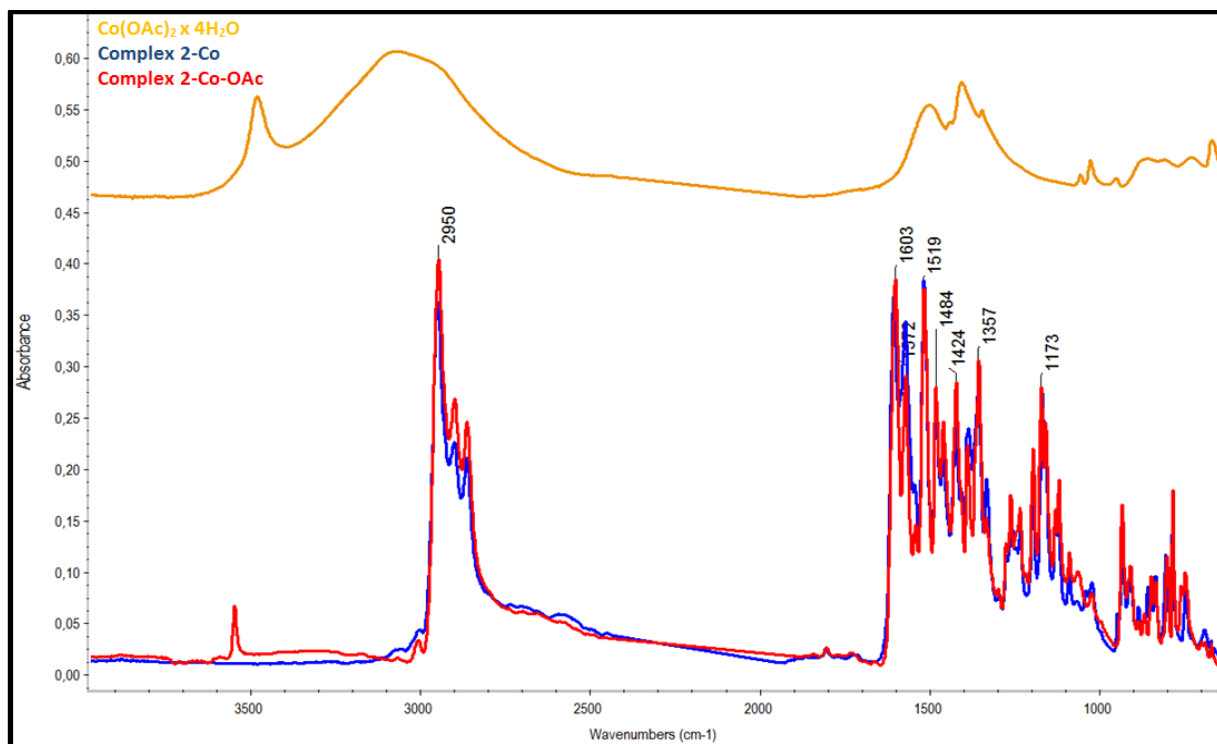
Spectrum 5.10: FT-IR spectra of complexes **2-Co** and **2-Co-DNP**



Spectrum 5.11: ^1H NMR spectrum of complex **2-Co-DNP** in DMSO

Complex **2-Co-OAc**

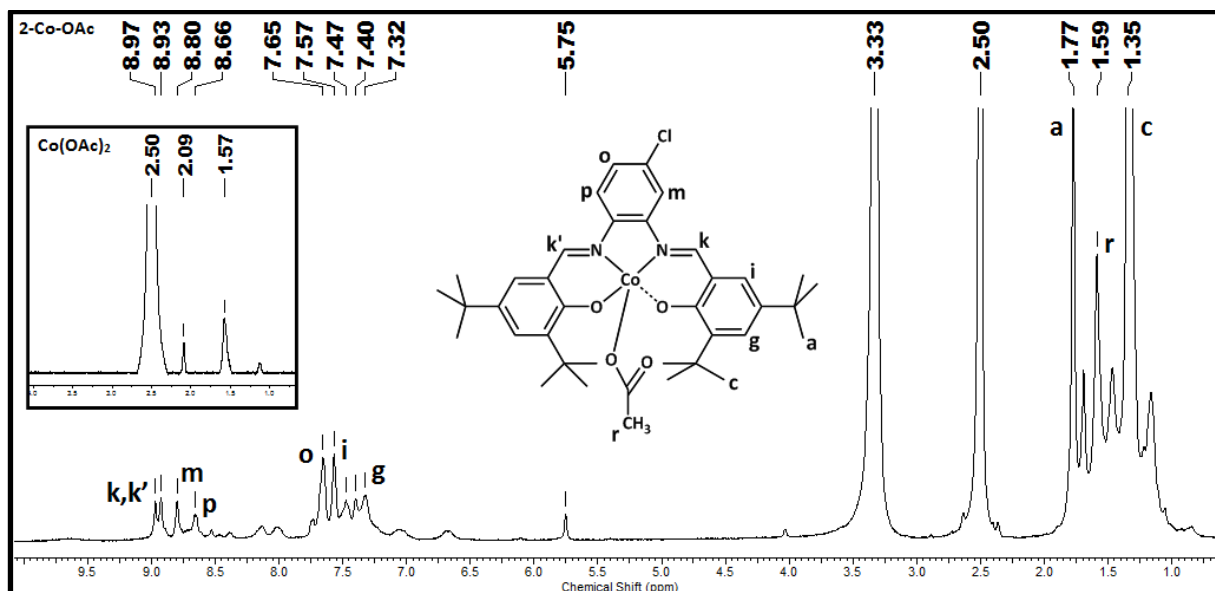
Mass spectrometry of complex **2-Co-OAc** confirmed only the presence of $[\text{2-Co}]^+$ cation (631.2484). The acetate counterion was not observed in MS-ESI⁺ spectrum. Displayed FT-IR spectrum of **2-Co-OAc** complex (Spectrum 5.12) shows the close coincidence with reference compound **2-Co**, which can be attributed to the fact that even unoxidized cobaltate (II) complex **2-Co** (prepared from $\text{Co}(\text{OAc})_2 \cdot 4\text{H}_2\text{O}$) could contain detectable amount of poorly attached acetate. Compared to **2-Co**, new peak at 3550 cm^{-1} in the spectrum **2-Co-OAc** is observed. This peak can be attributed to the Co(III)-attached acetate as it was observed in the reference spectrum of $\text{Co}(\text{OAc})_2 \cdot 4\text{H}_2\text{O}$ (orange line in Spectrum 5.12).



Spectrum 5.12: FT-IR spectra of complexes **2-Co** and **2-Co-OAc**

Compared to complex **2-Co**, which was perfectly soluble in organic solvents, allowing entire ¹H and ¹³C characterization (Spectrum 8.1 - Spectrum 8.6 in supplementary data), complex **2-Co-OAc** was very poorly soluble. Therefore, displayed ¹H NMR spectrum of **2-Co-OAc** in DMSO (Spectrum 5.13) is not quantitative. In the spectrum, we can observe peak at δ 1.59 ppm which could be ascribed to the acetate group attached to the Co metal. To confirm this presumption, solely Co(OAc)₂·4H₂O was analyzed by ¹H NMR spectroscopy in DMSO. Position of methyl moiety of cobalt acetate tetrahydrate at δ 1.57 ppm is coincident with peak **r** in spectrum of **2-Co-OAc** (1.59 ppm), which can be considered as an evidence of the presence of acetate group in the complex.

The indirect evidence of acetate anion in **2-Co-OAc** complex afforded also elemental analysis where the best correlation of found and theoretical composition was achieved for single acetate anion attached to Co metal. EA calculated for [C₃₆H₄₅N₂O₂ClCo.(C₂H₃O₂)1.30] (%): C 65.40; H 6.95; N 3.95; Found: C 65.43; H 7.25; N 4.18.



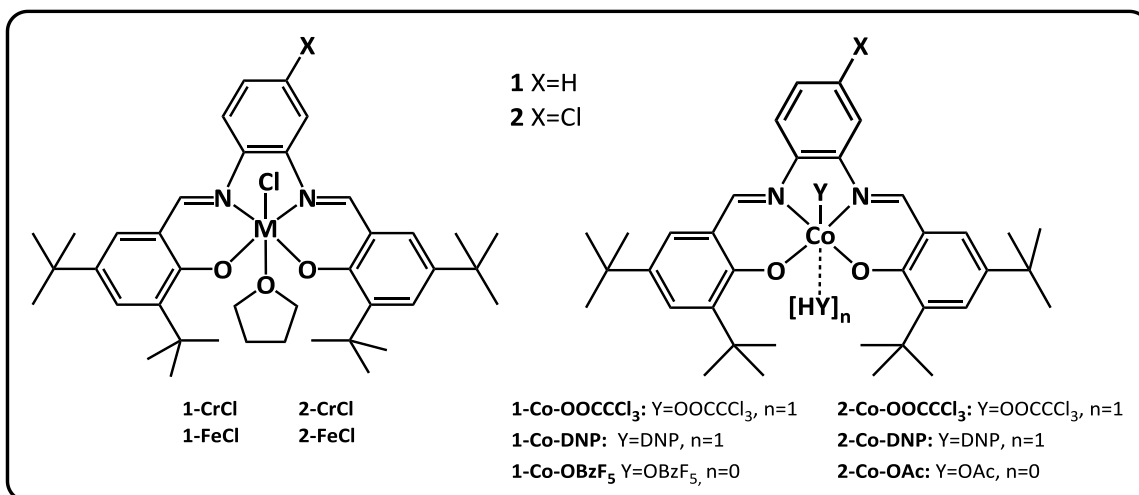
Spectrum 5.13: ^1H NMR spectrum of complex **2-Co-OAc** in DMSO with embedded ^1H NMR spectrum of solely cobalt(II) acetate tetrahydrate in DMSO

5.1.4 Conclusion

All salphen complexes were prepared in 50-100% yields as microcrystalline reddish/brown powders, which were characterized by MS-ESI spectrometry, IR spectroscopy and elemental analysis and in case of Co complexes also by NMR.

Limitation of Cr and Fe complexes to be analyzed by NMR due to their paramagnetic nature resulted in lower level of complexes structure characterization. Whereas complex cations were clearly confirmed by MS, IR neither EA analysis gave a clear information about complex counteranions. The coordination of two different ligands (anionic Cl and neutral THF) to the central metal was concluded as suggested from elemental analysis (Scheme 5.4).

Diamagnetic Co salphen complexes, with the highest catalytic potential (see next chapters), were characterized in detail by all common techniques including NMR. In the case of **1-Co-OBzF₅**, a single crystal suitable for X-ray measurement was obtained allowing full solid state structure characterization. Prepared Co salphen complexes were found to be rather a mixture of pentacoordinated and hexacoordinated [YH] complexes (adducts with trichloroacetic acid, dinitrophenol, pentafluorobenzoic acid or acetic acid) (Scheme 5.4). This is in contrast with the literature data according to which analogous salen complexes were described to be pentacoordinated in all reported cases.



Scheme 5.4: Proposed structures of salen chromium, iron and cobalt complexes

5.2 Copolymerization of epoxides with carbon monoxide

5.2.1 Copolymerization of PO and CO with 2-CrCl/Co₂(CO)₈

Coates groups reported a combination of carbonylation catalysts **6** and **7** (Figure 2.3, page 9) and ROP catalysts **10b** (Figure 2.5, page 10) and **42b,c** (Figure 2.18, page 24) for the carbonylation of PO to BBL followed by its immediate ROP to form PHB. The limitation of this approach lies in the need for mutual tolerance of both catalysts and their catalytic activity at same (selected) reaction conditions.

Therefore, we attempted the one pot synthesis of PHB by a dual catalytic system using chromium salphen complex **2-CrCl** intended for the ROP of in-situ formed BBL by the carbonylation of PO catalyzed by well know carbonylation catalyst Co₂(CO)₈.

First, blank experiments of PO with CO copolymerization were performed at 75°C for 20 h in the presence of solely Co₂(CO)₈ or **2-CrCl** (Exp. 1_1 and 2_1 in Table 5.3). ¹H NMR analysis of reaction mixtures showed very low conversion to products (cyclic ester and polyester). Subsequent prolongation of the polymerization period by another 20 h (exp. 1_2, 2_2), together with increase of temperature to 100°C did not result in increase of ester nor polyester formation.

Table 5.3: Copolymerization of PO with CO using **2-CrCl/Co₂(CO)₈**

Exp.	Catalyst	2-CrCl/ Co ₂ (CO) ₈	T (°C)	t _p (h)	Y _w POL (%) ^a	TOF _{POL} (h ⁻¹) ^b	TOF _{BBL} (h ⁻¹) ^c	[POL]/[BBL]/ [PO]/[Acetone] (%) ^d	Ester linkage (%) ^e	M _n ^f (kg.mol ⁻¹)	D ^f
1_1	Co ₂ (CO) ₈	-	75	20	-	-	0.6	1:2:92:5	-	-	-
1_2			100	+20	7	1.7	0.5	2:2:88:8	≈ 82	1.0	1.3
2_1	2-CrCl	-	75	20	-	-	0.1	0:0.2:99:0.8	-	-	-
2_2			100	+20	5	1.3	0.1	0.6:0.4:98:1	≈ 30	0.9	1.6
3_1	2-CrCl/ Co ₂ (CO) ₈	1:1	75	20	-	-	4.4	68:8:21:2	-	-	-
3_2			100	+20	38	10.3	0.3	82:1:15:2	≈ 90	1.1	1.4

p_{CO}=1MPa, [PO]/[Cr]=1000:1;

^a Based on isolated polymer yield;

^b Turnover frequency to polymer;

^c Turnover frequency to BBL (For details see experimental part);

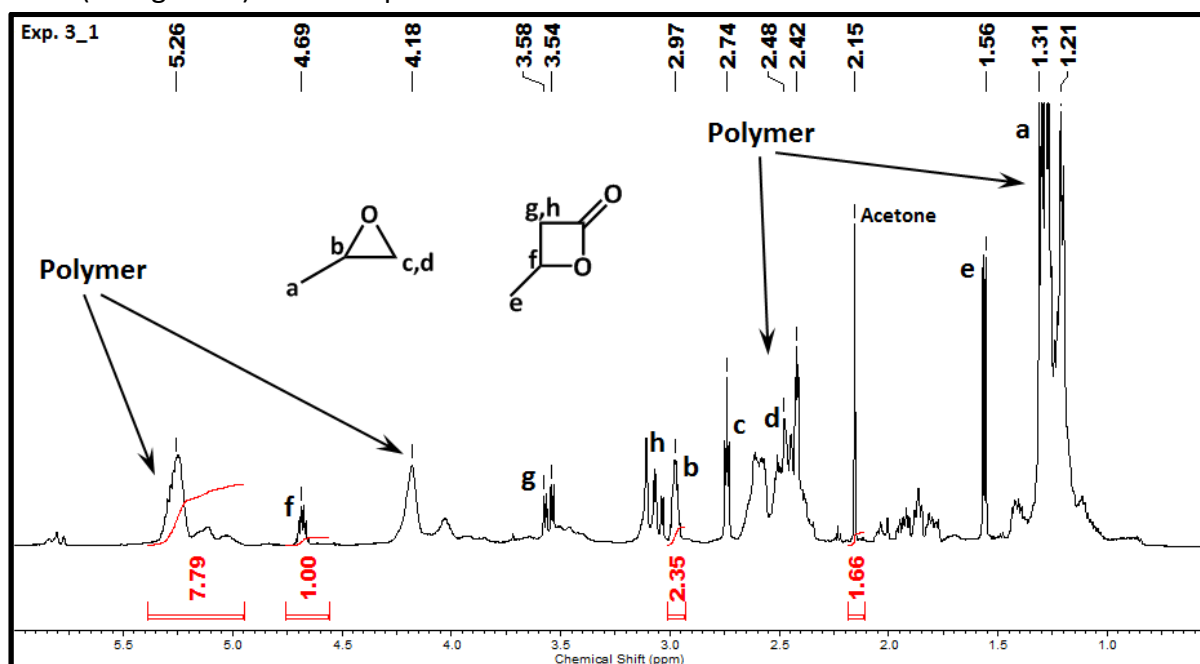
^d Composition of reaction mixture at the end of experiment, determined by ¹H NMR spectroscopy, (POL= polyester);

^e Determined from dried polymer by ¹H NMR spectroscopy;

^f Determined by SEC-PS calibration in THF at 35°C

Further, a combination of **2-CrCl** with Co₂(CO)₈ lead to the formation of cyclic ester (β-butyrolactone) together with polyester-co-ether copolymer as determined by ¹H NMR spectroscopy (Exp. 3, Table 5.3 and Spectrum 5.14). Small amount of acetone (side product of epoxide carbonylation) was also found in ¹H NMR spectrum. Comparison of reaction mixtures after 20 h (at 75°C) and after another 20 h of copolymerization performed at 100°C shows the decrease of β-butyrolactone concentration which suggests its incorporation into

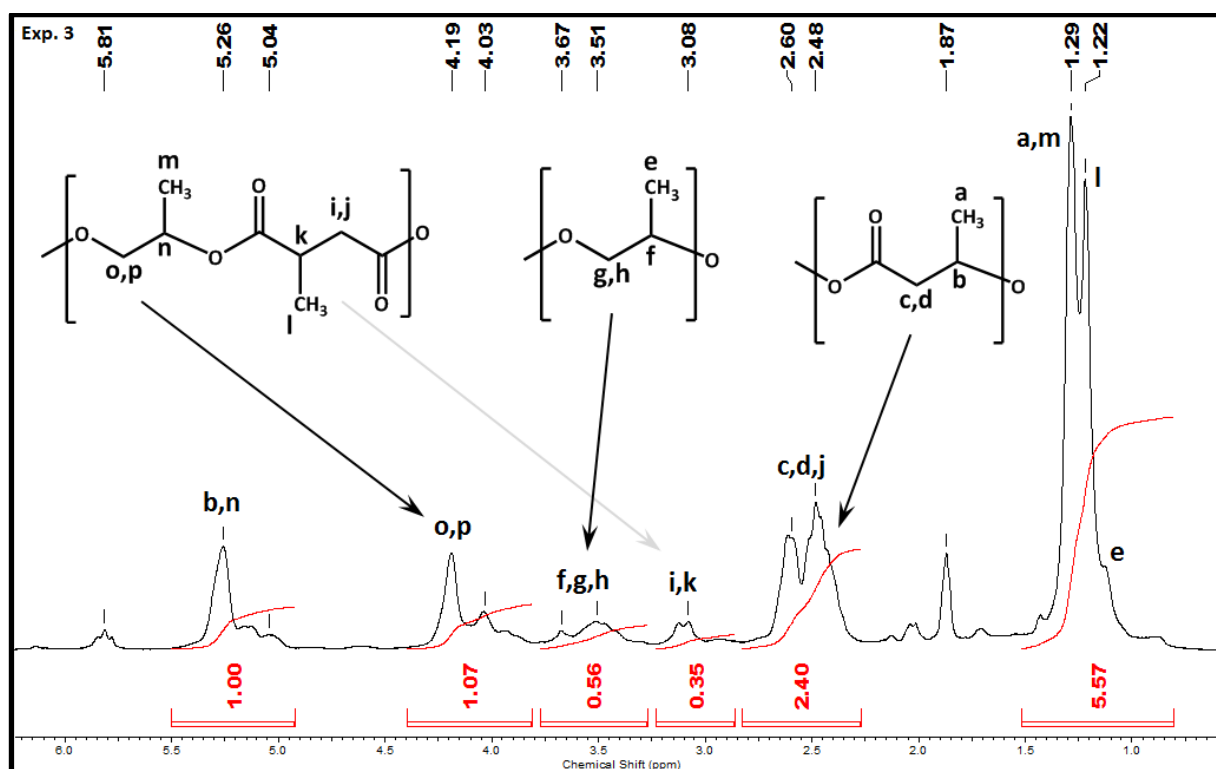
polymer during the copolymerization. Final polymer was obtained in the form of low molar mass ($\approx 1 \text{ kg}\cdot\text{mol}^{-1}$) viscous liquid.



Spectrum 5.14: ^1H NMR spectra of reaction mixture of exp. 3_1 ($t_p=20 \text{ h}$, $T=75^\circ\text{C}$)

More detailed insight into ^1H NMR spectrum of polymer (Spectrum 5.15) showed multiple peaks corresponding to PHB-like polyester with $\approx 20\%$ of ether units (peaks at δ 3.50 ppm). Peaks at area δ 3.9-4.3 ppm (*o,p*) could be assigned probably to the methylene hydrogens originated from the polyester obtained from the copolymerization of PO with succinic anhydride, which is probably formed by double carbonylation of propylene oxide. Similar chemical shifts were observed in the case of polyesters prepared by the copolymerization of epoxides with anhydrides (see chapter 5.3.7).

Further experiments (Table 5.4) were performed at 100°C with a new batch of **2-CrCl** complex. The modification of experimental conditions did not lead to significant improvement of catalytic performance. Increase of pressure to 5MPa (exp. 5) led to higher conversion of PO to both BBL and polymer, On the other hand, addition of 3 eq. of dicobaltoctacarbonyl instead of equimolar ratio led to higher production of polymer (exp. 6 vs. 4). Nevertheless, in all cases, only low molar-mass poly(ester-co-ether)s were obtained.



Spectrum 5.15: ^1H NMR spectrum of polyester-co-ether copolymer prepared by copolymerization of PO with carbon monoxide by $2\text{-CrCl}/\text{Co}_2(\text{CO})_8$ (exp. 3)

Table 5.4: Copolymerization of epoxides with CO using $2\text{-CrCl}/\text{Co}_2(\text{CO})_8$

Exp.	$2\text{-CrCl}/\text{Co}_2(\text{CO})_8$	Epoxide	T (p) ($^{\circ}\text{C}$; MPa)	$Y_{\text{w POL}}$ (%) ^a	TOF_{POL} (h^{-1}) ^b	TOF_{BBL} (h^{-1}) ^c	$[\text{POL}]/[\text{BBL}]/$ $[\text{PO}]/[\text{Ketone}]$ ^d (%)	EL ^e (%)	M_n ^f ($\text{kg}\cdot\text{mol}^{-1}$)	\bar{D} ^f
4	1:1	PO	100 (1)	34	17	10	58:12:26:5	≈ 89	1.1	1.3
5	1:1	PO	100 (5)	35	18	33	41:54:3:2	≈ 81	1.4	1.5
6	1:3	PO	100 (1)	47	24	7	72:6:15:7	≈ 91	1.1	1.4
7	1:3	CHO	100 (1)	33	11	0	26:0:43:31	≈ 40	1.2	1.6
8	1:3	MUO ^g	100 (1)	0	0	0	0:0:100:0	-	-	-
9	10:1	PO	100 (5)	23	11	5	61:5:34:0	≈ 83	1.0	1.3

Catalyst: $2\text{-CrCl}/\text{Co}_2(\text{CO})_8$, $t_p=20\text{h}$, $[\text{Epoxide}]/[\text{Cr}]=1000:1$;

^a Based on isolated polymer yield;

^b Turnover frequency to polymer;

^c Turnover frequency to BBL (For details see experimental part);

^d Composition of reaction mixture at the end of experiment, determined by ^1H NMR spectroscopy, (POL= polyester; Ketone = acetone or cyclohexanone);

^e Ester linkage determined from dried polymer by ^1H NMR spectroscopy;

^f Determined by SEC-PS calibration in THF at 35°C ;

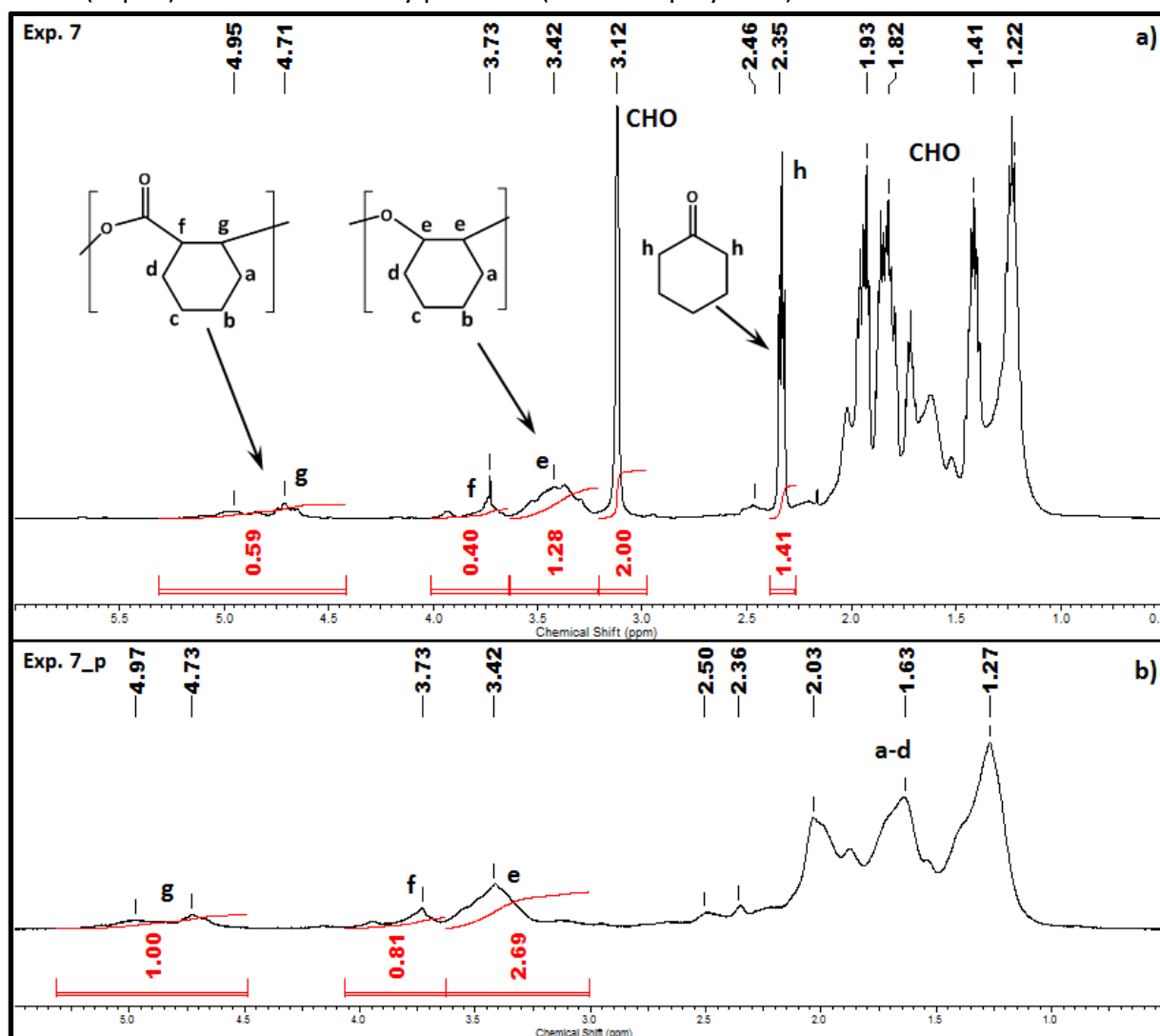
^g $[\text{MUO}]/[\text{Cr}]=500:1$

The formation of higher molar mass polyesters is probably inhibited by $\text{Co}_2(\text{CO})_8$, which acts as a chain transfer agent during the copolymerization. The negative role of $\text{Co}_2(\text{CO})_8$ was confirmed when one equivalent of $\text{Co}_2(\text{CO})_8$ was added to 2-CrCl catalyzing the ROP of β -butyrolactone at 100°C . As a result, polyesters with molar mass of only $1.7\text{ kg}\cdot\text{mol}^{-1}$ were obtained, while blank ROP of BBL using solely 2-CrCl at 100°C afforded high molar mass PHB ($58\text{ kg}\cdot\text{mol}^{-1}$, $\bar{D} = 5.9$). Decrease of $\text{Co}_2(\text{CO})_8$ concentration was tested with respect to compromise between chain transfer and ROP reactions (exp. 9). However, the

copolymerization with decreased concentration of $\text{Co}_2(\text{CO})_8$ did not afford higher molar mass polyester too. Interestingly, the formation of acetone was not observed during the reaction.

5.2.2 Copolymerization of CHO or MUO with CO catalyzed by $2\text{-CrCl}/\text{Co}_2(\text{CO})_8$

Further, the copolymerization of CO with CHO or MUO using dual $2\text{-CrCl}-\text{Co}_2(\text{CO})_8$ catalytic system was investigated. Cyclohexene oxide with CO (exp. 7, Table 5.4) led to similar low molar mass polymer (Spectrum 5.16a). In contrast to PO/CO copolymerization, no cyclic ester was present in the reaction mixture and cyclohexanone side product was formed significantly (peak **h** in Spectrum 5.16a). ^1H NMR spectrum of separated polymer revealed that resulting copolymer is composed of approximately 40% of ester (peaks **f** + **g**) and 60% ether units (**e**), (Spectrum 5.16b). The copolymerization of methylundec-10-enoate oxide (exp. 8) did not lead to any products (ester nor polyester).



Spectrum 5.16: ^1H NMR spectra of CHO/CO copolymerization (exp. 7) a) reaction mixture, b) dried polymer

5.2.3 Conclusion

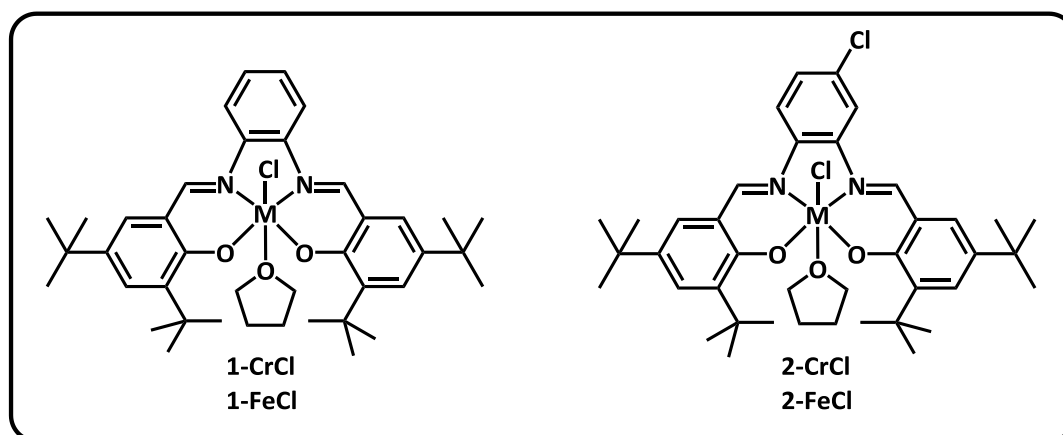
Dual catalyst **2-CrCl**/ $\text{Co}_2(\text{CO})_8$ led to cyclic lactone and low molar mass polyester ($1 \text{ kg}\cdot\text{mol}^{-1}$) with 80-90% of ester linkage in the copolymer. The formation of acetone by-product was observed during PO/CO copolymerization. ^1H NMR spectrum of oligomer suggests also the presence of epoxide double carbonylation leading to anhydrides during the reaction. The optimization of experimental conditions did not lead to significant improvement of catalytic performance. The formation of oligomeric product with 40% of ester linkage was observed also during cyclohexene oxide/CO copolymerization while the methylundec-10-enoate oxide/CO coupling reaction did not afford any product. Although **2-CrCl** proved to be excellent catalyst in BBL ROP,^{42b} it is incompatible with $\text{Co}_2(\text{CO})_8$ carbonylation catalyst, which causes chain transfer side reactions.

5.3 Copolymerization of epoxides with anhydrides

5.3.1 Copolymerization of epoxides and anhydrides catalyzed by Cr and Fe salen complexes

Salphen complexes of aluminium, cobalt and especially chromium are well known as the most efficient catalysts in epoxide/anhydride copolymerization.⁵⁸ Herein, we attempted to copolymerize basic epoxides available on large scale (PO, CHO, SO) with PA using chromium and iron salen complexes.

Synthesized salen chromium and iron complexes **1-CrCl**, **2-CrCl** and **1-FeCl**, **2-FeCl** (Scheme 5.5) were first used in the copolymerization of PA with CHO.



Scheme 5.5: Proposed structure of salen chromium and iron complexes

It was found, that **1-CrCl**, **1-FeCl** and **2-FeCl** alone (Table 5.5, exp. 1-3) were not able to catalyze the copolymerization reaction, whereas combined with PPNCI (1:1), all complexes afforded highly alternating polyesters. Complexes **1-FeCl** and **2-FeCl** afforded polyesters in low yields. **1-CrCl**/PPNCI afforded highly alternating polyesters in 76% yield within 1 h (exp. 5). Our complex **1-CrCl** was nevertheless less active in the ROCOP of PA with CHO compared to already reported results obtained with the same complex at identical conditions (98% conversion after 1 h)⁵⁸. Except of the significant role of monomer (PA) purity (see Table 5.8 in chapter 5.3.2, page 84), another major factor influencing the copolymerization is a structure/purity of chromium complex, which can contain different attached ligands, which is strongly dependent on synthesis procedure as already reported earlier by Rieger et al.^{42b}

Catalytic system **1-CrCl**/PPNCI exhibited slightly better catalytic performance compared to **2-CrCl**/PPNCI. The reason is probably lower nucleophilicity of complex **1-CrCl** resulting in weaker interactions between metal and nucleophile (initiating Cl⁻ group or polymer chain, i.e. oxypolymeryl group) allowing faster monomer insertion into the metal-oxygen bond. The copolymerization of PA and CHO with solely PPNCI (Table 5.5, exp. 4) surprisingly afforded also highly alternating polyesters with narrow dispersity, therefore PPNCI was further

explored for the copolymerization of epoxides with anhydrides in following sub-chapters 5.3.2-5.3.7.

Table 5.5: Copolymerization of PA with CHO catalyzed with salphen Cr and Fe complexes

Exp.	Catalyst	Y_w^a (%)	M_n^b (kg.mol ⁻¹)	\bar{D}^b	Ester Linkage ^c (%)
1	1-CrCl	0	-	-	-
2	1-FeCl	0	-	-	-
3	2-FeCl	0	-	-	-
4	PPNCl	8	3.5	1.07	95
5	1-CrCl/PPNCl	76	6.7	1.17	96
6	2-CrCl/PPNCl	64	5.5	1.17	95
7	1-FeCl/PPNCl	17	3.7	1.27	92
8	2-FeCl/PPNCl	11	4.2	1.14	94

$t_p=1h$, $T=110^\circ C$, $n_{CAT}=10\mu mol$, $[PA]/[CHO]/[Cat.]/[PPNCl]=250:250:1:1$, $V_{SOLVENT}=1.5mL$ (dry); Crude new PA from Alfa Aesar was used in all polymerizations;
^a Based on isolated polymer yield;
^b Determined by SEC-PS calibration in THF at 35°C;
^c Determined by ¹H NMR of dried polymer samples in CDCl₃

Use of twice sublimed PA (exp. 9, Table 5.6) for PA/CHO copolymerization afforded higher molar mass polyesters compared to crude PA (exp. 5). Corresponding SEC traces (Figure 5.2) exhibit a bimodal character. This phenomenon is further explored in chapter 5.3.2. The copolymerization of PA with PO and SO with **1-CrCl** afforded polyesters with > 99% of ester units and molar masses 6-10 kg.mol⁻¹ (exp. 11, 12). The copolymerization of CHA with PO and CHO using **1-CrCl** resulted in low molar mass polyesters (exp. 13 and 14).

Table 5.6: Copolymerization of epoxides and anhydrides catalyzed with salphen Cr complexes

Exp.	Anhydride	Epoxide	Catalyst	Y_w^a (%)	M_n^b (kg.mol ⁻¹)	\bar{D}^b	Ester Linkage ^c (%)
5	PA ^e	CHO	1-CrCl/PPNCl	76	6.7	1.17	96
9	PA ^f	CHO	1-CrCl/PPNCl	64	8.1	1.22	98
10	PA ^f	CHO	2-CrCl/PPNCl	57	5.8	1.22	97
11	PA ^f	PO	1-CrCl/PPNCl	39	6.5	1.24	> 99
12	PA ^f	SO	1-CrCl/PPNCl	81	9.0	1.20	> 99
13 ^d	CHA ^g	PO	1-CrCl/PPNCl	86	2.2	1.59	≈ 91
14 ^d	CHA ^g	CHO	1-CrCl/PPNCl	86	1.4	1.20	> 98

$t_p=1h$, $T=110^\circ C$, $n_{CAT}=10\mu mol$, $[Anhydride]/[Epoxide]/[Cr]/[PPNCl]=250:250:1:1$, $V_{SOLVENT}=1.5mL$ (dry);
^a Based on isolated polymer yield;
^b Determined by SEC-PS calibration in THF at 35°C;
^c Determined by ¹H NMR of dried polymer samples in CDCl₃;
^d $t_p = 5h$;
^e Crude PA (new, Alfa Aesar);
^f 2x sublimed PA (new, Alfa Aesar);
^g CHA distilled under N₂ atmosphere

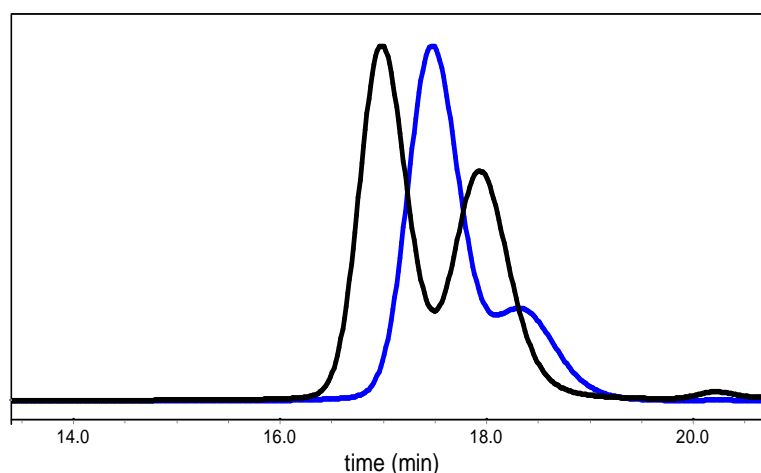


Figure 5.2: SEC traces of CHO-PA copolymers prepared with **1-CrCl**/PPNCl using crude PA (blue, exp. 5) and twice sublimed PA (black, exp. 9)

Additional attempt to copolymerize bio-based epoxides α -pinene oxide (APO) and β -pinene oxide (BPO) with PA using **1-CrCl**/PPNCl was performed in a bulk at 130°C (Table 5.7, for the monomer structures see Figure 5.13, page 97). Although the experiments were performed at prolonged reaction time (24 h) we did not observe high-molar mass polyester formation (no polymer could be precipitated at the end of the polymerization). ^1H NMR spectra of obtained viscous liquids confirmed the formation of ester bonds, nevertheless, the large number of signals in the spectra did not allow a proper characterization of the products (Spectrum 8.7 and Spectrum 8.8 in supplementary data, page 130). The copolymerization of methylundec-10-enoate oxide (MUO) with PA catalyzed with **1-CrCl**/PPNCl (exp. 17) give access to polyester with moderate molar mass in 70% yield.

Table 5.7: Copolymerization of phthalic anhydride with bio-based epoxides

Exp.	Epoxide	Catalyst	T (°C)	t_p (%)	Y_w^a (%)	M_n^b ($\text{kg}\cdot\text{mol}^{-1}$)	\mathcal{D}^b	Ester Linkage (%) ^c
15	APO ^d	1-CrCl /PPNCl	130	24	86	0.8	1.09	n.d.
16	BPO ^d	1-CrCl /PPNCl	130	24	77	0.8	1.07	n.d.
17	MUO ^e	2-CrCl /PPNCl	110	5	70	7.1	1.22	n.d.

$T=110^\circ\text{C}$, $n_{\text{CAT}}=10\mu\text{mol}$, $[\text{PA}]/[\text{Epoxide}]/[\text{Cr}]/[\text{PPNCl}]=250:250:1:1$, $V_{\text{SOLVENT}}=1.5\text{mL}$ (dry); Crude new PA from Alfa Aesar was used in all polymerizations;

^a Based on isolated polymer yield;

^b Determined by SEC-PS calibration in THF at 35°C;

^c Determined by ^1H NMR in CDCl_3 of dried polymer samples;

^d Copolymerization in bulk;

^e Copolymerization in toluene (1mL)

5.3.2 Copolymerization of PA with CHO catalyzed with PPNCl - initial screening

Since PPNCl alone surprisingly produced highly alternating polyester even in the absence of metal complexes (see exp. 4, Table 5.5), we decided to explore its potential as a catalyst in epoxide/anhydride copolymerization.

The most reactive monomers, cyclohexene oxide (CHO) and phthalic anhydride (PA), were selected as the substrates for further reaction initiated by PPNCl. Significant

differences in the reproducibility of experiments performed in longer time period were observed (Table 5.8, exp. 1 vs 2). Therefore, the effect of monomer and catalyst purity was explored in more detail.

Recently purchased PA (2015, (A)) afforded higher molar masses polyesters compared to 2 years old PA (Table 5.8, exp. 3 vs. 2). Such a difference is caused probably by a fact, that old batch PA contains higher amount of absorbed water, which acts as a chain transfer agent during the copolymerization. Another slight improvement was achieved when freshly recrystallized PPNCl was used as a catalyst (exp. 4), however, additional multiple recrystallization of PPNCl (exp. 5) did not lead to further increase of molar masses as observed earlier for (Salphen)Cr(III)Cl/PPNCl catalytic system.⁵⁸

Table 5.8: Copolymerization of PA-CHO with phthalic anhydrides in toluene at 110°C

Exp.	PPNCl (recr.)	PA ^a (Supplier)	Y _w ^b (%)	M _n ^{THEOR c} (kg.mol ⁻¹)	M _n ^{PS d} (kg.mol ⁻¹)	Đ ^{PS d}	M _n ^{MALLS e} (kg.mol ⁻¹)	Ester Linkage (%) ^f
1 ^g	1x	2013 (A)	51	31.4	12.8	1.31	-	98.5
2 ^h	Old (1x)	2013 (A)	71	43.7	4.4	1.10	5.9	93.2
3	Old (1x)	2015 (A)	65	40.0	6.7	1.17	8.8	96.2
4	Fresh (1x)	2015 (A)	64	39.4	8.1	1.23	10.5	97.5
5	Fresh (3x)	2015 (A)	50	30.8	6.9	1.23	9.2	97.5
6	Fresh (1x)	2015 (S)	73	44.9	7.2	1.14	9.6	96.3
7	Fresh (1x)	2015 (A) subl.	57	35.0	11.7	1.31	14.6	98.0
8	Fresh (1x)	2015 (A) 2x subl.	73	44.9	11.2	1.32	13.7	98.4
9	Fresh (1x)	2015 (A) recr.	62	38.1	10.0	1.28	12.5	98.7

T=110°C, t_p=5h, n_{PPNCl}=20μmol, [PA]/[CHO]/[PPNCl]=250:250:1, V_{Toluene}=3mL (dry);

^a Year of shipping, (supplier: A – Alfa Aesar, S – Sigma Aldrich);

^b Based on isolated polymer yield;

^c Theoretical molar mass (For details see experimental part);

^d Determined by SEC-PS calibration in THF at 35°C;

^e Determined by SEC-MALLS in THF at 35°C using dn/dc increment 0.139 mL.g⁻¹;

^f Determined by ¹H NMR of dried polymer samples in CDCl₃;

^g Experiment performed in 2013 with freshly purchased PA;

^h Recently performed blank experiment (02/2015) with PA purchased in 2013

FT-IR spectroscopy of purchased phthalic anhydrides (Figure 5.3) revealed the presence of hydrolyzed PA in all batches. Sigma Aldrich PA contained higher amount of hydrolyzed PA (peak at 1675 cm⁻¹), compared to PA from Alfa Aesar (Figure 5.3, spectrum I vs. II). Further purification was therefore performed to remove phthalic acid from PA. Sublimation and recrystallization of PA led to appreciable decrease of hydrolyzed PA (Figure 5.3, spectrum III and IV).

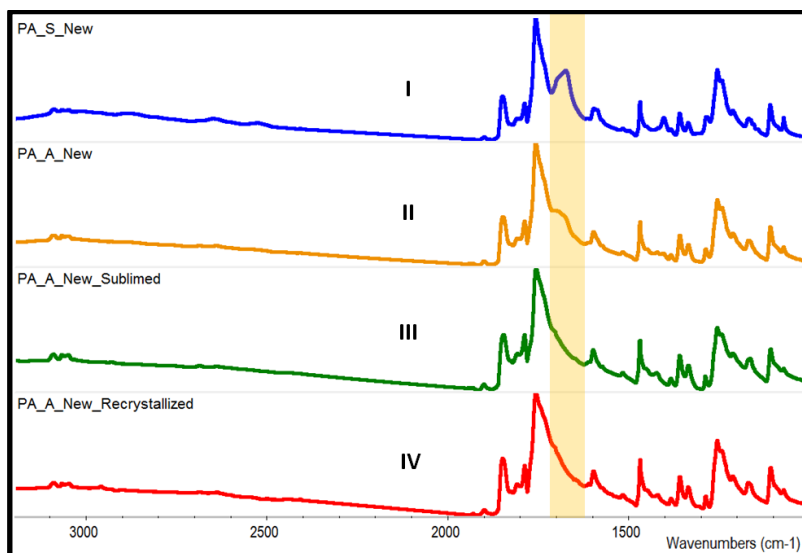


Figure 5.3: FT-IR spectra of phthalic anhydrides purified by different methods (I-PA(S)_New; II-PA(A)_New; III-PA(A)_New_Sublimed; IV-PA(A)_New_Recrystallized)

Copolymerizations with different batches of PA (Table 5.8) showed differences in molar masses of polyesters. The highest molar mass was achieved when sublimed PA was copolymerized with dried CHO. Approximately 50% increase in molar mass was achieved when using sublimed PA (exp. 8; $11.7 \text{ kg}\cdot\text{mol}^{-1}$) compared to unpurified PA grades (≈ 8.1 and $7.2 \text{ kg}\cdot\text{mol}^{-1}$ in exp. 4 and 6, respectively). With decreasing amount of phthalic acid in PA (as determined by FT-IR spectroscopy, Figure 5.3) a decrease of polymerization activity was observed, reflecting the fact that phthalic acid acts as an initiator. SEC analyses showed bimodal traces for all polyesters (Figure 5.4) and higher molar mass fraction was always of double molar mass compared to the lower molar mass one. This phenomenon was already observed in metal catalyzed ROCOP of epoxides and anhydrides⁵⁸ and it was explained by the presence of bifunctional initiating species such as phthalic acid (product of anhydride hydrolysis) or water. SEC traces of the copolymers show that lower molar mass fraction in the copolymer obtained from sublimed PA (exp. 7) is significantly larger compared to lower molar mass fraction in copolymer obtained from crude PA (exp. 4), which contains higher amount of phthalic acid (GPC curve III vs. II in Figure 5.4). This clearly indicates phthalic acid being a bifunctional initiator.

Multiple sublimation did not lead to further increase of molar mass, however, we observed higher yield of copolymerization (Table 5.8, exp. 8 vs. 7).

Additionally, the recrystallization of PA from hot (dry) chloroform was used as a method of PA purification. Decrease of phthalic acid in PA was confirmed by FT-IR spectroscopy (Spectrum IV, Figure 5.3).

SEC trace of copolyester prepared from sublimed PA (Table 5.8, exp. 7) showed the highest ratio of lower to higher molar mass fractions (Figure 5.4, spectrum III), i.e. the highest ratio of monoinitiated chains towards those formed on bifunctional initiators.

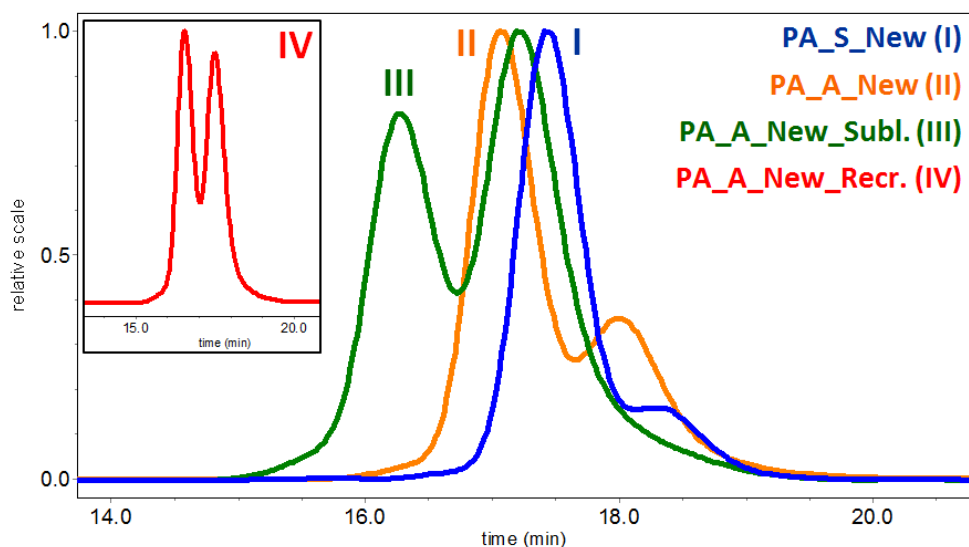


Figure 5.4: SEC-traces of PA-CHO copolymers prepared from PA with various amount of hydrolyzed PA (PA_S_New - blue, PA_A_New - orange, PA_A_New_Subl. - green, PA_A_New_Recr. - red)

To confirm further the role of phthalic acid as a bifunctional initiator we performed the copolymerizations of CHO with sublimed PA on purpose contaminated by phthalic acid (Table 5.9). Decrease of molar mass from $12.5 \text{ kg}\cdot\text{mol}^{-1}$, when using sublimed PA (exp. 10), to 8.3 and $3.5 \text{ kg}\cdot\text{mol}^{-1}$ for PA with added 1 and 5 wt % of phthalic acid (exp. 11 and 12) was observed.

Table 5.9: Copolymerizations of CHO with PA contaminated on purpose by phthalic acid

Exp.	Phthalic acid (wt %)	Y_w^a (%)	M_n^b ($\text{kg}\cdot\text{mol}^{-1}$)	\mathcal{D}^b	Ester Linkage ^c (%)
10	0	65	12.5 (20.4+10.1)	1.14	98.8
11	1	66	8.3 (10.6+4.9)	1.07	96.7
12	5	70	3.5 (4.0)	1.01	90.3

$t_p=5\text{h}$, $n_{\text{PPNCl}}=20\mu\text{mol}$, $V_{\text{SOLVENT}}=3\text{mL}$ (dry), $[\text{PA}+\text{Ph. Acid}]/[\text{CHO}]/[\text{PPNCl}]=250:250:1$; Freshly sublimed PA from Alfa Aesar was used in all polymerizations;

^a Based on isolated polymer yield;

^b Determined by SEC-PS calibration in THF at 35°C ; Values in brackets correspond to maxima of peaks (M_p);

^c Determined by ^1H NMR of dried polymer samples in CDCl_3

The copolymerization of CHO with PA containing 1 wt % of phthalic acid further resulted in a significant decrease of lower-molar mass fraction (Figure 5.5, grey vs. black chromatogram). 5 wt % of phthalic acid afforded single distribution, which suggests that dominant initiating species was phthalic acid in that case.

Above results demonstrate that even using PA with the lowest content of phthalic acid, the monofunctional initiator (Cl^- anions from PPNCl) represents on maximum $\approx 60\%$ of growing centers, the rest of the polymer chains being grown on bifunctional centers. This corresponds also with 3-4 times lower than expected molar mass values, which were in range $30\text{-}45 \text{ kg}\cdot\text{mol}^{-1}$ (Table 5.8). Different initiating groups has to be reflected in the structure of formed polymer. Detail MALDI-TOF MS analysis (next chapter 5.3.3) was therefore used to investigate the nature of end-groups formed at the initiation step.

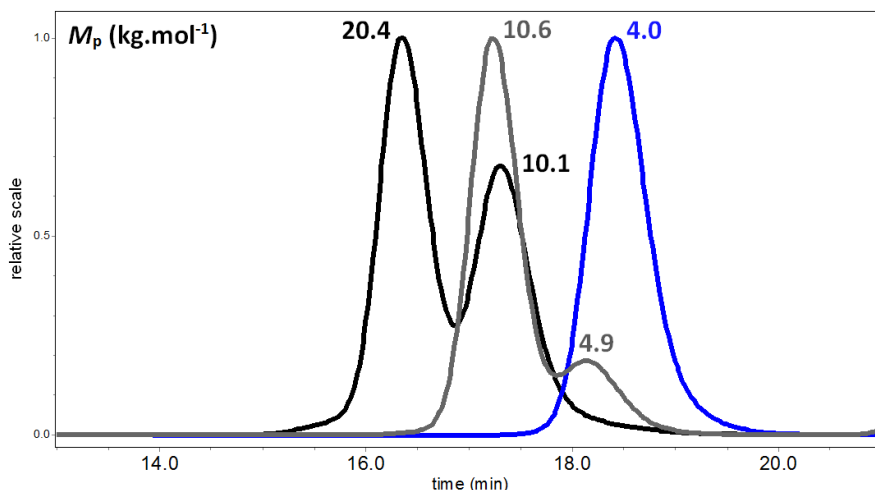


Figure 5.5: Copolymerization of PA with CHO using sublimed PA (black) and sublimed PA with addition of 1 wt % (grey) and 5 wt % (blue) of phthalic acid

5.3.3 MALDI-TOF analysis of PA-CHO polyesters – mechanism of initiation

The MALDI-TOF MS analysis of PA-CHO copolymer was performed with respect to determine the microstructure of polyester and to reveal the mechanism of initiation. Considering the fact, that high molar mass copolyesters are more difficult to ionize, we selected a low molar mass polyester ($M_p = 4.0 \text{ kg.mol}^{-1}$) obtained only after 1 h of polymerization (exp. 25, Table 5.13, page 94). Relatively narrow molar mass distribution of PA-CHO copolymers ($\mathcal{D} < 1.20$ according to SEC) was also suitable for reliable MALDI-TOF MS analysis.

MALDI-TOF mass spectrum of PA-CHO copolymer (Figure 5.6) shows two distributions with $M_p = 1.9 \text{ kg.mol}^{-1}$ and 3.9 kg.mol^{-1} . A lower molar mass fraction is composed of 4 series of peaks (peaks 1-4 in Figure 5.6) while a higher molar mass fraction is composed of 6 series of peaks (peaks 5-10).

The lower molar mass fraction contains two different microstructures **A** and **B** (Scheme 5.6). Microstructure **A** with Cl and PPN-OMe end groups was assigned to peaks 1 and 3 that corresponds to the polymer with the same end-groups but different amounts of ether units (different perfection of alternating structure). **Peak 1:** $M_{\text{Peak1}} (1834.70) = M_{\text{Cl}} (34.97) + 5 \times M_{\text{PA-CHO}} (1230.45) + M_{\text{PPN}^+} (538.19) + M_{\text{OCH}_3} (31.03) = 1834.64 \text{ g.mol}^{-1}$. Peak 3 is different by a factor of 98 to peak 1, which corresponds to one additional ether unit in the polymer chain. **Peak 3:** $M_{\text{Peak3}} (1932.78) = M_{\text{Peak1}} (1834.64) + 1 \times M_{\text{CHO}} (98.07) = 1932.71 \text{ g.mol}^{-1}$.

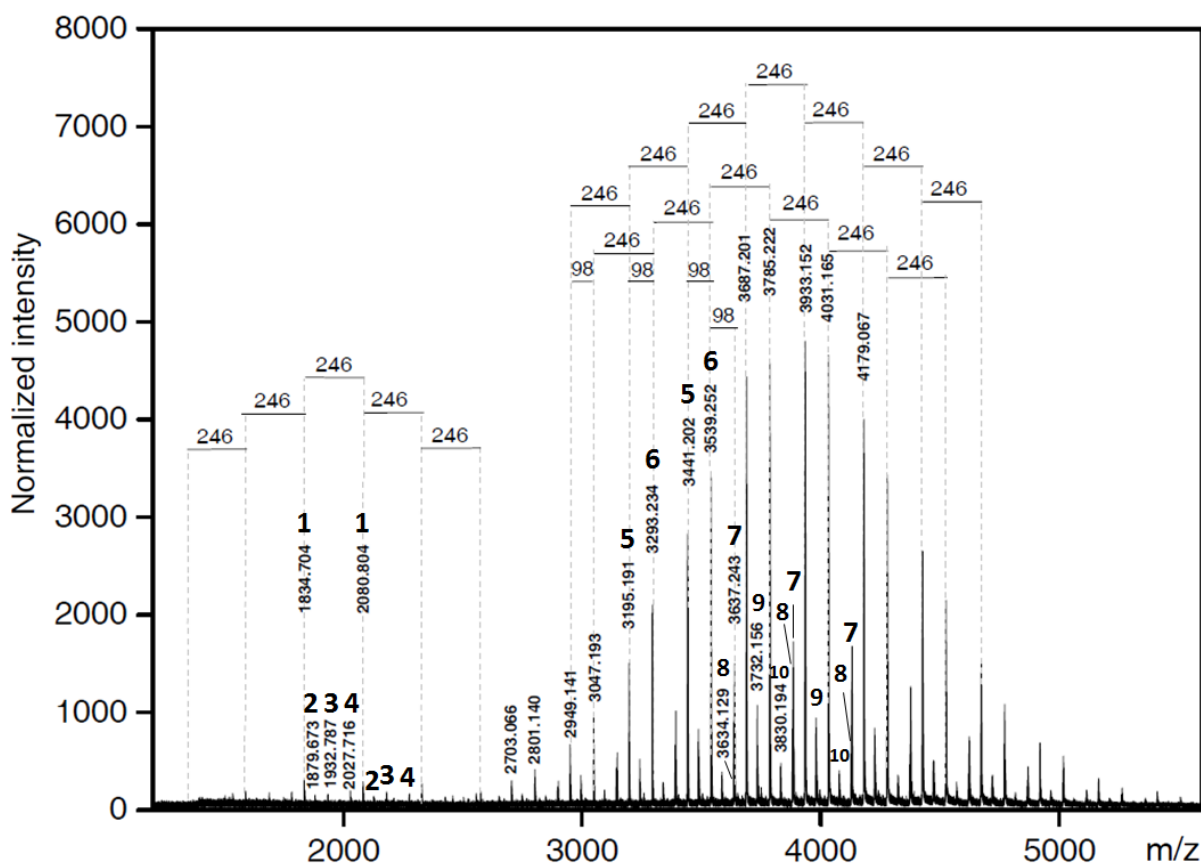
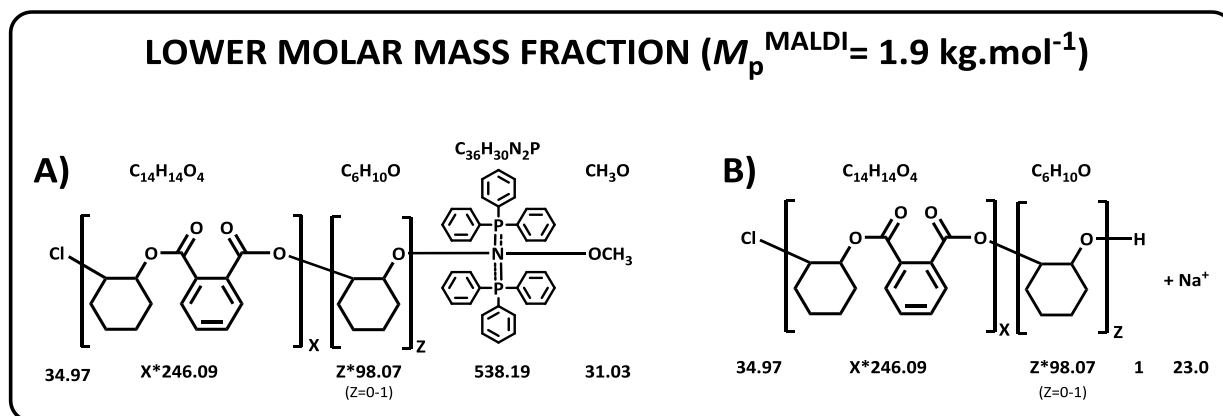


Figure 5.6: MALDI-TOF mass spectrum of PA-CHO copolymer catalyzed with PPnCl (exp. 25)

Peaks 2 and 4 were attributed to microstructure **B** with Cl and COOH (or OH) end groups.

Peak 4: $M_{\text{Peak4}} (2027.72) = M_{\text{Cl}} (34.97) + 8 \times M_{\text{PA-CHO}} (1968.71) + M_{\text{H}} (1) + M_{\text{Na}^+} (23.0) = 2027.68$ g.mol⁻¹. Peak 2 is higher of factor 98 to Peak 4, which again corresponds to one CHO unit.

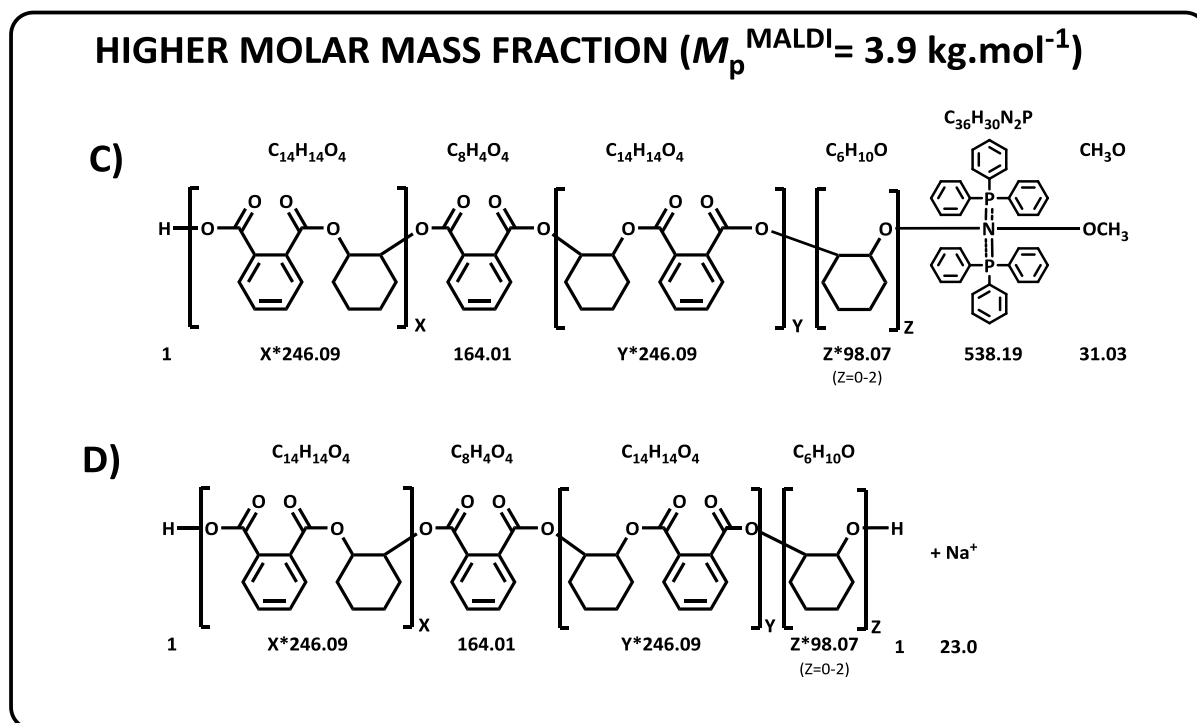
Peak 2: $M_{\text{Peak2}} (2125.81) = M_{\text{Peak4}} (2027.68) + 1 \times M_{\text{CHO}} (98.07) = 2125.75$ g.mol⁻¹.



Scheme 5.6: Microstructure of PA-CHO copolyesters (lower molar mass fraction)

The higher molar mass fraction is also composed of two different microstructures (microstructures **C** and **D**; Scheme 5.7). We found, that both microstructures (**C**, **D**) contain phthalic acid in the middle of polymer chain as it was stated in chapter 5.3.2, thus we can definitely confirm the role of phthalic acid as a bifunctional initiating species. Microstructure **C** with -COOH (or -OH) and PPN⁺-OMe end groups (Scheme 5.7) was assigned to peaks 5, 6

and 7 (Figure 5.6). **Peak 5:** $M_{\text{Peak5}} (3687.20) = M_{\text{H}} (1) + 12xM_{\text{PA-CHO}} (2953.07) + M_{\text{Ph.Acid}} (164.01) + M_{\text{PPN}^+} (538.19) + M_{\text{OCH}_3} (31.03) = 3687.30 \text{ g.mol}^{-1}$. Peaks 6 and 7 are different by a factor of 98 and 196 to peak 5, which correspond to one and two ether units in the copolymer. **Peak 6:** $M_{\text{Peak6}} (3785.22) = M_{\text{Peak5}} (3687.30) + 1xM_{\text{CHO}} (98.07) = 3785.37 \text{ g.mol}^{-1}$. **Peak 7:** $M_{\text{Peak7}} (3883.12) = M_{\text{Peak5}} (3687.30) + 2xM_{\text{CHO}} (196.14) = 3883.44 \text{ g.mol}^{-1}$.



Scheme 5.7: Microstructure of PA-CHO copolyesters (higher molar mass fraction)

Microstructure **D** (Scheme 5.7) is represented by peaks 8-10 (Figure 5.6), which contains two -COOH groups (one -COOH and one -OH or two -OH end groups are also possible).

Peak 8: $M_{\text{Peak8}} (3634.13) = 2xM_{\text{H}} (2) + 14xM_{\text{PA-CHO}} (3445.25) + M_{\text{Ph.Acid}} (164.01) + M_{\text{Na}^+} (23) = 3634.26 \text{ g.mol}^{-1}$. Peaks 9 and 10 are again higher by a factor of 98 (+1xCHO) and 196 (+2xCHO) compared to peak 8. **Peak 9:** $M_{\text{Peak9}} (3732.20) = M_{\text{Peak8}} (3634.26) + 1xM_{\text{CHO}} (98.07) = 3732.33 \text{ g.mol}^{-1}$. **Peak 10:** $M_{\text{Peak10}} (3830.19) = M_{\text{Peak8}} (3634.26) + 2xM_{\text{CHO}} (196.14) = 3830.40 \text{ g.mol}^{-1}$.

Interestingly, an additional MALDI-TOF MS analysis using Na^+ salt to ionize PA-CHO copolymer (Figure 5.7b) showed significant increase in intensity of **peaks 8,9** and **10**, whereas the **peaks 5-7** were not detected in the spectrum. This is due to two different charges (neutral vs. ionized) of analyzed polyester: microstructure **D** (**peaks 8-10**) with neutral -OH or -COOH end groups, which requires Na^+ salt to be ionized, and microstructure **C** (**peaks 5-7**), which already poses easily ionizable $\text{PPN}^+\text{-OMe}$ groups.

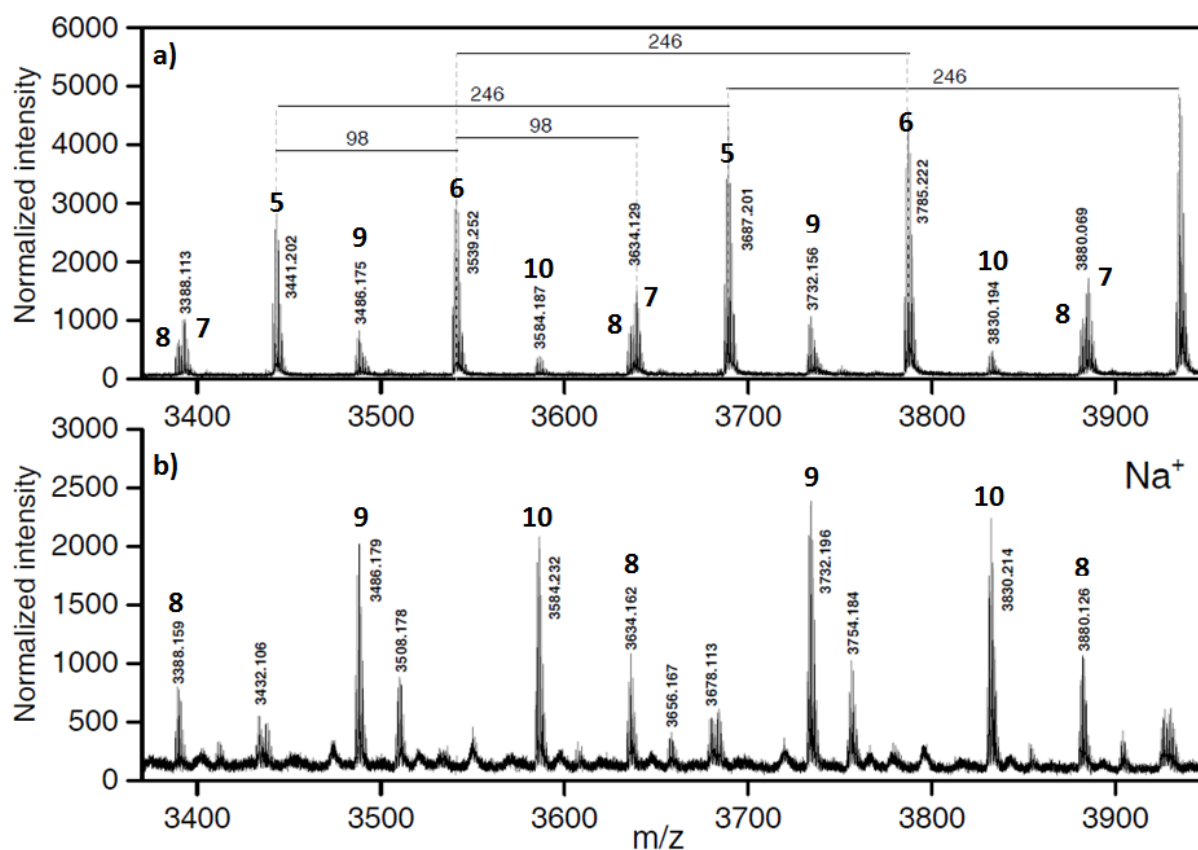
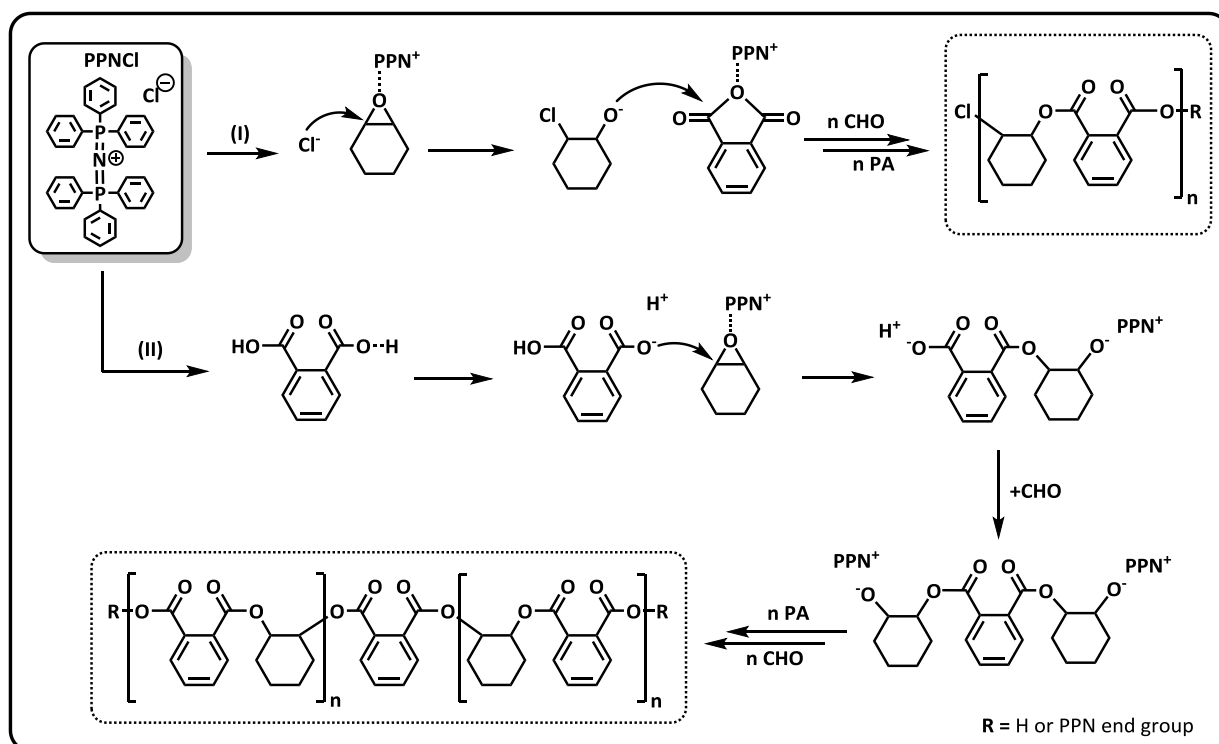


Figure 5.7: MALDI-TOF mass spectrum of PA-CHO copolymer catalyzed with PPNCI ionized in absence (a) or in presence (b) of Na salt

MALDI-TOF mass spectrum clearly shows, that both PPNCI and phthalic acid can initiate the copolymerization (proposed initiation mechanism is depicted in Scheme 5.8). The lower molar mass fraction contain in-built Cl atom as α end group in copolyester. This is an evidence that epoxide (or anhydride) is initiated via nucleophilic Cl⁻ anion (Scheme 5.8, route I). We can assume, that PPN⁺ cation helps to activate the epoxide and thus facilitates the epoxide opening via Cl⁻ nucleophile. On the contrary, the higher molar mass fraction does not contain Cl atoms at the ends of the polymer chains in agreement with an idea of phthalic acid initiation where the end-groups are not formed in the initiation step (Scheme 5.8, route II). While the presence of phthalic acid in PA generally led to significant decrease of the lower molar mass fraction (Figure 5.4 and Figure 5.5) and also to decrease of overall molar mass of the polyesters, we can also assume lower activation energy of phthalic acid initiated epoxide ring-opening compared to the activation via Cl⁻ anion. Polymer chains grow preferentially from bifunctional phthalic acid. ω -end groups of both lower and higher molar mass fractions were either free carboxylic and hydroxyl groups or μ -oxo bridged PPN cation with attached methoxy group, which is visible also in ¹H NMR spectrum (Spectrum 8.9 in supplementary data).



Scheme 5.8: Proposed mechanism of initiation by PPNCI (I) and phthalic acid (II)

5.3.4 The effect of PA-CHO stoichiometry, reaction temperature and solvent (incl. bulk)

The effect of PA-CHO ratio to determine a potential role of nonstoichiometry of the comonomers was also investigated (Table 5.10). A slight decrease in monomer conversion (62% vs 67%) was observed when PA was used in 10% excess over CHO (exp. 13) while an opposite 10% excess of CHO (exp. 15) resulted in almost the same conversion (69%). Interestingly, the increase of CHO concentration over PA did not lead to higher appearance of consecutive ether connections in the copolymer. Observed molar masses and carbonate linkage content were comparable (exp. 13-15).

Table 5.10: Nonstoichiometric copolymerization of PA with CHO at 110°C in toluene

Exp.	[PA]:[CHO]/[PPNCl] ^a	Y _w ^b (%)	Y _{NMR} ^c (%)	M _n ^d (kg.mol ⁻¹)	Đ ^d	Ester Linkage ^e (%)
13	250:225:1	62	66	7.1	1.21	97.8
14	250:250:1	67	71	7.8	1.23	97.4
15	225:250:1	69	81	7.8	1.34	97.6

t_p=5h, n_{PPNCl}=20μmol, V_{SOLVENT}=3mL (dry); Crude new PA from Alfa Aesar was used in all polymerizations;

^a The average error of monomer dosage in all experiments within this chapter (5.3) was in range of 0-2% excess of one comonomer, while maximal deviation from equimolar ratio was 5% (1.05 eq.);

^b Based on isolated polymer yield;

^c Based on ¹H NMR analysis of reaction mixture;

^d Determined by SEC-PS calibration in THF at 35°C;

^e Determined by ¹H NMR of dried polymer samples in CDCl₃

Copolymerizations of PA with CHO at various temperatures (Table 5.11) were performed as well. Increase of temperature from 100 to 110°C in toluene (exp. 4 vs 16) resulted in increase of polymer yield by ≈ 1/3 and almost doubled molar mass. To see the catalytic performance of PPNCl at temperatures above 110°C, toluene was replaced by xylene. Interestingly, the polymer yield in xylene at 110°C was higher by 10% compared to toluene at 110°C (Table 5.11, exp. 4 vs. 17). Molar mass of the polyester obtained in xylene was comparable of that obtained in toluene. At 130°C in xylene, polymer yield was the highest one and the molar mass was also higher compared to the experiments performed at 110°C (exp. 18 vs. 4 and 17). High copolymer yield and molar mass was also observed in xylene at 130°C with an alternative catalyst DMAP (exp. 19).

Table 5.11: Effect of solvent and temperature in copolymerization of CHO with PA

Exp.	Catalyst	Solvent	T (°C)	Y _w ^a (%)	M _n ^b (kg.mol ⁻¹)	Đ ^b	Ester Linkage (%) ^c
16	PPNCl	TOLUENE	100	46	4.9	1.13	95.0
4		TOLUENE	110	64	8.1	1.23	97.5
17		XYLENE	110	73	8.4	1.21	96.5
18		XYLENE	130	95	10.4	1.67	97.5
19	DMAP	XYLENE	130	85	9.1	1.32	97.0

t_p=5h, n_{BASE}=20μmol, [PA]/[CHO]/[Base]=250:250:1, V_{SOLVENT}=3mL (dry); Crude new PA from Alfa Aesar was used in all polymerizations;

^a Based on isolated polymer yield;

^b Determined by SEC-PS calibration in THF at 35°C;

^c Determined by ¹H NMR of dried polymer samples in CDCl₃

Compared to the solution polymerization, the copolymerization of PA with CHO in a bulk provided slightly higher molar masses, while dispersity remains low. However, decreased ester linkage content was observed (Table 5.12, exp. 20-23), probably due to the effect of increased viscosity during the copolymerization in bulk causing slower migration of more bulky comonomer (phthalic anhydride) to propagating centers compared to CHO. Consequently, a faster CHO approach to the growing centers could result in consecutive epoxide insertions.

Table 5.12: Copolymerization of PA with CHO at 110°C in bulk

Exp.	Base	t_p (h)	Y_w^a (%)	M_n^b (kg.mol ⁻¹)	\mathcal{D}^b	Ester Linkage ^c (%)
20	PPNCl	1	49	6.7	1.17	89.0
21	PPNCl	3	86	10.7	1.16	91.6
22	PPNCl	5	89	11.4	1.16	92.0
23	DMAP	5	85	14.5	1.13	93.6

$T=110^\circ\text{C}$, $n_{\text{BASE}}=20\mu\text{mol}$, $[\text{PA}]/[\text{CHO}]/[\text{Base}]=250:250:1$; Crude new PA from Alfa Aesar was used in all polymerizations;

^a Based on isolated polymer yield;

^b Determined by SEC-PS calibration in THF at 35°C;

^c Determined by ¹H NMR of dried polymer samples in CDCl₃

5.3.5 Kinetic studies of CHO-PA copolymerization

Kinetic experiments were performed in toluene at 110°C with [PA]/[CHO]/[PPNCl] ratio 250:250:1. Conversions were determined either by a ¹H NMR analysis of the reaction mixture and by a gravimetric method. The gravimetric method provided slightly lower conversions, which could be explained by non-complete precipitation of the reaction mixture in MeOH, when a small oligomeric product could remain in MeOH solution and by losses of polymer during its isolation. Conversion curve (determined by ¹H NMR) (Figure 5.8a) suggests no induction period and linear plot of $\ln(M_0/M_t)$ to time dependence indicates 1st order of the reaction with respect to the monomer (Figure 5.8b).

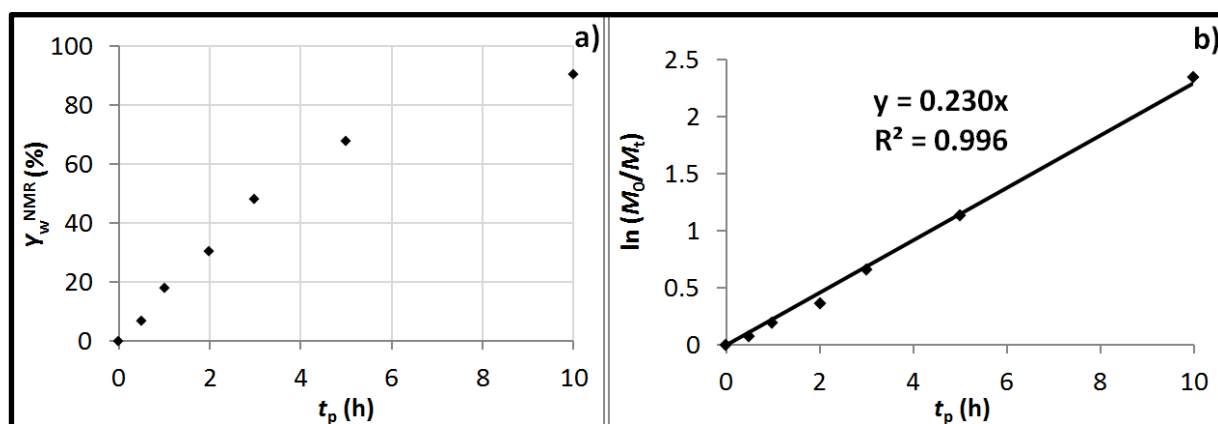


Figure 5.8: a) Conversion curve of PA/CHO copolymerization at 110°C catalyzed with PPNCl; b) Linear plot of $\ln(M_0/M_t)$ vs time

SEC traces of separated polyesters shows a nascent bimodal character with increasing conversion (Figure 5.9a). The fact, that the bimodality is not visible in early stage of the copolymerization could be probably attributed to a poor separation ability of SEC method in low molar mass range.

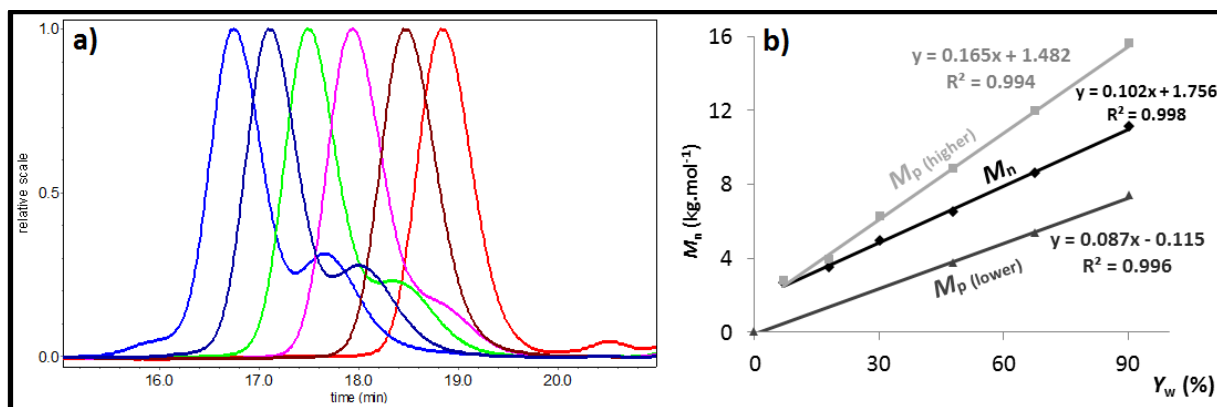


Figure 5.9: a) SEC traces of CHO-PA copolymers (exp. 24-29) and b) linear increase of PES molar mass with conversion

Close coincidence of M_n with M_p (at peak maximum) values of higher-molar mass fraction (see Figure 5.9b) is clearly visible in the early stage of the copolymerization. Linear evolution of M_n with conversion (Figure 5.9b) and low dispersities even at high monomer conversions further suggest living behavior of the polymerization system. The fact that the linear dependence of M_n to conversion does not pass through the origin is caused by bimodality of obtained polymers. Indeed, when M_p values of lower-molar mass fraction were related to the conversion, a linear curve passing through the origin was obtained.

Table 5.13: Kinetic study of PA/CHO copolymerization initiated by PPNCI in toluene at 110°C

Exp.	t_p (h)	Y_w^a (%)	Y_{NMR}^b (%)	$M_n^{THEOR}^c$ (kg.mol ⁻¹)	M_n (M_p) ^d (kg.mol ⁻¹)	\mathcal{D}^d	N_{PM}/N_{PPNCI}^e	EL^f (%)
24	0.5	1	7	4.3	2.6 (2.8)	1.07	1.38	-
25 ^g	1	8	18	10.9	3.5 (3.9)	1.07	1.30	94.7
26	2	27	30	19.2	4.9 (6.2)	1.15	3.43	-
27	3	46	48	34.0	6.5 (8.8+3.7)	1.18	4.27	96.6
28	5	65	68	44.5	8.6 (11.9+5.4)	1.19	4.86	-
29	10	84	90	57.7	11.1 (15.6+7.4)	1.22	4.71	96.6

$T=110^\circ\text{C}$, $n_{PPNCI}=20\mu\text{mol}$, $[\text{PA}]/[\text{CHO}]/[\text{PPNCI}]=250:250:1$, $V_{\text{SOLVENT}}=3\text{mL}$ (dry); Crude new PA from Alfa Aesar was used in all polymerizations;

^a Based on isolated polymer yield;

^b Based on ¹H NMR analysis of reaction mixture;

^c Theoretical molar mass (For details see experimental part);

^d Determined by SEC-PS calibration in THF at 35°C, Values in brackets correspond to maxima of peaks (M_p);

^e Number of polymer molecules to PPNCI;

^f Ester linkage, determined by ¹H NMR of dried polymer samples in CDCl₃;

^g $M_p^{MALDI-TOF} = 3.9 + 1.9 \text{ kg.mol}^{-1}$

Significant increase of number of polymer molecules per initiator molecule (N_{PM}/N_{PPNCI}) (Table 5.13) indicates substantial extent of transfer reactions in the system. However, the low dispersity observed even at longer polymerization period exclude the presence of transesterification reactions. The possible explanation of these contradictory observations could be very fast transfer reactions between propagating and dormant polymer chains that would have to be present during the reaction. To prove such a hypothesis one would need more experimental data.

Increase of catalyst loading to 100:100:1 (exp. 30-32, Table 5.14) resulted in higher number of initiating species and probably also to faster chain transfer leading to expected decrease in molar mass (Figure 5.11). Proportional decrease of propagation rate at low catalyst loading (500:500:1) was observed as could be expected (Figure 5.10). Surprisingly, molar masses of obtained copolymers (exp. 33-35) were comparable with those from copolymerizations performed at 250:250:1 ratio. This is probably due to the presence of phthalic acid, which acts as initiating species, thus the decrease of [PPNCl] to ½ did not result to proportional decrease of active sites in the system. Low dispersity even at high conversion of monomers suggests that no concurrent transesterification reaction occurs during the copolymerization.

Table 5.14: Copolymerization of PA with CHO at different loadings of PPNCl

Exp.	[PA]/[CHO] /[PPNCl]	t_p (h)	Y_w^c (%)	$M_n^{THEOR^d}$ ($kg \cdot mol^{-1}$)	M_n^e ($kg \cdot mol^{-1}$)	\mathcal{D}^e	N_{PM}/N_{PPNCl}^f	Ester Linkage
30		1	26	6.2	2.8 (3.3)	1.11	2.3	95.9
31	100:100:1 ^a	3	67	16.8	5.1 (7.0+3.1)	1.19	3.3	96.9
32		5	86	21.0	6.0 (8.4+3.8)	1.20	3.5	97.2
33		5	38	46.6	5.6 (6.6)	1.12	8.3	92.2
34	500:500:1 ^b	10	69	84.0	8.2 (10.1)	1.13	10.4	93.9
35		20	89	109.2	11.5 (14.8+7.0)	1.17	9.6	96.2

Polymerization run in toluene; $T=110^\circ C$, $V_{TOL}=3mL$ (dry), ^a $n_{PPNCl}=40\mu mol$, ^b $n_{PPNCl}=10\mu mol$; Crude new PA from Alfa Aesar was used in all polymerizations;

^c Based on isolated polymer yield;

^d Theoretical molar mass (For details see experimental part);

^e Determined by SEC-PS calibration in THF at $35^\circ C$; Values in brackets correspond to maxima of peaks (M_p);

^f Number of polymer molecules to PPNCl;

^g Determined by 1H NMR of dried polymer samples in $CDCl_3$

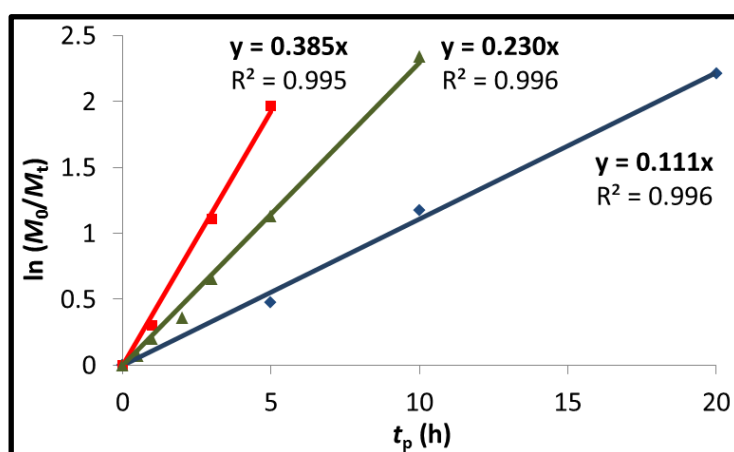


Figure 5.10: Linear plot of $\ln(M_0/M_t)$ vs time at different monomer/PPNCl loadings (100:1-red; 250:1-green and 500:1-blue)

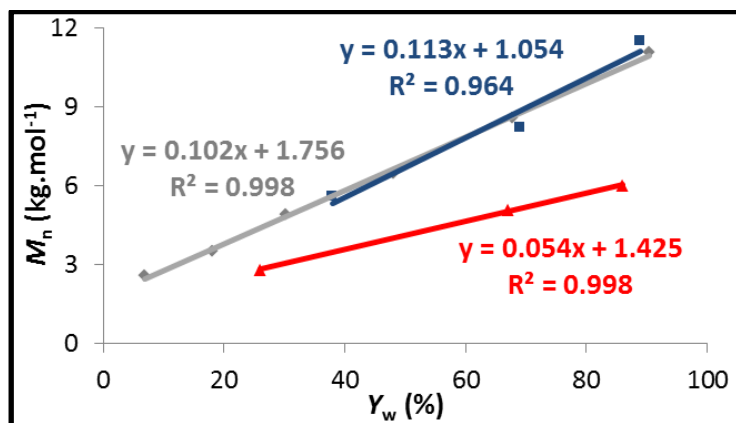


Figure 5.11: Linear increase of polyester molar mass with conversion at different monomer/PPNCl loadings (100:1-red; 250:1-grey and 500:1-blue)

5.3.6 Copolymerization of PA with CHO catalyzed by various organic bases

Other common organic bases were studied as potential initiators for the ROCOP of PA with CHO. Figure 5.12 shows that, at our conditions, PPNCl is the most effective initiator producing polyester with the highest molar mass compared to other neutral and ionic bases. Sufficiently high conversions in PA-CHO copolymerizations were achieved also with simple organic bases *n*-Bu₄NCl and *n*-Bu₄NBr, which afforded polyesters with molar masses $\approx 7 \text{ kg.mol}^{-1}$ and low $\bar{D} < 1.14$. Ester linkage in PA-CHO copolymers prepared with the four most effective bases were in range 96–98%. Triphenylphosphine salt (PPh₃) and bicyclic organic bases 1,5,7-Triazabicyclo[4.4.0]dec-5-ene (TBD) and 1,4-diazabicyclo[2.2.2]octane (DABCO) exhibited very poor catalytic performance and obtained polyesters had only 58% (PPh₃) and 81% (DABCO) of ester linkage. All synthesized polyesters had low dispersities ($\bar{D} < 1.21$).

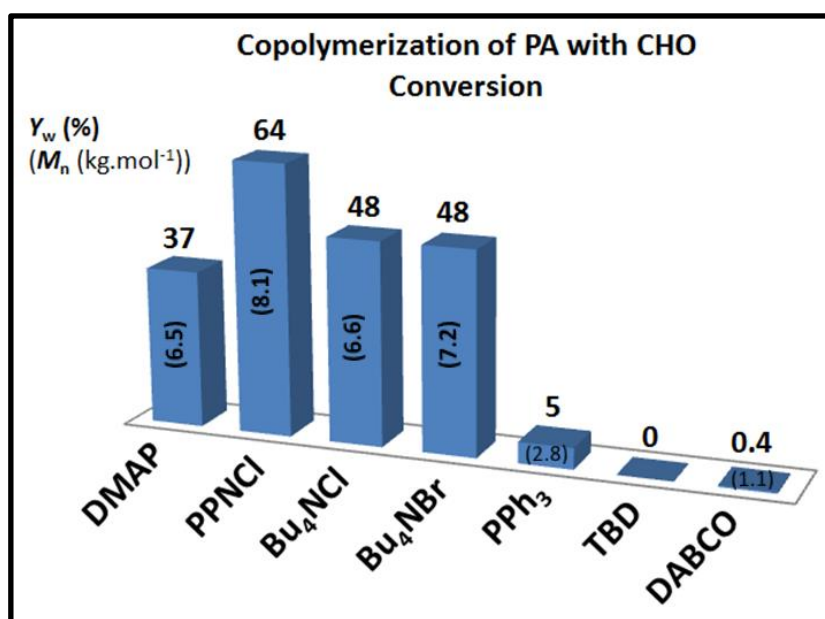


Figure 5.12: Copolymerization of PO with PA (crude, new Alfa Aesar) at 110°C after 5h in toluene catalyzed by various organic bases ([PA]/[CHO]/[Base]=250:250:1)

5.3.7 Copolymerization of various epoxides and anhydrides

PPNCl was shown to be the most efficient catalyst for CHO/PA copolymerization (see above). Therefore it was selected as a catalyst for the copolymerization of various epoxides and anhydrides (Figure 5.13). Anhydrides were purified by sublimation or distillation and the reaction were performed in toluene at 110°C and [Epoxide]/[Anhydride]/[PPNCl] ratio 250:250:1.

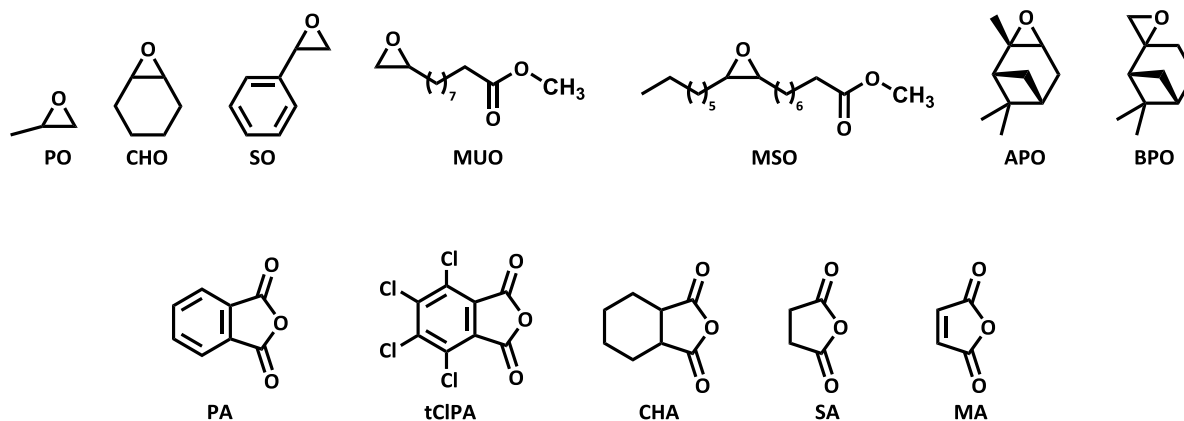


Figure 5.13: Listing of epoxides and anhydrides used for alternating ROCOP

The versatility of PPNCl in the copolymerization of selected epoxides with anhydrides is depicted in Table 5.15. All synthesized polyesters had molar mass 7-21 kg.mol⁻¹ and high content of ester linkage 88-99%. In the case of PA more than 99% of ester units were achieved in its copolymerization with other epoxides (exp. 36-39). Obtained polyesters were amorphous with T_g between -19 - +138°C reflecting the rigidity of built-in epoxide.

Table 5.15: Copolymerization of various epoxides and anhydrides initiated by PPNCI

Exp.	Anhydride	Epoxide	Y_w^a (%)	M_n^b (kg.mol ⁻¹)	\mathcal{D}^b	Ester Linkage (%) ^c	T_g^d (°C)	$T_{deg.(5\%)}^e$ (°C)
36	PA	PO	87	21.1	1.23	> 99	55	269
37	PA	CHO	93	14.5	1.49	99	138	295
38	PA	SO	83	13.5	1.21	> 99	85	275
39	PA	MUO	77	7.2	1.29	> 99	-18	277
40	PA	MSO	0	-	-	-	-	-
41 ^f	MA	CHO	27	-	-	-	41	243
42 ^f	SA	CHO	0	-	-	-	-	-
43	tCIPA	PO	66	5.3	2.07	97	84	218
44	tCIPA	CHO	94	5.5	2.22	94	154	268
45	tCIPA	SO	n.d.	0.8	1.07	n.d.	n.d.	n.d.
46	tCIPA	MUO	74	4.0	1.66	> 95	-0.5	245
47 ^g	CHA	PO	42	1.6	1.25	99	37	257
48 ^g	CHA	CHO	60	1.2	1.19	89	81	295

$T=110^\circ\text{C}$, $t_p=10\text{h}$, $n_{PPNCI}=20\mu\text{mol}$, $[\text{Anhydride}]/[\text{Epoxide}]/[\text{PPNCI}]=250:250:1$, $V_{\text{Toluene}}=3\text{mL}$ (dry); PA and tCIPA (New, Alfa Aldrich) were purified by sublimation;

^a Based on isolated polymer yield;

^b Determined by SEC-PS calibration in THF at 35°C ;

^c Determined by ^1H NMR spectroscopy;

^d Determined by DSC from 2nd run (heating $10^\circ\text{C}/\text{min}$);

^e Determined by TGA, as 5% polymer loss (heating $10^\circ\text{C}/\text{min}$);

^f $t_p=5\text{h}$, MA and SA were used as received;

^g $t_p=20\text{h}$, CHA was purified by distillation

The copolymerization of epoxides with tCIPA resulted in polyesters with lower M_n and broader dispersity suggesting the presence of transesterification reactions during the copolymerization (exp. 43-46). Related copolymers possess higher T_g due to bulkier and more polar tCIPA, while all polyesters have lower thermal stability compared to polyesters from PA, which is due to low dissociation energy of C-Cl bond in tCIPA/epoxide copolymers. The copolymerization of aliphatic CHA with PO and CHO (exp. 47, 48) ran very slowly and afforded low molar mass polyesters with T_g 37 and 81°C , respectively. The copolymerization of MA resulted in a dark brown solid insoluble in organic solvents, which is due to crosslinking of copolymer during the copolymerization.^{54b} The copolymerization of PA with MSO (exp. 40) and SA with CHO (exp. 42) did not result in polyester formation. ^1H NMR spectra of all prepared polyesters are listed in supplement (Spectrum 8.10 - Spectrum 8.18, page 131).

5.3.8 Conclusion

Salphen chromium complexes **1-CrCl** and **2-CrCl** alone were inactive in PO/CHO copolymerization. In combination with PPNCI, they were 5x faster in PA/CHO copolymerization compared to solely organic base PPNCI, however, they did not exceed PPNCI in term of polyester molar mass and ester linkage content. The copolymerization of sterically demanding epoxides α -pinene oxide and β -pinene oxide (catalyzed with **1-CrCl**) led only to the formation of oligomers.

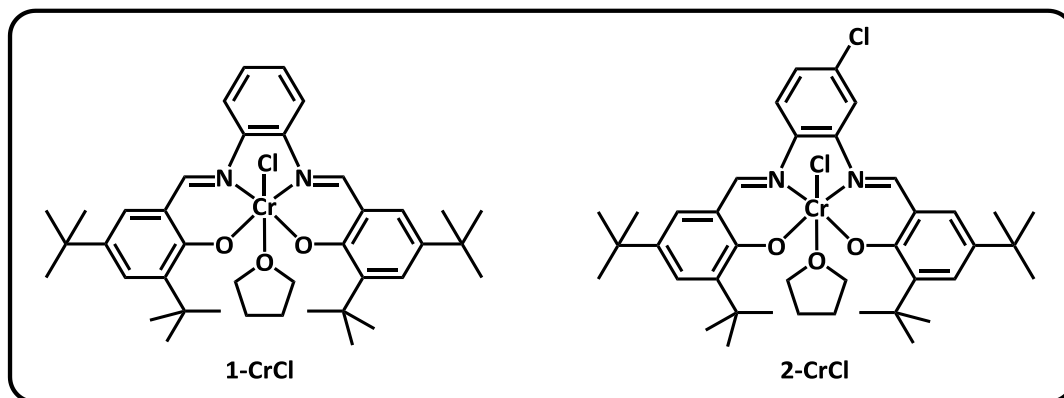
Further, the simple organic bases proved to be efficient catalysts for epoxide/anhydride copolymerization. Although the organic bases are slower compared to the metal catalysts, obtained polyesters exhibit sufficiently high molar masses 4-17 kg.mol⁻¹ and high content of ester linkage. Detailed kinetic investigation revealed controlled copolymerization and determination of α - and ω -end groups helped to clarify the mechanism of initiation.

Organic bases, namely the most efficient PPNCI, proved their versatility in the copolymerization of various epoxide and anhydride substrates producing aliphatic polyesters with various thermal properties. New bio-based epoxide methylundec-10-enoate oxide was further successfully copolymerized with phthalic anhydride and tetrachlorophthalic anhydride to produce polyester with molar mass 7 and 4 kg.mol⁻¹, high ratio of ester linkage and low T_g -18 and -0.5°C, respectively.

5.4 Copolymerization of epoxides with CO₂

5.4.1 Alternating copolymerization of PO or CHO with CO₂ catalyzed by Cr salphen complexes

More than 10 years ago, Rieger et al. reported the copolymerization of PO with CO₂ using **1-CrCl**/DMAP.^{75d} Herein, we decided to briefly reinvestigate this topic and explore the effect of the substitution in salphen ligand framework on overall catalytic performance in epoxide/CO₂ copolymerization in the presence of highly efficient PPNCl cocatalyst.



Scheme 5.9: Proposed structure of salphen chromium complexes

First, we tested the catalytic performance of salphen-chromium complex **2-CrCl** (Table 5.16). With **2-CrCl** alone, copolymer of molar mass 14 kg.mol⁻¹ was obtained with activity (TOF) 28 h⁻¹, nevertheless, the carbonate linkage of such copolymer was low (\approx 60%) (exp. 1). Addition of 0.5 eq. of neutral cocatalyst (DMAP) resulted in decrease of activity, but in all cases significantly higher ratio of carbonate units in the copolymer was achieved (exp. 2-4). Significantly lower activity and selectivity of **2-CrCl** complex compared to reported salen complex **1-CrCl (31a)**^{75d} is probably due to higher Lewis acidity of metal center resulting in stronger interaction of metal-nucleophile, which slows down the coordination of epoxide (PO) and also its attack by nucleophile in initiation and propagation step. Lower selectivity to polycarbonate is caused by strong Cr-nucleophile (DMAP) interactions, which disfavor the coordination of free polymer chains, a step preceding formation of cyclic carbonate by back-biting (especially at higher temperatures). Although the reproducibility of experiments was generally good (exp. 3 vs. 4), after prolonged time, we observed a significant drop-off in catalytic performance of **2-CrCl**. Since we manipulated the catalyst in air, we assume that the decrease of catalytic activity is observed due to slow exchange of chlorine atoms by hydroxyl groups.

Table 5.16: Copolymerization of PO/CO₂ catalyzed with salphen Cr complexes **2-CrCl**/DMAP

Exp.	Catalyst	[PO]/[Cr]	$Y_{w\text{POL}}$ (%) ^a	TOF_{POL} (h ⁻¹) ^b	TOF_{CC} (h ⁻¹) ^c	M_n^d (kg.mol ⁻¹)	\bar{D}^d	Selectivity ^e (% PPC)	Carbonate Linkage (%)
1	2-CrCl	1000:1	56	28	13	14.3	1.40	69	60.8
2	2-CrCl /DMAP	1000:1	38	18	30	13.5	1.05	38	93.7
3	2-CrCl /DMAP	2000:1	17	17	28	9.7	1.14	38	94.0
4	2-CrCl /DMAP	2000:1	17	17	28	11.7	1.12	37	95.6
5	2-CrCl regen.	1000:1	40	20	15	14.2	1.15	57	55.9
6	2-CrCl regen. /DMAP	1000:1	38	20	28	5.4	1.04	42	80.5
7	2-CrCl regen. /DMAP	2000:1	50	49	23	11.7	1.25	60	72.6

Polymerizations run in neat epoxide; $V_{\text{PO}}=1.5\text{-}2\text{mL}$, $T=75^\circ\text{C}$, $t_p=20\text{h}$, $p_{\text{CO}_2}=1\text{MPa}$, $[\text{Cr}]/[\text{DMAP}]=1:0.5$;

^a Based on isolated polymer yield;

^b Turnover frequency to polycarbonate;

^c Turnover frequency to cyclic carbonate (For details see experimental part);

^d Determined by SEC-MALLS in THF at 35°C using dn/dc increment 0.050 mL.g^{-1} ;

^e Selectivity to PPC over cyclic carbonate

To regenerate the catalyst, we treated the complex in HCl vapors for several days. Subsequent copolymerization of PO with CO₂ using regenerated **2-CrCl** (exp. 5) revealed increase of activity and selectivity towards polycarbonate compared to the original aged complex **2-CrCl**, but interestingly, significant decrease of carbonate linkage was observed in the final copolymer compared to the non-regenerated complex. Despite no further analysis of regenerated Cr complex was performed, we can only assume, that such a discrepancy can be caused by a modification of catalyst structure. Probably, the complex could bear two chlorine atoms attached to Cr instead of one in the original complex **2-CrCl**. Increase of activity and selectivity to polycarbonate with regenerated complex (exp. 7 vs. 4) is probably due to higher concentration of initiating species (especially Cl⁻) together with lowered Lewis acidity of active center (second Cl⁻ attached to chromium can decrease Lewis acidity of the metal due to M⁺ effect), which allow easier and faster coordination of growing polymer chains to both sides of the metal center. Enhanced catalytic performance could markedly fasten PO insertion compared to CO₂ resulting in lower carbonate linkage ratio in the copolymer.

The copolymerization of PO with CO₂ catalyzed by **1-CrCl** and **2-CrCl** using more nucleophilic cocatalyst PPNCI (Table 5.17) resulted in significant increase in activity, while the selectivity remained rather low. Prepared polycarbonates had 94-98% of carbonate linkage, which is significantly higher compared to the relevant copolymerization using DMAP cocatalyst with complex **2-CrCl** (Exp. 6, 7 in Table 5.16 vs. exp. 8, 9 in Table 5.17).

Table 5.17: Copolymerization of PO/CO₂ catalyzed by **1-CrCl** and **2-CrCl** with PPNCI cocatalyst

Exp.	Catalyst	[PO]/[Cr]	Y_{wPOL}^a (%)	TOF_{POL}^b (h ⁻¹)	TOF_{CC}^c (h ⁻¹)	M_n^d (kg.mol ⁻¹)	\bar{D}^d	Selectivity ^e (% PPC)	Carbonate Linkage (%)
8	2-CrCl regen. /PPNCI	1000:1	43	85.6	45.9	12.4	1.36	65	94.0
9	2-CrCl regen. /PPNCI	2000:1	25	103.3	215.6	13.1	1.13	32	96.7
10	1-CrCl /PPNCI ^f	2000:1	19	79.9	27.6	5.1	1.07	74	98.3
11	1-CrCl /PPNCI ^g	2000:1	38	152.9	33.4	7.2	1.70	82	96.1

Polymerizations run in neat epoxide; $V_{PO}=1.5-2\text{mL}$, $T=75^\circ\text{C}$, $t_p=5\text{h}$, $p_{CO_2}=1\text{MPa}$, $[\text{Cr}]/[\text{PPNCI}]=1:0.5$;

^a Based on isolated polymer yield;

^b Turnover frequency to polycarbonate;

^c Turnover frequency to cyclic carbonate (For details see experimental part);

^d Determined by SEC-MALLS in THF at 35°C using dn/dc increment 0.050 mL.g⁻¹;

^e Selectivity to PPC over cyclic carbonate (CC);

^f Synthesized 10/2012;

^g Synthesized 7/2015

The copolymerization of CHO with CO₂ catalyzed with **2-CrCl**/PPNCI proceeded markedly slower compared to PO/CO₂ copolymerization, due to higher steric hindrance of cyclohexene oxide. **2-CrCl** afforded highly alternating polycarbonates with > 99% carbonate units in the copolymers and 100% selectivity to polycarbonate (Table 5.18). Blank experiment with a new batch of **2-CrCl** (synthesized 10/2014), which was performed approximately 5 month after the catalyst synthesis (04/2015) revealed decreased catalytic performance compared to early experiments with **2-CrCl** from 2011 (exp. 14 vs. 13). The regeneration of **2-CrCl** again led to the significant increase in catalytic performance, which was coincident with previous copolymerization experiments (exp. 15 vs. 13).

Table 5.18: Effect of catalyst (**2-CrCl**) aging in CHO/CO₂ copolymerization

Exp.	Catalyst	t_p (h)	Y_{wPOL}^a (%)	TOF_{POL}^b (h ⁻¹)	M_n^c (kg.mol ⁻¹)	\bar{D}^c
12	2-CrCl ^d regen. /PPNCI	8	37	45.9	12.3	1.22
13	2-CrCl ^d regen. /PPNCI	20	51	26.6	15.5	1.25
14	2-CrCl ^e (5 months old) /PPNCI	20	23	11.8	8.8	1.16
15	2-CrCl ^e regen. /PPNCI	20	52	26.7	16.2	1.13

Polymerizations run in neat epoxide; $V_{PO}=1.5-2\text{mL}$, $T=75^\circ\text{C}$, $t_p=5\text{h}$, $p_{CO_2}=1\text{MPa}$, $[\text{CHO}]/[\text{Cr}]/[\text{PPNCI}]=1000:1:0.5$; Selectivity to polycarbonate as determined by ¹H NMR spectroscopy was >99% in all cases; All poly(cyclohexene carbonate)s have >99% carbonate linkages as determined by ¹H NMR spectroscopy;

^a Based on isolated polymer yield;

^b Turnover frequency to polycarbonate;

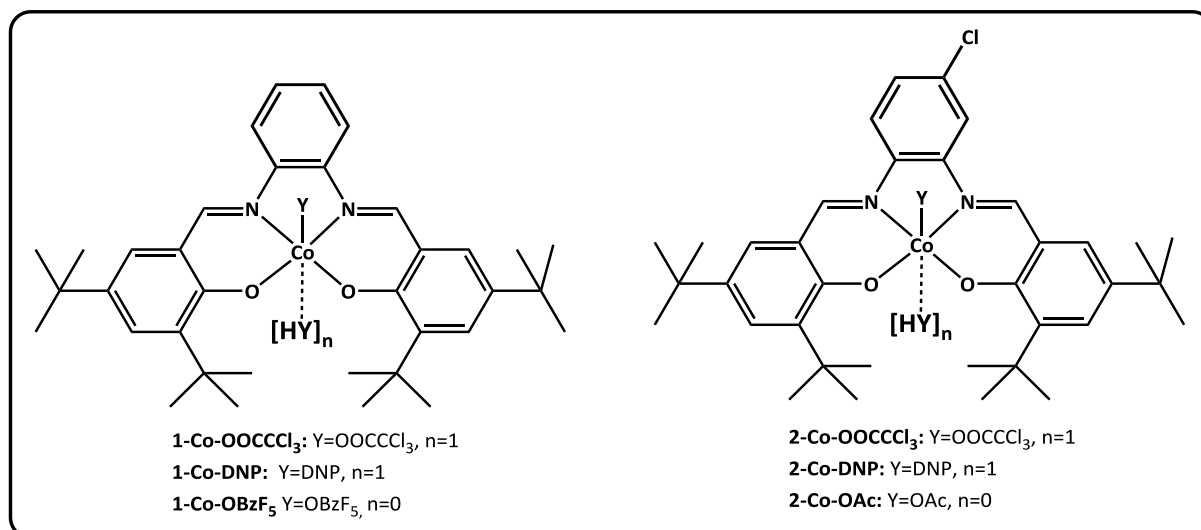
^c Determined by SEC-MALLS in THF at 35°C using dn/dc increment 0.087 mL.g⁻¹;

^d Synthesized 11/2011;

^e Synthesized 10/2014

5.4.2 Alternating copolymerization of PO and CO₂ catalyzed by Co salphen complexes

Compared to salen-chromium, cobalt-salen complexes usually exhibit better catalytic performance in terms of activity, molar mass and selectivity and usually they provide perfectly alternating polycarbonates. Therefore, we synthesized salphen-cobalt complexes with different nucleophilic counterions. We selected nucleophiles, which proved to be the most effective in combination with chiral cyclohexylene framework,^{76a} namely trichloroacetate, dinitrophenolate, pentafluorobenzoate and acetate (Scheme 5.10).



Scheme 5.10: Proposed structure of salphen cobalt complexes

5.4.2.1 Copolymerization of PO/CO₂ with 1-Co-OOCCl₃

Initial screening of experimental conditions was performed with symmetric salphen complex **1-Co-OOCCl₃** combined with PPNCI - the most frequent and efficient cocatalyst for salen complexes. Copolymerization performed at ambient temperature and 1 MPa pressure afforded highly alternating polycarbonate with molar mass $\approx 25 \text{ kg}\cdot\text{mol}^{-1}$. Comparison of catalytic performance of **1-Co-OOCCl₃**/PPNCI with chiral *R,R'* salen complexes (e.g. **52b**/PPNCI; Figure 2.24) showed that selectivity to polymer formation and TOF of **1-Co-OOCCl₃** are significantly lower. It can be explained by a stronger interaction of nucleophile Y group or growing polymer chain with Co center as a result of higher Lewis acidity of π -conjugated salphen complex. This limits the ring-opening of activated epoxide molecules (during initiation and propagation step) by nucleophile, which has to be released from Co center (in the case that nucleophile does not come from the cocatalyst). It could be further expected that higher Lewis acidity of salphen complex should lead to better selectivity to polycarbonate vs. cyclic carbonate as it was observed in the case of salphen Cr(III) complex compared to its salen analogue.^{75d} However, the selectivity of salphen Co (III) complex **1-Co-OOCCl₃** to polycarbonate formation was lower in all conditions compared to the salen complex. This shows the complexity of the copolymerization reactions where many parameters play a role and can work in the opposite manner. Enhanced activity was observed at elevated temperature 50°C and even at 75°C. An optimal polymerization temperature of **1-Co-OOCCl₃** from point of view of both high TOF and selectivity to PPC

(80%) was 50°C. Decrease of selectivity to PPC observed at higher temperatures is a general phenomenon of these catalytic systems due to higher activation energy for the formation of cyclic PC than for the formation of PPC.⁷⁸ Decrease of pressure resulted in decrease of activity, molar mass and at 0.1 MPa also to significant decrease of selectivity to PPC (Exp. 3, 4, Table 5.19). However, even at 0.1 MPa, the polymer consists of more than 99% of carbonate linkage suggesting the insertion of CO₂ into metal-alkoxy bond is sufficiently fast.

Table 5.19: Effect of temperature and reaction pressure to PO/CO₂ copolymerization catalyzed by **1-Co-OOCCCl₃**/PPNCl

Exp.	<i>T</i> (°C)	<i>p</i> (MPa)	<i>t_p</i> (h)	<i>Y_wPOL</i> ^a (%)	<i>TOF_{POL}</i> ^b (h ⁻¹)	<i>TOF_{CC}</i> ^c (h ⁻¹)	<i>M_n</i> ^{d,e} (kg.mol ⁻¹)	<i>D</i> ^{d,e}	Selectivity ^f (% PPC)
1	25	1	4	37	190	27	25.0 (34+18)	1.09	88
2	50	1	2	43	454	110	34.4 (48+25)	1.16	80
3	50	0.2	2	20	206	51	18.1 (27+14)	1.13	80
4	50	0.1	2	10	98	94	11.8 (13+7)	1.24	51
5	75	1	1	27	558	391	26.5 (43+21)	1.25	59

Polymerizations run in neat epoxide; [PO]/[Co]/[PPNCl]=2000:1:1, *V_{PO}*=1.5-2mL; Carbonate linkage of all polymers were >99% as determined by ¹H NMR spectroscopy;

^a Based on isolated polymer yield;

^b Turnover frequency to polycarbonate;

^c Turnover frequency to cyclic carbonate (For details see experimental part);

^d Determined by SEC-MALLS in THF at 35°C with *dn/dc* increment 0.050 mL.g⁻¹;

^e All polymers exhibit bimodal distributions (values in brackets correspond to maxima of peaks (*M_p*));

^f Selectivity to PPC over cyclic carbonate (CC)

We further investigated the influence of catalyst/cocatalyst ratio on activity and selectivity of copolymerization catalyzed with **1-Co-OOCCCl₃** (Figure 5.14) In contrast to salphen chromium complexes, which produced poly(ether-*co*-carbonate) even without any cocatalyst, complex **1-Co-OOCCCl₃** alone was almost completely inactive and produced only trace amount of cyclic carbonate (*TOF_{CC}* ≈ 2 h⁻¹) showing the crucial role of nucleophilic cocatalyst, which helps in ring-opening of the epoxide as the rate determining step of the copolymerization. The highest activity, molar mass and selectivity was observed at equimolar ratio of catalyst to cocatalyst. Further increase of cocatalyst loading (above 1:1 ratio) resulted in significant decrease of activity, selectivity and molar mass. This is due to the displacement of growing polymer chains from active metal centers by nucleophilic cocatalyst moieties that is notably promoted at higher cocatalyst concentration. This generally results in increased back-biting of free polymer chains leading to CC formation. Additionally, PPNCl was tested as a single catalyst. At identical conditions, only trace amount of cyclic carbonate (*TOF_{CC}* ≈ 3 h⁻¹) was detected in ¹H NMR spectrum of the reaction mixture.

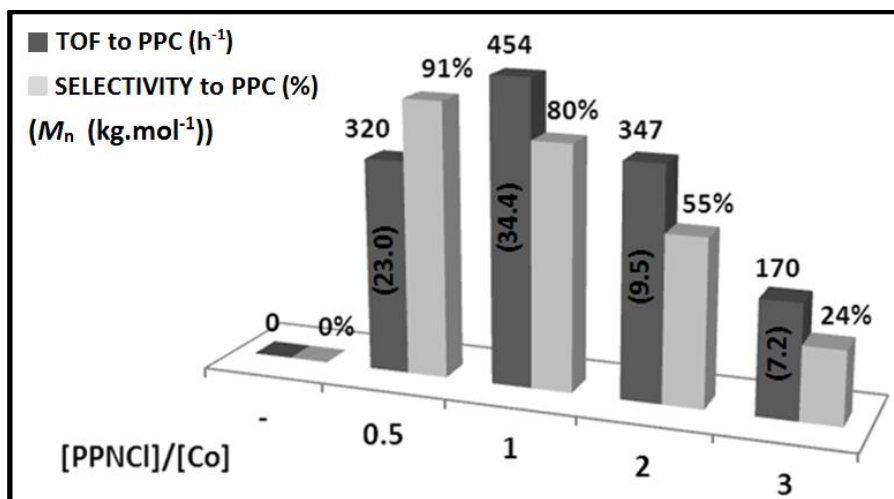


Figure 5.14: Effect of **1-Co-OOCCl₃**/PPNCl loading to PO/CO₂ copolymerization at 1MPa and 50°C ([PO]/[Co]=2000:1, t_p=2h)

5.4.2.2 Copolymerization of epoxide with series of salphen complexes **1-Co-Y** and **2-Co-Y**

To compare the catalytic performance of synthesized salphen cobalt complexes, we selected conditions, which proved to be the best compromise between the activity and selectivity as observed for catalyst **1-Co-OOCCl₃**/PPNCl. Table 5.20 shows comparison of catalytic behavior of symmetric salphen complexes **1-Co-Y** with phenylene backbone and asymmetric complexes **2-Co-Y** with 3-chlorophenylene backbone. Complex **1-Co-OOCCl₃** with the weakest nucleophile – trichloroacetate (*p*K_a of conjugated acid 0.65) proved to be the most effective for PO/CO₂ copolymerization to produce PPC with the highest activity, molar mass and selectivity up to 80% towards polymer. Complexes bearing stronger nucleophiles, such as **1-Co-OBzF₅** with pentafluorobenzoate (*p*K_a = 1.60) and **1-Co-DNP** with 2,4-dinitrophenolate (*p*K_a = 4.11) exhibit lower activity, molar mass and their selectivity was decreased to 60%. The decrease of catalyst activity with increase of Y nucleophilicity is caused by the fact that the stronger nucleophile dissociates from the metal center slower and thus the coordination and subsequent epoxide activation is slower. Similarly, higher affinity of more nucleophilic Y group to the metal center leads to higher concentration of uncoordinated polymer chains which undergo the back-biting reaction to CC, which leads to decreased selectivity.

Table 5.20: Copolymerization of PO/CO₂ catalyzed with complexes **1-Co-Y** and **2-Co-Y**

Exp.	Catalyst	Y_{wPOL}^a (%)	TOF_{POL}^b (h ⁻¹)	TOF_{CC}^c (h ⁻¹)	$M_n^{d,e}$ (kg.mol ⁻¹)	$\bar{D}^{d,e}$	Selectivity ^f (% PPC)	HT linkage ^g (%)
6	1-Co	0	0	243	-	-	0	-
2	1-Co-OOCCCl₃	43	454	110	34.4 (48+25)	1.16	80	92
7	1-Co-DNP	38	391	251	21.3 (40+21)	1.30	61	-
8	1-Co-OBzF₅	37	374	228	25.0 (41+21)	1.28	62	-
9	2-Co-OOCCCl₃	38	386	72	29.4 (43+23)	1.13	84	95
10	2-Co-DNP	33	340	87	14.8 (23+11)	1.10	80	-
11	2-Co-OAc	13	124	184	10.3 (10+9)	1.05	40	-

Polymerizations run in neat epoxide; [PO]/[Co]/[PPNCl]=2000:1:1, V_{PO} =1.5-2mL, T =50°C, t_p =2h, p_{CO_2} =1MPa; Carbonate linkage of all polymers were >99% as determined by ¹HNMR spectroscopy;

^a Based on isolated polymer yield;

^b Turnover frequency to polycarbonate;

^c Turnover frequency to cyclic carbonate (For details see experimental part);

^d Determined by SEC-MALLS in THF at 35°C with dn/dc increment 0.050 mL.g⁻¹;

^e All polymers exhibit bimodal distributions (values in brackets correspond to maxima of peaks (M_p));

^f Selectivity to PPC over cyclic carbonate (CC);

^g Head-to-tail linkage determined by ¹³C NMR spectroscopy

The substitution of phenylene backbone by Cl atom was further investigated as analogous Cr complex **11c (2-CrCl)** was found to be highly active in similar catalytic ROP of β -butyrolactone.^{42b} However, in the case of CO₂/PO copolymerization, the activity of chloro-substituted Co complexes **2-Co-OOCCCl₃** and **2-Co-DNP** was lower compared to unsubstituted derivatives **1-Co-OOCCCl₃** and **1-Co-DNP** (Table 5.20 runs 9 and 10 vs. 2 and 7). This can be explained by increased Lewis acidity of Co metal center in **2-Co-OOCCCl₃** and **2-Co-DNP**, which lowers the activity of salphen complexes due to stronger interaction of nucleophile and metal, which slows down PO coordination and its attack by nucleophile in initiation and propagation step. As expected, complex **2-Co-OAc** combining chloro-substitution on phenylene backbone and the strongest Y nucleophile (acetate group, $pK_a = 4.76$) displayed the lowest activity and selectivity in CO₂/PO copolymerization.

Comparison of temperature dependence of activity and selectivity of salphen complexes **1-Co-OOCCCl₃** and **2-Co-OOCCCl₃** in PO/CO₂ copolymerization shows that **1-Co-OOCCCl₃** continuously increases its activity up to 75°C, while the selectivity simultaneously decreases. Complex **2-Co-OOCCCl₃** reaches the maximum activity and selectivity at 50°C (Figure 5.15). This shows the importance of optimization of reaction conditions for each of the catalyst to achieve its best catalytic performance. In addition, asymmetric salphen complex **2-Co-OOCCCl₃** exhibited slightly higher regioselectivity (expressed as HT linkage %) compared to corresponding symmetric complex **1-Co-OOCCCl₃** (Table 5.20, exp. 2 vs. 9). For comparison reasons we also used unoxidized (salphen)Co(II) complex **1-Co** (without attached nucleophile) for PO/CO₂ copolymerization (Table 5.20, exp. 6). In combination with PPNCl the complex **1-Co** was able to catalyze the cyclization reaction to CC at much higher TOF (243 h⁻¹) than PPNCl alone (3 h⁻¹).

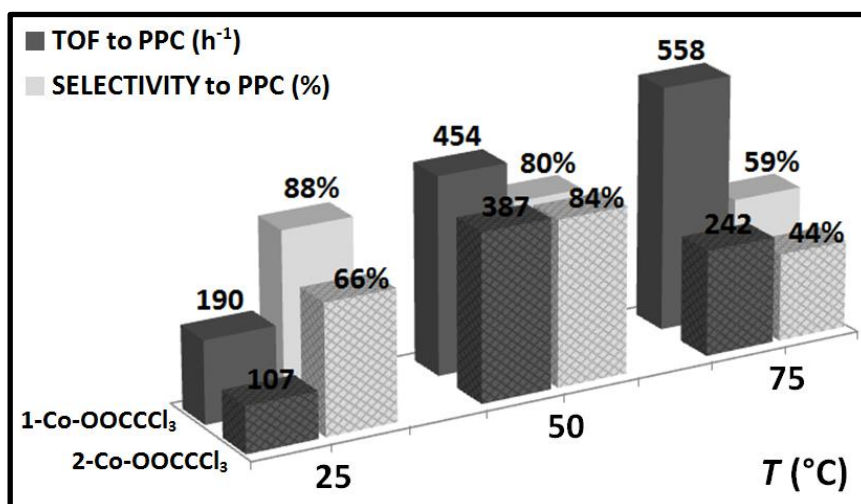


Figure 5.15: Effect of catalyst and temperature to overall activity and selectivity of PO/CO₂ copolymerization catalyzed by complexes **1-Co-OOCCl₃**/PPNCl and **2-Co-OOCCl₃**/PPNCl at 1MPa ([PO]/[Co]/[PPNCl]=2000:1:1)

5.4.2.3 Mechanism of activation and insight into PO/CO₂ copolymer microstructure

All prepared polypropylene carbonates displayed the bimodal molar mass distributions as already observed for the other salen complexes earlier.^{120,180} M_n value of the higher-molar-mass peak was twice as large as that of the lower-molar-mass one in all prepared polycarbonates. This was previously described and explained due to the presence of contaminant water, which works as a bifunctional initiating group to give telechelic polymers.^{120,146,180} This indicates that the copolymerization can be initiated by several different active species such as axial Y group of catalyst and chlorine anion, which is a part of PPNCl cocatalyst or also by the contaminant water.

To confirm the role of water as the bifunctional initiator, we performed the copolymerization of propylene oxide containing different amount of water (10 ppm, 100 ppm and 0.5 mol %) with **2-Co-OOCCl₃**/PPNCl. Whereas the selectivity of copolymerizations carried out at 10 ppm and 100 ppm H₂O level was identical ($\approx 70\%$), there was a significant difference in molar mass distribution profiles of polypropylene carbonates (Figure 5.16). One can clearly see the increase of the proportion of the higher molar mass peak with respect to the one of lower molar mass in the case of more contaminated system (100 ppm H₂O). This indicates the role of water as the bifunctional initiator. Overall molar mass is slightly decreased as could be expected when increasing number of initiating species by the addition of water. The copolymerization of CO₂ with wet PO (0.5 mol. % H₂O) afforded only cyclic carbonate with TOF 69 h⁻¹ as determined by ¹H NMR spectroscopy.

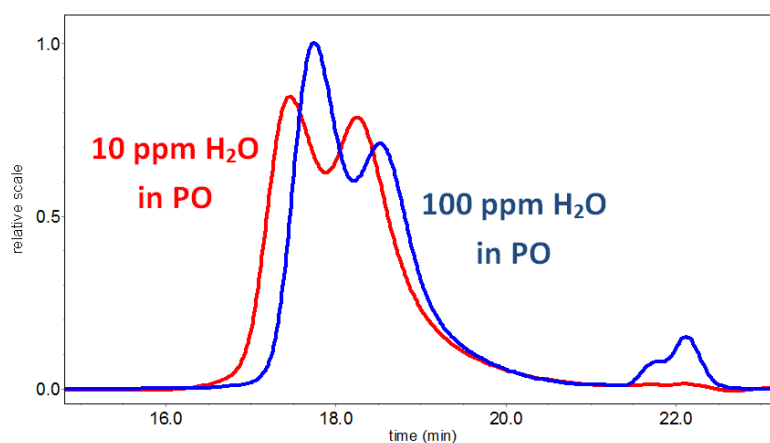


Figure 5.16: SEC traces of polypropylene carbonate prepared with PO containing various amount of water

To investigate the mechanism of activation in detail, the MALDI-TOF MS analysis of prepared polycarbonates was used to determine end-groups of final polymer (Figure 5.17). Probably due to poor ionization of polycarbonate samples and their fragmentation, only low molar mass fractions of polymers up to $3 \text{ kg}\cdot\text{mol}^{-1}$ were detected. Therefore it was not possible to confirm the role of contaminant water as the bifunctional initiator, which is believed to provide higher molar mass fractions. Obtained spectra for PPC prepared by **2-Co-DNP**/PPNCl demonstrated the presence of DNP (α -end group) and salphen catalyst adduct (ω -end group). Catalyst ω -end group can be attached either to ether or carbonate oxygen (Figure 5.17).

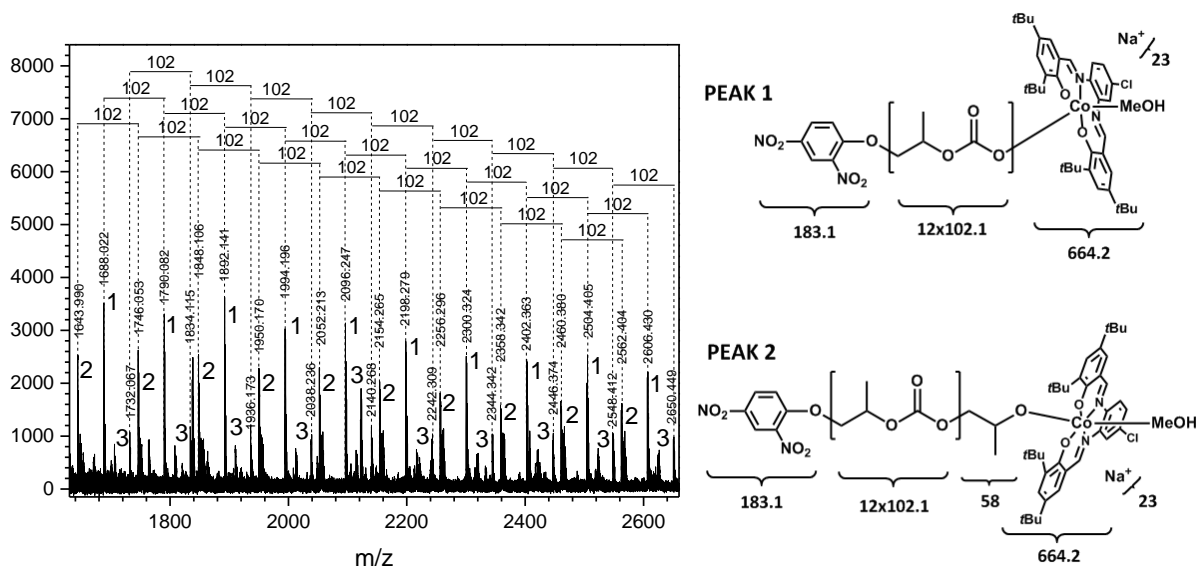


Figure 5.17: MALDI-TOF mass spectrum of PPC prepared by **2-Co-DNP**/PPNCl (exp. 10)

For **peak 1** we detected molar mass corresponding to initiation by DNP^- and termination by adduct **2-Co**-MeOH attached to carbonate oxygen (see Figure 5.17): $M_{\text{Peak1}} (2096.2) = M_{\text{DNP}} (183.1) + M_{\text{Na}^+} (23) + 12M_{\text{C}_4\text{H}_6\text{O}_3} (1225.1) + M_{\text{2-co-MeOH}} (664.2) = 2095.4 \text{ g}\cdot\text{mol}^{-1}$. **Peak 2** correspond to initiation by DNP^- and termination by adduct **2-Co**-MeOH attached to ether oxygen: $M_{\text{Peak2}} (2052.2) = M_{\text{DNP}} (183.1) + M_{\text{Na}^+} (23) + 11M_{\text{C}_4\text{H}_6\text{O}_3} (1123) + M_{\text{C}_3\text{H}_6\text{O}} (58) + M_{\text{2-co-MeOH}} (664.2) = 2051.3 \text{ g}\cdot\text{mol}^{-1}$. **Peak 3** was attributed to the structure where DNP^- and **2-Co**-

H₂O adduct attached to ether oxygen are present as end groups of polycarbonate: $M_{\text{Peak3}} (2038.2) = M_{\text{DNP}} (183.1) + M_{\text{Na}^+} (23) + 11 \times M_{\text{C}_4\text{H}_6\text{O}_3} (1123) + M_{\text{C}_3\text{H}_6\text{O}} (58) + M_{2\text{-Co-H}_2\text{O}} (650.2) = 2037.3 \text{ g.mol}^{-1}$.

5.4.3 Alternating copolymerization of CHO with CO₂ in presence of 1-Co-Y and 2-Co-Y complexes

The series of salphen Co(III) complexes were further tested for the copolymerization of another substrate - CHO with CO₂ (Table 5.21) in order to prepare polycarbonates with higher T_g when using a more rigid epoxide. Copolymerization conditions were optimized with salphen complex **2-Co-OAc**. We found that [Co]/[PPNCl]=1:1, [CHO]/[Co]=1000-2000:1, $p_{\text{CO}_2} = 1 \text{ MPa}$ and $T = 75^\circ\text{C}$ are the optimal experimental conditions affording PCHC with molar mass around 20 kg.mol^{-1} and TOF 260-290 h⁻¹ (Table 5.21, exp. 13, 14). A 100% selectivity to copolymer without formation of cyclohexene carbonate by-product during CHO/CO₂ copolymerization is attributed to high (86 kJ.mol^{-1}) difference of activation barriers for the cyclic carbonate formation compared to the formation of PCHC.⁷⁸ Decrease of reaction temperature from 75°C to 50°C or decrease of pressure from 1 MPa to 0.1 MPa resulted in 50% decrease of molar mass of formed polycarbonate and 2-5 times polymerization rate reduction (Table 5.21, exp. 13 vs. 12 and 16).

Table 5.21: Copolymerization of CHO with CO₂ with salphen complex **2-Co-OAc**/PPNCl

Exp.	T (°C)	p (MPa)	[CHO]/[Co] /[PPNCl]	Y_{wPOL}^a (%)	$\text{TOF}_{\text{POL}}^b$ (h ⁻¹)	$M_n^{c,d}$ (kg.mol ⁻¹)	$\bar{D}^{c,d}$
12	50	1	1000:1:1	28	133	13.8 (18+10)	1.08
13	75	1	1000:1:1	46	263	21.5 (30+16)	1.12
14	75	1	2000:1:1	29	287	23.1 (29+16)	1.08
15 ^e	75	1	1000:1:0.5	45	161	23.8 (36+19)	1.15
16	75	0.1	1000:1:1	13	64	8.9	1.07

Polymerizations run in neat epoxide; $V_{\text{CHO}}=1.5\text{-}2\text{ mL}$, $t_p=2\text{ h}$; Selectivity to polycarbonate as determined by ¹H NMR spectroscopy was >99% in all cases; All poly(cyclohexene carbonate)s have >99% carbonate linkages as determined by ¹H NMR spectroscopy;

^a Based on isolated polymer yield;

^b Turnover frequency to polycarbonate (For details see experimental part);

^c Determined by SEC-MALLS in THF at 35°C using dn/dc increment 0.087 mL.g^{-1} ;

^d All polymers exhibit bimodal distributions (values in brackets correspond to maxima of peaks (M_p));

^e $t_p=3\text{ h}$

The variation of nucleophile Y (Table 5.22) has a negligible effect to Co complexes activity and molar mass of resulted polycarbonates, except for complex **1-Co-OOCCCl₃**, which was significantly less active compared to all other cobalt complexes. Surprisingly, the complexes **1-Co-OOCCCl₃** and **2-Co-OOCCCl₃** containing the same nucleophile show considerable different activity, which is not possible to ascribe to the ligand substitution by Cl atom in **2-Co-OOCCCl₃** as the same ligands in **1-Co-DNP** and **2-Co-DNP** have no effect on their activity (exp. 18 and 21). All complexes produced polycyclohexene carbonate with 100% selectivity to polymer (no formation of cyclic carbonate) and > 99% of carbonate linkage at 75°C and

1 MPa. Number average molar mass values of polycyclohexene carbonates prepared by **1-Co-DNP**, **1-Co-OBzF₅** and all **2-Co-Y** were in the range of 15 to 23 kg.mol⁻¹, again displaying a bimodal molar mass distribution as in the case of polypropylene carbonates described above.

Table 5.22: Copolymerization of CHO with CO₂ with salphen Co complexes **1-Co-Y** and **2-Co-Y**

Exp.	Catalyst	Y _{wPOL} ^a (%)	TOF _{F_{POL}} ^b (h ⁻¹)	M _n ^{c,d} (kg.mol ⁻¹)	Đ ^{c,d}
17	1-Co-OOCCCl₃	21	106	8.7 (14+7)	1.41
18	1-Co-DNP	46	222	20.0 (29+15)	1.14
19	1-Co-OBzF₅	47	236	21.0 (30+16)	1.22
20	2-Co-OOCCCl₃	42	276	18.4 (30+15)	1.27
21	2-Co-DNP	45	230	17.3 (26+13)	1.10
13	2-Co-OAc	46	263	23.0 (29+15)	1.09

Polymerizations run in neat epoxide; V_{CHO}=1.5-2mL, T=75°C, t_p=2h, p_{CO₂}=1MPa, [CHO]/[Co]/[PPNCl]=1000:1:1; In all cases cyclohexene carbonate by-product is not observed and all poly(cyclohexene carbonate)s have >99% carbonate linkages as determined by ¹H NMR spectroscopy;

^a Based on isolated polymer yield;

^b Turnover frequency to polycarbonate (For details see experimental part);

^c Determined by SEC-MALLS in THF at 35°C using dn/dc increment 0.087 mL.g⁻¹;

^d All polymers exhibit bimodal distributions; Values in brackets correspond to maxima of peaks (M_p)

5.4.3.1 Kinetics of copolymerization CHO/CO₂ and insight into copolymer microstructure

The M_n and M_p values of poly(cyclohexene carbonates) prepared with catalytic system **1-Co-OOCCCl₃**/PPNCl increases linearly with the conversion in the range of 0–30% (Figure 5.18), while dispersity remained relatively low (Đ = 1.1-1.4) in initial phase of these catalytic polymerizations.¹⁸¹

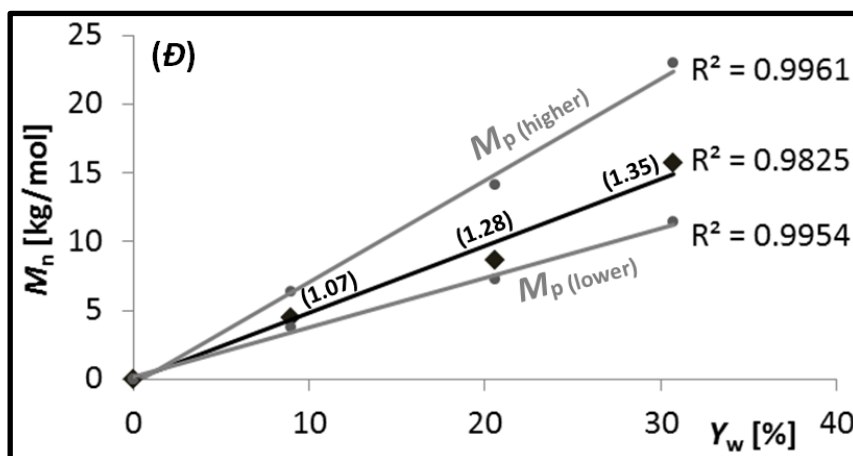


Figure 5.18: Linear increase of PCHC molar mass with conversion (catalytic system **1-Co-OOCCCl₃**/PPNCl, [PO]/[Co]/[PPNCl]=1000:1:1, t_p=0.5, 2 and 4h, T=75°C, p=1MPa)

MALDI-TOF MS analysis of synthesized poly(cyclohexene carbonate) prepared by **1-Co-OOCCCl₃**/PPNCl (Figure 5.19) confirmed the presence of OOCCCl₃⁻ or Cl⁻ anions (α-end groups) and PPN⁺ or (salphen)Co.MeOH (ω-end groups), respectively. In contrast to PPC,

PCHC contains (salphen)Co⁺ and PPN⁺ ω-end groups attached solely to the carbonate oxygen meaning that the last monomer unit comes from CO₂ insertion, probably due to higher steric hindrance of cyclohexene oxide units compared to propylene oxide ones.

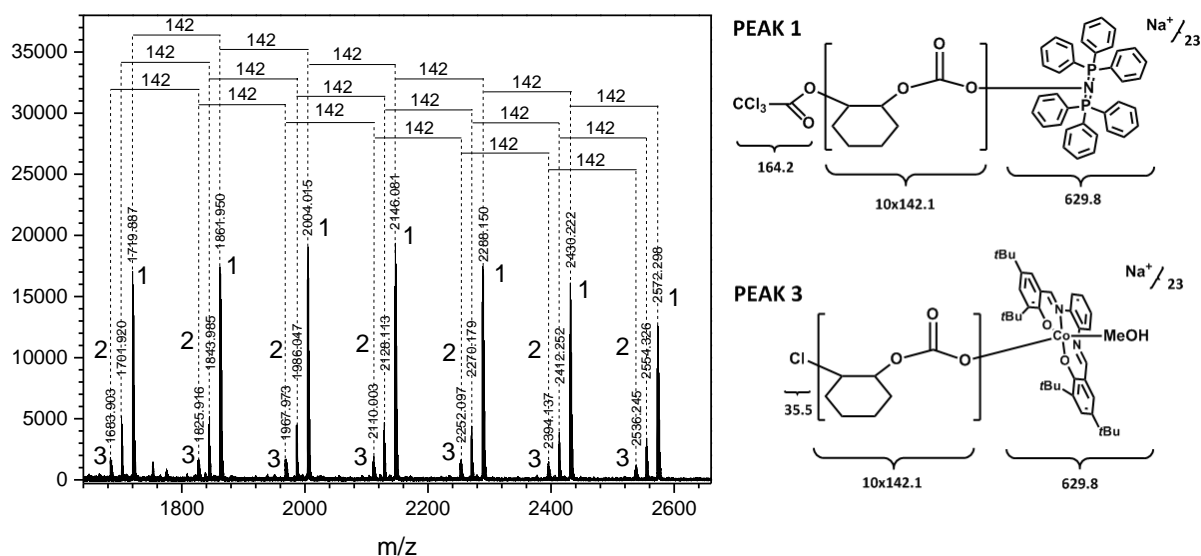


Figure 5.19: MALDI-TOF mass spectrum of PCHC prepared by 1-Co-OOCCl₃/PPNCl (exp. 17)

Peak 1 was attributed to polycarbonate with OOCCL₃⁻ and PPN⁺ end groups: $M_{\text{Peak1}} (2146.1) = M_{\text{OOCCL}_3} (162.4) + M_{\text{Na}^+} (23) + 10 \times M_{\text{C}_7\text{H}_{10}\text{O}_3} (1421.5) + M_{\text{PPN}^+} (538.6) = 2145.5 \text{ g.mol}^{-1}$. **Peak 3** was attributed to polycarbonate with Cl⁻ (α-end groups) and 1-Co-MeOH adduct (ω-end group): $M_{\text{Peak3}} (2110.0) = M_{\text{Cl}^-} (35.5) + M_{\text{Na}^+} (23) + 10 \times M_{\text{C}_7\text{H}_{10}\text{O}_3} (1421.5) + M_{1\text{-Co-MeOH}} (629.8) = 2109.8 \text{ g.mol}^{-1}$ (Figure 5.19). **Peak 2** could be composed of same α and ω-end groups as peak 3 with one more water molecule attached to Co metal: $M_{\text{Peak2}} (2128.1) = M_{\text{Cl}^-} (35.5) + M_{\text{Na}^+} (23) + 10 \times M_{\text{C}_7\text{H}_{10}\text{O}_3} (1421.5) + M_{1\text{-Co-MeOH}} (629.8) + M_{\text{H}_2\text{O}} (18) = 2127.8 \text{ g.mol}^{-1}$.

MALDI TOF mass spectrum of PCHC shows that both nucleophiles (OOCCL₃⁻, Cl⁻) initiate the growth of polycarbonate chain and both counter-cations can be connected as the ω-end group.

5.4.4 Coupling of alternative epoxides with CO₂ catalyzed with 2-CrCl and 2-Co-OAc

The copolymerization of other epoxides (Figure 5.20) mostly based on natural alkene precursors, with CO₂ was attempted. However, the only products of the reactions, as determined by ¹H NMR spectroscopy, were cyclic carbonates (Figure 5.21).

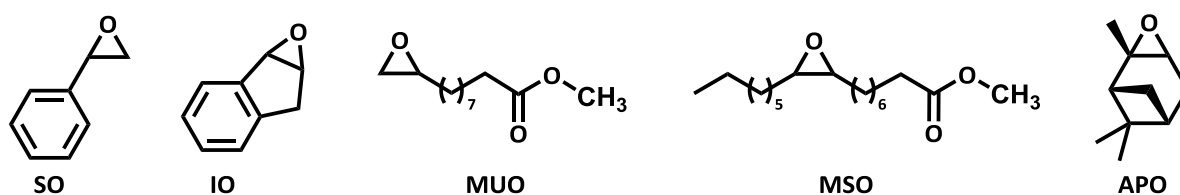


Figure 5.20: Epoxides used for carbonylation to cyclic carbonates

Very low TOF to cyclic carbonate in MSO/CO₂ coupling catalyzed with **2-CrCl** compared to MUO is attributed mainly to low purity of MSO ($\approx 85\%$, based from biodiesel, main impurities being ketones and other esters), although the TOF is expected to be lower also due to a higher steric hindrance of internal epoxy group (MSO) compared to the terminal epoxide (MUO). The MSO was not further purified due to very limited amount of this monomer (≈ 5 mL). Selected epoxides (SO, IO, MUO) were attempted to copolymerize also with salphen cobalt complex **2-Co-OAc**. As in the case of chromium complex, only cyclic carbonates were produced. This is in contrast with our expectation as IO and SO monomers were already successfully copolymerized with CO₂ using similar chiral salenCo-DNP catalysts yielding high-molar mass polycarbonates.^{165,168} Except for SO/CO₂, **2-Co-OAc** is generally slower catalyst compared to **2-CrCl**.

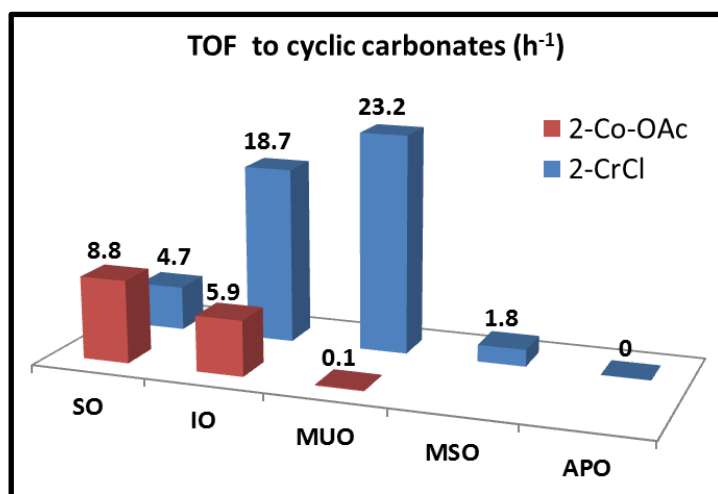


Figure 5.21: Activity of **2-CrCl** in coupling of epoxides with CO₂ at 1MPa and 75°C ([Epoxide]/[Co]/[PPNCl]=500:1:1, $t_p=20h$)

5.4.5 Screening of catalytic activity of Al, Zn and Mg complexes for copolymerization of epoxides with CO₂

Despite CO₂/epoxide copolymerization are studied for relatively long time, the library of catalysts in use and particularly of those with acceptable activity is very limited in terms of central metals used as well as in the variation of ligand structures. This is in sharp contrast with the development of catalysis for olefin polymerization that lead in the last 30 years in the development of huge amount of structurally distinct catalytic systems from which several hits were identified as highly active systems.

All complexes tested in this sub-chapter exceed partially the main focus of the Thesis, salphen complexes, the systems that were proved to be one of the most active in epoxide/CO₂ copolymerization at present time. However, activities of even the best complexes are still far from activities interesting for further scale-up of this catalysis towards their industrial application. Therefore, a long-term collaboration with group of Prof. Růžička, was initiated during the course of this Thesis, intended for the search of novel catalyst structures. The choice of ligands is driven by their potentially high activation ability even to substrates with such a low reactivity as CO₂ displays.

Following the previous research of epoxide/CO₂ copolymerization with β-diiminate complexes of tin carried in our laboratory,¹⁸² other new β-diiminate, ketiminate and aminidate complexes of Al, Zn and Mg (Figure 5.22) were tested in PO/CO₂ and CHO/CO₂ copolymerization. New β-diiminate aluminium complexes (**4-AlMe₂**, **4-AlBu₂**) are central metal varied version of efficient Zn BDI complexes published by Coates⁷⁴ and ketiminate complexes of Zn and Al (**3-ZnEt**, **3-AlMe₂**, **3-AlMeCl**) are *N,O*-chelated alternative to *N,N*-chelated BDI complexes. Furthermore, magnesium aminidate complex **5-MgBu** was tested, since analogous aminidate Al complexes proved to be highly reactive in the ROP of ε-caprolactone and TMC.¹⁸³ Moreover, these complexes contain nontoxic Al, Zn or Mg metals and their use as catalysts would not require additional purification of synthesized polymers, which is usually necessary when harmful metal complexes are used.

Whereas PO/CO₂ copolymerization using both β-diiminate and ketiminate complexes of Al and Zn did not afford any product, the copolymerization of CHO with CO₂ led to the formation of polyether or poly (ether-*co*-carbonate) (Table 5.23) The highest content of carbonate units was observed in the copolymer prepared with ketiminate complexes **3-ZnEt**, formed from ketiminate ligand (**3**) with ZnEt₂. The activity (TOF) of copolymerization with **3-ZnEt** was very low.

Significantly higher turnover frequency was observed with aluminium complexes **3-AlMe₂** and **3-AlMeCl**, nevertheless all obtained polymers were almost 100% polyethers. All complexes afford polymers with very broad dispersity indicating significant extent of chain transfer during the copolymerization. It is worthy to note the potential use of **3-AlMeCl** in epoxide homopolymerization, as **3-AlMeCl** afforded PCHO with very high molar mass over 300 kg.mol⁻¹ (*D* = 1.64) with TOF 860 h⁻¹ (bulk polymerization; [CHO]:[**3-AlMeCl**] = 2000:1, *T* = 50°C, *t_p* = 0.5h).

β-Diiminate complexes **4-AlMe₂** and **4-AlBu₂** were poorly active and afforded only polyether similarly as the aminidate complex **5-MgBu**.

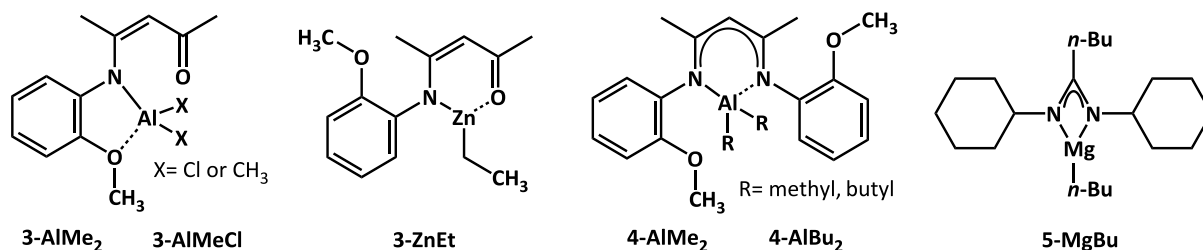


Figure 5.22: Aluminium, zinc and magnesium complexes for CHO/CO₂ copolymerization

Table 5.23: Copolymerization of CHO with CO₂ catalyzed with various Al, Zn and Mg complexes

Exp.	Catalyst	T (°C)	t _p (h)	Y _{w POL} ^a (%)	TOF _{POL} ^b (h ⁻¹)	M _n ^c (kg.mol ⁻¹)	Đ ^c	CL ^d (%)
1	3-AlMe ₂	50	6	21	18	27.1	3.82	0.1
2	3-AlMe ₂	100	3	36	61	17.0	5.54	0.3
3	3-AlMeCl	50	3	30	50	102.0	1.93	0
4	3-AlMeCl	100	3	58	98	16.3	7.08	2.3
5	3-AlMeCl	100	1	54	275	18.1	6.43	2.1
6	3-ZnEt	50	24	4	0.9	45.0	5.62	42.6
7	3-ZnEt	100	24	3	0.7	23.2	4.78	76.3
8	4-AlMe ₂	100	20	17	4.3	11.2 (94.3+4.7+2.0)	6.63	1.4
9	4-AlBu ₂	100	20	3	0.8	34.9	2.47	0
10	5-MgBu	75	16	7	2.0	62.1	2.98	4.4

Polymerizations run in neat epoxide; V_{CHO}=1.5-2mL, p_{CO₂}=1MPa, [CHO]/[Co]=500:1;
^a Based on isolated polymer yield;
^b Turnover frequency to polycarbonate (For details see experimental part);
^c Determined by SEC-MALLS in THF at 35°C using dn/dc increment 0.101 mL.g⁻¹ for PCHO polymers and 0.087 mL.g⁻¹ for PCHC (exp. 6, 7);
^d Carbonate linkage determined by ¹H NMR spectroscopy of dried polymer samples in CDCl₃

5.4.6 Conclusion

Salphen chromium (**1-CrCl**, **2-CrCl**) and cobalt (**1-Co-Y**, **2-Co-Y**) complexes were effective for both PO/CO₂ and CHO/CO₂ copolymerization leading to polycarbonates with molar mass 5-16 and 15-30 kg mol⁻¹, respectively. Aging of catalysts is an important parameter in overall catalytic performance of chromium complexes (**1-CrCl**, **2-CrCl**). To keep the best performance, they need to be regenerated periodically or kept at strictly inert conditions despite the fact that short term manipulation on air does not affect their catalytic activity at all. Both chromium complexes provide polycarbonates with variable content of carbonate linkage (60-98%) depending to the catalyst age and regeneration process.

Cobalt complexes showed better catalytic performance compared to salphen-chromium complexes and afforded polycarbonates with carbonate linkage > 99%. The substitution of hydrogen in the phenylene framework of salphen ligand by chlorine atom led to decrease of activity in PO/CO₂ copolymerization while the variation of Y counteranions showed significant differences in activity, selectivity and molar mass. The best results were obtained with complexes bearing the weakest nucleophile trichloroacetate. PO/CO₂ copolymerization catalyzed by salphen Co complexes was accompanied by the formation of cyclic carbonate. The selectivity to polycarbonates varied from 40 to 80% depending to the nucleophilicity of attached counterions and Lewis acidity of metal center.

Activity and selectivity of all salphen Co (III) complexes in CHO/CO₂ copolymerization was almost independent on ligand structure and counteranion. No cyclic carbonate was formed

in CHO/CO₂ copolymerization even at low CO₂ pressure. Attempts to prepare polycarbonates from other disponible epoxides (styrene oxide, indene oxide and bio-based methylundec-10-enoate oxide and methyl stearate oxide) were not successful. Only products of epoxide/CO₂ coupling were cyclic carbonates.

The search for highly active catalysts for epoxide/CO₂ copolymerizations is a long term task with the key focus on catalyst design.

6 GENERAL CONCLUSIONS

We demonstrated three different routes to renewable polymers. Copolymerizations of epoxides with various comonomers (CO, CO₂ or anhydrides) were performed with easily synthesized salphen complexes of Cr, Co or Fe. Several new cobalt complexes were prepared and fully characterized. For the first time salphen complexes based on abundant and non-toxic iron metal were used in epoxide copolymerization reactions. Detailed characterization of chromium and cobalt complexes showed their hexacoordinated structure for the first time

One-pot copolymerization of epoxides with CO was performed with dual catalytic system **2-CrCl** - Co₂(CO)₈ for epoxide carbonylation to BBL and its consequent ROP to low molar mass PHB with 20% of ether defects. Cyclic lactones and ketones were formed as side products too. The significant extent of transfer reactions, which suppress the formation of higher-molar mass polyesters, demonstrated the poor compatibility of salphen chromium complex with Co₂(CO)₈.

Synthesized chromium complexes combined with organic bases were further efficient catalysts for the copolymerization of epoxides with anhydrides. Unexpectedly, only organic bases proved to be good catalysts for this type of reaction providing highly alternating polyesters with low dispersity and molar mass up to 21 kg.mol⁻¹. The versatility of organic bases were confirmed by the copolymerization of various epoxides and anhydrides (especially PA) including also bio-based monomer methylundec-10-enoate oxide, which afforded new partially renewable polyesters with molar mass 7 kg.mol⁻¹ and low *T_g* -20°C when copolymerized with PA.

Salphen chromium and cobalt complexes were finally used in CO₂ with epoxides (PO, CHO) copolymerization. Better catalytic performance in the copolymerization was achieved with salphen cobalt complexes. Symmetric salphen cobalt complex with weak nucleophile trichloroacetate **1-Co-OOCCCl₃** exhibited the best activity in PO/CO₂ copolymerization from all tested complexes providing highly alternating poly(propylene carbonate) with molar mass 30 kg.mol⁻¹. It is however worthy of note that all displayed salphen cobalt complexes had lower activity and selectivity to polycarbonate (max. 91% at 25°C) compared to salen cobalt complexes. Salphen complexes catalyzed the copolymerization of CHO with CO₂, which was also slower compared to salen cobalt catalysts, but in this case, no formation of cyclic carbonate by-product was observed. The copolymerization of other epoxides with CO₂ led only to cyclic carbonate formation.

Salphen complexes represent simple and efficient catalysts for transformation of renewable monomers (epoxides, anhydrides, CO_x, lactones) into valuable materials - polyesters and polycarbonates. Their advantage lies in the ease of salphen ligand modification. The variation of nucleophilic counteranions represents another efficient structural parameter that influences the selectivity and activity of these catalysts.

Future perspectives: Copolymerization of functionalized epoxides with CO₂ or anhydrides with respect to prepare water-soluble biodegradable polymers (polycarbonates and polyesters) could be an interesting continuation of the present work. Search for new highly effective catalysts for epoxide/CO₂ copolymerization is another long-term goal. These catalysts should be based on nontoxic and non-coloring metal complexes probably coordinated to novel highly activating ligand frameworks.

7 REFERENCES

- [1] in *Plastics – the Facts 2014/2015, An analysis of European plastics production, demand and waste data, Vol.* Plastics Europe, **2014**.
- [2] Al-Salem, S. M.; Lettieri, P.; Baeyens, J., *Waste Management* **2009**, *29*, 2625-2643.
- [3] Butler, E.; Devlin, G.; McDonnell, K., *Waste and Biomass Valorization* **2011**, *2*, 227-255.
- [4] Goto, M.; Sasaki, M.; Hirose, T., *Journal of Materials Science* **2006**, *41*, 1509-1515.
- [5] a) Drent, E.; Budzelaar, P. H. M., *Chemical Reviews* **1996**, *96*, 663-681; b) Brulé, E.; Guo, J.; Coates, G. W.; Thomas, C. M., *Macromolecular Rapid Communications* **2011**, *32*, 169-185.
- [6] Sun, H.; Zhang, J.; Liu, Q.; Yu, L.; Zhao, J., *Angewandte Chemie - International Edition* **2007**, *46*, 6068-6072.
- [7] Coates, G. W.; Moore, D. R., *Angewandte Chemie - International Edition* **2004**, *43*, 6618-6639.
- [8] Economy, J.; Parkar, Z., *ACS Symp. Ser.* **2011**, *1080*, 93-103.
- [9] Ulery, B. D.; Nair, L. S.; Laurencin, C. T., *Journal of Polymer Science, Part B: Polymer Physics* **2011**, *49*, 832-864.
- [10] Albertsson, A.-C.; Varma, I. K., *Adv. Polym. Sci.* **2002**, *157*, 1-40.
- [11] Vert, M., *Journal of Materials Science: Materials in Medicine* **2009**, *20*, 437-446.
- [12] a) Reichardt, R.; Rieger, B., *Adv. Polym. Sci.* **2012**, *245*, 49-90; b) Allmendinger, M., Eberhardt, R., Luinstra, A. G., Molnar, F., Rieger, B. The Alternating Copolymerization of Epoxides and Carbon Monoxide: A Novel Way to Polyesters, in *Beyond Metallocenes*, 857 (Ed. Patil, A. O., Hlatky, G. G.), ACS Symposium Series, Washington, DC, **2003**, *9*, 114-130.
- [13] Dunn, E. W.; Coates, G. W., *Journal of the American Chemical Society* **2010**, *132*, 11412-11413.
- [14] Furukawa, J.; Iseda, Y.; Saegusa, T.; Fujii, H., *Die Makromolekulare Chemie* **1965**, *89*, 263-268.
- [15] Allmendinger, M.; Eberhardt, R.; Luinstra, G.; Rieger, B., *Journal of the American Chemical Society* **2002**, *124*, 5646-5647.
- [16] Allmendinger, M.; Molnar, F.; Zintl, M.; Luinstra, G. A.; Preishuber-Pfluegl, P.; Rieger, B., *Chem. - Eur. J.* **2005**, *11*, 5327-5332.
- [17] a) Eisenmann, J. L.; Yamartino, R. L.; Howard Jr, J. F., *Journal of Organic Chemistry* **1961**, *26*, 2102-2104; b) Eisenmann, J. L., *Journal of Organic Chemistry* **1962**, *27*, 2706; c) Heck, R. F., *Journal of the American Chemical Society* **1963**, *85*, 1460-1463.
- [18] a) Pollock, J. M.; Shipman, A. J. Preparation of polymers of β -lactones. Patent GB 1020575, 23. Fevrier, **1966**; b) Kamiya, Y.; Kawato, K.; Ohta, H., *Chemistry Letters* **1980**, *9*, 1549-1552; c) Shimizu, I.; Maruyama, T.; Makuta, T.; Yamamoto, A., *Tetrahedron Letters* **1993**, *34*, 2135-2138.
- [19] Drent, E.; Kragtwijk, E. Carbonylation of epoxides. Patent EP 0577206 A2, 29 June, **1994**.
- [20] Lee, J. T.; Thomas, P. J.; Alper, H., *Journal of Organic Chemistry* **2001**, *66*, 5424-5426.
- [21] Takeuchi, D.; Sakaguchi, Y.; Osakada, K., *Journal of Polymer Science, Part A: Polymer Chemistry* **2002**, *40*, 4530-4537.
- [22] Allmendinger, M.; Eberhardt, R.; Luinstra, G. A.; Rieger, B., *Macromolecular Chemistry and Physics* **2003**, *204*, 564-569.
- [23] Lee, J. T.; Alper, H., *Macromolecules* **2004**, *37*, 2417-2421.
- [24] Carpentier, J.-F., *Macromol. Rapid Commun.* **2010**, *31*, 1696-1705.

- [25] Wang, Y.; Tennyson, R. L.; Romo, D., *Heterocycles* **2004**, *64*, 605-658.
- [26] a)Orr, R. K.; Calter, M. A., *Tetrahedron* **2003**, *59*, 3545-3565; b)Yang, H. W.; Romo, D., *Tetrahedron* **1999**, *55*, 6403-6434.
- [27] Church, T. L.; Getzler, Y. D. Y. L.; Byrne, C. M.; Coates, G. W., *Chemical Communications* **2007**, 657-674.
- [28] Mahadevan, V.; Getzler, Y. D. Y. L.; Coates, G. W., *Angewandte Chemie - International Edition* **2002**, *41*, 2781-2784.
- [29] Getzler, Y. D. Y. L.; Mahadevan, V.; Lobkovsky, E. B.; Coates, G. W., *Journal of the American Chemical Society* **2002**, *124*, 1174-1175.
- [30] Getzler, Y. D. Y. L.; Mahadevan, V.; Lobkovsky, E. B.; Coates, G. W., *Pure and Applied Chemistry* **2004**, *76*, 557-564.
- [31] Kramer, J. W.; Lobkovsky, E. B.; Coates, G. W., *Organic Letters* **2006**, *8*, 3709-3712.
- [32] Kramer, J. W.; Coates, G. W., *Tetrahedron* **2008**, *64*, 6973-6978.
- [33] a)Schmidt, J. A. R.; Mahadevan, V.; Getzler, Y. D. Y. L.; Coates, G. W., *Org. Lett.* **2004**, *6*, 373-376; b)Schmidt, J. A. R.; Lobkovsky, E. B.; Coates, G. W., *J. Am. Chem. Soc.* **2005**, *127*, 11426-11435.
- [34] Rowley, J. M.; Lobkovsky, E. B.; Coates, G. W., *Journal of the American Chemical Society* **2007**, *129*, 4948-4960.
- [35] Woelfle, H.; Kopacka, H.; Wurst, K.; Preishuber-Pfluegl, P.; Bildstein, B., *J. Organomet. Chem.* **2009**, *694*, 2493-2512.
- [36] Dechy-Cabaret, O.; Martin-Vaca, B.; Bourissou, D., *Chem. Rev.* **2004**, *104*, 6147-6176.
- [37] Thomas, C. M., *Chemical Society Reviews* **2010**, *39*, 165-173.
- [38] Labet, M.; Thielemans, W., *Chemical Society Reviews* **2009**, *38*, 3484-3504.
- [39] a)Kricheldorf, H. R.; Lee, S.-R.; Scharnagl, N., *Macromolecules* **1994**, *27*, 3139-3146; b)Kemnitzer, J. E.; McCarthy, S. P.; Gross, R. A., *Macromolecules* **1993**, *26*, 6143-6150; c)Jedlinski, Z.; Kowalczyk, M.; Kurcok, P.; Adamus, G.; Matuszowicz, A.; Sikorska, W.; Gross, R. A.; Xu, J.; Lenz, R. W., *Macromolecules* **1996**, *29*, 3773-3777.
- [40] Hori, Y.; Hagiwara, T., *Int. J. Biol. Macromol.* **1999**, *25*, 237-245.
- [41] Rieth, L. R.; Moore, D. R.; Lobkovsky, E. B.; Coates, G. W., *J. Am. Chem. Soc.* **2002**, *124*, 15239-15248.
- [42] a)Zintl, M.; Molnar, F.; Urban, T.; Bernhart, V.; Preishuber-Pfluegl, P.; Rieger, B., *Angew. Chem., Int. Ed.* **2008**, *47*, 3458-3460; b)Reichardt, R.; Vagin, S.; Reithmeier, R.; Ott, A. K.; Rieger, B., *Macromolecules* **2010**, *43*, 9311-9317.
- [43] Vagin, S. I.; Reichardt, R.; Klaus, S.; Rieger, B., *J. Am. Chem. Soc.* **2010**, *132*, 14367-14369.
- [44] a)Amgoune, A.; Thomas, C. M.; Ilinca, S.; Roisnel, T.; Carpentier, J.-F., *Angew. Chem., Int. Ed.* **2006**, *45*, 2782-2784; b)Ajellal, N.; Bouyahyi, M.; Amgoune, A.; Thomas, C. M.; Bondon, A.; Pillin, I.; Grohens, Y.; Carpentier, J.-F., *Macromolecules* **2009**, *42*, 987-993.
- [45] Grunova, E.; Kirillov, E.; Roisnel, T.; Carpentier, J.-F., *Dalton Trans.* **2010**, *39*, 6739-6752.
- [46] Ajellal, N.; Lyubov, D. M.; Sinenkov, M. A.; Fukin, G. K.; Cherkasov, A. V.; Thomas, C. M.; Carpentier, J.-F.; Trifonov, A. A., *Chem. - Eur. J.* **2008**, *14*, 5440-5448.
- [47] Ajellal, N.; Durieux, G.; Delevoye, L.; Tricot, G.; Dujardin, C.; Thomas, C. M.; Gauvin, R. M., *Chem. Commun.* **2010**, *46*, 1032-1034.
- [48] Xu, C.; Yu, I.; Mehrkhodavandi, P., *Chem. Commun.* **2012**, *48*, 6806-6808.

- [49] a) Klitzke, J. S.; Roisnel, T.; Kirillov, E.; de L. Casagrande, O., Jr.; Carpentier, J.-F., *Organometallics* **2014**, *33*, 309-321; b) Pappalardo, D.; Bruno, M.; Lamberti, M.; Pellecchia, C., *Macromolecular Chemistry and Physics* **2013**, *214*, 1965-1972.
- [50] Paul, S.; Zhu, Y.; Romain, C.; Brooks, R.; Saini, P. K.; Williams, C. K., *Chem. Commun.* **2015**, *51*, 6459-6479.
- [51] Fischer, R. F., *J. Polym. Sci.* **1960**, *44*, 155-172.
- [52] a) Inoue, S.; Kitamura, K.; Tsuruta, T., *Makromol. Chem.* **1969**, *126*, 250-265; b) Hsieh, H. L., *J. Macromol. Sci., Chem.* **1973**, *7*, 1526-1537; c) Kuran, W.; Nieslochowski, A., *Polym. Bull.* **1980**, *2*, 411-416.
- [53] a) Aida, T.; Inoue, S., *J. Am. Chem. Soc.* **1985**, *107*, 1358-1364; b) Aida, T.; Sanuki, K.; Inoue, S., *Macromolecules* **1985**, *18*, 1049-1055.
- [54] a) Huijser, S.; HosseiniNejad, E.; Sablong, R.; de Jong, C.; Koning, C. E.; Duchateau, R., *Macromolecules* **2011**, *44*, 1132-1139; b) Hosseini Nejad, E.; Paoniasari, A.; Koning, C. E.; Duchateau, R., *Polym. Chem.* **2012**, *3*, 1308-1313.
- [55] Bernard, A.; Chatterjee, C.; Chisholm, M. H., *Polymer* **2013**, *54*, 2639-2646.
- [56] Jeske, R. C.; DiCiccio, A. M.; Coates, G. W., *J. Am. Chem. Soc.* **2007**, *129*, 11330-11331.
- [57] DiCiccio, A. M.; Coates, G. W., *J. Am. Chem. Soc.* **2011**, *133*, 10724-10727.
- [58] Nejad, E. H.; van Melis, C. G. W.; Vermeer, T. J.; Koning, C. E.; Duchateau, R., *Macromolecules* **2012**, *45*, 1770-1776.
- [59] Nejad, E. H.; Paoniasari, A.; van Melis, C. G. W.; Koning, C. E.; Duchateau, R., *Macromolecules* **2013**, *46*, 631-637.
- [60] Liu, J.; Bao, Y.-Y.; Liu, Y.; Ren, W.-M.; Lu, X.-B., *Polym. Chem.* **2013**, *4*, 1439-1444.
- [61] Liu, D.-F.; Wu, L.-Y.; Feng, W.-X.; Zhang, X.-M.; Wu, J.; Zhu, L.-Q.; Fan, D.-D.; Lu, X.-Q.; Shi, Q., *J. Mol. Catal. A: Chem.* **2014**, *382*, 136-145.
- [62] Wu, L.-y.; Fan, D.-d.; Lu, X.-q.; Lu, R., *Chin. J. Polym. Sci.* **2014**, *32*, 768-777.
- [63] Saini, P. K.; Romain, C.; Zhu, Y.; Williams, C. K., *Polym. Chem.* **2014**, *5*, 6068-6075.
- [64] Robert, C.; Ohkawara, T.; Nozaki, K., *Chem. - Eur. J.* **2014**, *20*, 4789-4795.
- [65] Rokicki, G.; Parzuchowski, P. G. 4.12 - ROP of Cyclic Carbonates and ROP of Macrocycles, in *Polymer Science: A Comprehensive Reference*, (Ed. Möller, K. M.), Elsevier, Amsterdam, **2012**. 247-308.
- [66] Abts, G.; Eckel, T.; Wehrmann, R. Polycarbonates, in *Ullmann's Encyclopedia of Industrial Chemistry*, Wiley-VCH Verlag GmbH & Co. KGaA, **2000**.
- [67] Ulery, B. D.; Nair, L. S.; Laurencin, C. T., *J. Polym. Sci., Part B: Polym. Phys.* **2011**, *49*, 832-864.
- [68] Pescarmona, P. P.; Taherimehr, M., *Catal. Sci. Technol.* **2012**, *2*, 2169-2187.
- [69] Klaus, S.; Lehenmeier, M. W.; Anderson, C. E.; Rieger, B., *Coord. Chem. Rev.* **2011**, *255*, 1460-1479.
- [70] Srivastava, R.; Bennur, T. H.; Srinivas, D., *J. Mol. Catal. A: Chem.* **2005**, *226*, 199-205.
- [71] Chisholm, M. H.; Zhou, Z., *J. Am. Chem. Soc.* **2004**, *126*, 11030-11039.
- [72] Darensbourg, D. J.; Mackiewicz, R. M.; Rodgers, J. L.; Phelps, A. L., *Inorg. Chem.* **2004**, *43*, 1831-1833.
- [73] Nakano, K.; Hashimoto, S.; Nozaki, K., *Chem. Sci.* **2010**, *1*, 369-373.
- [74] Moore, D. R.; Cheng, M.; Lobkovsky, E. B.; Coates, G. W., *J. Am. Chem. Soc.* **2003**, *125*, 11911-11924.

- [75] a) Lu, X.-B.; Wang, Y., *Angew. Chem., Int. Ed.* **2004**, *43*, 3574-3577; b) Cohen, C. T.; Coates, G. W., *J. Polym. Sci., Part A: Polym. Chem.* **2006**, *44*, 5182-5191; c) Darensbourg, D. J.; Mackiewicz, R. M., *J. Am. Chem. Soc.* **2005**, *127*, 14026-14038; d) Eberhardt, R.; Allmendinger, M.; Rieger, B., *Macromol. Rapid Commun.* **2003**, *24*, 194-196; e) Rao, D.-Y.; Li, B.; Zhang, R.; Wang, H.; Lu, X.-B., *Inorg. Chem.* **2009**, *48*, 2830-2836.
- [76] a) Lu, X.-B.; Shi, L.; Wang, Y.-M.; Zhang, R.; Zhang, Y.-J.; Peng, X.-J.; Zhang, Z.-C.; Li, B., *J. Am. Chem. Soc.* **2006**, *128*, 1664-1674; b) Lu, X.-B.; Darensbourg, D. J., *Chemical Society Reviews* **2012**, *41*, 1462-1484.
- [77] Brule, E.; Guo, J.; Coates, G. W.; Thomas, C. M., *Macromol. Rapid Commun.* **2011**, *32*, 169-185.
- [78] Darensbourg, D. J.; Bottarelli, P.; Andreatta, J. R., *Macromolecules* **2007**, *40*, 7727-7729.
- [79] Darensbourg, D. J.; Wilson, S. J., *Green Chem.* **2012**, *14*, 2665-2671.
- [80] Taherimehr, M.; Pescarmona, P. P., *J. Appl. Polym. Sci.* **2014**, *131*, 41141/41141-41141/41117.
- [81] Inoue, S.; Koinuma, H.; Tsuruta, T., *J. Polym. Sci., Part B* **1969**, *7*, 287-292.
- [82] a) Kobayashi, M.; Inoue, S.; Tsuruta, T., *Macromolecules* **1971**, *4*, 658-659; b) Kobayashi, M.; Tang, Y.-L.; Tsuruta, T.; Inoue, S., *Makromol. Chem.* **1973**, *169*, 69-81; c) Kobayashi, M.; Inoue, S.; Tsuruta, T., *J. Polym. Sci., Polym. Chem. Ed.* **1973**, *11*, 2383-2385; d) Inoue, S.; Kobayashi, M.; Koinuma, H.; Tsuruta, T., *Makromol. Chem.* **1972**, *155*, 61-73.
- [83] Kuran, W.; Pasynkiewicz, S.; Skupinska, J.; Rokicki, A., *Makromol. Chem.* **1976**, *177*, 11-20.
- [84] Soga, K.; Imai, E.; Hattori, I., *Polym. J.* **1981**, *13*, 407-410.
- [85] a) Darensbourg, D. J.; Holtcamp, M. W., *Macromolecules* **1995**, *28*, 7577-7579; b) Darensbourg, D. J.; Holtcamp, M. W.; Struck, G. E.; Zimmer, M. S.; Niezgodna, S. A.; Rainey, P.; Robertson, J. B.; Draper, J. D.; Reibenspies, J. H., *J. Am. Chem. Soc.* **1999**, *121*, 107-116.
- [86] a) Darensbourg, D. J.; Wildeson, J. R.; Yarbrough, J. C.; Reibenspies, J. H., *J. Am. Chem. Soc.* **2000**, *122*, 12487-12496; b) Darensbourg, D. J.; Zimmer, M. S.; Rainey, P.; Larkins, D. L., *Inorg. Chem.* **2000**, *39*, 1578-1585.
- [87] Hampel, O.; Rode, C.; Walther, D.; Beckert, R.; Gorls, H., *Z. Naturforsch., B: Chem. Sci.* **2002**, *57*, 946-956.
- [88] Cheng, M.; Moore, D. R.; Reczek, J. J.; Chamberlain, B. M.; Lobkovsky, E. B.; Coates, G. W., *J. Am. Chem. Soc.* **2001**, *123*, 8738-8749.
- [89] Moore, D. R.; Cheng, M.; Lobkovsky, E. B.; Coates, G. W., *Angew. Chem., Int. Ed.* **2002**, *41*, 2599-2602.
- [90] Allen, S. D.; Moore, D. R.; Lobkovsky, E. B.; Coates, G. W., *J. Am. Chem. Soc.* **2002**, *124*, 14284-14285.
- [91] Kröger, M.; Folli, C.; Walter, O.; Döring, M., *Advanced Synthesis & Catalysis* **2005**, *347*, 1325-1328.
- [92] Eberhardt, R.; Allmendinger, M.; Luinstra, G. A.; Rieger, B., *Organometallics* **2003**, *22*, 211-214.
- [93] Piesik, D. F. J.; Range, S.; Harder, S., *Organometallics* **2008**, *27*, 6178-6187.
- [94] Darensbourg, D. J.; Fitch, S. B., *Inorg. Chem.* **2007**, *46*, 5474-5476.
- [95] Bok, T.; Yun, H.; Lee, B. Y., *Inorg. Chem.* **2006**, *45*, 4228-4237.
- [96] Kissling, S.; Lehenmeier, M. W.; Altenbuchner, P. T.; Kronast, A.; Reiter, M.; Deglmann, P.; Seemann, U. B.; Rieger, B., *Chem. Commun.* **2015**, *51*, 4579-4582.

- [97] Abbina, S.; Du, G., *Organometallics* **2012**, *31*, 7394-7403.
- [98] Ellis, W. C.; Jung, Y.; Mulzer, M.; Di Girolamo, R.; Lobkovsky, E. B.; Coates, G. W., *Chem. Sci.* **2014**, *5*, 4004-4011.
- [99] Rajendran, N. M.; Haleel, A.; Reddy, N. D., *Organometallics* **2014**, *33*, 217-224.
- [100] Jacobsen, E. N., *Acc. Chem. Res.* **2000**, *33*, 421-431.
- [101] a) Lu, X.-B.; He, R.; Bai, C.-X., *J. Mol. Catal. A: Chem.* **2002**, *186*, 1-11; b) Lu, X.-B.; Zhang, Y.-J.; Liang, B.; Li, X.; Wang, H., *J. Mol. Catal. A: Chem.* **2004**, *210*, 31-34.
- [102] Paddock, R. L.; Nguyen, S. T., *J. Am. Chem. Soc.* **2001**, *123*, 11498-11499.
- [103] Lu, X.-B.; Liang, B.; Zhang, Y.-J.; Tian, Y.-Z.; Wang, Y.-M.; Bai, C.-X.; Wang, H.; Zhang, R., *J. Am. Chem. Soc.* **2004**, *126*, 3732-3733.
- [104] Darensbourg, D. J.; Rainey, P.; Yarbrough, J., *Inorg. Chem.* **2001**, *40*, 986-993.
- [105] Darensbourg, D. J.; Yarbrough, J. C., *J. Am. Chem. Soc.* **2002**, *124*, 6335-6342.
- [106] Li, B.; Zhang, R.; Lu, X.-B., *Macromolecules* **2007**, *40*, 2303-2307.
- [107] Paddock, R. L.; Nguyen, S. T., *Macromolecules* **2005**, *38*, 6251-6253.
- [108] Cohen, C. T.; Chu, T.; Coates, G. W., *J. Am. Chem. Soc.* **2005**, *127*, 10869-10878.
- [109] Cohen, C. T.; Thomas, C. M.; Peretti, K. L.; Lobkovsky, E. B.; Coates, G. W., *Dalton Trans.* **2005**, 237-249.
- [110] Shi, L.; Lu, X.-B.; Zhang, R.; Peng, X.-J.; Zhang, C.-Q.; Li, J.-F.; Peng, X.-M., *Macromolecules* **2006**, *39*, 5679-5685.
- [111] Niu, Y.; Zhang, W.; Li, H.; Chen, X.; Sun, J.; Zhuang, X.; Jing, X., *Polymer* **2009**, *50*, 441-446.
- [112] Wang, Y.; Qin, Y.; Wang, X.; Wang, F., *ACS Catal.* **2015**, *5*, 393-396.
- [113] Niu, Y.; Li, H., *Colloid Polym. Sci.* **2013**, *291*, 2181-2189.
- [114] Guo, L.; Wang, C.; Zhao, W.; Li, H.; Sun, W.; Shen, Z., *Dalton Trans.* **2009**, 5406-5410.
- [115] Fuchs, M. A.; Altesleben, C.; Zevaco, T. A.; Dinjus, E., *Eur. J. Inorg. Chem.* **2013**, *2013*, 4541-4545.
- [116] Kember, M. R.; Buchard, A.; Williams, C. K., *Chem. Commun.* **2011**, *47*, 141-163.
- [117] Nakano, K.; Nakamura, M.; Nozaki, K., *Macromolecules* **2009**, *42*, 6972-6980.
- [118] Darensbourg, D. J.; Ulusoy, M.; Karroonnirum, O.; Poland, R. R.; Reibenspies, J. H.; Cetinkaya, B., *Macromolecules* **2009**, *42*, 6992-6998.
- [119] Mandal, M.; Chakraborty, D.; Ramkumar, V., *RSC Adv.* **2015**, *5*, 28536-28553.
- [120] Nakano, K.; Kamada, T.; Nozaki, K., *Angew. Chem., Int. Ed.* **2006**, *45*, 7274-7277.
- [121] Liu, B.; Gao, Y.; Zhao, X.; Yan, W.; Wang, X., *J. Polym. Sci., Part A: Polym. Chem.* **2010**, *48*, 359-365.
- [122] Nakano, K.; Hashimoto, S.; Nakamura, M.; Kamada, T.; Nozaki, K., *Angew. Chem., Int. Ed.* **2011**, *50*, 4868-4871.
- [123] Noh, E. K.; Na, S. J.; S, S.; Kim, S.-W.; Lee, B. Y., *J. Am. Chem. Soc.* **2007**, *129*, 8082-8083.
- [124] Min, S. S. J. K.; Seong, J. E.; Na, S. J.; Lee, B. Y., *Angew. Chem., Int. Ed.* **2008**, *47*, 7306-7309.
- [125] Na, S. J.; S, S.; Cyriac, A.; Kim, B. E.; Yoo, J.; Kang, Y. K.; Han, S. J.; Lee, C.; Lee, B. Y., *Inorg. Chem.* **2009**, *48*, 10455-10465.
- [126] Ren, W.-M.; Liu, Z.-W.; Wen, Y.-Q.; Zhang, R.; Lu, X.-B., *J. Am. Chem. Soc.* **2009**, *131*, 11509-11518.

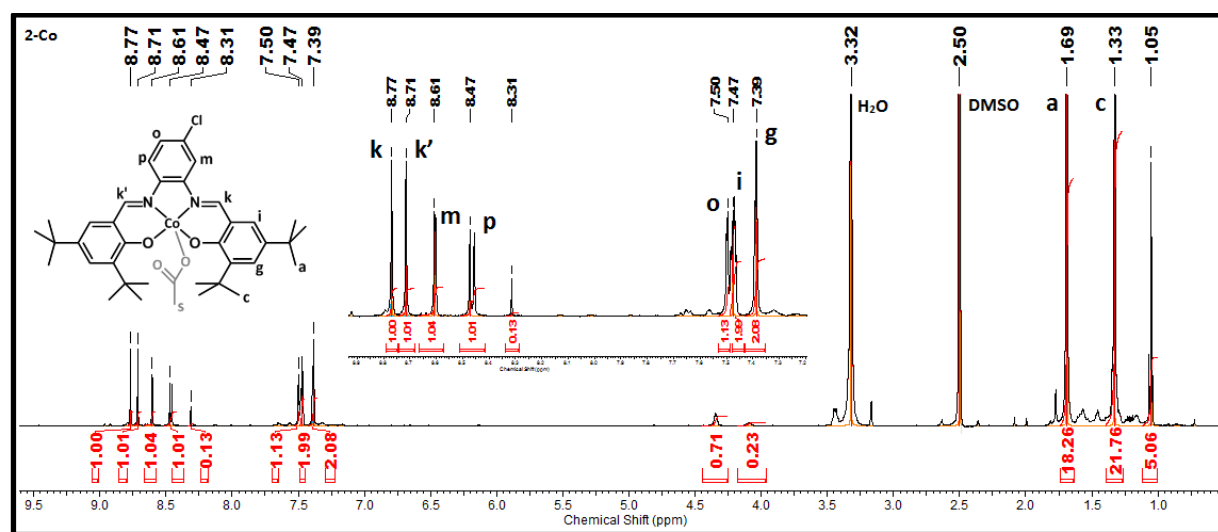
- [127] Ren, W. M.; Zhang, W. Z.; Lu, X. B., *Sci. China: Chem.* **2010**, *53*, 1646-1652.
- [128] Ren, W.-M.; Liu, Y.; Wu, G.-P.; Liu, J.; Lu, X.-B., *J. Polym. Sci., Part A: Polym. Chem.* **2011**, *49*, 4894-4901.
- [129] Takeda, N.; Inoue, S., *Bull. Chem. Soc. Jpn.* **1978**, *51*, 3564-3567.
- [130] a) Takeda, N.; Inoue, S., *Makromol. Chem.* **1978**, *179*, 1377-1381; b) Aida, T.; Inoue, S., *Macromolecules* **1982**, *15*, 682-684.
- [131] Aida, T.; Ishikawa, M.; Inoue, S., *Macromolecules* **1986**, *19*, 8-13.
- [132] Chatterjee, C.; Chisholm, M. H.; El-Khaldy, A.; McIntosh, R. D.; Miller, J. T.; Wu, T., *Inorg. Chem.* **2013**, *52*, 4547-4553.
- [133] Sugimoto, H.; Kuroda, K., *Macromolecules* **2008**, *41*, 312-317.
- [134] Anderson, C. E.; Vagin, S. I.; Hammann, M.; Zimmermann, L.; Rieger, B., *ChemCatChem* **2013**, *5*, 3269-3280.
- [135] Mang, S.; Cooper, A. I.; Colclough, M. E.; Chauhan, N.; Holmes, A. B., *Macromolecules* **2000**, *33*, 303-308.
- [136] Kruper, W. J.; Dellar, D. D., *Journal of Organic Chemistry* **1995**, *60*, 725-727.
- [137] Sugimoto, H.; Ohshima, H.; Inoue, S., *J. Polym. Sci., Part A: Polym. Chem.* **2003**, *41*, 3549-3555.
- [138] Anderson, C. E.; Vagin, S. I.; Xia, W.; Jin, H.; Rieger, B., *Macromolecules* **2012**, *45*, 6840-6849.
- [139] Jiang, X.; Gou, F.; Jing, H., *J. Catal.* **2014**, *313*, 159-167.
- [140] Wu, W.; Qin, Y.; Wang, X.; Wang, F., *J. Polym. Sci., Part A: Polym. Chem.* **2013**, *51*, 493-498.
- [141] a) Sheng, X.; Wang, Y.; Qin, Y.; Wang, X.; Wang, F., *RSC Adv.* **2014**, *4*, 54043-54050; b) Wu, W.; Sheng, X.; Qin, Y.; Qiao, L.; Miao, Y.; Wang, X.; Wang, F., *J. Polym. Sci., Part A: Polym. Chem.* **2014**, *52*, 2346-2355; c) Sheng, X.; Wu, W.; Qin, Y.; Wang, X.; Wang, F., *Polym. Chem.* **2015**, *6*, 4719-4724.
- [142] a) Xiao, Y.; Wang, Z.; Ding, K., *Chem. - Eur. J.* **2005**, *11*, 3668-3678; b) Xiao, Y.; Wang, Z.; Ding, K., *Macromolecules* **2006**, *39*, 128-137.
- [143] Sugimoto, H.; Ogawa, A., *React. Funct. Polym.* **2007**, *67*, 1277-1283.
- [144] a) Kember, M. R.; Williams, C. K., *J. Am. Chem. Soc.* **2012**, *134*, 15676-15679; b) Kember, M. R.; Knight, P. D.; Reung, P. T. R.; Williams, C. K., *Angew. Chem., Int. Ed.* **2009**, *48*, 931-933; c) Kember, M. R.; White, A. J. P.; Williams, C. K., *Macromolecules* **2010**, *43*, 2291-2298; d) Buchard, A.; Kember, M. R.; Sandeman, K. G.; Williams, C. K., *Chem. Commun.* **2011**, *47*, 212-214.
- [145] Saini, P. K.; Romain, C.; Williams, C. K., *Chem. Commun.* **2014**, *50*, 4164-4167.
- [146] Klaus, S.; Vagin, S. I.; Lehenmeier, M. W.; Deglmann, P.; Brym, A. K.; Rieger, B., *Macromolecules* **2011**, *44*, 9508-9516.
- [147] Liu, Y.; Ren, W.-M.; Liu, J.; Lu, X.-B., *Angew. Chem., Int. Ed.* **2013**, *52*, 11594-11598.
- [148] Liu, Y.; Ren, W.-M.; Liu, C.; Fu, S.; Wang, M.; He, K.-K.; Li, R.-R.; Zhang, R.; Lu, X.-B., *Macromolecules* **2014**, *47*, 7775-7788.
- [149] Li, C.-H.; Chuang, H.-J.; Li, C.-Y.; Ko, B.-T.; Lin, C.-H., *Polym. Chem.* **2014**, *5*, 4875-4878.
- [150] Taherimehr, M.; Al-Amsyar, S. M.; Whiteoak, C. J.; Kleij, A. W.; Pescarmona, P. P., *Green Chem.* **2013**, *15*, 3083-3090.
- [151] Dean, R. K.; Dawe, L. N.; Kozak, C. M., *Inorg. Chem.* **2012**, *51*, 9095-9103.

- [152] Chen, H.; Dawe, L. N.; Kozak, C. M., *Catal. Sci. Technol.* **2014**, *4*, 1547-1555.
- [153] Langanke, J.; Wolf, A.; Hofmann, J.; Boehm, K.; Subhani, M. A.; Mueller, T. E.; Leitner, W.; Guertler, C., *Green Chem.* **2014**, *16*, 1865-1870.
- [154] Chen, S.; Hua, Z.; Fang, Z.; Qi, G., *Polymer* **2004**, *45*, 6519-6524.
- [155] Zhou, T.; Zou, Z.; Gan, J.; Chen, L.; Zhang, M., *J. Polym. Res.* **2011**, *18*, 2071-2076.
- [156] Sebastian, J.; Darbha, S., *RSC Adv.* **2015**, *5*, 18196-18203.
- [157] Inoue, S., *J. Macromol. Sci., Chem.* **1979**, *A13*, 651-664.
- [158] Duchateau, R.; van, M. W. J.; Yajjou, L.; Staal, B. B. P.; Koning, C. E.; Gruter, G.-J. M., *Macromolecules* **2006**, *39*, 7900-7908.
- [159] Kim, J. G.; Cowman, C. D.; LaPointe, A. M.; Wiesner, U.; Coates, G. W., *Macromolecules* **2011**, *44*, 1110-1113.
- [160] Tan, C.-S.; Juan, C.-C.; Kuo, T.-W., *Polymer* **2004**, *45*, 1805-1814.
- [161] Hu, Y.; Qiao, L.; Qin, Y.; Zhao, X.; Chen, X.; Wang, X.; Wang, F., *Macromolecules* **2009**, *42*, 9251-9254.
- [162] Wu, G.-P.; Xu, P.-X.; Lu, X.-B.; Zu, Y.-P.; Wei, S.-H.; Ren, W.-M.; Darensbourg, D. J., *Macromolecules* **2013**, *46*, 2128-2133.
- [163] Darensbourg, D. J.; Moncada, A. I., *Macromolecules* **2010**, *43*, 5996-6003.
- [164] Darensbourg, D. J.; Moncada, A. I., *Macromolecules* **2009**, *42*, 4063-4070.
- [165] Wu, G.-P.; Wei, S.-H.; Lu, X.-B.; Ren, W.-M.; Darensbourg, D. J., *Macromolecules* **2010**, *43*, 9202-9204.
- [166] Wei, R.-J.; Zhang, X.-H.; Du, B.-Y.; Sun, X.-K.; Fan, Z.-Q.; Qi, G.-R., *Macromolecules* **2013**, *46*, 3693-3697.
- [167] Wu, G.-P.; Xu, P.-X.; Zu, Y.-P.; Ren, W.-M.; Lu, X.-B., *J. Polym. Sci., Part A: Polym. Chem.* **2013**, *51*, 874-879.
- [168] a)Darensbourg, D. J.; Wilson, S. J., *J. Am. Chem. Soc.* **2011**, *133*, 18610-18613;
b)Darensbourg, D. J.; Wilson, S. J., *Macromolecules* **2013**, *46*, 5929-5934.
- [169] Ren, W.-M.; Liang, M.-W.; Xu, Y.-C.; Lu, X.-B., *Polym. Chem.* **2013**, *4*, 4425-4433.
- [170] Gu, L.; Qin, Y.; Gao, Y.; Wang, X.; Wang, F., *J. Polym. Sci., Part A: Polym. Chem.* **2013**, *51*, 2834-2840.
- [171] Geschwind, J.; Frey, H., *Macromol. Rapid Commun.* **2013**, *34*, 150-155.
- [172] Konieczynska, M. D.; Lin, X.; Zhang, H.; Grinstaff, M. W., *ACS Macro Lett.* **2015**, *4*, 533-537.
- [173] Byrne, C. M.; Allen, S. D.; Lobkovsky, E. B.; Coates, G. W., *J. Am. Chem. Soc.* **2004**, *126*, 11404-11405.
- [174] Zhou, J.; Wang, W.; Villarroya, S.; Thurecht, K. J.; Howdle, S. M., *Chem. Commun.* **2008**, 5806-5808.
- [175] Zhang, Y.-Y.; Zhang, X.-H.; Wei, R.-J.; Du, B.-Y.; Fan, Z.-Q.; Qi, G.-R., *RSC Adv.* **2014**, *4*, 36183-36188.
- [176] Mundil, R.; Hostalek, Z.; Sedenkova, I.; Merna, J., *Macromolecular Research* **2015**, *23*, 161-166.
- [177] Darensbourg, D. J.; Mackiewicz, R. M.; Rodgers, J. L.; Fang, C. C.; Billodeaux, D. R.; Reibenspies, J. H., *Inorg. Chem.* **2004**, *43*, 6024-6034.
- [178] Peretti, K. L.; Ajiro, H.; Cohen, C. T.; Lobkovsky, E. B.; Coates, G. W., *J. Am. Chem. Soc.* **2005**, *127*, 11566-11567.

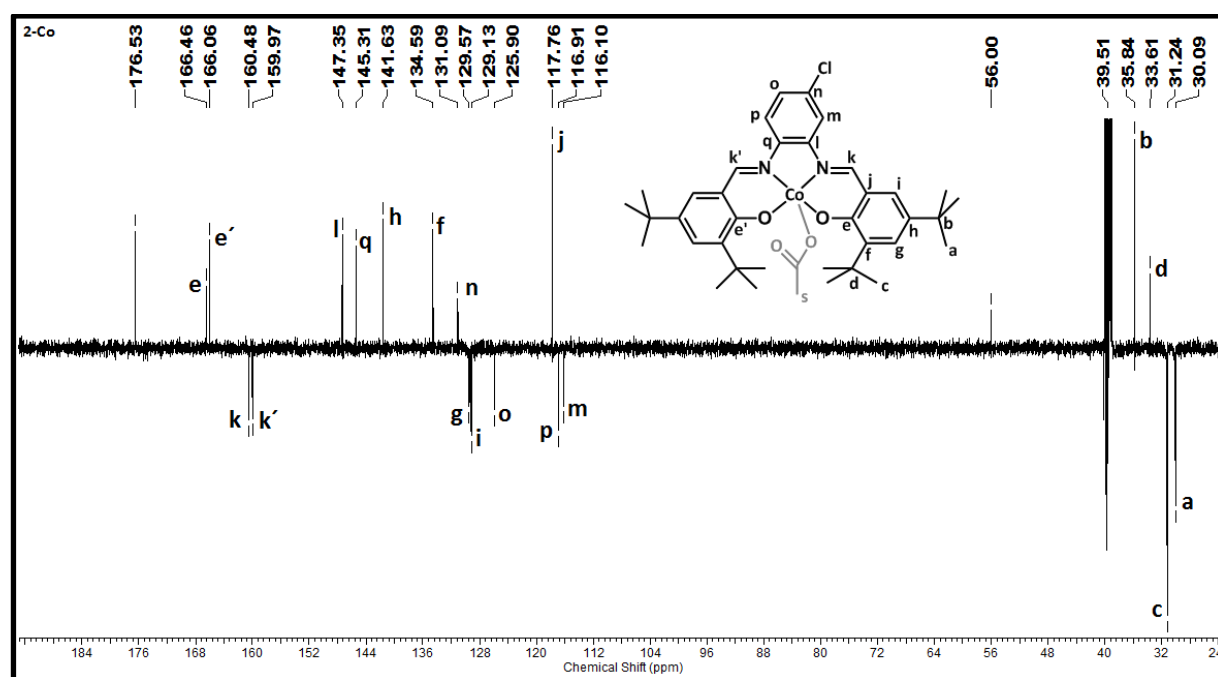
- [179] Leamen, M. J.; McManus, N. T.; Penlidis, A., *J. Appl. Polym. Sci.* **2004**, *94*, 2545-2547.
- [180] Sugimoto, H.; Ohtsuka, H.; Inoue, S., *J. Polym. Sci., Part A: Polym. Chem.* **2005**, *43*, 4172-4186.
- [181] Cyriac, A.; Lee, S. H.; Varghese, J. K.; Park, E. S.; Park, J. H.; Lee, B. Y., *Macromolecules* **2010**, *43*, 7398-7401.
- [182] Olejnik, R.; Padelkova, Z.; Mundil, R.; Merna, J.; Ruzicka, A., *Appl. Organomet. Chem.* **2014**, *28*, 405-412.
- [183] Kampova, H.; Riemlova, E.; Klikarova, J.; Pejchal, V.; Merna, J.; Vlasak, P.; Svec, P.; Ruzickova, Z.; Ruzicka, A., *J. Organomet. Chem.* **2015**, *778*, 35-41.
- [184] Host'alek, Z.; Mundil, R.; Cisarova, I.; Trhlikova, O.; Grau, E.; Peruch, F.; Cramail, H.; Merna, J., *Polymer* **2015**, *63*, 52-61.

8 SUPPLEMENTARY DATA

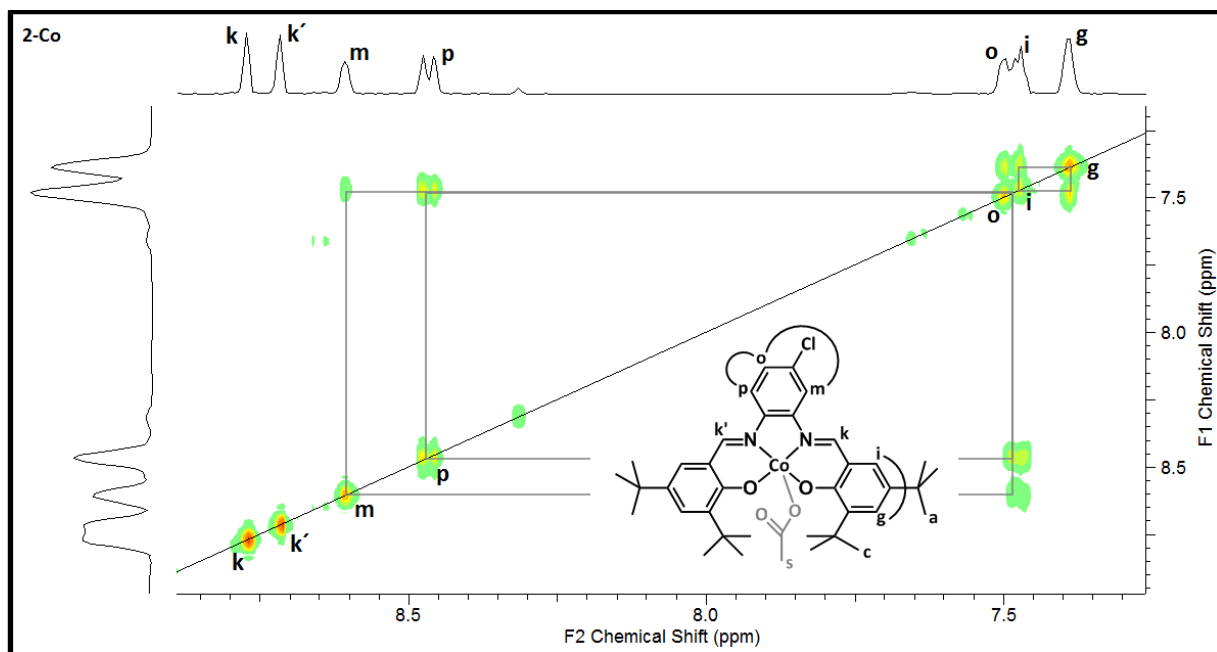
8.1 Full NMR characterization of complex 2-Co



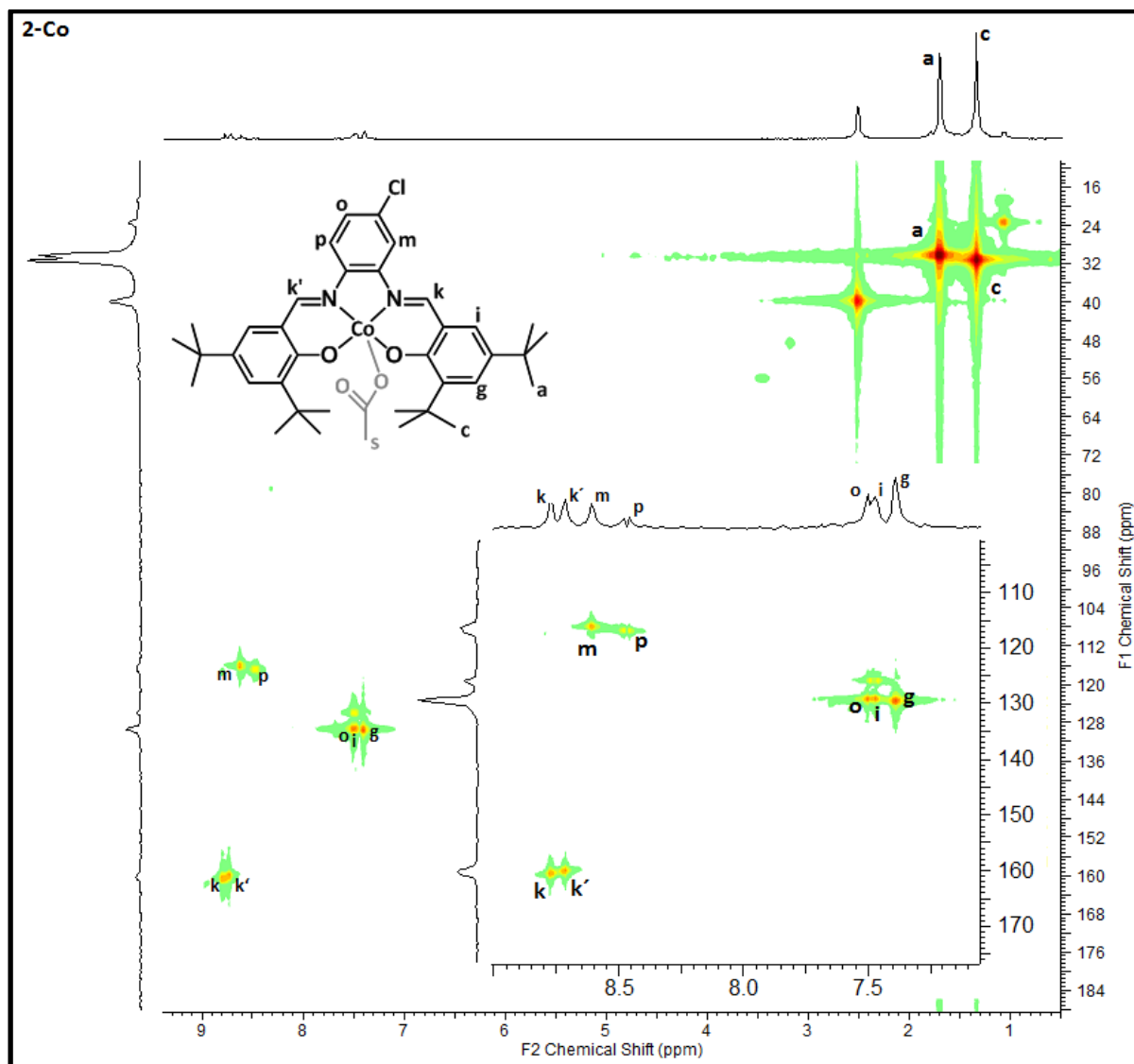
Spectrum 8.1: ¹H NMR spectrum of complex 2-Co in DMSO



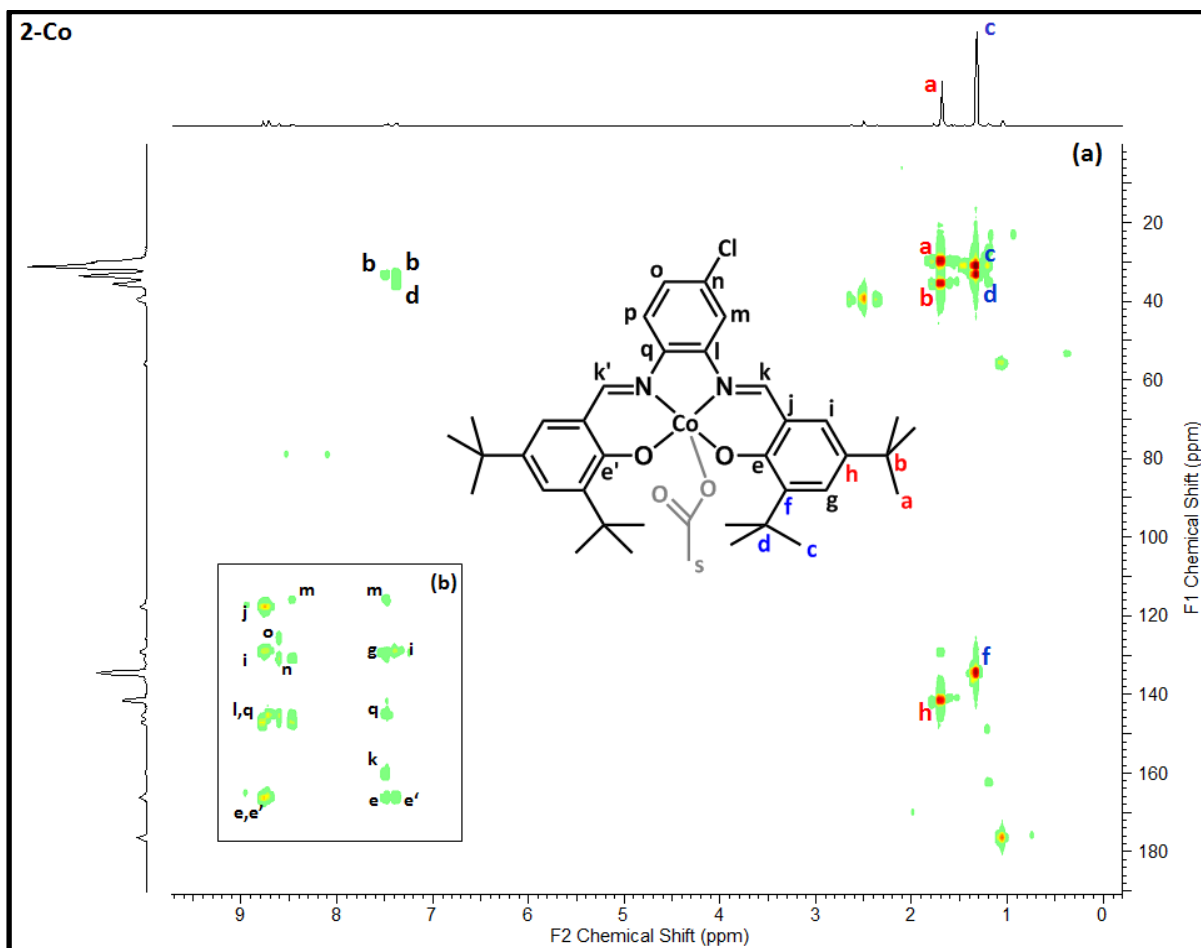
Spectrum 8.2: ¹³C APT NMR spectrum of complex 2-Co in DMSO



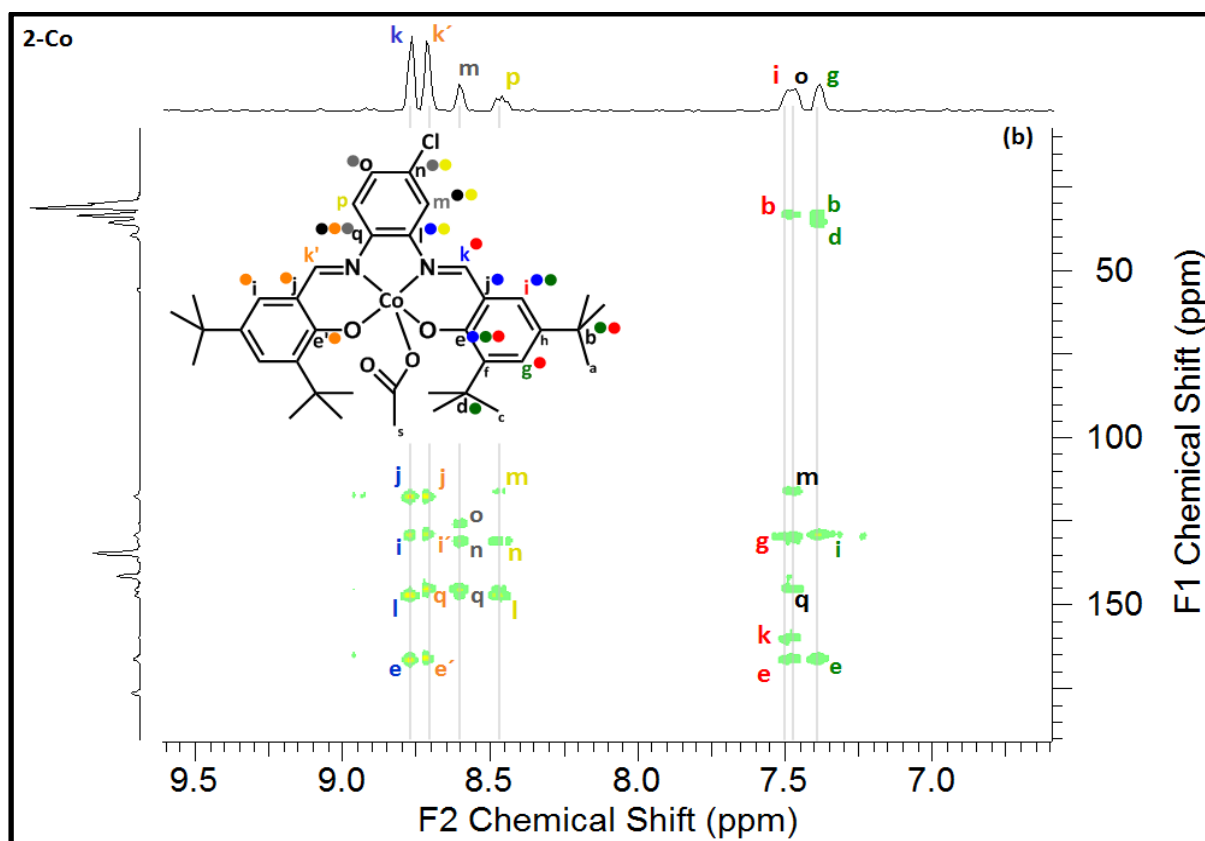
Spectrum 8.3: ^1H COSY NMR of complex **2-Co** (aromatic region) in DMSO



Spectrum 8.4: ^1H - ^{13}C NMR of complex **2-Co** in DMSO



Spectrum 8.5: HMBC NMR of complex 2-Co



Spectrum 8.6: HMBC NMR of complex 2-Co: expanded aromatic region (6.5 ppm – 9.5 ppm)

8.2 Crystallographic data for complex **1-Co-OBzF₅**

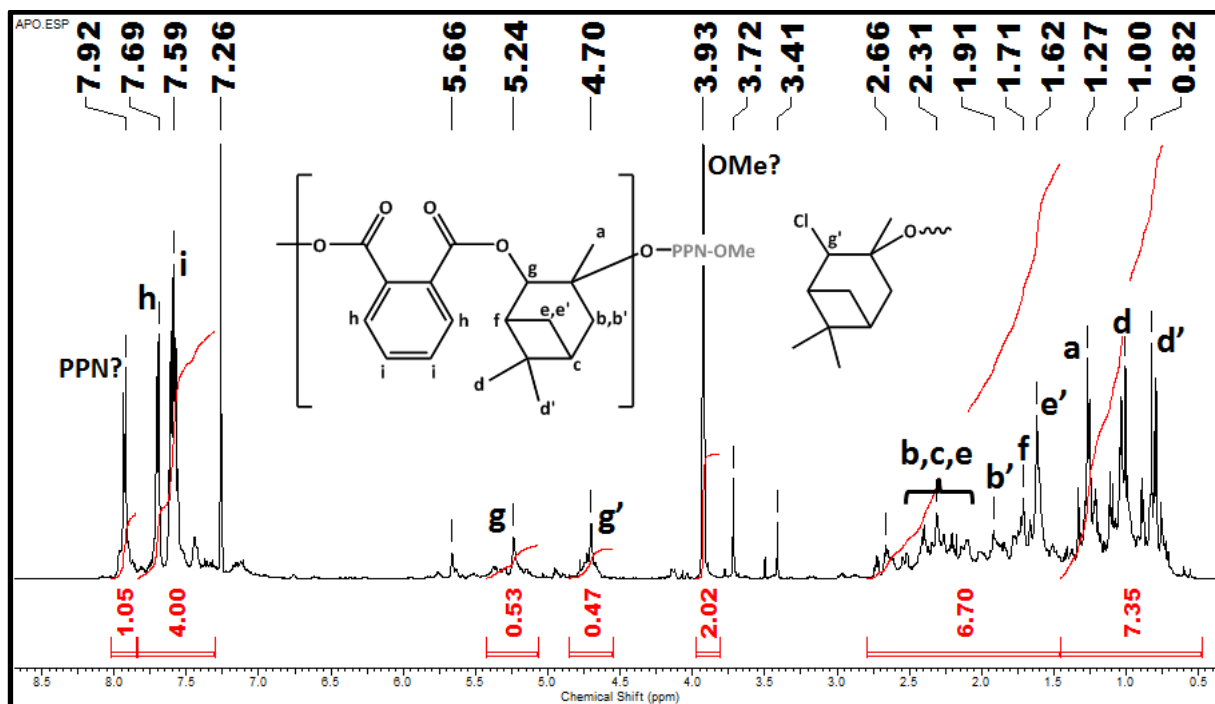
Crystal data for complex **1-Co-OBzF₅**: C₅₀H₄₇CoF₁₀N₂O₆, $M_r = 1020.83$, triclinic, $P-1$ (No 2), $a = 13.6323$ (6) Å, $b = 14.3118$ (6) Å, $c = 14.4602$ (6) Å, $\alpha = 76.884$ (2)°, $\beta = 85.260$ (2)°, $\gamma = 65.678$ (2)°; $Z = 2$, $D_x = 1.354$ Mg.m⁻³, dark red crystal of dimensions 0.40 × 0.31 × 0.18 mm, the multi-scan absorption correction was applied was ($\mu = 0.43$ mm⁻¹), $T_{\min} = 0.846$, $T_{\max} = 0.925$; 31019 diffraction collected ($\theta_{\max} = 27^\circ$), 10924 independent ($R_{\text{int}} = 0.032$) and 8543 observed ($I > 2\sigma(I)$). The refinement converged ($\Delta/\sigma_{\max} = 0.001$) to $R = 0.046$ for observed reflections and $wR(F^2) = 0.127$, $GOF = 1.08$ for 634 parameters and all 10924 reflections. The final difference map displayed no peaks of chemical significance ($\Delta\rho_{\max} = 0.79$, $\Delta\rho_{\min} = 0.51$ e.Å⁻³)

Crystal data

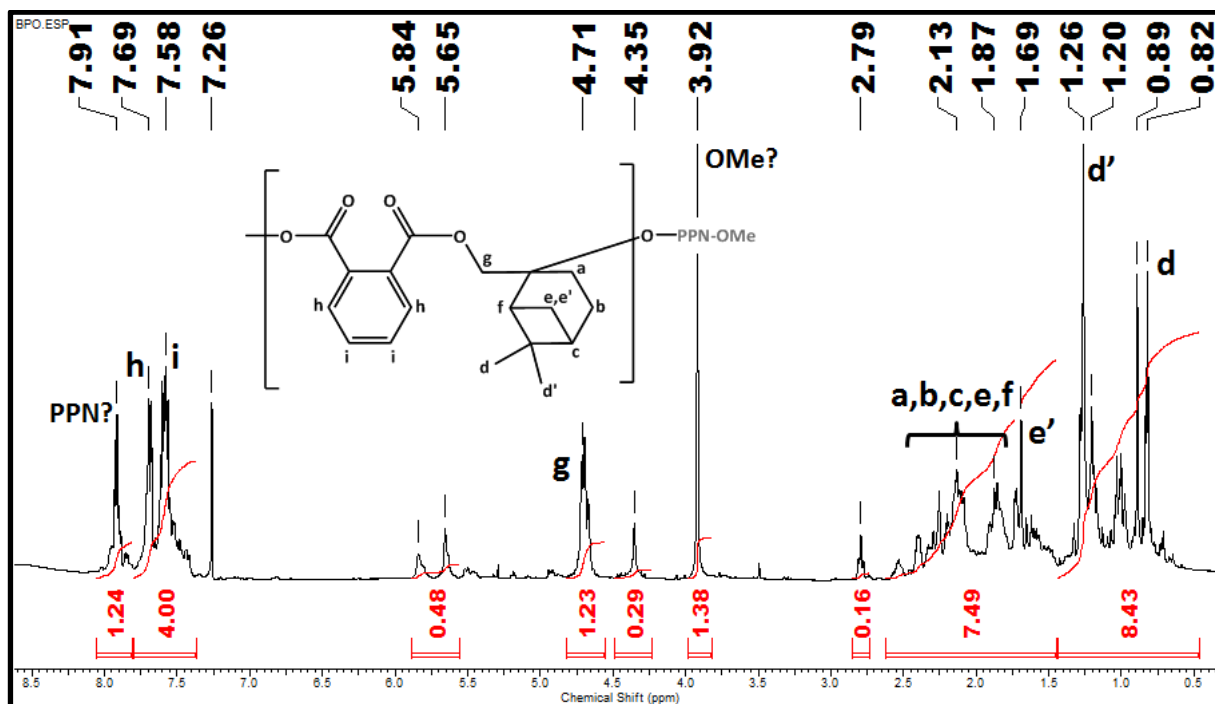
C ₅₀ H ₄₇ CoF ₁₀ N ₂ O ₆	$Z = 2$
$M_r = 1020.83$	$F(000) = 1052$
Triclinic, $P-1$	$D_x = 1.354$ Mg m ⁻³
$a = 13.6323$ (6) Å	Mo $K\alpha$ radiation, $\lambda = 0.71073$ Å
$b = 14.3118$ (6) Å	Cell parameters from 9942 reflections
$c = 14.4602$ (6) Å	$q = 2.7-27.0^\circ$
$\alpha = 76.884$ (2)°	$m = 0.43$ mm ⁻¹
$\beta = 85.260$ (2)°	$T = 150$ K
$\gamma = 65.678$ (2)°	Prism, dark red
$V = 2503.58$ (18) Å ³	0.40 × 0.31 × 0.18 mm

Complete crystallographic data for structural analysis of complex **1-Co-OBzF₅** have been deposited with the Cambridge Crystallographic Data Centre, CCDC no. **1024696**. Copies of this information may be obtained free of charge from The Director, CCDC, 12 Union Road, Cambridge CB2 1EY, UK (e-mail: deposit@ccdc.cam.ac.uk or [www: http://www.ccdc.cam.ac.uk](http://www.ccdc.cam.ac.uk)). Crystallographic data for the complex can be further found also in supporting information of related publication (reference 184).

8.3 ^1H NMR spectra of “polyesters” obtained by copolymerization of APO or BPO with PA

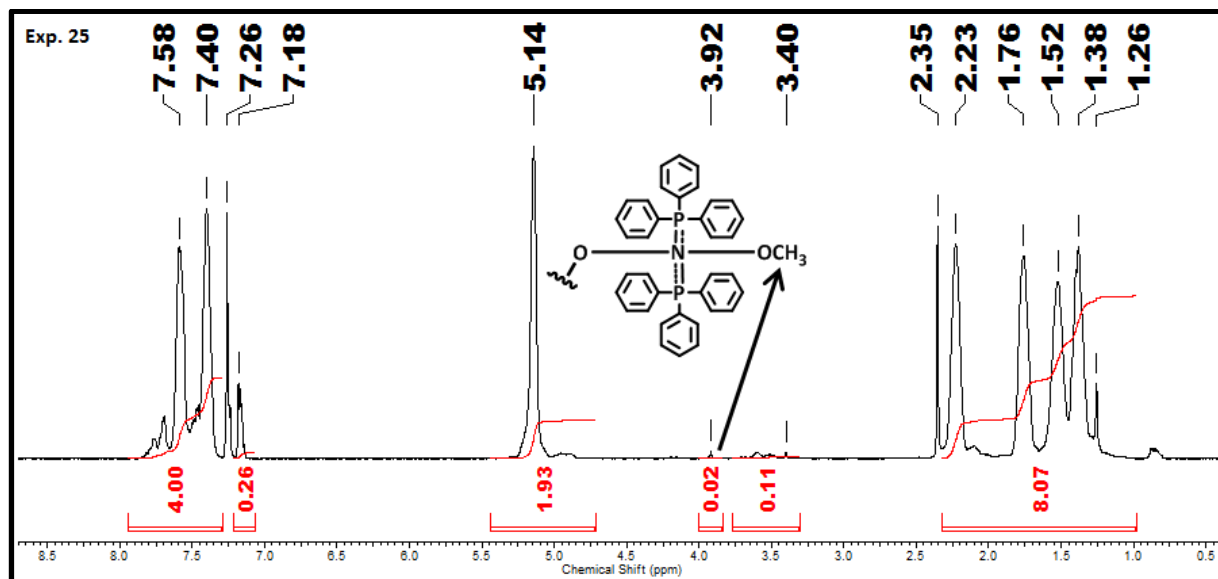


Spectrum 8.7: ^1H NMR spectrum of PA-APO copolymer with proposed peak assignment (exp. 15)



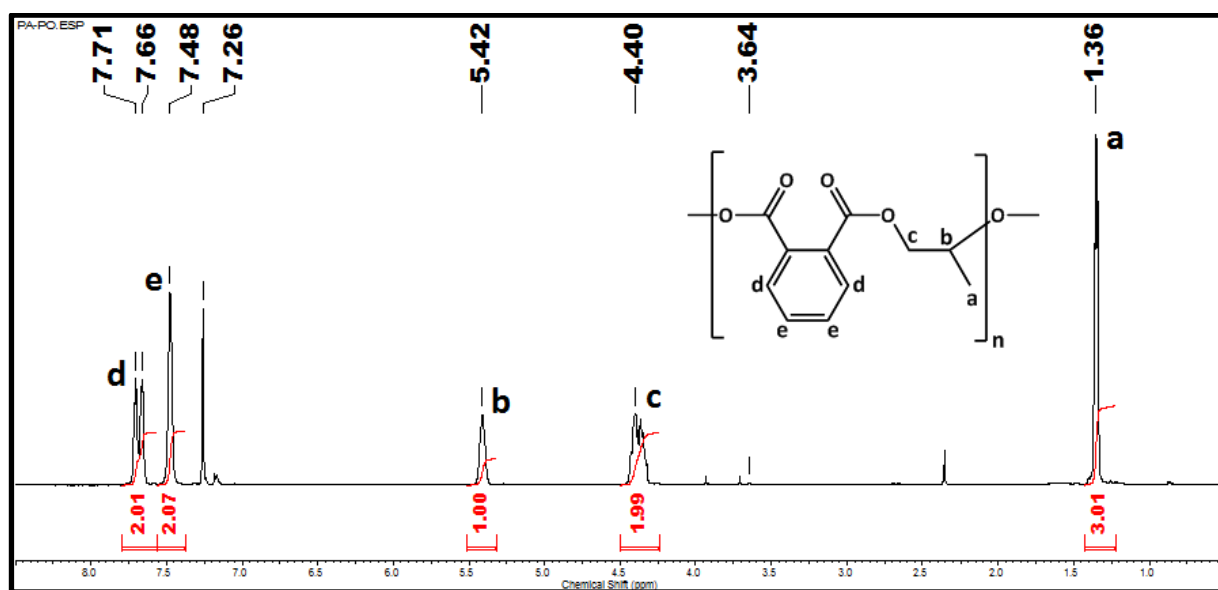
Spectrum 8.8: ^1H NMR spectrum of PA-BPO copolymer with proposed peak assignment (exp. 16)

8.4 Spectrum of PA-CHO copolymer with PPN-OMe terminal group

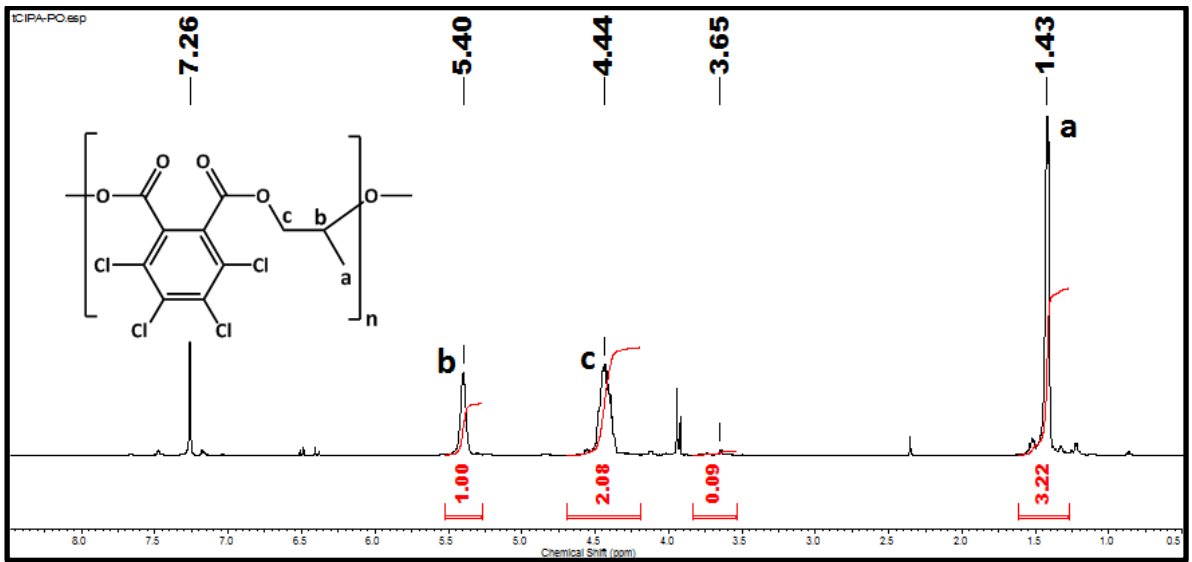


Spectrum 8.9: ^1H NMR spectrum of PA-CHO copolymer with PPN-OMe terminal group (exp. 25)

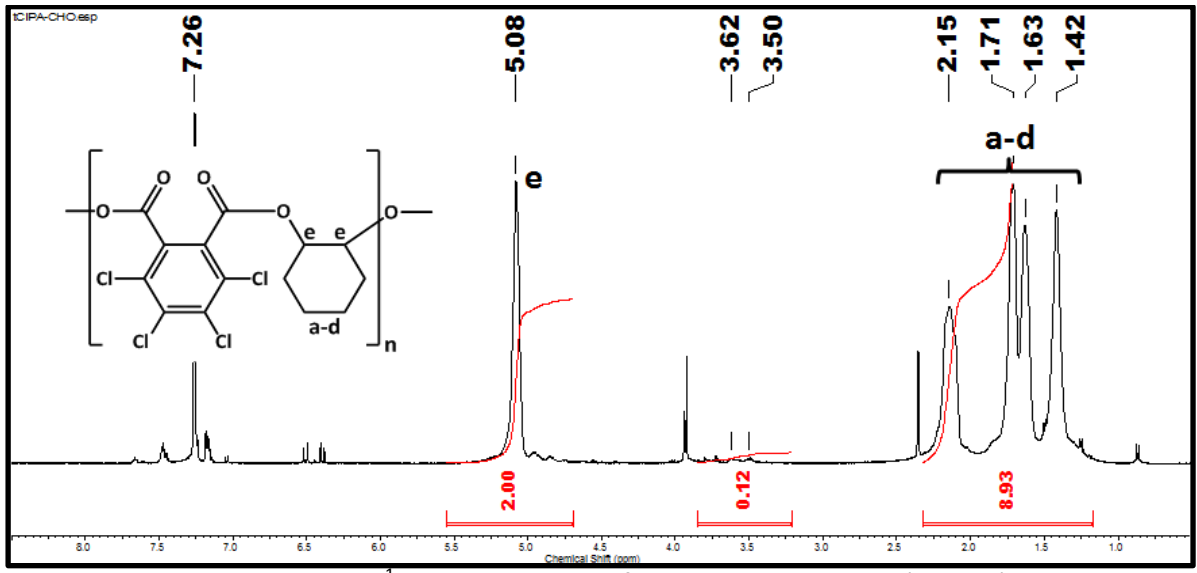
8.5 ^1H NMR spectra of copolyesters prepared with PPNCl catalyst



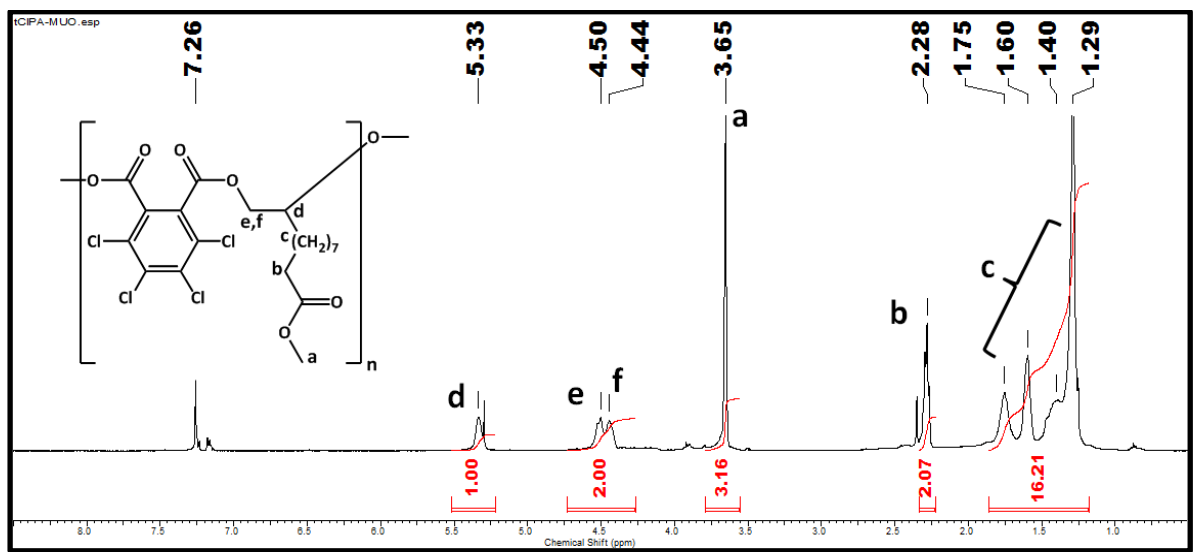
Spectrum 8.10: ^1H NMR spectrum of PA-PO copolymer (exp. 36)



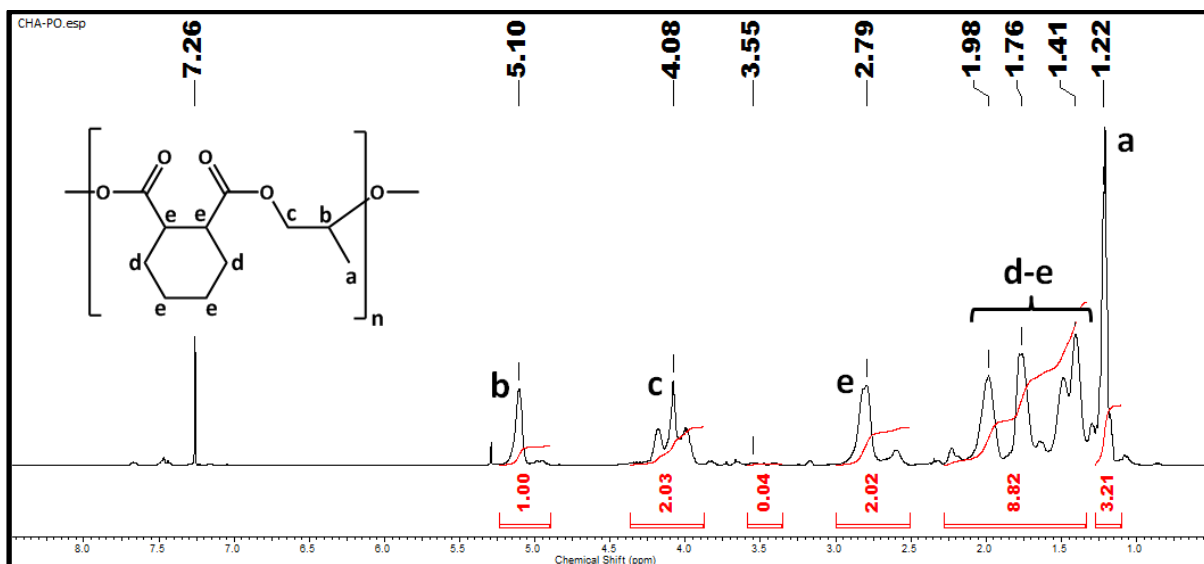
Spectrum 8.14: ^1H NMR spectrum of tCIPA-PO copolymer (exp. 43)



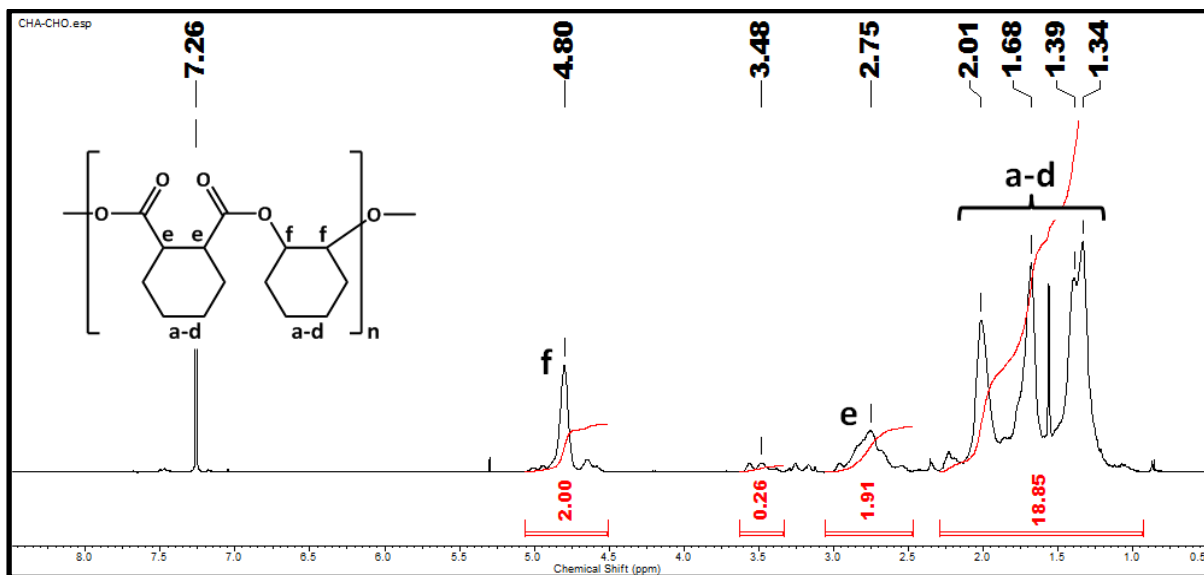
Spectrum 8.15: ^1H NMR spectrum of tCIPA-CHO copolymer (exp. 44)



Spectrum 8.16: ^1H NMR spectrum of tCIPA-MUO copolymer (exp. 46)



Spectrum 8.17: ^1H NMR spectrum of CHA-PO copolymer (exp. 47)



Spectrum 8.18: ^1H NMR spectrum of CHA-CHO copolymer (exp. 48)

8.6 Polymerization apparatuses used for epoxide/ CO_x copolymerizations



Figure 8.1: Fisher-Porter bottle (100 mL) used for copolymerizations up to 1 MPa of CO_2



Figure 8.2: Metallic minireactor (10 mL) for high pressure (5 MPa) copolymerizations

9 LIST OF TABLES

Table 2.1: Bulk polymerization of epoxides with selected BDI Zinc complexes	27
Table 2.2: Binary salen and salan complexes for epoxide/CO ₂ copolymerization in bulk	32
Table 2.3: Bifunctional salen and porphyrin complexes for PO/CO ₂ copolymerization	39
Table 2.4: Dinuclear and bimetallic bridged complexes for epoxide/CO ₂ copolymerization	44
Table 5.1: Elemental analysis of 1-CrCl and 2-CrCl	64
Table 5.2: Elemental analysis of 1-FeCl and 2-FeCl	64
Table 5.3: Copolymerization of PO with CO using 2-CrCl/Co₂(CO)₈	76
Table 5.4: Copolymerization of epoxides with CO using 2-CrCl/Co₂(CO)₈	78
Table 5.5: Copolymerization of PA with CHO catalyzed with salphen Cr and Fe complexes.....	82
Table 5.6: Copolymerization of epoxides and anhydrides catalyzed with salphen Cr complexes.....	82
Table 5.7: Copolymerization of phthalic anhydride with bio-based epoxides.....	83
Table 5.8: Copolymerization of PA-CHO with phthalic anhydrides in toluene at 110°C.....	84
Table 5.9: Copolymerizations of CHO with PA contaminated on purpose by phthalic acid	86
Table 5.10: Nonstoichiometric copolymerization of PA with CHO at 110°C in toluene	92
Table 5.11: Effect of solvent and temperature in copolymerization of CHO with PA	92
Table 5.12: Copolymerization of PA with CHO at 110°C in bulk	93
Table 5.13: Kinetic study of PA/CHO copolymerization initiated by PPNCI in toluene at 110°C.....	94
Table 5.14: Copolymerization of PA with CHO at different loadings of PPNCI	95
Table 5.15: Copolymerization of various epoxides and anhydrides initiated by PPNCI	98
Table 5.16: Copolymerization of PO/CO ₂ catalyzed with salphen Cr complexes 2-CrCl/DMAP	101
Table 5.17: Copolymerization of PO/CO ₂ catalyzed by 1-CrCl and 2-CrCl with PPNCI cocatalyst.....	102
Table 5.18: Effect of catalyst (2-CrCl) aging in CHO/CO ₂ copolymerization	102
Table 5.19: Effect of temperature and reaction pressure to PO/CO ₂ copolymerization catalyzed by 1-Co-OCCCCl₃/PPNCI	104
Table 5.20: Copolymerization of PO/CO ₂ catalyzed with complexes 1-Co-Y and 2-Co-Y	106
Table 5.21: Copolymerization of CHO with CO ₂ with salphen complex 2-Co-OAc/PPNCI	109
Table 5.22: Copolymerization of CHO with CO ₂ with salphen Co complexes 1-Co-Y and 2-Co-Y	110
Table 5.23: Copolymerization of CHO with CO ₂ catalyzed with various Al, Zn and Mg complexes ...	114

10 LIST OF SCHEMES

Scheme 2.1: Synthetic routes to polyesters	3
Scheme 2.2: Expansion carbonylation of propylene oxide with CO and subsequent ring-opening polymerization.....	4
Scheme 2.3: Mechanism of direct epoxide/CO copolymerization proposed by Rieger et al.	5
Scheme 2.4: Copolymerization of propylene oxide with CO performed by Drent and Kragtwijk.....	6
Scheme 2.5: Preparation methods to β -lactones	7
Scheme 2.6: Mechanism of carbonylative expansion of epoxides to cyclic β -lactones	8
Scheme 2.7: Double carbonylation of epoxides to anhydrides	13
Scheme 2.8: General scheme of metal catalyzed ROCOP of epoxides and anhydrides	13
Scheme 2.9: Synthetic routes to polycarbonates	17
Scheme 2.10: Products of epoxide/CO ₂ copolymerization	18
Scheme 2.11: General initiation and propagation mechanisms for epoxide/CO ₂ copolymerization ...	20
Scheme 2.12: Formation of cyclic carbonates via back-biting mechanism	21
Scheme 2.13: Bifunctional initiation by contaminant water	22
Scheme 2.14: Chain transfer reaction by contaminant water during the copolymerization	22
Scheme 2.15: Mechanism of PO/CO ₂ copolymerization for salen/salan type catalysts with DMAP ...	31
Scheme 5.1: Synthesis of salphen ligands 1 and 2	63
Scheme 5.2: General synthesis procedure of salphen Cr and Fe complexes.....	63
Scheme 5.3: General scheme of salphen Co-Y synthesis.....	65
Scheme 5.4: Proposed structures of salphen chromium, iron and cobalt complexes	75
Scheme 5.5: Proposed structure of salphen chromium and iron complexes.....	81
Scheme 5.6: Microstructure of PA-CHO copolyesters (lower molar mass fraction).....	88
Scheme 5.7: Microstructure of PA-CHO copolyesters (higher molar mass fraction)	89
Scheme 5.8: Proposed mechanism of initiation by PPNCl (I) and phthalic acid (II).....	91
Scheme 5.9: Proposed structure of salphen chromium complexes	100
Scheme 5.10: Proposed structure of salphen cobalt complexes.....	103

11 LIST OF FIGURES

Figure 2.1: Bipyridine derivatives as cocatalysts for epoxides/CO copolymerization	6
Figure 2.2: Cyclopentadienyl titanium complex for carbonylative expansion of epoxides	9
Figure 2.3: Salen and porphyrin complexes for carbonylative expansion of epoxides to lactones.....	9
Figure 2.4: Chiral indole-based Cr(III) catalysts for carbonylation of epoxides to BBL.....	10
Figure 2.5: Catalysts for ROP of β -butyrolactone	10
Figure 2.6: Conformationally flexible dimeric chromium salphen complexes.....	11
Figure 2.7: Rare earth metal catalysts for syndiospecific polymerization of β -butyrolactone.....	12
Figure 2.8: Newest yttrium complexes for syndiospecific β -butyrolactone polymerization.....	12
Figure 2.9: β -diiminate (BDI) zinc catalysts for ROP of in-situ formed BBL	13
Figure 2.10: Metal-porphyrin complexes for copolymerization of epoxides with anhydrides.....	14
Figure 2.11: β -diiminate (BDI) zinc complexes for ROCOP of epoxides and anhydrides	15
Figure 2.12: Series of salen complexes for copolymerization of epoxides with anhydrides	15
Figure 2.13: Bi- and tri-metallic salan and salen complexes for copolymerization of epoxides with anhydrides.....	16
Figure 2.14: Di-magnesium and zinc catalysts for ROCOP of PA with CHO	16
Figure 2.15: Metal corolle complexes for copolymerization of epoxides with anhydrides	16
Figure 2.16: Early discrete zinc-phenoxide complexes	23
Figure 2.17: Diimine quinoxaline-derived zinc alkoxide complex for CHO/CO ₂ copolymerization.....	24
Figure 2.18: β -diiminate (BDI) zinc catalysts for epoxide-CO ₂ copolymerization	24
Figure 2.19: BDI zinc complexes with modified framework	25
Figure 2.20: Ethyl sulfinato BDI complexes synthesized by Rieger	25
Figure 2.21: BDI-derived dizinc complex.....	26
Figure 2.22: New amido-oxazolate and BDI complexes for asymmetric copolymerization of CHO with CO ₂	26
Figure 2.23: New BDI complexes with <i>para</i> CN substituents.....	27
Figure 2.24: Early metal salen complexes for production of cyclic carbonates and polycarbonates...	28
Figure 2.25: First salicyl-aldimine complex producing PCHC.....	28
Figure 2.26: Metal salen complexes for copolymerization of epoxides with CO ₂	29
Figure 2.27: Salan and salalen Cr and Zr complexes for CHO and PO copolymerization.....	32
Figure 2.28: Salen(Co) complexes with pieridinium end-capping arms.....	33
Figure 2.29: (Salen)Co complexes with tertiary amine end-capping arms	34
Figure 2.30: Salen Co complexes with pendant tertiary amine cocatalyst.....	35
Figure 2.31: Multichiral BINOL salen Co(III) complexes	35
Figure 2.32: Metal porphyrin complexes for copolymerization of epoxides with CO ₂	36
Figure 2.33: New metal porphyrin complexes for copolymerization of epoxides with CO ₂	37
Figure 2.34: Cobalt porphyrin complexes with tetrabutylammonium side arms.....	37
Figure 2.35: Series of aluminium porphyrin complexes with tetraalkylammonium side arms	38

Figure 2.36: Metal corolle complexes for copolymerization of epoxides with CO ₂	38
Figure 2.37: Trost phenolate complexes.....	40
Figure 2.38: Dinuclear Robson-type complexes.....	40
Figure 2.39: Dinuclear methylene-bridged salen complexes.....	41
Figure 2.40: Conformationally flexible dimeric chromium salphen complexes.....	41
Figure 2.41: Enantiopure dinuclear Co salen complexes	42
Figure 2.42: Biphenyl-linked dinuclear cobalt complexes with restricted rotation.....	42
Figure 2.43: Ni(II), Co(II) and Zn(II)bis(benzotriazole iminophenolate) catalysts	43
Figure 2.44: Metal amino triphenolate complexes.....	43
Figure 2.45: Structure of Zn ₃ [Co(CN) ₆] double metal cyanide (DMC) complex	44
Figure 2.46: Scope of noncommercial and biobased epoxides.....	46
Figure 4.1: Methylundec-10-enoate oxide (MUO).....	58
Figure 4.2: Correlation of molar masses of PPC (a) and PCHC (b) obtained by SEC-MALLS and PS calibration method.....	62
Figure 5.1: View on the molecular structure of complex 1-Co-OBzF₃ , determined by X-Ray crystallography	70
Figure 5.2: SEC traces of CHO-PA copolymers prepared with 1-CrCl /PPNCl using crude PA (blue, exp. 5) and twice sublimed PA (black, exp. 9).....	83
Figure 5.3: FT-IR spectra of phthalic anhydrides purified by different methods (I-PA(S)_New ; II-PA(A)_New ; III-PA(A)_New_Sublimed ; IV-PA(A)_New_Recrystallized).....	85
Figure 5.4: SEC-traces of PA-CHO copolymers prepared from PA with various amount of hydrolyzed PA (PA_S_New - blue, PA_A_New - orange, PA_A_New_Subl. - green, PA_A_New_Recr. - red)	86
Figure 5.5: Copolymerization of PA with CHO using sublimed PA (black) and sublimed PA with addition of 1 wt % (grey) and 5 wt % (blue) of phthalic acid	87
Figure 5.6: MALDI-TOF mass spectrum of PA-CHO copolymer catalyzed with PPNCl (exp. 25).....	88
Figure 5.7: MALDI-TOF mass spectrum of PA-CHO copolymer catalyzed with PPNCl ionized in absence (a) or in presence (b) of Na salt.....	90
Figure 5.8: a) Conversion curve of PA/CHO copolymerization at 110°C catalyzed with PPNCl; b) Linear plot of ln(M ₀ /M _t) vs time.....	93
Figure 5.9: a) SEC traces of CHO-PA copolymers (exp. 24-29) and b) linear increase of PES molar mass with conversion.....	94
Figure 5.10: Linear plot of ln(M ₀ /M _t) vs time at different monomer/PPNCl loadings (100:1-red; 250:1-green and 500:1-blue).....	95
Figure 5.11: Linear increase of polyester molar mass with conversion at different monomer/PPNCl loadings (100:1-red; 250:1-grey and 500:1-blue)	96
Figure 5.12: Copolymerization of PO with PA (crude, new Alfa Aesar) at 110°C after 5h in toluene catalyzed by various organic bases ([PA]/[CHO]/[Base]=250:250:1)	96
Figure 5.13: Listing of epoxides and anhydrides used for alternating ROCOP	97
Figure 5.14: Effect of 1-Co-OOCCL₃ /PPNCl loading to PO/CO ₂ copolymerization at 1MPa and 50°C ([PO]/[Co]=2000:1, t _p =2h)	105

Figure 5.15: Effect of catalyst and temperature to overall activity and selectivity of PO/CO ₂ copolymerization catalyzed by complexes 1-Co-OOCCl₃ /PPNCl and 2-Co-OOCCl₃ /PPNCl at 1MPa ([PO]/[Co]/[PPNCl]=2000:1:1)	107
Figure 5.16: SEC traces of polypropylene carbonate prepared with PO containing various amount of water	108
Figure 5.17: MALDI-TOF mass spectrum of PPC prepared by 2-Co-DNP /PPNCl (exp. 10).....	108
Figure 5.18: Linear increase of PCHC molar mass with conversion (catalytic system 1-Co-OOCCl₃ /PPNCl, [PO]/[Co]/[PPNCl]=1000:1:1, $t_p=0.5, 2$ and 4h, $T=75^\circ\text{C}$, $p=1\text{MPa}$)	110
Figure 5.19: MALDI-TOF mass spectrum of PCHC prepared by 1-Co-OOCCl₃ /PPNCl (exp. 17)	111
Figure 5.20: Epoxides used for carbonylation to cyclic carbonates.....	111
Figure 5.21: Activity of 2-CrCl in coupling of epoxides with CO ₂ at 1MPa and 75°C ([Epoxide]/[Co]/[PPNCl]=500:1:1, $t_p=20\text{h}$)	112
Figure 5.22: Aluminium, zinc and magnesium complexes for CHO/CO ₂ copolymerization.....	113
Figure 8.1: Fisher-Porter bottle (100 mL) used for copolymerizations up to 1 MPa of CO ₂	135
Figure 8.2: Metallic minireactor (10 mL) for high pressure (5 MPa) copolymerizations.....	135

12 LIST OF SPECTRA

Spectrum 5.1: FT-IR spectra of complexes 1-Co and 1-Co-OOCCl₃	66
Spectrum 5.2: ¹ H NMR spectrum of complex 1-Co-OOCCl₃ in DMSO	66
Spectrum 5.3: FT-IR spectra of complexes 1-Co and 1-Co-DNP	67
Spectrum 5.4: ¹ H NMR spectrum of complex 1-Co-DNP in DMSO	68
Spectrum 5.5: FT-IR spectra of complexes 1-Co and 1-Co-OBzF₅	68
Spectrum 5.6: ¹ H NMR spectrum of complex 1-Co-OBzF₅ in DMSO.....	69
Spectrum 5.7: ¹⁹ F NMR of complex 1-Co-OBzF₅	69
Spectrum 5.8: FT-IR spectra of complexes 2-Co and 2-Co-OOCCl₃	70
Spectrum 5.9: ¹ H NMR spectrum of complex 2-Co-OOCCl₃ in DMSO	71
Spectrum 5.10: FT-IR spectra of complexes 2-Co and 2-Co-DNP	72
Spectrum 5.11: ¹ H NMR spectrum of complex 2-Co-DNP in DMSO	72
Spectrum 5.12: FT-IR spectra of complexes 2-Co and 2-Co-OAc	73
Spectrum 5.13: ¹ H NMR spectrum of complex 2-Co-OAc in DMSO with embedded ¹ H NMR spectrum of solely cobalt(II) acetate tetrahydrate in DMSO	74
Spectrum 5.14: ¹ H NMR spectra of reaction mixture of exp. 3_1 (<i>t_p</i> =20 h, <i>T</i> =75°C).....	77
Spectrum 5.15: ¹ H NMR spectrum of polyester-co-ether copolymer prepared by copolymerization of PO with carbon monoxide by 2-CrCl/Co₂(CO)₈ (exp. 3).....	78
Spectrum 5.16: ¹ H NMR spectra of CHO/CO copolymerization (exp. 7) a) reaction mixture, b) dried polymer	79
Spectrum 8.1: ¹ H NMR spectrum of complex 2-Co in DMSO.....	126
Spectrum 8.2: ¹³ C APT NMR spectrum of complex 2-Co in DMSO	126
Spectrum 8.3: ¹ H COSY NMR of complex 2-Co (aromatic region) in DMSO	127
Spectrum 8.4: ¹ H - ¹³ C NMR of complex 2-Co in DMSO	127
Spectrum 8.5: HMBC NMR of complex 2-Co	128
Spectrum 8.6: HMBC NMR of complex 2-Co : expanded aromatic region (6.5 ppm – 9.5 ppm)	128
Spectrum 8.7: ¹ H NMR spectrum of PA-APO copolymer with proposed peak assignment (exp. 15). 130	
Spectrum 8.8: ¹ H NMR spectrum of PA-BPO copolymer with proposed peak assignment (exp. 16). 130	
Spectrum 8.9: ¹ H NMR spectrum of PA-CHO copolymer with PPN-OMe terminal group (exp. 25)... 131	
Spectrum 8.10: ¹ H NMR spectrum of PA-PO copolymer (exp. 36)	131
Spectrum 8.11: ¹ H NMR spectrum of PA-CHO copolymer (exp. 37).....	132
Spectrum 8.12: ¹ H NMR spectrum of PA-SO copolymer (exp. 38)	132
Spectrum 8.13: ¹ H NMR spectrum of PA-MUO copolymer (exp. 39)	132
Spectrum 8.14: ¹ H NMR spectrum of tCIPA-PO copolymer (exp. 43).....	133
Spectrum 8.15: ¹ H NMR spectrum of tCIPA-CHO copolymer (exp. 44)	133
Spectrum 8.16: ¹ H NMR spectrum of tCIPA-MUO copolymer (exp. 46).....	133
Spectrum 8.17: ¹ H NMR spectrum of CHA-PO copolymer (exp. 47).....	134
Spectrum 8.18: ¹ H NMR spectrum of CHA-CHO copolymer (exp. 48).....	134

13 LIST OF PUBLICATIONS

Hostalek, Z.; Mundil, R.; Cisarova, I.; Trhlikova, O.; Grau, E.; Peruch, F.; Cramail, H.; Merna, J. Salphen-Co(III) complexes catalyzed copolymerization of epoxides with CO₂. *Polymer* **2015**, *63*, 52-61

Mundil, R.; **Hostalek, Z.;** Sedenkova, I.; Merna, J. Alternating Ring-Opening Copolymerization of cyclohexene oxide with phthalic anhydride catalyzed by Iron(III) salen complexes. *Macromol. Res.* **2015**, *23*, 161-166

Olejnik, R.; Bilek, M.; Ruzickova, Z.; **Hostalek, Z.;** Merna, J.; Ruzicka, A. Zinc complexes chelated by bifunctional ketiminate ligands: Structure, reactivity and possible applications in initiation of ROP and copolymerization of epoxides with carbon dioxide. *J. Organomet. Chem.* **2015**, *794*, 237-246.

Olejnik, R.; Bazantova, J.; Ruzickova, Z.; Merna, J.; **Hostalek, Z.;** Ruzicka, A. Methoxyaryl substituted aluminum ketiminate complexes and its activity in ring opening polymerization processes. *Inorg. Chem. Commun.* **2015**, *55*, 161-164

Hostalek, Z.; et al. Copolymerization of epoxides with anhydrides initiated with organic bases – environmentally friendly route to polyesters; manuscript in preparation

Lectures

Hošťálek, Z.; Martinez, T.; Trhliková, O.; Cramail, H.; Merna, J. Copolymerization of epoxides with anhydrides catalyzed with organic bases 47. *Symposium on Catalysis*, Prague (Czech Republic), 2-4.11.2015

Hošťálek, Z.; Peruch, F.; Grau, E.; Cramail, H.; Merna, J. Copolymerization of epoxides with CO₂ initiated by Salphen-Co complexes. 45. *Symposium on Catalysis*, Prague (Czech Republic), 4-6.11.2013

Hošťálek, Z.; Cramail, H.; Peruch, F.; Grau, E.; Merna, J. Coupling of epoxides with CO_x: Production of degradable polymers and cyclic carbonates/esters. *Journées de rencontres des Polyméristes du Sud-Ouest*, Sabres (France), 27-28.5.2013

Posters

Hošťálek, Z.; Peruch, F.; Cramail, H.; Merna, J. Coupling of CO₂ with commercial and biobased epoxides. 46. *Symposium on Catalysis*, Prague (Czech Republic), 3.-5.11.2014

Hošťálek, Z.; Cramail, H.; Peruch, F.; Grau, E.; Merna, J. Direct coupling of CO_x with epoxides: Production of cyclic carbonates/esters and polycarbonates. JEDSC Bordeaux (France) 25.04.2013

Hošťálek Z.; Merna J. Direct coupling of CO_x with epoxides: Catalytic production of biodegradable polymers. 4th EuCheMS Chemistry Congress, Prague (Czech Republic), 26.-30.8.2012

Hošťálek, Z.; Cramail, H.; Merna, J. Kopolymerizace epoxidů s CO_x iniciované Salenovými komplexy. *Polymery 2012*, Smolenice (Slovakia) 26.-29.11.2012

Hošťálek, Z.; Štekrová, M.; Cramail, H.; Merna, J. Copolymerization of CO₂ with epoxides initiated by salen complexes. 44. *Symposium on Catalysis*, Prague (Czech Republic), 5.-6.11.2012